AD NUMBER

AD822519

NEW LIMITATION CHANGE

TO

Approved for public release, distribution unlimited

FROM

Distribution authorized to U.S. Gov't. agencies and their contractors; Administrative/Operational Use; SEP 1967. Other requests shall be referred to Air Force Materials Laboratory, Wright-Patterson AFB, OH 45433.

AUTHORITY

AFSC ltr dtd 26 May 1972

AFML-TR-67-310

SEMI-RIGID OR NON-RIGID STRUCTURES FOR RE-ENTRY APPLICATIONS

J. F. Keville

Space-General, a Division of
Aerojet-General Corporation

September 1967

FINAL TECHNICAL REPORT AFML-TR-67-310

Project No. 7-943b

Part 1 Evaluation and Design

This document is subject to special export controls and each transmittal to foreign governments or foreign nationals may be made only with prior approval of the Air Force Materials Laboratory (MATF) Wright-Patterson Air Force Base, Ohio 45433.

Air Force Materials Laboratory
Research and Technology Division
Air Force Systems Command
Wright-Patterson Air Force Base, Ohio

NOTICE

AFML-TR-67-310

SEMI-RIGID OR NON-RIGID STRUCTURES FOR RE-ENTRY APPLICATIONS

J. F. Keville

Space-General, a Division of
Aerojet-General Corporation

September 1967

FINAL TECHNICAL REPORT AFML-TR-67-310

Project No. 7-943b

Part 1 Evaluation and Design

Air Force Materials Laboratory
Research and Technology Division
Air Force Systems Command
Wright-Patterson Air Force Base, Ohio

FOREWORD

This Final Technical Report covers all work performed under contract AF 33(657)-10252 from 15 January 1963 to 15 January 1967. The manuscript was released by the author September 1967 for publication as an RTD Technical Report.

This contract with the Space-General Plant, Aerojet-General Corporation, El Monte, California, was initiated under ASD (subsequently RTD) Project Number 7-943b, entitled "Semi-Rigid or Non-Rigid Structures for Reentry Applications." It was accomplished under the technical directic of Mr. Thomas Campbell, MATF (now ASKMM), of the Manufacturing Technology Division, Air Force Materials Laboratory, Wright-Patterson Air Force Base, Ohio.

Mr. J. F. Keville was the Program Manager for Space-General. Others who participated in the development, fabrication, and test work in this project were:

A. F. Baca, Stress and Loads Analyst
M. K. Barsh, Materials Systems Specialist
C. J. Barton, Vehicle Design Engineer
C. R. Burnett, Materials Engineer
J. E. Crawford, Manager, Expandable Structures Department
G. H. Fredy Jr., Test Engineering Supervisor
W. A. Grant, Welding Engineering
J. G. Guidero, Project Staff Engineer
W. Hatalsky, Aerodynamicist
J. S. Haynes, Test Engineer
C. S. Horine, Senior Engineer
J. C. Huisking, Manufacturing Engineer
J. D. McNerney, Aerodynamicist
J. V. Miller, Design Specialist
J. E. Misselhorn, Thermodynamicist
R. A. Morrison, Design Specialist
A. H. Olsen, Senior Engineer
R. B. Robinson, Materials and Processes Engineer
J. R. Schrink, Manufacturing Engineer
S. L. Tomkinson, Project Staff Engineer
F. Warren, Program Management Office
J. A. Wrede, Materials Scientist

In addition to these Space-General technical personnel, numerous other technicians and project support personnel, as well as subcontractor technical personnel, participated significantly in the completion of this work.

FOREWORD (Continued)

This project has been accomplished as a part of the Air Force Manufacturing Methods Program, the primary objective of which is to develop, on a timely basis, manufacturing processes, techniques and equipment for use in economical production of USAF materials and components.

Suggestions concerning additional manufacturing methods development required on this or other subjects will be appreciated.

This technical report has been reviewed and is approved.

C. H. Nelson

C. H. NELSON, Assistant Chief
Manufacturing Technology Division
Air Force Materials Laboratory

ABSTRACT

This study, fabrication and test program was undertaken to determine the most suitable structural design, using available materials, for inflatable re-entry vehicles and space structures, to develop suitable manufacturing processes and techniques, and to perform tests on the resulting components of a typical re-entry paraglider. The results are applicable to other types of structures. This final technical report covers the period 15 January 1963 to 15 January 1967. Materials system development was conducted in conjunction with re-entry, aero-thermodynamic studies and vehicle structural design. A two-ply, ultra-fine, multifilament, nickel-chromium metal fabric, impregnated and coated with two different types of silicone rubber, was chosen as the basic structural and inflatable membrane of the re-entry vehicle. Major areas of technology advancement included development of manufacturing and processing techniques for the utilization of ultra-fine metal filament in the manufacture of special metal fabrics; stress analysis, and confirmation by test, of structures constructed of anisotropic woven materials; design and construction of a special, deep-throat, semi-automatic metal fabric welder capable of producing flexible, welded seams of approximately 90 percent efficiency in two through five layers of metal fabric; techniques for thorough impregnation and coating of metal fabric with high-temperature and ablative silicone elastomers, and fabrication methods for the construction of expandable space structures.

CONTENTS

Part 1 Evaluation and Design

CONTENTS (Continued)

Part 2 Fabrication and Test

Part 3 Appendices

ILLUSTRATIONS

Part 1 Evaluation and Design

ILLUSTRATIONS (Continued)

ILLUSTRATIONS (Continued)

ILLUSTRATIONS (Continued)

ILLUSTRATIONS (Continued)

ILLUSTRATIONS (Continued)

ILLUSTRATIONS (Continued)

ILLUSTRATIONS (Continued)

ILLUSTRATIONS (Continued)

ILLUSTRATIONS (Continued)

ILLUSTRATIONS (Continued)

ILLUSTRATIONS (Continued)

TABLES

Part 1 Evaluation and Design

TABLES (Continued)

Part 2 Fabrication and Test

LIST OF SYMBOLS

A	Reference Area
A_n	Acceleration, Normal
A_t	Acceleration, Tangential
c	Specific Heat of Materials, Btu/lb °F
c_p	Specific Heat, Btu/lb °F
C_D	Drag Coefficient
C_L	Lift Coefficient
C_n	Normal Force Coefficient
C_p	Pressure Coefficient
D	Boom Diameter, inches
E	Young's Modulus
Fg	Load due to Acceleration, pounds/inch
f_o	Force per Unit Length
f_s	Shear Fiber Load
f_t	Tension Fiber Load Due to Internal Pressure
F	Force
$\bar{i}$	Unit Vector in the x Direction
I	Moment of Inertia
$\bar{j}$	Unit Vector in the y Direction
$\bar{k}$	Unit Vector in the z Direction
k	Thermal Conductivity Btu/hr ft^2 °F/ft
Ku	Effective Sharp-Edged Gust Velocity, ft/sec
ℓ	Length of Boom from Apex

L/D	Lift-to-Drag Ratio
$\dot{m}$	Mass Ablation Rate
m	Mass per Unit Length
M_v	Keel Moment, inch-pound
M_y	Moment About the Horizontal Axis, inch-pound
M_z	Moment About the Vertical Axis, inch-pound
M	Bending Moment
n_g	Gust Load Factor, Normal to Flight Path
n_z	Gust Load Factor, Normal to Keel
N'/ql	Normal Span Loading
N_θ	Unit Hoop Load, pounds/inch
$N_{\phi B}$	Unit Longitudinal Bending Load, pounds/inch
$N_{\phi p}$	Unit Longitudinal Force Due to Internal Pressure pounds/inch
p	Internal Pressure, pounds/sq. inch
p_s	Boom Shear Unit Loads, pounds/inch
P_s	Increment of Internal Pressure Applied to a Strand
q	Dynamic Pressure, pounds/sq. ft.
$\dot{q}$	Heat Flux, Btu/sec ft^2
q_{cw}	Cold Wall Heat Flux, Btu/sq. ft., sec
$\dot{q}$	Pseudo Heat Flux, Btu/sq. ft., sec
q_ℓ	Heat Flux on Boom
q_s	Heat Flux on Boom at Stagnation Point

Q	Shear Force
Q_c	Heating Rate, Btu/sq. ft., sec
Q^*_c	Effective Heat of Ablation, Btu/lb
r_1	Radius of Curvature
r_2	Distance from Neutral Axis
R	Apex Radius
R_i	Instantaneous Radius
t	Time, sec., or Wall Thickness, in.
T_{av}	Average Temperature of Material During Time (dt), ^oR
T_i	Inside Surface Temperature, ^oR
T_i	Effective Average Inside Temperature of Material, ^oR
T_m	Ablation Temperature, ^oF
T_{psm}	Pseudo Melting Temperature, ^oF
T_s	Tension in a Longitudinal Strand
T_i	Inside Surface Temperature, ^oF
T_o	Outside Surface Temperature, ^oR
T_H	Tension in a Hoop Strand
V	Shear Load, pounds
w	Unit weight pounds/in
W	Weight, Pounds
W/C_DA	Ballistic Coefficient
W/s	Wing Loading
x, y, z	Coordinate System
$x'/q\ell$	Axial Span Loading

x/ℓ	Keel Station
y/ℓ	Span Station
α	Angle of Attack - Degrees
γ	Cone Semivertex Angle, Degrees
ϵ	External Emissivity at T_o
δ	Thickness of Material, ft.
η	Angle Between Velocity Vector and the Normal to the Surface
θ	Angular Change
θ_i	Re-entry Angle, Degrees
$\iota(\xi)$	E_ξ/E_{ξ_o}, Normalized to Unity at ξ
ξ	Nondimensional Length Coordinate, x/ℓ
Λ	Sweep Angle of L. E. Boom Relative to y-Axis
ρ	Ambient Air Density, lb/ft^3
ρ_m	Density of Material, lb/ft^3
σ	Stefan-Boltzmann Constant
σ_c	Pressure Stress in Cylindrical Section
σ_p	Pressure Stress
σ_s	Shear Stress
σ_t	Pressure Stress in Toroidal Section
$\varphi(\xi)$	Nondimensional Force Distribution Parameter
ψ	Nondimensional Parameter, $\frac{\ell^2 F}{EI_o}$
$\omega''(x)$	Transverse Beam Deflection
Ω	Nondimensional Frequency Parameter, $\frac{\ell^4 \omega^2 m_o}{EI_o}$

Subscripts

a	Aft Station
f	Forward Station
n	Normal Component
o	Apex

Section 1

INTRODUCTION

Future space activities will require the utilization of expandable structures capable of being pre-packaged in a small volume and expanded in space to create strong and, in many cases, high-temperature-resistant structures. The objective of this program was the development, construction, and test of typical inflatable, high-temperature structures. As an object for design and demonstration of design and manufacturing capabilities, the manned, emergency re-entry paraglider was chosen. The vehicle would be capable of returning a man from orbit by re-entering the earth's atmosphere at hypersonic velocity and decelerating to effect a subsonic, controlled landing on earth. The research and development program described in this report was initiated by the Manufacturing and Technology Division, Air Force Materials Laboratory, Research and Technology Division, USAF, Wright-Patterson Air Force Base, under the title "Semi-Rigid or Non-Rigid Structures for Re-Entry Applications."

Space-General assigned the program the title "Project FIRST" which is an acronym for "Fabrication of Inflatable Re-Entry Structures for Test." A description of the paraglider vehicle and its application is contained in Section 3.1 of this report.

One of the project criteria was that available materials must be used, which was interpreted to mean that development of new alloys or new formulations of coating materials was outside the project's scope.

This report, which contains a review of all technical effort during the four-year program, describes early analytical studies of the aero- and thermodynamic design criteria affecting the materials and structural configuration. These studies subsequently led to the actual design and fabrication of sub-scale and full-scale structural components. A special welder was constructed and used to fabricate the complex metal fabric structures which were then impregnated and coated with silicone rubber. These components were tested in environments simulating the hypersonic re-entry conditions which a paraglider would encounter, and the results of the tests were analyzed and compared with the analytical predictions. The results of the tests exceeded the design goals in most cases and definitely established the applicability of the welded, impregnated metal fabric structure for high-strength, high-temperature applications.

Section 2

SUMMARY

To proceed with design and material selection, it was necessary to first determine the critical environment of an inflated, flexible-wing paraglider during atmospheric re-entry. Aeromechanical analysis during the first phase of this program permitted determination of structural loads and other design criteria. A sub-optimized re-entry trajectory corresponding to minimal thermodynamic heating effect was selected using digital computer programs in which the heating of the materials system and ablation of the silicone rubber surface were accounted for. Initial evaluation of the materials, particularly the silicone elastomers to be used in impregnating and coating the metal fabric, was conducted by exposing specimens to an air-arc plasma jet at heat fluxes and related conditions simulating the environment of the hypersonic re-entry vehicle. As a result of these tests a silicone rubber (S-6510, manufactured by Dow Corning) was selected as the ablative coating material. Subsequent evaluation of techniques for producing void-free saturation or impregnation of the metal fabric with silicone rubber resulted in the selection of another high-temperature silicone rubber (RTV 655, manufactured by General Electric Co.) which exists as a liquid prior to polymerization.

A large number of metal fabric joining methods were evaluated experimentally. These included sewing, continuous weaving, and various brazing and welding techniques. In the early part of the program, monofilament, type 304 stainless steel cloth was used for joining experiments and to construct small 7-inch-diameter test cylinders. Subsequently, the multifilament yarn, nickel-chromium fabric was woven in a 2 by 2 basket weave and the "pilot run" of this fabric permitted the optimization of the final joining technique. Spot welding was selected as the best joining method, not only because it avoided the disadvantages of the need for inert atmosphere, brazing fluxes, and attendant handling problems, but also because it produced an extremely strong, flexible joint which could be made rapidly. Although attempts to produce a portable hand-held welding "gun" were unsuccessful, laboratory work indicated that welds exceeding 80 percent joint efficiency could be made by using two rows of closely spaced small spot welds. A large, semi-automatic welding machine was designed and constructed to produce such spot welded seams at operational speeds of about 1 to 8 inches per minute. Two rows of spot welds, approximately 0.3 inches apart, are produced. Each row contains 40, approximately 0.015-inch-diameter, spot welds per inch using 1/2- to 3/4-inch overlap of the fabric layers. At least five layers of fabric can be joined so that intersecting seams and multiple plies can be accommodated permitting the construction of surfaces with compound curvatures.

The welder has a 7-foot-deep throat and two different arm arrangements which support the lower welding head. This permits the welding of

longitudinal and circumferential seams in cylindrical shapes as well as the welding of curved shapes such as the toroidal apex of the paraglider. The heads can be rotated at various angles and indexed so that joints may be made at angles to the axis of the machine.

The extensive qualification testing on this welding system showed that the weld strength exceeds 89 percent of the parent fabric strength for a large population of tensile test coupons at the 90 percent confidence level. The original goal was a weld efficiency of 85 percent and statistical analysis of the qualification test results indicated that there is more than 99.95 percent confidence that the average tensile strength of a two-layer weld exceeds this value. In welding the complicated, toroidally-shaped apex of the paraglider, the average efficiency of process control coupons was 92 percent for two layers and 87 percent for five layers.

The entire fabrication technology which was developed began with a very careful cutting of the metal fabric using templates which were previously fitted to master forms. The fabric was then laid-up on these forms and "basted" in place using a small capacitance-discharge power supply and a hand-held copper electrode. The other electrode was a thin copper back-up strip inserted under the proposed joint. After basting, the form was removed from the fabric structure (in the case of the compound curvature apex, the form was disassembled from within the structure) and the unsupported flexible material was taken to the large welder.

For a structure with maximum shear strength in the reinforcing skin, permitting torsional loads, two similar structures were assembled with one having the fabric in bias or 45° yarn relationship to the other. One of these plies was then inserted within the other and the form again placed within the two-ply fabric assembly. This fabric assembly on the form tool was then vacuum-impregnated with a liquid silicone rubber. The impregnated fabric was then overlaid or coated with additional high-temperature protective ablative coating of the gum-type silicone rubber, except in the case of the apex which was not coated.

The objectives of this program included not only the development of materials systems and manufacturing techniques but the testing of a number of paraglider components using simulated re-entry loads and temperatures to verify the design technology as well as the fabrication methods. Fifteen small components (including 7-inch-diameter by 15-inch-long cylinders and 30-inch-long frustums tapering from 10-inch-diameter to 7-inch-diameter, with open ends) were fabricated including impregnation and ablative coating. These were tested with end closures in place and internal pressures producing the proper reinforcing fabric loading, while torsion, shear, and bending loads were applied, both at room temperature and temperatures simulating those of the re-entry regime. In most high-temperature tests the structure was heated non-uniformly (as in flight), where the coating of ablative silicone rubber was 1/8-inch thick, until the metal fabric substrate reached 700-900°F.

The 15-inch-long cylinders were tested as single-ply and two-ply, with and without impregnation, to determine the individual performance of the materials components. The 30-inch-long frustums were tested with combined loads, under cyclic loads, folded, packaged, and vibrated, vibrated in the inflated condition, before heating, during heating, and after heating to maximum temperatures. Finally, most of these frustums were burst either at high temperature or at room temperature to determine the structural integrity and any degradation caused by the various loads, vibration, folding, and heating experiments. There was no evidence to indicate that the burst strength was significantly affected by any of these conditions.

The folding and packaging of one of the 30-inch-long frustums indicated that it could be packaged into a box with a volume of only 7.9 percent of its inflated volume. Also, its packaged volume was only twice that of the volume of the material from which it was constructed.

Similarly, the large, full-scale, 17-foot-long paraglider boom which tapered from 32-inch-diameter to 13-inch-diameter was folded and found to occupy a volume of only 4.9 percent of its original 48 cubic feet inflated. The package occupied a volume only 3.1 times greater than the material volume.

The boom was exposed to the complete series of environments that the paraglider would be expected to encounter during re-entry. While the frustums were exposed to these tests separately to determine their individual effects, the boom was successively tested for permeability and leakage, packaging and packaged vibration, inflated resonant vibration, static design loads and cyclic loads. It was then heated to a metal fabric substrate temperature 850°F under a bank of high-temperature quartz heating lamps. Permeability and leak tests were again performed, followed by resonant vibration and cyclic loads at high-temperature before being allowed to cool. The boom encountered severe charring due to several unexpected events, including the rupture of the inert atmosphere enclosure (simulating the low oxygen content of the re-entry environment) which caused infiltration of additional oxygen and melting of the quartz lamp aluminum reflectors with the result that molten aluminum ran over the surface of the boom. The boom withstood all of these drastic environments without any serious damage except to the ablative silicone rubber coating. The impregnated metal fabric appeared to be essentially unaffected although leakage rates increased somewhat.

After cooling, the boom was subjected to permeability and leakage tests again, followed by additional resonant vibration exposure, static design loads and cyclic loads, with final combined loads to 240 percent of design limit. At this point, the large, 32-inch-diameter supporting closure fixture failed to hold the boom and the boom pulled out of the closure clamps with consequent damage to the large end of the boom. Since it was intended to take the boom to failure either through application of loads or by pressure burst, the test program on the boom was complete.

The large toroidal apex section of the paraglider was constructed using over 200 separate fabric segments welded together in a jigsaw pattern to produce a load carrying skin with compound curvature. The two-ply metal fabric structure was "mummy" wrapped with 1.6-inch-wide metal tape to reinforce the highly loaded crotch areas between the center keel boom and the leading edge booms. The entire structure was vacuum-impregnated with silicone rubber. The final test component was about 8 feet from the forward surface of the apex to the end of the center stub boom and nearly 12 feet between outer tips of the leading edge stub booms, with a 32-inch cross-sectional diameter.

The apex was subjected to pressure tests until it burst although it had an unusually high leakage rate apparently due to improper curing of the silicone rubber impregnant. It appears that the improper cure of the silicone rubber was due to poisoning and contamination of the impregnant. While the apex was expected to have a minimum burst pressure of 21 psig, it failed at 9.0 psig. This was attributed not only to the improper cure of the impregnant but to wrinkling of the bias ply and unequal sharing of the loads between the layers of fabric.

While the 10-inch-diameter frustums were expected to have a minimum burst pressure of 68 psig, they all failed between pressures of 78 and 102 psig, the latter indicating essentially 100 percent weld joint efficiency throughout with negligible stress concentrations. The boom, on the other hand, was not tested above 11 psig but did carry 240 percent of combined (shear, torsion and bending) limit loads before showing incipient buckling. This compared favorably with the frustum which was tested to buckling at 250 percent of combined design limit loads.

Other tests on the apex included folding and packaging which indicated that it could be reduced to a volume of 3.4 percent of its inflated size or 6.6 times its actual materials volume. Due to the tape wraps amounting to some 25 layers in the crotches, the apex was less flexible than the frustums and the boom, although the fact that it could be folded to this small package size indicated considerably more flexibility and packageability than had been anticipated.

Structural analysis of the failure of the apex indicates that most of the reasons for the failure are known and that construction of a similar structure in the future could be successfully carried out with reasonable assurance provided a somewhat more sophisticated structural design is employed and certain fabrication problems are avoided.

Briefly, the program has resulted in the development of four main technologies:

a. Design of specialized metal fabrics woven from multifilament yarn, for high-temperature, high-strength structural applications.

b. Analytical techniques for stress analysis of anisotropic structural fabrics with extensive empirical test results to reinforce the analytical techniques.

c. Production of high-strength, high-temperature, flexible seams in metal fabric with a special semi-automatic welding machine. These seams have joint efficiencies relative to parent fabric strength of about 90 percent and can be made through two to five layers of metal fabric permitting the construction of large structures of compound curvature.

d. Vacuum impregnation and overlaid coatings of various silicone rubber elastomers to produce void-free, high-temperature-resistant and ablative structures which retain adequate flexibility after heating.

Section 3

DISCUSSION

3.1 PROGRAM OBJECTIVES

As a model for the development of manufacturing technology for non-rigid structures for re-entry applications, the re-entry paraglider was chosen. The mission of the vehicle would be to return a single crew member to earth from an orbiting space station. The proposed vehicle (Figure 1) is a modification of the micrometeoroid sensing paraglider developed by Space-General for NASA/Langley under Contract No. NAS 1-1732.

In general, the design concept of this paraglider requires that it be a flexible, inflatable-type of structure capable of being packaged in the uninflated condition into a small volume similar to the manner in which a rubber liferaft is packaged. The vehicle would be stored in its container within or on the wall of the space station. In the event of a requirement for emergency return to earth, a crewman would enter the crew capsule of the paraglider through a hatch opening to the interior of the space station. The compartment section would then be sealed and the vehicle ejected away from the space station. After inflation by nitrogen from high-pressure gas bottles or through umbilical from the space station (see Figure 2), attitude control jets would be used to align the vehicle in proper retrofire attitude. Solid rockets mounted on top of the keel boom would then be used to reduce the velocity sufficiently to de-orbit. The attitude control jets would be supplied with gas from the vehicle pressurizing supply. Since the pressurizing gas in the inflated sections will be heated during re-entry, the excess gas would also be available for this control system. A constant pressure differential between interior and ambient environment pressure would be maintained. After re-entry and subsequent cooling, additional gas would be available from the pressurizing bottles to maintain proper inflation pressure as the vehicle entered the lower atmosphere.

Since the vehicle will re-enter the earth's atmosphere at a velocity of approximately 26,000 feet per second, it is necessary to select materials which will withstand high temperatures resulting from aerodynamic heating. The high angle-of-attack of the vehicle will cause the entire lower surface of the structure, as well as the nose section, to be exposed to the high heating effect. Control of this heating would be accomplished through the use of ablating silicone rubber coating materials.

After entering the sensible atmosphere, aerodynamic control may be obtained by the deflection of the aft edge of the sail membrane or by de-pressurizing or pressurizing the leading edge booms to permit them to bend more or less, thus permitting maneuverability through wing warping. It is expected that the landing footprint for a vehicle of this type would be approximately 450 miles wide and 1400 miles long (Reference 1). The landing maneuver would be accomplished by reducing vertical velocity by a

05-051

Figure 1. Emergency Re-entry Paraglider

07/092

Figure 2. Deployment of Escape Vehicle (Artist's Concept)

conventional aircraft-type flare maneuver. It is not anticipated that landing skids would be necessary since the glider would be capable of absorbing ground impact loads.

Although a rigid capsule would be required in the center keel boom of the paraglider (containing the crewman, life support system, and autopilot instrumentation) the scope of this program did not include the design or development of the capsule section. The program included the design, development and construction of prototype and full-scale sections of the vehicle. No portion of the actual skin of the vehicle, including the toroidal nose or apex, was to be rigid material and, therefore, the development effort concentrated on the design and construction of flexible, inflatable load carrying structures of complex geometry which would be capable of high strength at high temperatures.

As will be discussed further in this report, the vehicle that evolved from this concept consists of an inflated body made up of three tapered booms attached to a common toroidal apex as shown in Figure 1. Attached between the center boom or keel and each leading edge boom is a thin, flexible wing membrane which takes on an approximately semi-conical shape during flight in the atmosphere. The booms taper from 32 inches in diameter at the forward end to 13 inches at the aft tip, with an overall vehicle length of approximately 23 feet and a wing spread of 28 feet. Since aerodynamic analysis indicated that the wing membrane itself carried relatively low loads, emphasis on deflection of a membrane structure was concentrated on the inflated booms and apex. The means of attaching the wings tangentially to the booms was developed also.

3.2 AERO-TRAJECTORY ANALYSIS

3.2.1 GENERAL CONSIDERATIONS

Evaluation of the re-entry dynamics and subsonic aerodynamic characteristics of the paraglider concept indicates a low-aspect ratio planform with a leading edge sweep angle of 55°. Survey of existing literature produced adequate aerodynamic data for the subsonic and supersonic flight realm, but data at the hypersonic speeds encountered during re-entry were lacking. Therefore, analytical estimates of the pressure distribution at hypersonic speeds were made using Newtonian concepts. The analyses not only define the overall aerodynamic characteristics but also provide detailed loading distribution for the structural design.

3.2.2 AERODYNAMICS

Estimate of the pressure distribution on the wing membrane and the keel at hypersonic velocities was made using an approximation to the Newtonian theory. This theory assumes that the entire vertical component of stream momentum is given up to the glider.

Strict Newtonian flow computations require that only the normal momentum be transmitted to the body. Comparison of the calculated results (using the aforementioned modified approach and the latter strict Newtonian flow approach) indicates that the pressure distribution across the wing (perpendicular to the semi-cone axis of symmetry) is similar in both cases and the difference is one of magnitude. The values obtained with the less complicated modified approach, wherein the entire vertical component of momentum is transmitted to the body, are approximately 15 percent larger than the strict Newtonian values. Since the wings are flexible and maneuverability may be achieved by wing or trailing edge warping, the higher values resulting from the less complicated approach have been used.

Based on the theory that the entire vertical component of stream momentum is given up to the vehicle, the following equation results:

$$C_p = \frac{\Delta p}{q} = 2 \sin^2 \left| \alpha - \tan^{-1} \frac{dz}{dx} \right| \tag{1}$$

The local flow deflection angle is $\alpha - \tan^{-1} \frac{dz}{dx}$. The local flow deflection angles were computed by assuming that each wing membrane inflated to the shape of half a right-circular cone, as shown in the sketch on the following page.

The streamwise airfoil sections are parts of parabolas formed by cutting vertical planes parallel to the keel. The leading and trailing edges of the membrane are described by the expressions:

$$x_{LE}/\ell = (y/\ell)(\tan 2\gamma)^{-1} \tag{1a}$$

and

$$x_{TE}/\ell = 1 - (y/\ell) \tan \gamma \tag{1b}$$

Taking the derivative, dz/dx, the pressure coefficient at any point on the panel is:

$$C_p = 2 \sin^2 \left[\alpha - \tan^{-1} \frac{\tan \gamma}{\tan^2 \gamma - 1 + 2 \frac{x}{y} \tan \gamma} \right] \tag{2}$$

For the vehicle proposed in this program, $\gamma = 17.5^\circ$ and $\ell = 17.35$ feet; therefore

$$C_p = 2 \sin^2 \left[\alpha - \tan^{-1} \frac{.3153}{.6306 \frac{x}{y} - .9006} \right] \tag{3}$$

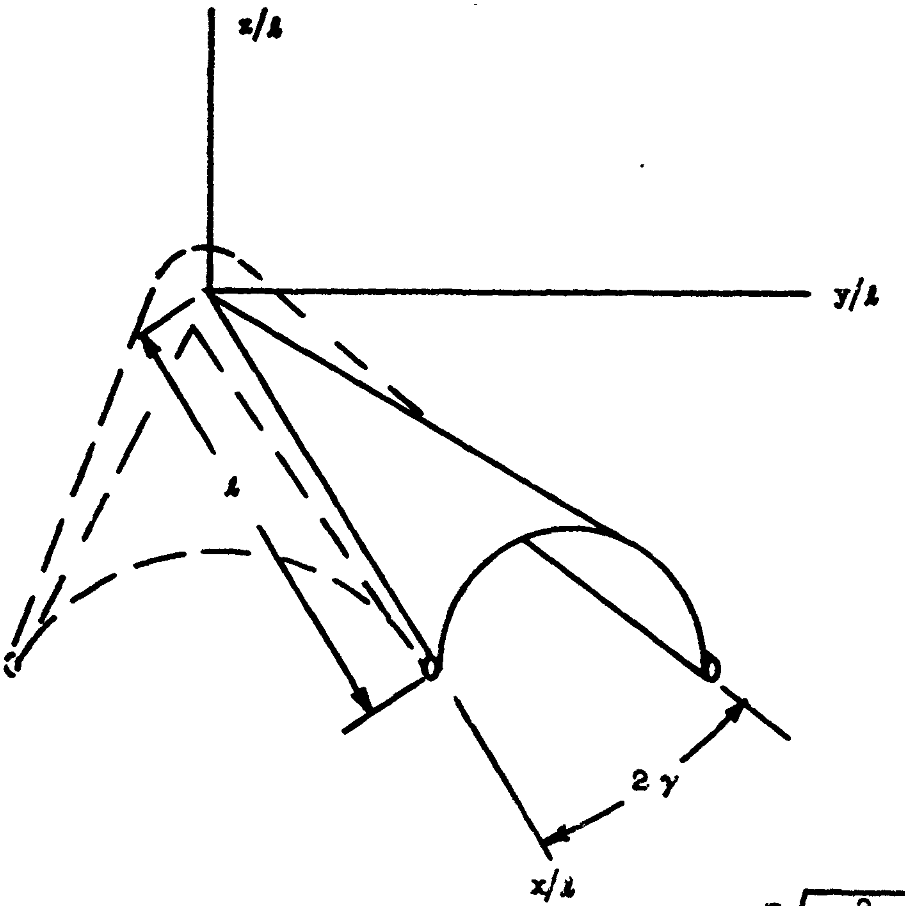

$$z/\ell = (y/\ell)\sqrt{\tan^2\gamma - 1 + 2(x/y)\tan\gamma}$$

Plots of the airfoil sections and the pressure distribution for $\alpha = 70^\circ$ for each quarter-span station are shown in Figure 3. The normal and axial force components resulting from these are shown in Figure 4. From these figures the normal membrane loading along strips parallel to the trailing edge were determined and then integrated chordwise to indicate the spanwise loading distribution as in Figure 5. Although Figure 5 indicates the normal span loading increasing at all points as the centerline of the keel is approached, there would actually be a dip in this curve where the membrane becomes tangent to the keel at spanwise station of zero. The total integrated normal force coefficient obtained from this analysis, however, compares very well with test data from the literature (Reference 2) since the present assumption that the wing membrane would become tangential to the side of the keel boom may not remain true during all flight perturbations and maneuvers. The assumption made in accordance with Figure 5 should be conservative.

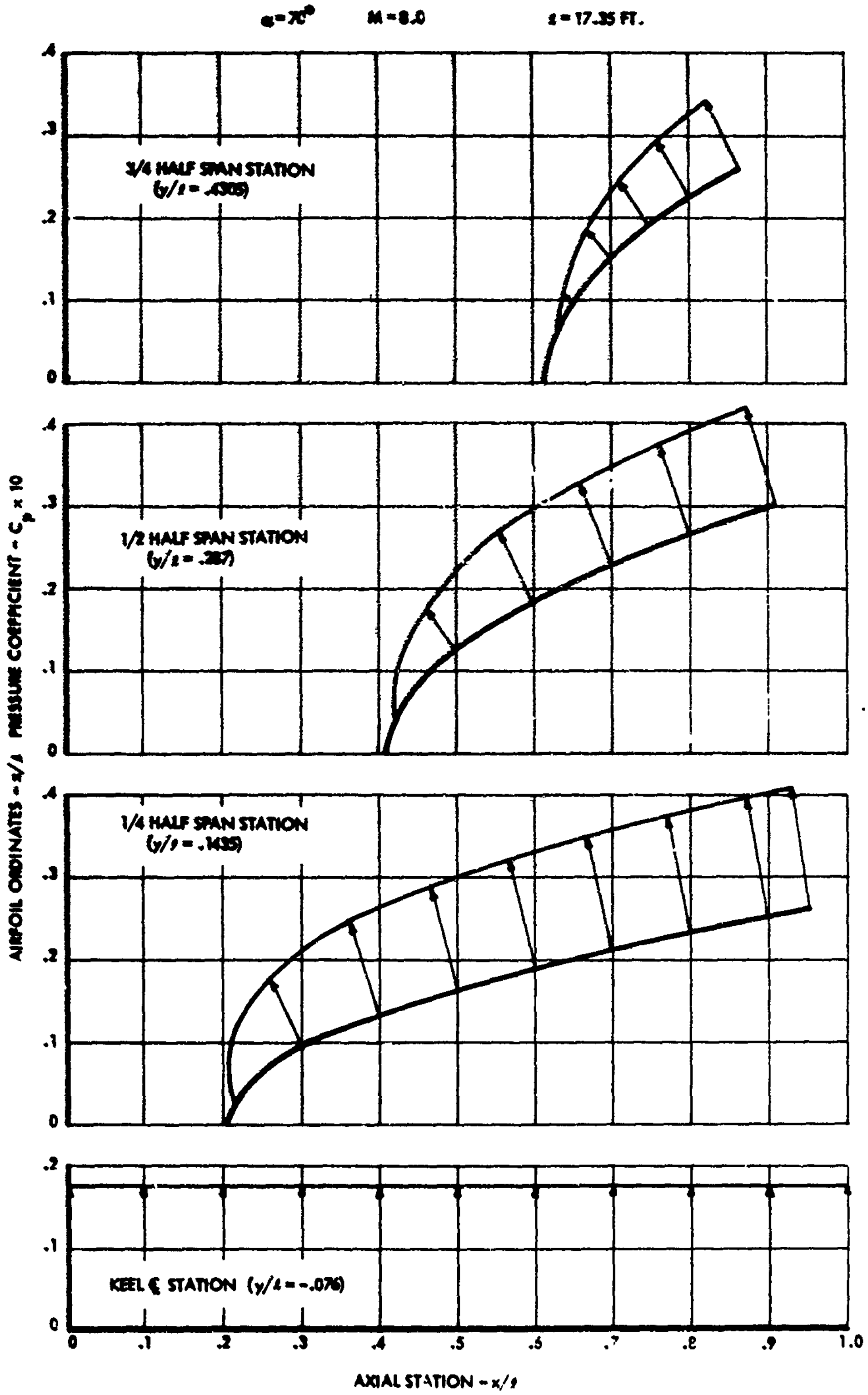

Figure 3. Membrane and Keel Chordwise Pressure Loading

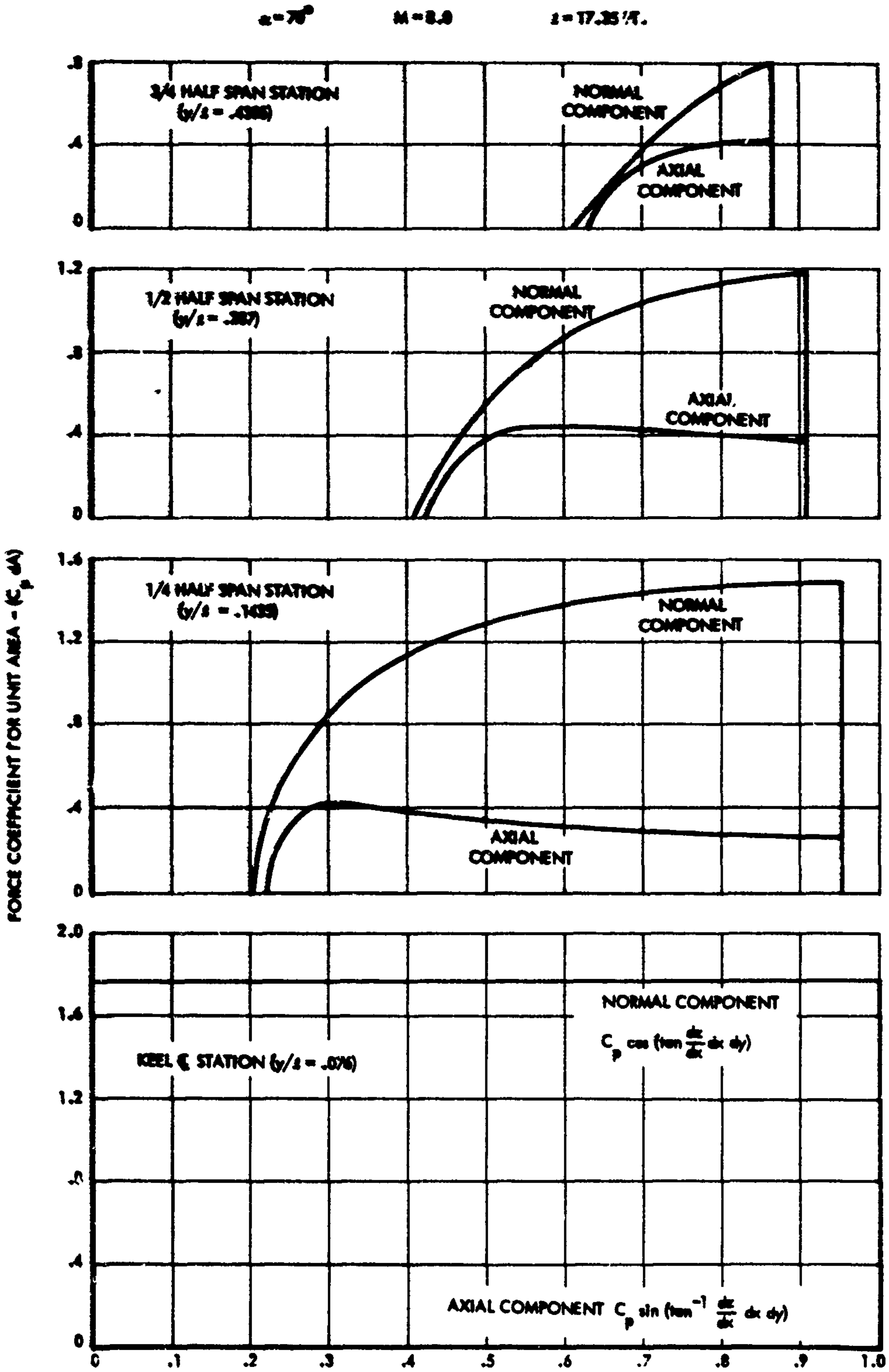

Figure 4. Membrane and Keel Chordwise Loading

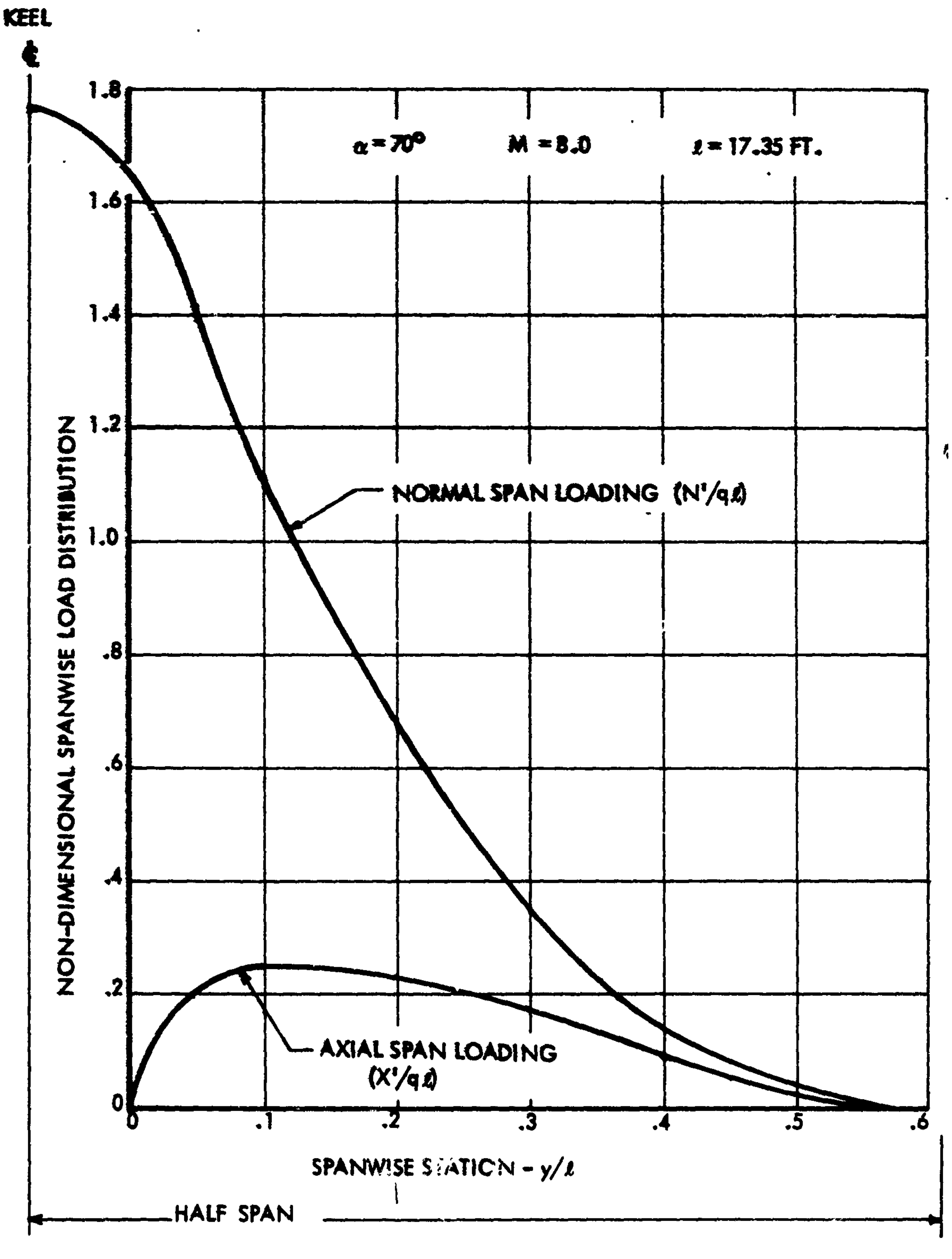

Figure 5. Membrane and Keel Spanwise Pressure Loading

Calculation of the airload distribution on the leading edge booms was made using Newtonian theory which presents the expression:

$$C_p = 2 \cos^2 (\theta - \alpha) \cos^2 (\Lambda \cos \alpha) \tag{4}$$

The local angle of the leading edge boom cross section relative to the x axis is θ, and the leading edge boom sweep angle measured from the y axis is Λ. A plot of the pressure distribution applicable to all cross-sections of the boom is shown in Figure 6. Pressures on the apex are approximately 10 percent higher. These pressures were integrated over the periphery of each cross-section and the resulting normal and transverse running loads are also plotted.

With the spanwise pressure distribution established, the resulting aerodynamic coefficients and the L/D ratio during hypersonic re-entry were determined as functions of angle-of-attack as shown in Figure 7. The variation of these coefficients with Mach number is small in the region of hypersonic re-entry velocities considered.

Consideration of a parametric study of heating rates indicated that minimum heating occurred near maximum lift coefficient. As a result, a re-entry angle of attack of 70°, which corresponds to a L/D of 0.5, was selected for the trajectory analysis.

3.2.3 RE-ENTRY TRAJECTORY

Several trajectories were investigated using an IBM 7090 digital computer. The program used determines a two-dimensional, point-mass trajectory and is based on the assumptions of a non-rotating spheroidal earth and that the mean flight path would not be affected appreciably by oscillatory motions while maintaining a constant L/D and without lag.

The aerothermal corridor corresponding to minimum re-entry heating was found to occur at re-entry angle (γ) of 1.0°, angle-of-attack (α) of 70°, and L/D of 0.5 (References 3, 4). Plots of the trajectory characteristics under these conditions are represented in Figures 8 through 14.

3.2.4 LOAD FACTORS

For structural analysis, a time history of the normal and axial inertia re-entry maneuver load factor was determined and is presented in Figure 15.

It is seen that a maximum re-entry normal load factor of 1.54 occurs at an altitude of approximately 250,000 feet. At this altitude the glider is expected to encounter atmospheric turbulence. At much lower

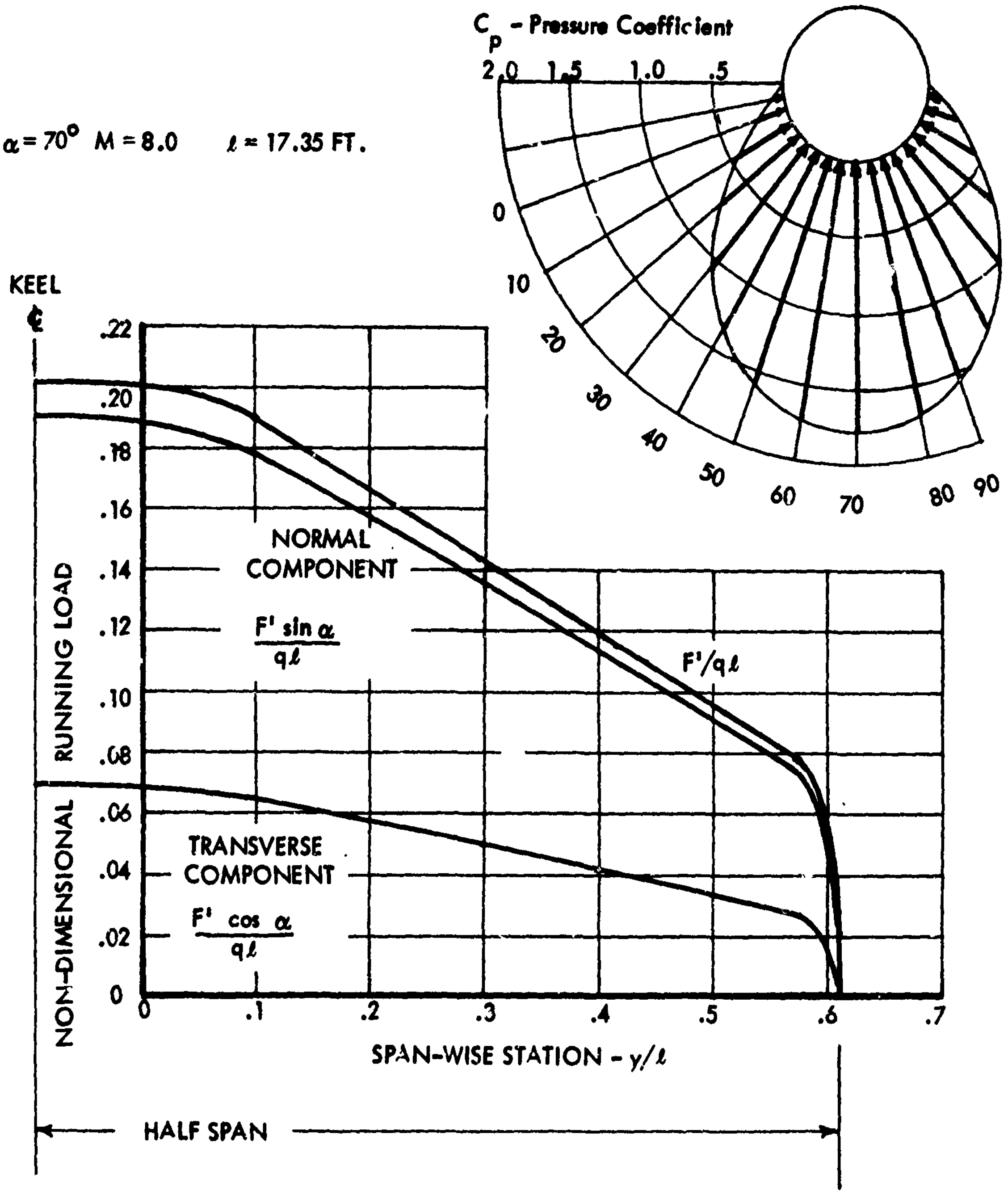

Figure 6. Hypersonic Pressure Distribution and Running Loads on Boom

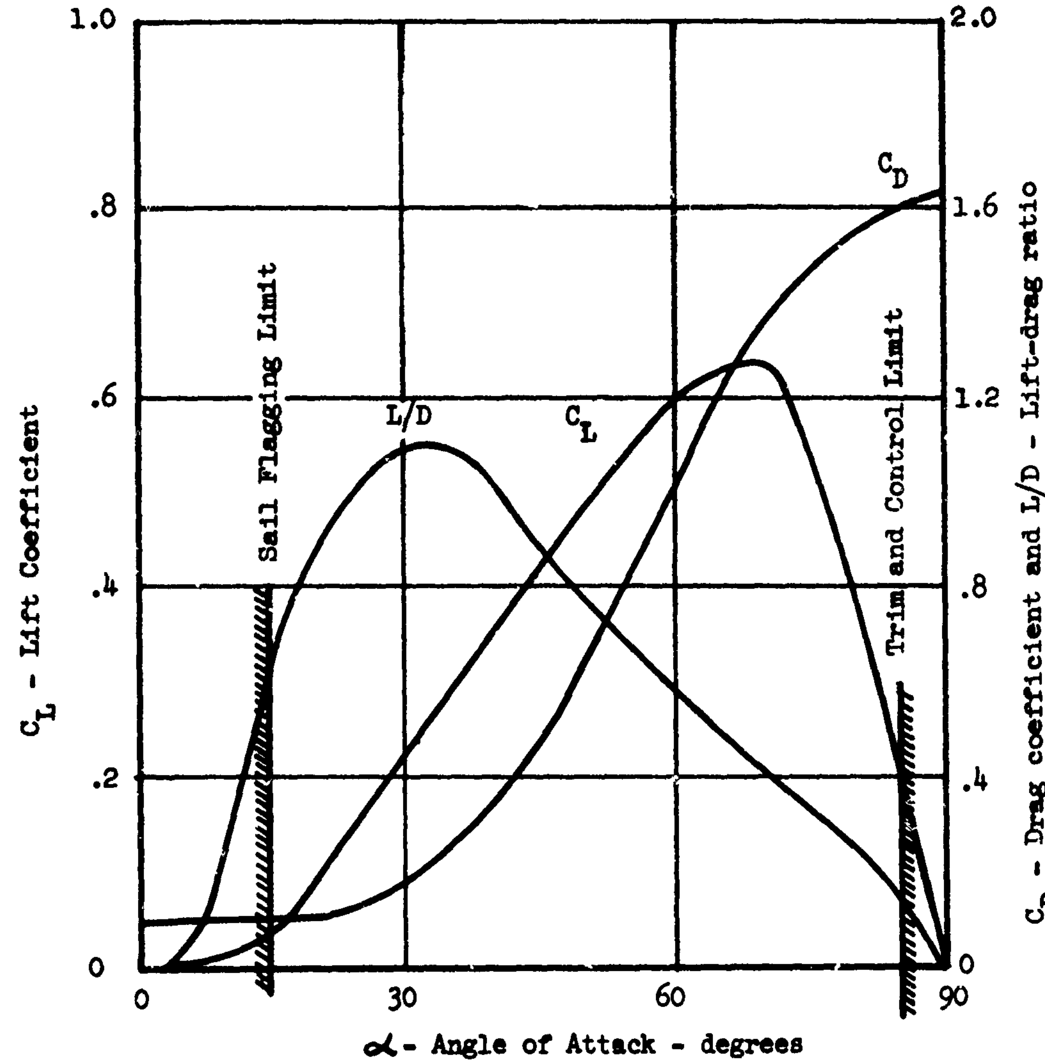

Figure 7. Aerodynamic Characteristics at Hypersonic Speeds

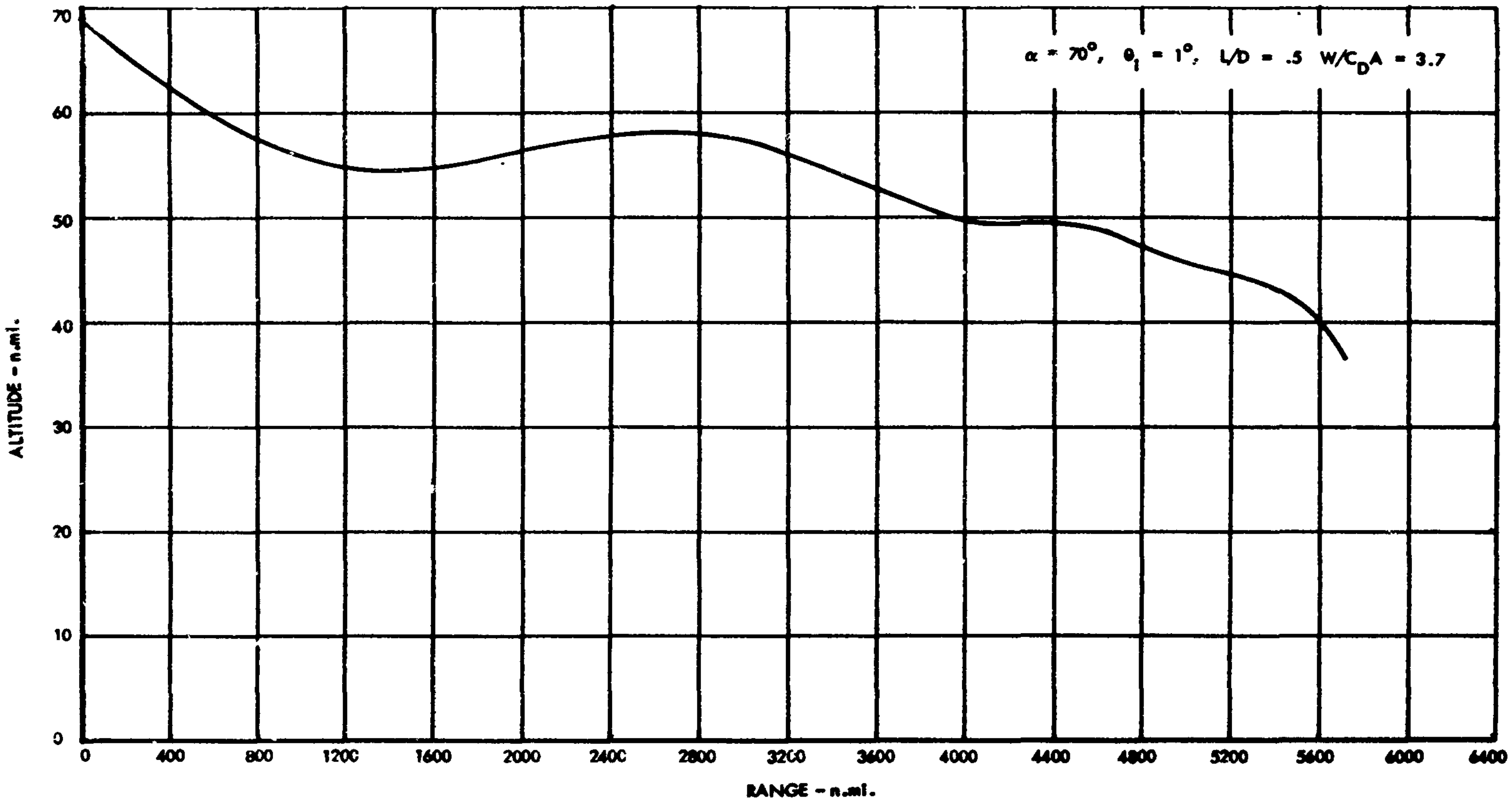

Figure 8. Re-Entry Trajectory Altitude Versus Range

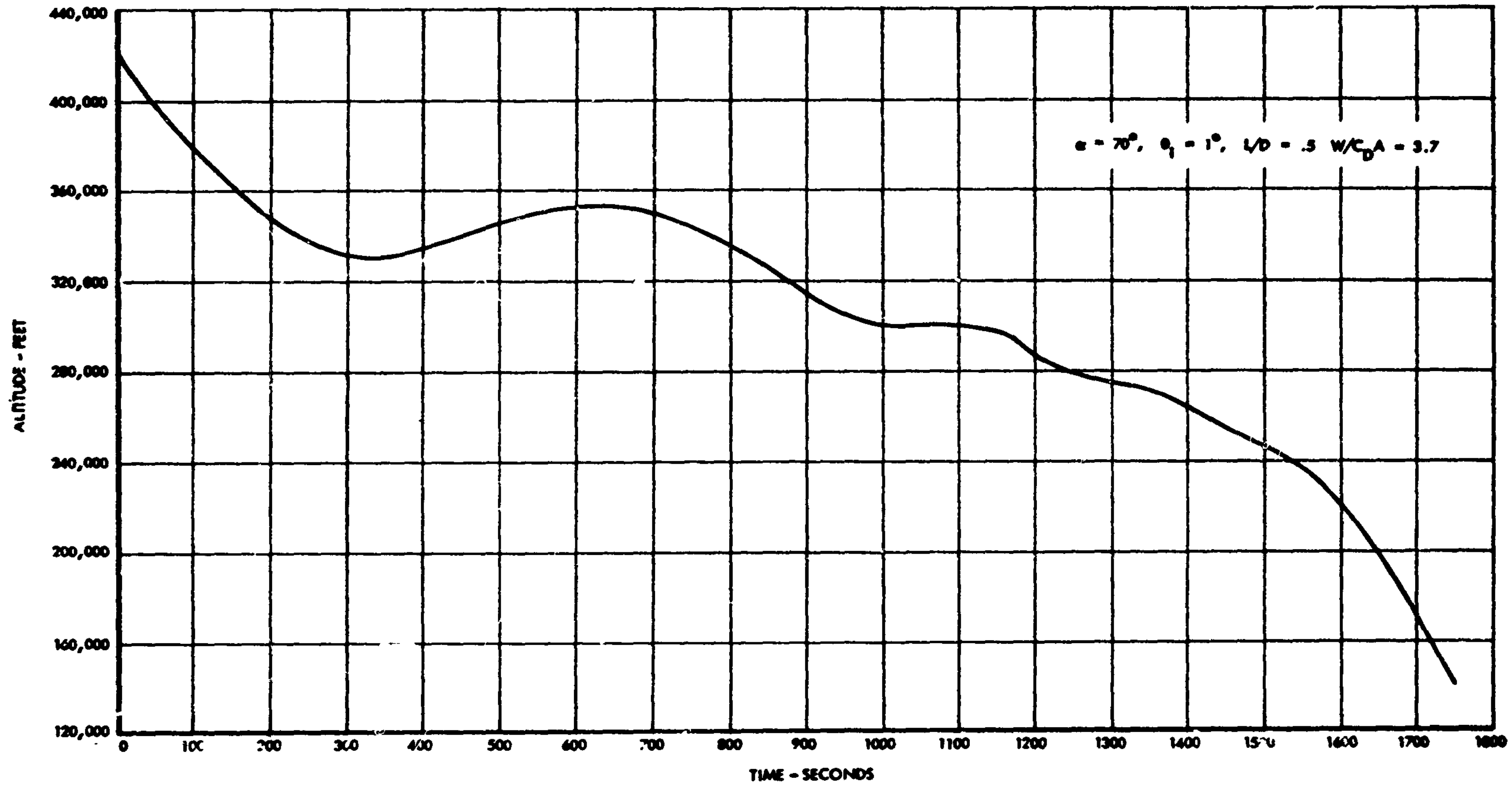

Figure 9. Altitude Time History

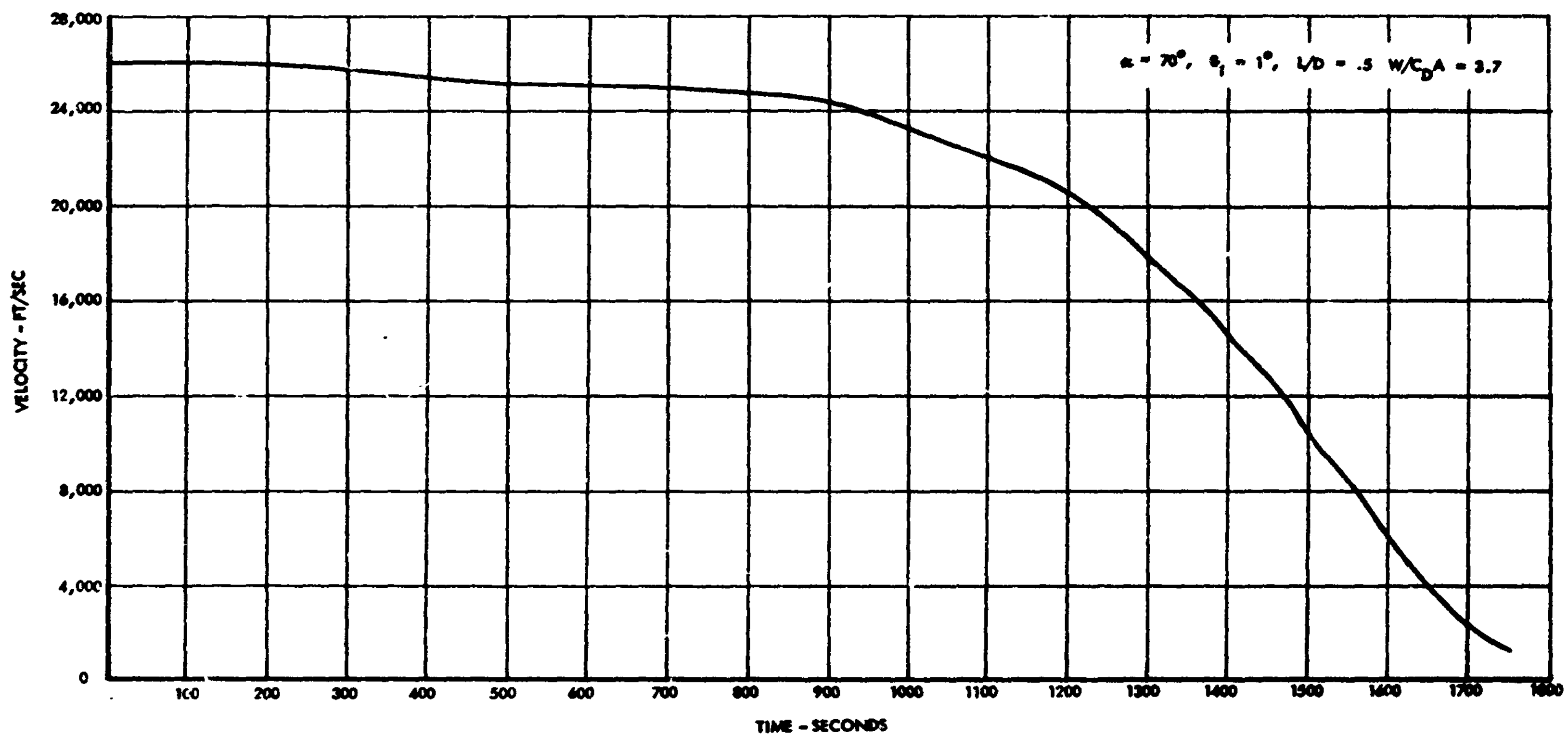

Figure 10. Velocity Time History

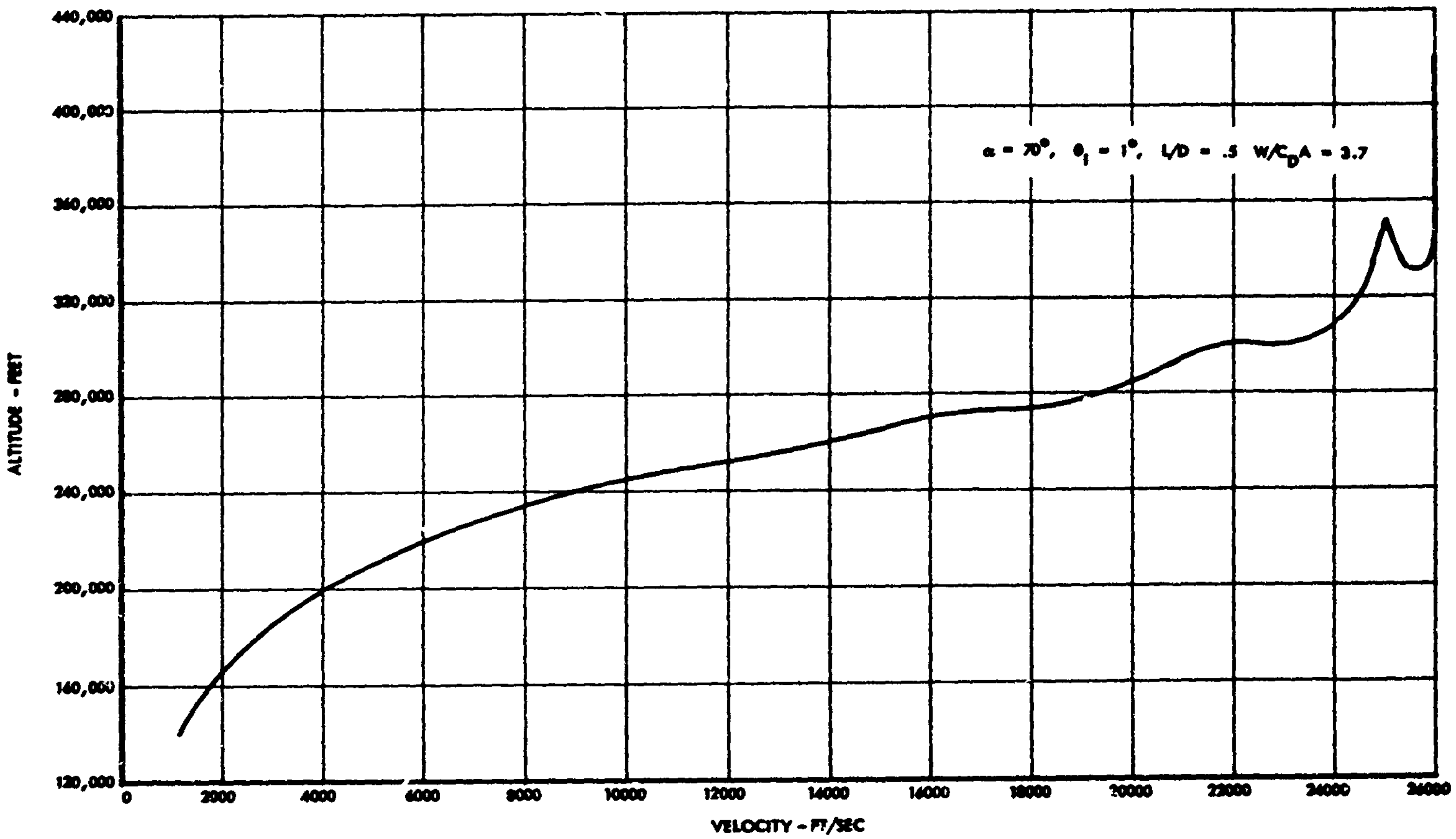

Figure 11. Re-Entry Trajectory - Altitude Versus Velocity

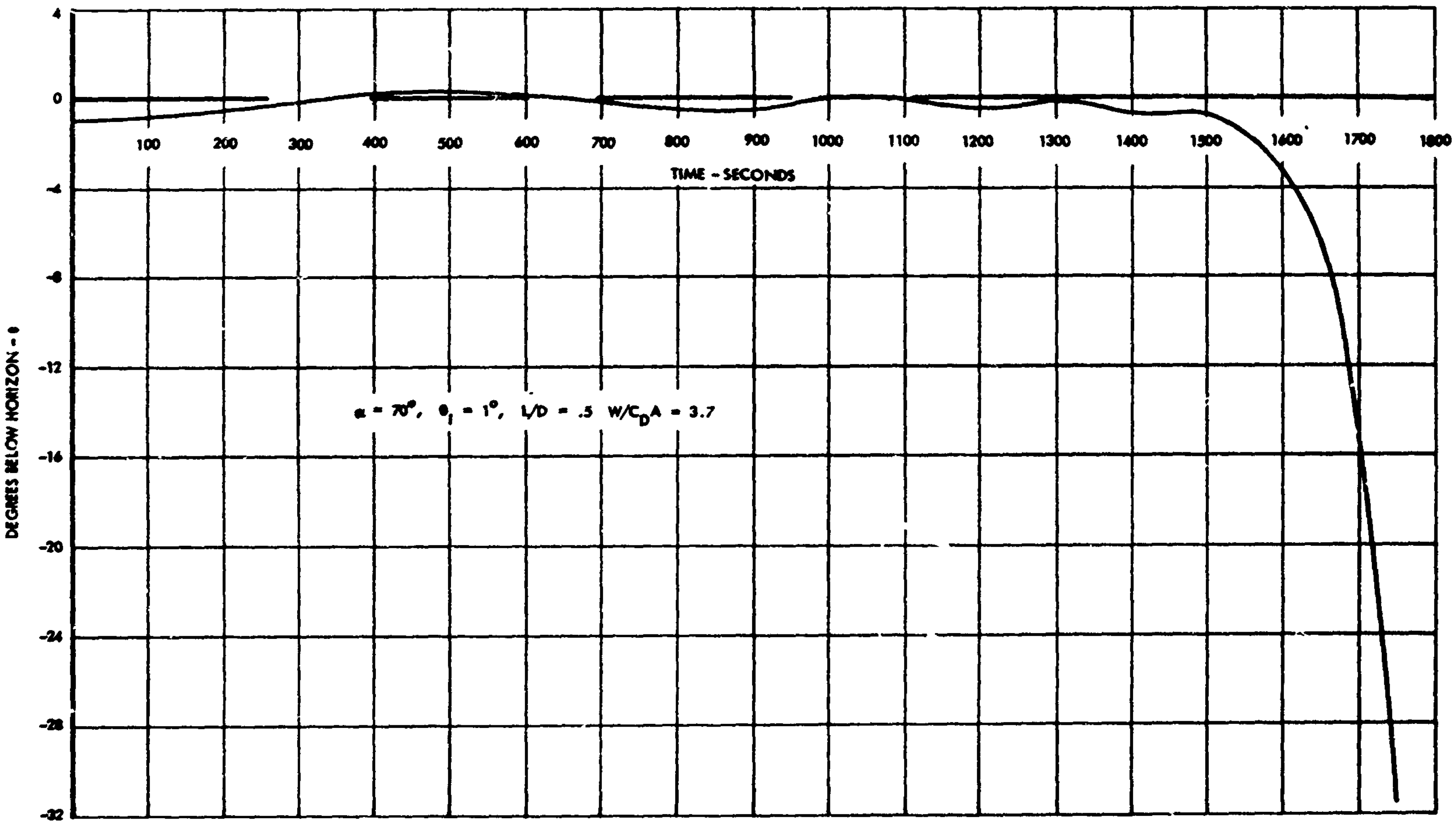

Figure 12. Glide Path Angle (θ) Time History

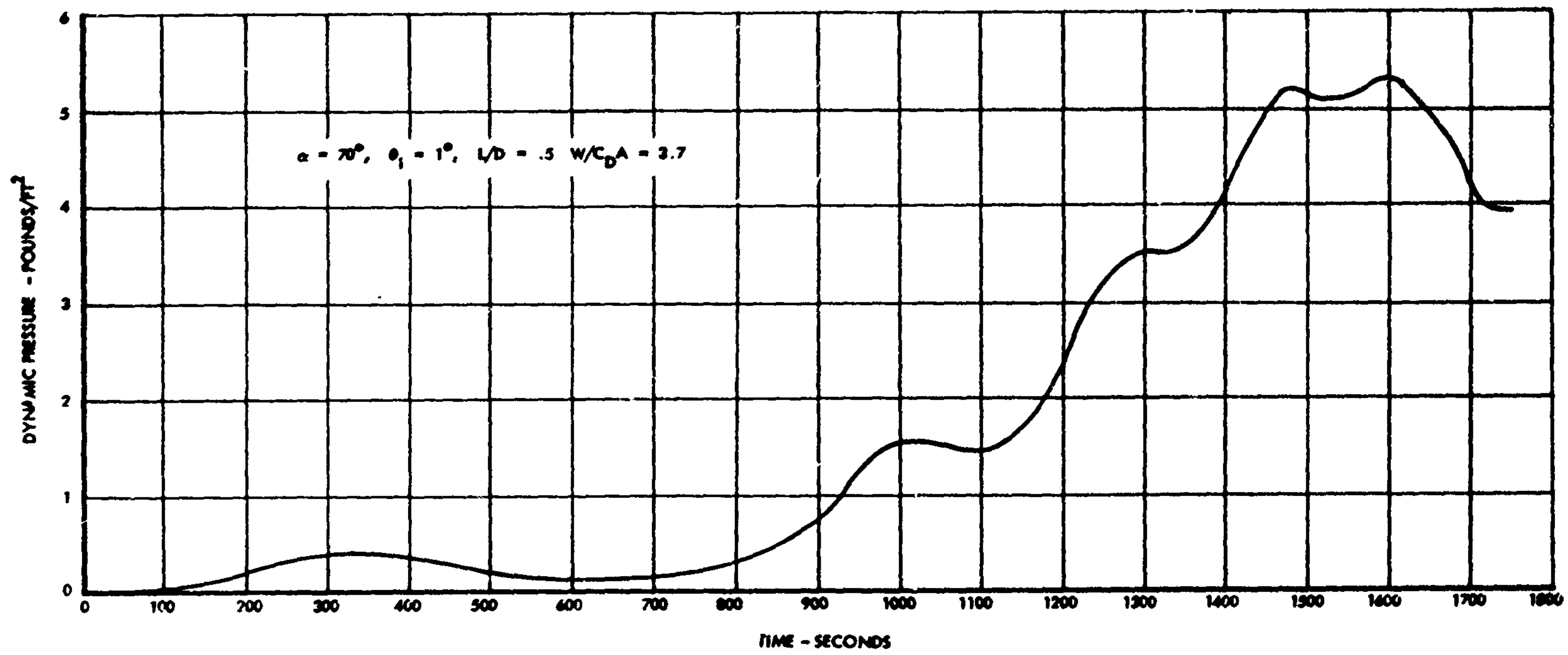

Figure 13. Dynamic Pressure (q) Time History

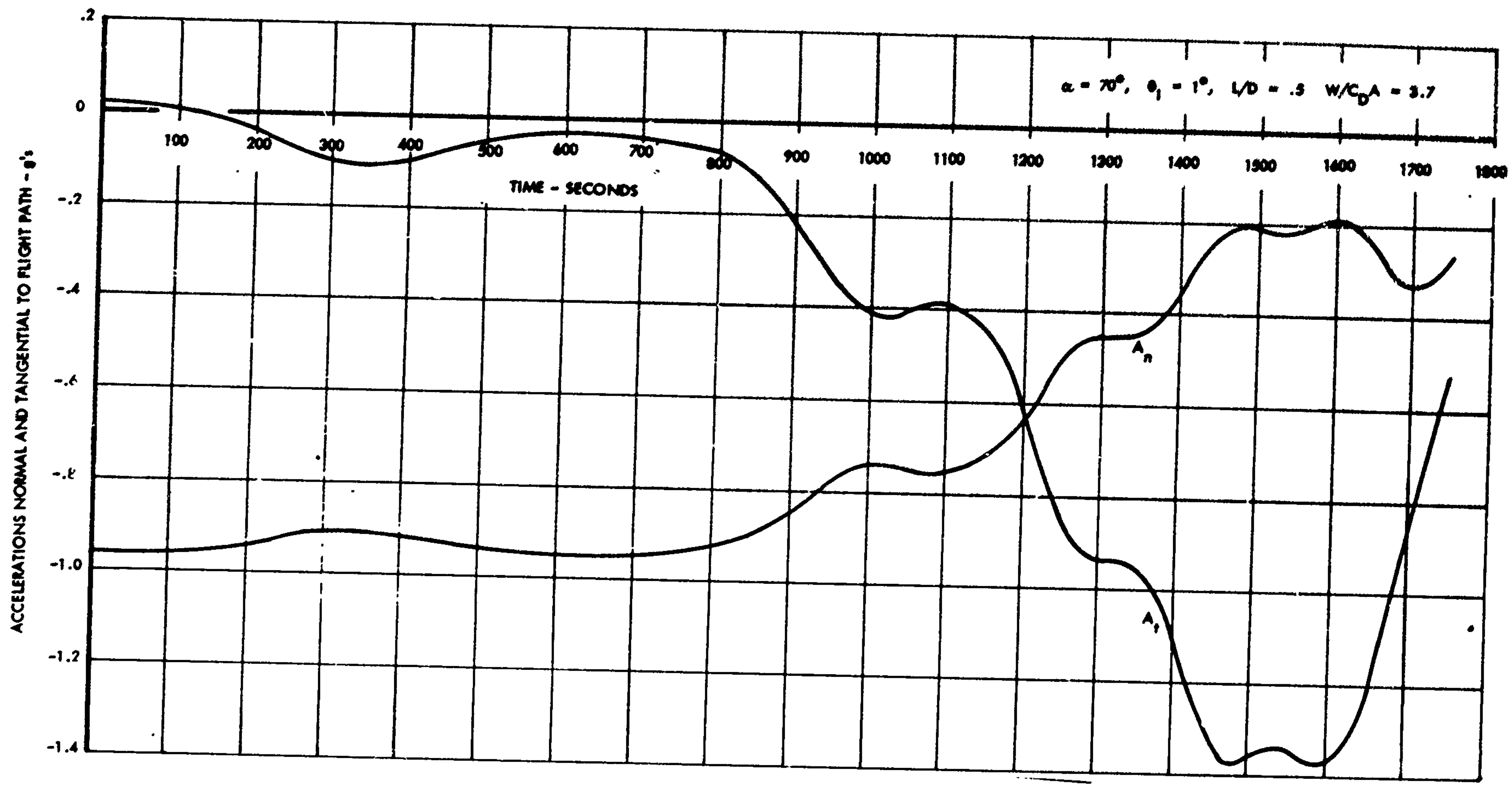

Figure 14. Acceleration Time History

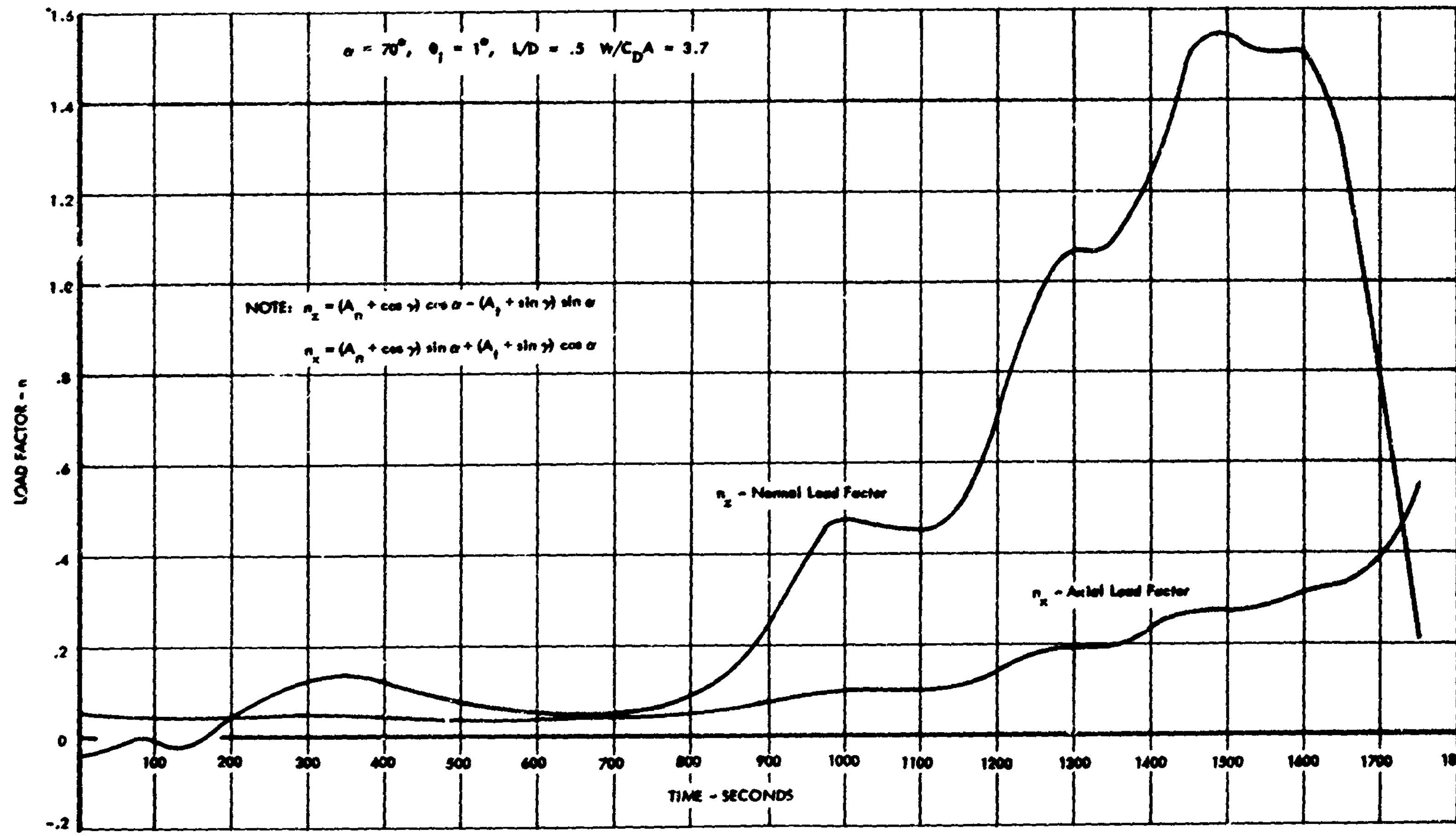

Figure 15. Normal and Axial Load Factors Time Histories

altitudes, however, the normal gust load factor, normal to the flight path, is given by the expression:

$$n_g = 1 + \frac{\rho (dc_z/d\alpha) \, Kuv}{2(W/S)} \tag{5}$$

Arbitrarily limiting the maximum permissible diving speed to 1.3 times the equilibrium gliding speed at the maximum lift-drag ratio:

$$v_{max} = 1.3 \sqrt{\frac{2(W/S)}{\rho \, C_L}} \tag{6}$$

Substituting this into the above expression, we have:

$$n_g = 1 + 1.3 \left(\frac{dC_z}{d\alpha}\right) (Ku) \sqrt{\frac{\rho}{2(W/S) C_L}} \tag{7}$$

The maximum gust load factor, therefore, occurs at sea level where the density (ρ) is a maximum and ($dC_z/d\alpha$) and (C_L) for maximum lift-drag ratio at subsonic speeds are 2.65 per radian and 0.6, respectively. The wing loading (W/S) = 3.57 and an "effective sharp-edged gust" velocity (Ku) of 30 ft/sec must be anticipated. Substituting these values into the above expressions, the maximum design gust load factor n_g = 5.85 and the maximum permissible indicated airspeed below 100,000 feet altitude should be established at 92 ft/sec, or 117 knots.

The gust load factor, n_z, normal to the paraglider keel, may be found from:

$$n_z = n_g \cos \alpha \approx 0.8 \, n_g \tag{8}$$

Therefore, the maximum normal gust load factor at sea level with a gust velocity of 30 ft/sec, is n_z = 4.68 g.

3.3 THERMODYNAMIC ANALYSIS

3.3.1 GENERAL CONSIDERATIONS

Thermodynamic analysis was undertaken to determine the effects of aerodynamic heating on the vehicle and establish the material requirements in terms of temperature resistance. Since the temperatures developed depend upon the heat capacity, thermal conductivity, emissivity, and other characteristics of the materials, the determination of temperatures and materials is necessarily iterative. Studies were performed to evaluate the nature of the temperature distribution at the apex and along and around the leading edge booms. Figures 16 and 17 illustrate heat flux relationships developed for the Space-General Micrometeorite Paraglider (NASA) which would also be applicable to the paraglider under consideration in this program since geometrical similarity exists.

Figure 16 shows the ratio of heat flux at any point on the stagnation line to the heat flux at the stagnation point on the apex as a function of distance along boom. The stagnation line is, in effect, the "leading edge" line along the outer booms of the vehicle. Due to the decrease in diameter of the tapered booms, it will be noted that the heat flux actually increases from fore to aft. At the aft end of the boom, the heat flux is actually greater than at the stagnation point on the apex, since the apex is much larger in diameter than the aft end of the boom. The heat flux along the boom also increases as the angle-of-attack increases, i.e., as the air approaches the leading element of a boom more perpendicularly.

Figure 17 illustrates the relationship of heat flux around the circumference of the boom to the heat flux at the stagnation line at a given cross-section as a function of the angle-of-departure from the stagnation line. It will be noted that the heat flux at 90° from the stagnation line is approximately 30 percent of the heat flux at the stagnation line. Therefore, the temperatures may be expected to fall off rapidly around the circumference of the boom from the hottest area.

Since the amount of material ablated is a function of the heat flux, optimization of vehicle weight may dictate a variation in thickness of ablated material around the periphery of the boom. It would be desirable to have the thickest material at the stagnation line with the material tapering to its thinnest cross-section 180° from the point of highest heat flux.

Basically, the temperature of the material is the result of the net heat stored which, in turn, is the difference between the heat gained and the heat lost. Since the heat transferred to the vehicle at any point on its surface increases from zero (at the time of retro-firing from orbit) to a maximum and then drops to a small value as subsonic velocity is approached, it is necessary to analyze the trajectories from the time of initial significant heating in order to account for the transient effects on heat storage. Basically, the heat stored may be illustrated by the following equation:

$$\underbrace{\int \rho_m c \, \delta \, d \, T_{av}}_{\text{heat stored}} = \underbrace{\int \dot{q} \, d t}_{\substack{\text{aero.} \\ \text{convect.}}} - \underbrace{\int \epsilon \sigma T_o^{\,4} \, d t}_{\text{reradiation}} - \underbrace{\int h_r (T_i - T_i') \, d t}_{\substack{\text{internal convect} \\ \text{and radiation}}} \qquad (9)$$

The above equation, although simplified, illustrates the following important points:

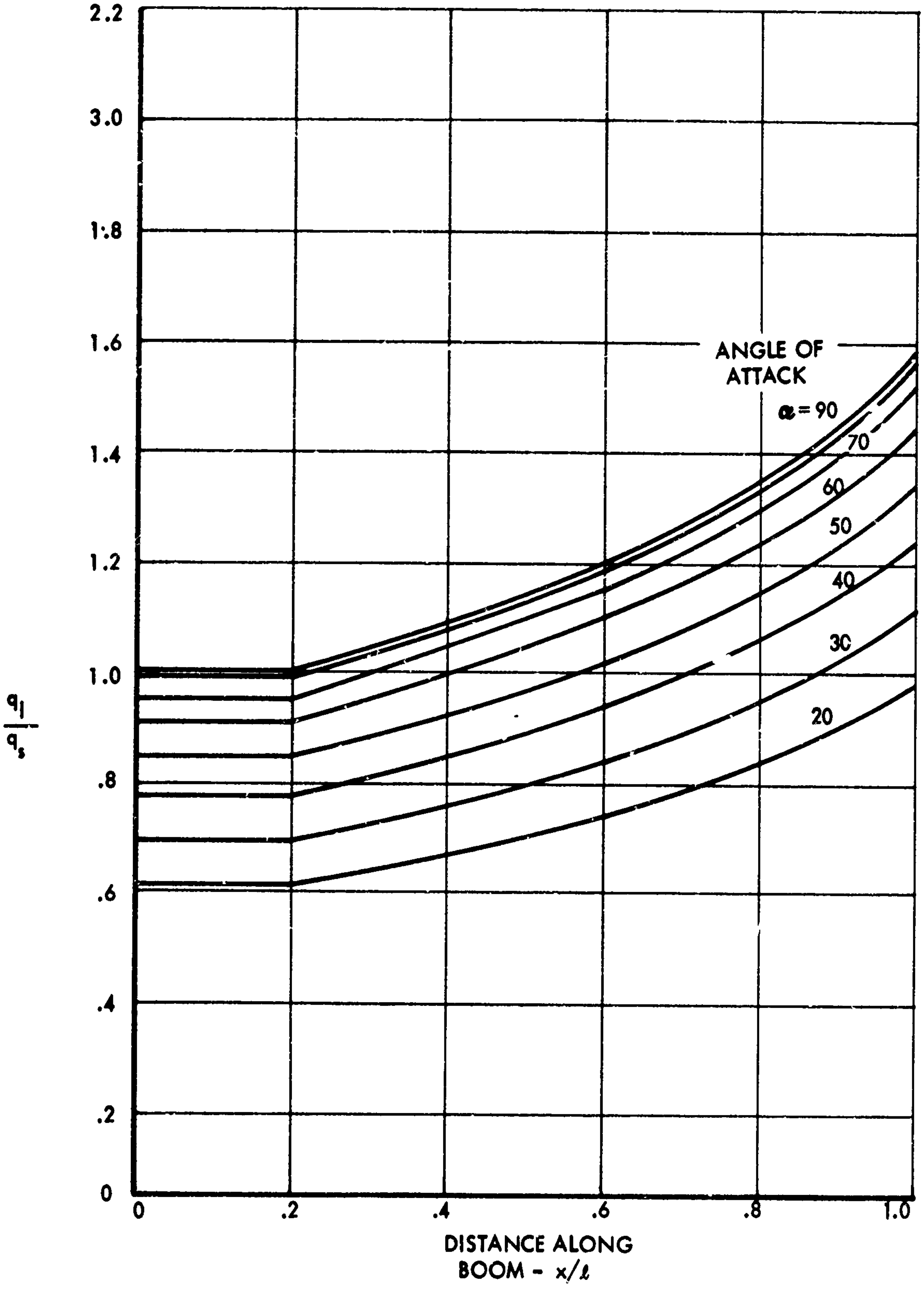

Figure 16. Heat Flux Versus Distance

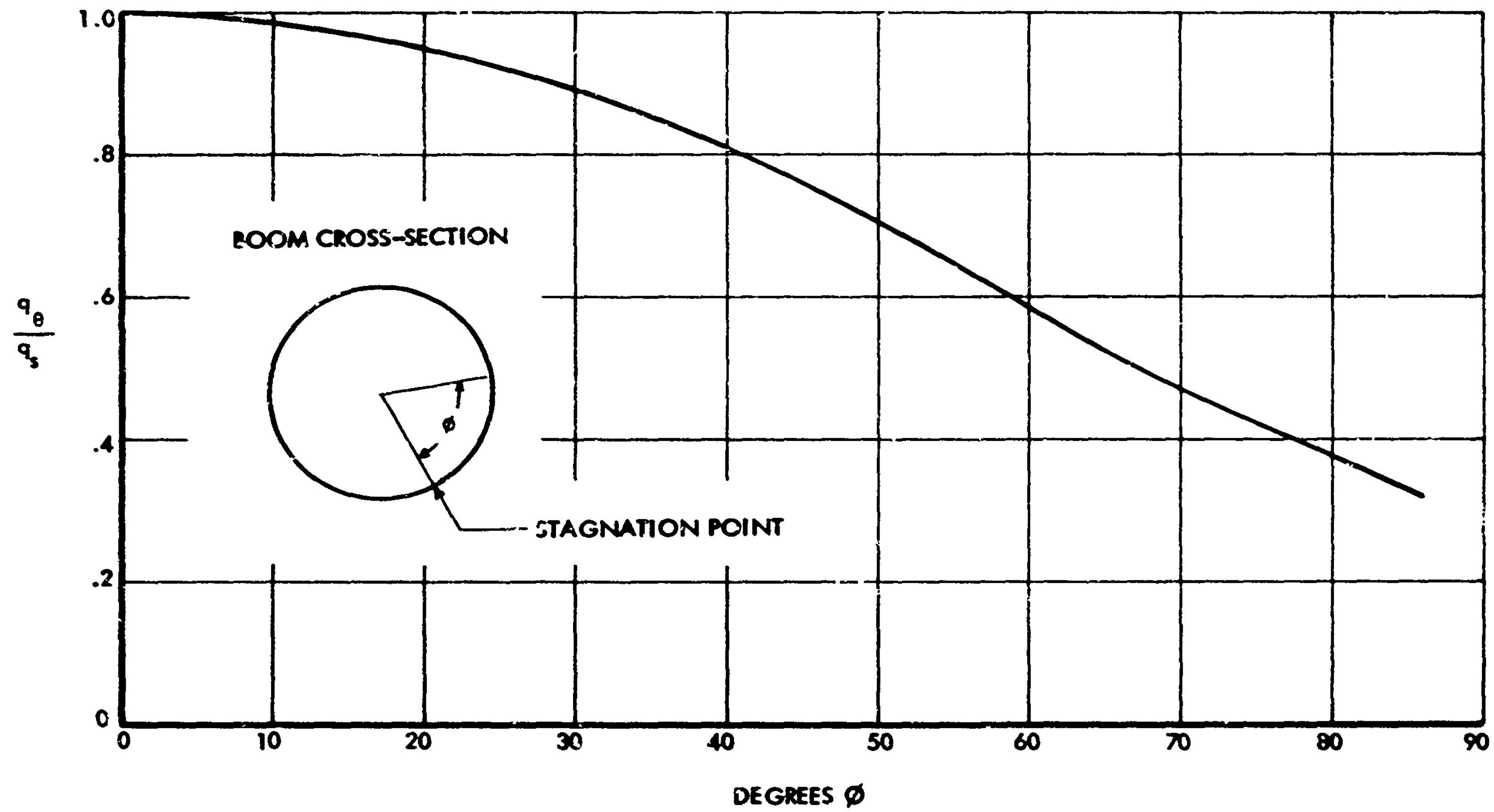

Figure 17. Heat Flux as a Function of Angle ϕ

a. The temperature of the material is a function of the aerodynamic convective heat flux.

b. Increasing the thickness, density or specific heat of the material will lower the temperature.

c. High re-radiative emissivities are desirable.

d. Internal convection to the pressurizing gas and radiation to other surfaces will decrease the temperature of the surface at the point under consideration. These effects must be considered with respect to increase of gas pressure and increase of temperature of the other surfaces, however.

Initial calculations performed manually indicated that stagnation point maximum material temperature would be nearly 2000°F while the material temperature at the stagnation line on the aft boom tip would reach 2100°F, provided that no ablation occurred.

Since the heat flux at the aft tip of the boom may be expected to be higher than the heat flux at the stagnation area on the apex, the ablation rate at the boom tip will be higher than at the apex, assuming similar construction. This leads to the conclusion that a rigid-nose ablation shield (e.g., phenolic reinforced linen) is no more important on the apex than it is on the boom tips. Since rigid ablation shields should be avoided (considering the flexible packaging requirements) it was reasonable to consider the possibility of using silicone rubber as the ablative material in both areas.

3.3.2 DIGITAL COMPUTER ANALYSIS

Space-General has developed an analytical heat transfer program, coded for the IBM 7090, which is an assembly of subprograms designed to solve the pertinent equations necessary to compute the heat transfer to the vehicle surface, the surface temperature, and internal heat conduction. The particular method used is an approximate procedure which calculates a pseudo-surface temperature in excess of the material melting temperature. This pseudo-temperature is expressed in terms of the heat of fusion and specific heat of the material at the melting temperature. The layers of material which are consumed by the pseudo-temperature formation are systematically accounted for and subtracted off. Up to 100 temperature (or ablation) planes can be handled.

To perform aerodynamic heating calculations, it was necessary to determine an effective heat of ablation in a form acceptable to the IBM 7090 computer program. The program uses a simplified step-wise procedure to allow for an ablating outside surface. The "effective heat of ablation" is converted to a pseudo-"melting" temperature, T_{psm}:

$$T_{psm} = \frac{Q_c^*}{c_p} + T_m \qquad (10)$$

where

Q_c^* is the corrected "effective heat of ablation" (Btu/lb)

c_p is the specific heat of the ablating material (Btu/lb^{o}F)

T_m is the melting temperature or the ablation temperature (^{o}F)

The heat of ablation, which is normally reported in the literature, is based on "cold wall" heat flux, $\dot{q}_{cw}$. Only a part of the cold wall heat flux (heat directed to the wall) actually contributes to the ablation or chemical degradation process. The rest of the cold wall heat flux is either reradiated from the hot surface or conducted and stored within the remaining matrix material. Some of the heat reaching the inner surface of the material is radiated or conducted away in the internal pressurizing gas of the inflated vehicle. All of these latter effects are taken into account in the computer heat transfer computations. It is, therefore, necessary to provide the computer with sufficient input such that it can utilize a true heat of ablation representing the actual endothermic effect of the chemical reaction. For design computations using this computer program, a value of Q_c^* is required which is defined as:

$$Q_c^* = \frac{\dot{q}_{pseu}}{\dot{m}} \qquad (11)$$

where

$\dot{q}_{pseu}$ is a pseudo-heat flux which not only includes the chemical degradation energy consumed, but permits the computer to calculate the correct ablation rate

$\dot{m}$ is mass ablation rate.

For materials which form char layers, the temperature of the surface of the char may be hundreds of degrees higher than the "melting" or ablation temperature at the point where the basic material turns into char. Because the computer program uses the "melting temperature", T_m, for calculating aerodynamic convection to the surface, radiation from the surface, and conduction into the material, it is necessary to correct the value of Q_c^* to account for the difference between the char temperature and the "melting temperature." Thus, in Equation (11)

$$\dot{q}_{pseu} = \dot{q}_{chem} + \Delta\dot{q}_{conv.} + \Delta\dot{q}_{rad.} \qquad (12)$$

where

$\dot{q}_{chem}$ is the heat flux which actually contributes to chemical reaction (ablation)

$\Delta\dot{q}_{conv.}$ is the difference between convection to a surface at the char temperature and a surface at the melting temperature, thus

$$\Delta\dot{q}_{conv.} = \left[\dot{q}_{conv}\right]_{T_m} - \left[\dot{q}_{conv}\right]_{T_{char}} \qquad (13)$$

$\Delta\dot{q}_{rad}$ is the difference between the radiation from a surface at the char temperature and a surface at the melting temperature, thus

$$\Delta\dot{q}_{rad} = \left[\dot{q}_{rad}\right]_{T_{char}} - \left[\dot{q}_{rad}\right]_{T_m} \qquad (14)$$

Because of the difficulty in evaluating $\dot{q}_{chem}$ and because the correction $\Delta\dot{q}_{rad}$ tends to overshadow the remaining terms, the value of $\Delta\dot{q}_{rad}$ plus an arbitrary percentage of $\dot{q}_{cw}$ were used to evaluate the corrected effective heat of ablation.

To evaluate the ablation temperature, the variation with time of the interior temperature of the test specimen, during plasma arc testing was recorded. Knowing the location of a thermocouple and the measured ablation rate, the time at which the ablating zone reached the thermocouple was determined. The temperature corresponding to this time was established as the "ablation temperature."

3.3.3 RESULTS OF ABLATION STUDIES

A number of trajectories were thermodynamically analyzed using the heat transfer program described in Section 3.3.2. These trajectory investigations utilized a range of input variables. Values of lift-to-drag ratio from 0.5 to 1.0 at various angles-of-attack, as described in Section 3.2.2, were investigated.

Early computer runs indicated that as much as one-half inch of silicone rubber would ablate with re-entry angles as great as -2°. Final sub-optimized matching of material thicknesses and re-entry trajectory characteristics resulted in the use of a rather flat or nose-up angle-of-attack of 70°. This, coupled with a -1° re-entry angle and a corresponding lift-to-drag ratio of 0.5, defines the trajectory which was selected.

Ablation data obtained from air-arc plasma testing was used to determine the rate of ablation under various heat fluxes. This investigation is discussed in Section 3.6.1.2.

The results of the thermodynamic analyses are shown in Figure 18 for silicone rubber S-6510 manufactured by Dow Corning. A similar plot was prepared for silicone rubber Y-3350 manufactured for Union Carbide and showed slightly greater quantities of material ablated.

Assuming that a metal fabric or a wire cloth is used as a structural reinforcing material (Figure 18) indications are that the maximum metal fabric temperature would be about 920°F, with an average metal fabric temperature of about 870°F. The total ablation thickness of S-6510 is 0.074 inches.

3.3.4 HEATING EFFECTS ON WING MEMBRANES

Although it was not intended that the wing membranes of the paraglider would be the subject of major design effort in this program, an analysis was undertaken to determine the heat transfer to the wing membranes. Although a 70° angle-of-attack permits significant acceleration in the low-density upper atmosphere, thus alleviating the extreme heating which would otherwise occur for a fast entry penetrating deep into the atmosphere, the high angle-of-attack creates greater heating effects on the wing membranes.

Since the maximum chord-wise wing element makes an angle of 20° with the axial plane of the booms, a nominal 70° body angle-of-attack will cause the wing membranes to have a maximum angle-of-attack to the air stream of about 50°.

Based on laminar flow with a maximum free-stream Reynolds number of approximately 35,000 (Reference 3), negligible mass transfer, negligible heat capacity with a surface emissivity of 0.8, and disassociated air in chemical equilibrium, and if shock-shock or shock-boundary layer interactions are neglected, the maximum aerodynamic convective heat flux is only 1.87 Btu/ft^2 sec with a radiation equilibrium temperature of 1040°F.

Since the effects of shock interaction was expected to be significant on the concave wing surfaces, Space-General conducted an auxiliary investigation in support of this contract, using Space-General research and development funds, to obtain empirical data.

Rhodes and Bloxsom, an applied physics research concern in Canoga Park, California, offered to run "hot-shot tunnel" model tests on a paraglider model supplied by Space-General. The model is shown in Figures 19 and 20. The model has a 10-inch span and is similar in configuration to the paraglider designed in this program.

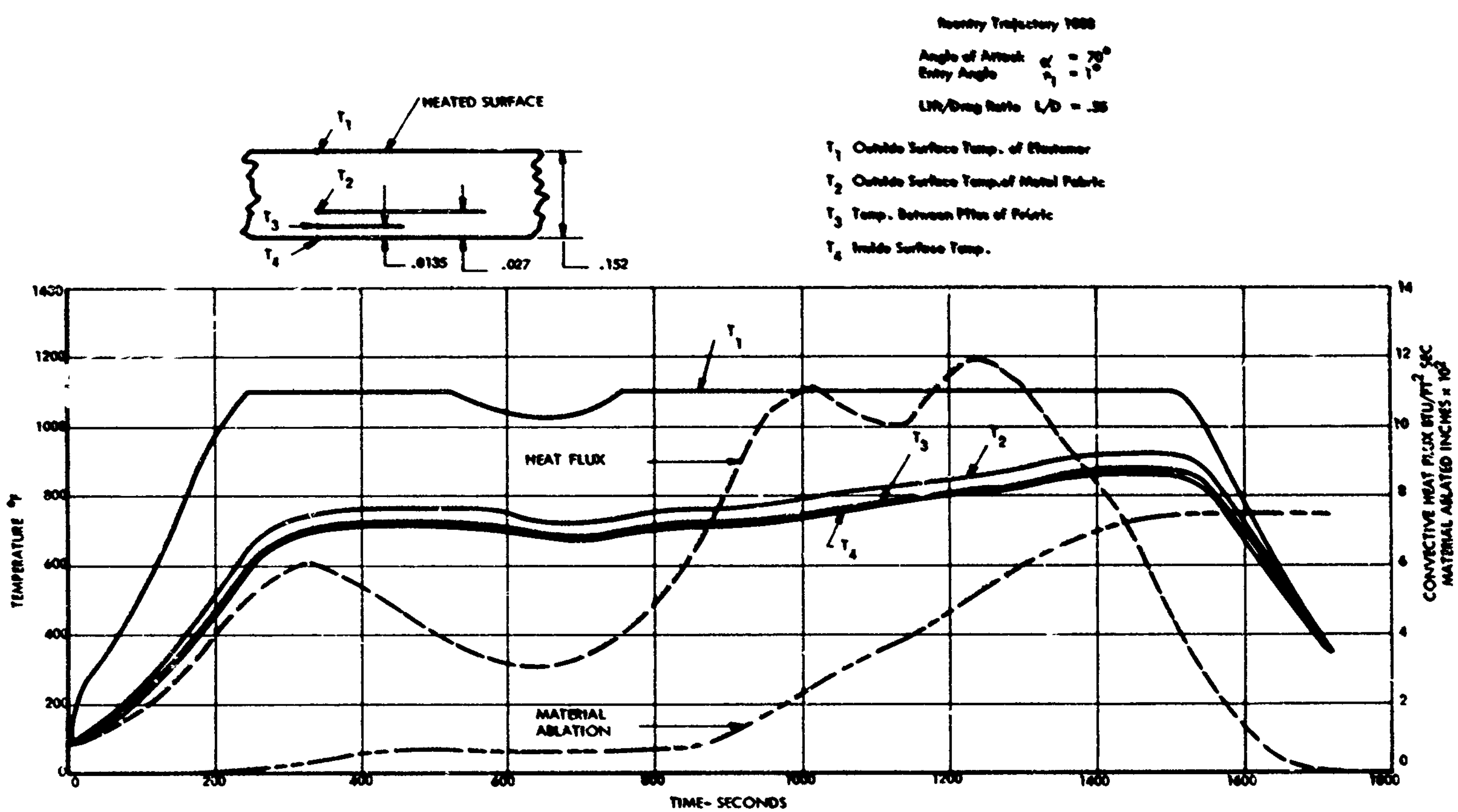

Figure 18. Project FIRST Paraglider Heating History at Tip of Leading Edge Boom for S-6510

4383/001

Figure 19. Space-General Paraglider Model

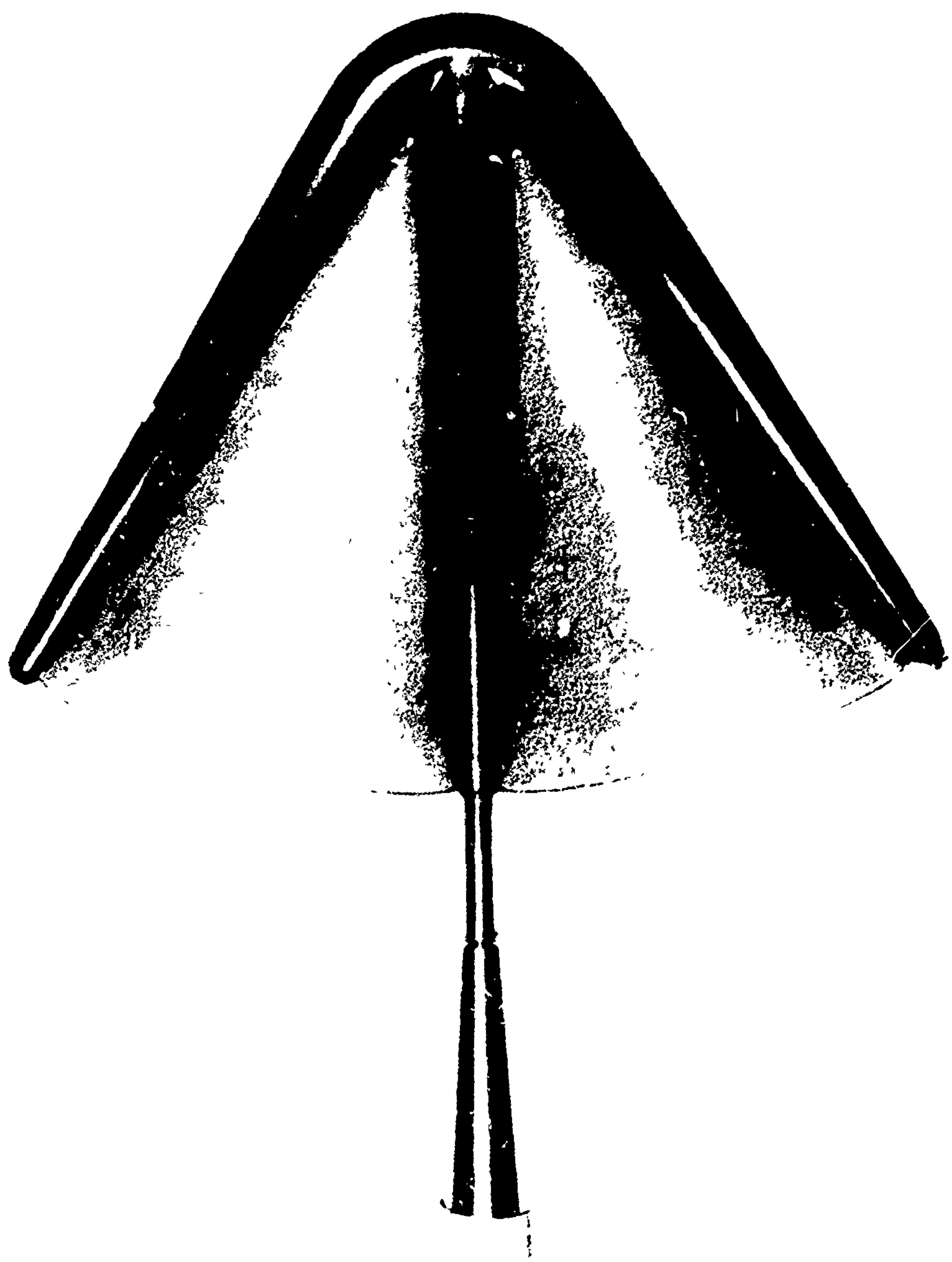

4383/002

Figure 20. Space-General Paraglider Model

The 60-inch diameter tunnel at Rhodes and Bloxsom uses a capacitor arc discharge to produce high-temperature, high-pressure, hypersonic flow with stagnation temperatures from 2500 to 16,000°K, Mach numbers up to 60, and Reynolds numbers from 30 to 10^7. The model was painted with a special temperature sensitive paint. Subjecting the model to shock tunnel environment causes different areas on the model to experience different temperature and heating effects. This affects the transparency of the paint film. After testing, the model appears to be covered with a series of colored rainbow-like areas which are indicative of the surface temperatures attained.

A calibration sphere is run into the tunnel concurrent with the model test. Using Lee's theory of blunt body heat transfer, the distribution of heating on the calibration sphere is known. Knowing the ratio of actual heat flux to stagnation heat flux at any point on the calibration sphere, the lines of constant heat flux ratio on the model can be determined by color matching of the model areas with areas on the sphere. The ratio of stagnation heat flux on the sphere to the stagnation heat flux on the model is inversely proportional to the square root of the relative radii. A photograph of the model mounted in the test chamber is shown in Figure 21. Figure 22 shows two successive frames taken with a Fastax camera at 5500 frames per second. The view is looking up on the under surface of the model and forward. The calibration sphere is seen above the model. The luminous shock impingement with the wing membrane is apparent not only in these photos but on the model paint surface.

The test conditions were selected to coincide with a trajectory point that produced the highest heat flux. This condition (as may be noted from Figures 9, 10, and 18 corresponds to an altitude of 280,000 feet with a velocity of 19,000 fps, Reynolds number equal to 24,400 and enthalpy of 1.8×10^8 ft^2/sec^2.

Because hot-shot tunnel experience indicated that the heating phenomena were most critical for a 45° angle-of-attack, Rhodes and Bloxsom elected to test the model so that the flow stream made a 45° angle with the uppermost element of the semi-conical wing, which corresponded to a 61° angle-of-attack to the keel boom centerline. Therefore, the air stream angle-of-attack was nearly as great as that developed for the proposed actual paraglider during re-entry.

The flight conditions in the tunnel did not exactly match those expected during proposed re-entry in that the Mach number obtained in the tunnel was 15.2 whereas the velocity of the paraglider at 280,000 feet is approximately Mach 23. Experience with the tunnel had indicated, however, that variation of the velocity above Mach 10 was not critical for this type of test. Actual conditions during the tunnel test were as follows:

Area ratio: 780
Enthalpy: 1.8×10^8 ft^2/sec^2
Length of Model: 0.716 feet
Stagnation temperature: 7300°K

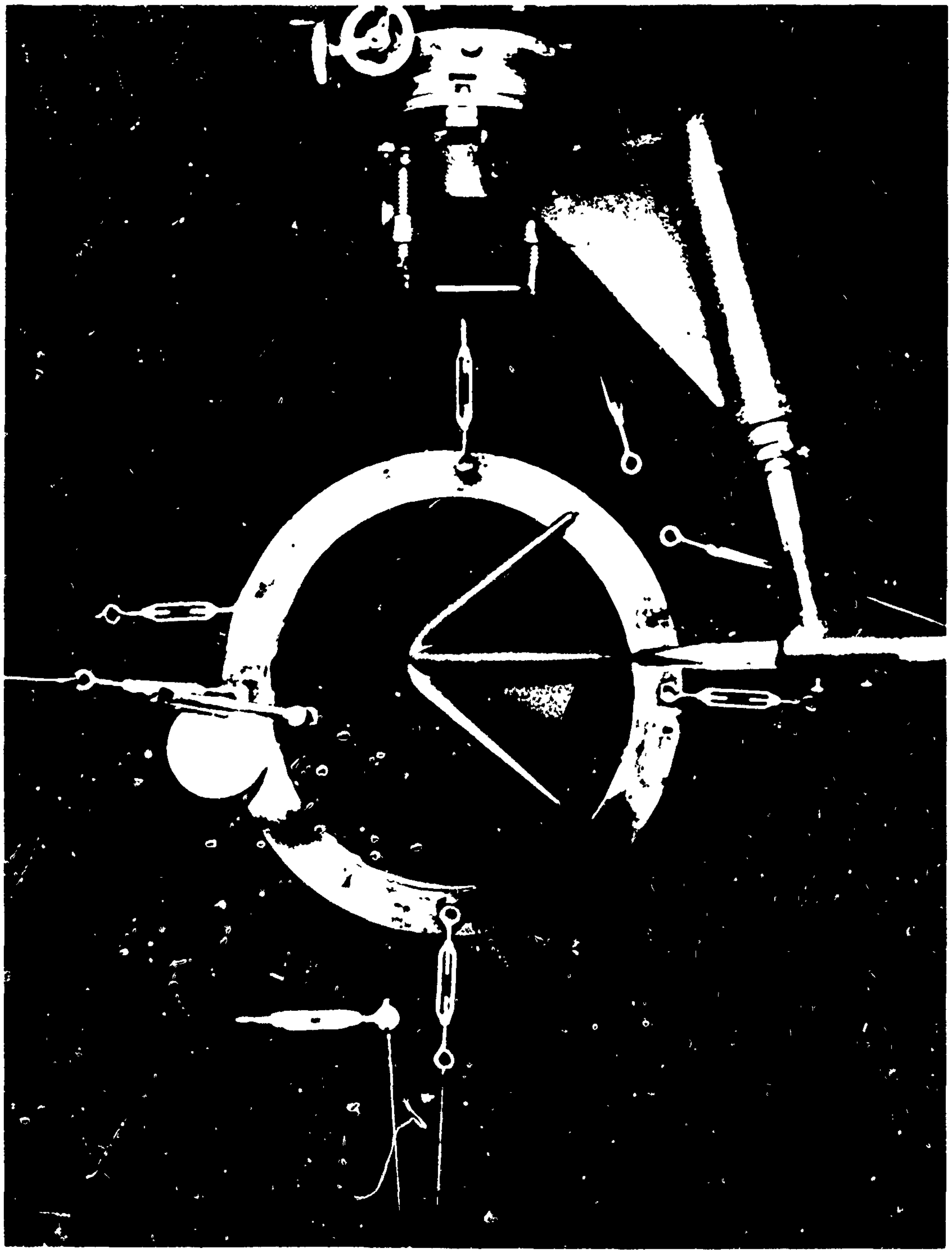

4383/002A

Figure 21. Top View of Model Installed in Test Chamber

This figure shows two successive frames taken with a Fastax camera at 5500 frames per sec. The view is looking up (on the under surface of the model) and forward. The calibration sphere is seen above the model. The luminous shock impingement with the wing membrane is seen clearly in these photos and on the model paint.

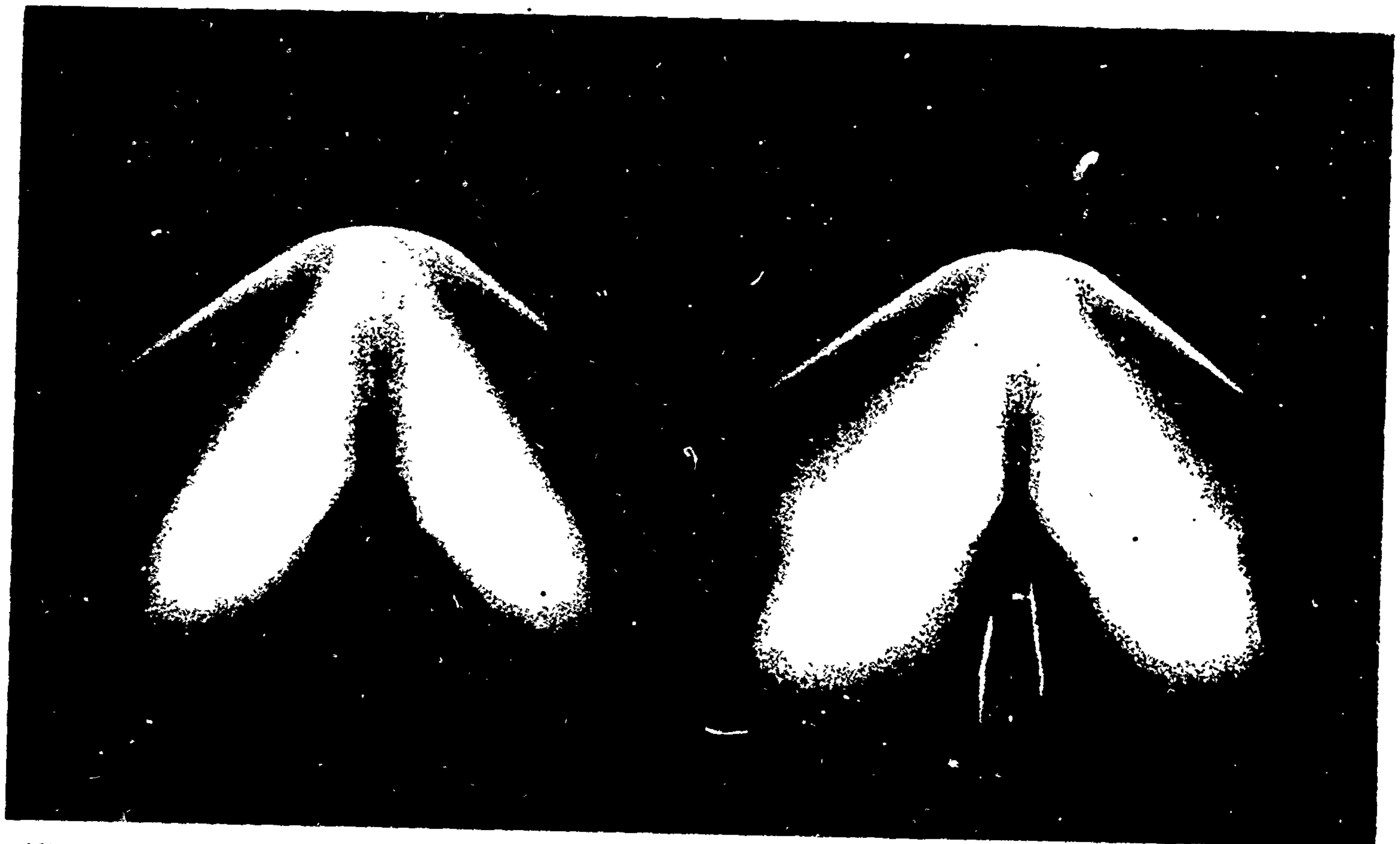

4383/001A

Figure 22. Paraglider Model Thermal Tests, Mach 15.2

Stagnation pressure: 21.5 atmospheric
Z 1.33, effective gamma for frozen flow: 1.50
Density in stagnation chamber: 0.778 x 10^{-3} gm/cm^3
Mach Number: 15.2
Static temperature: 124°K
Static density: 2.35 + 10^{-7} gm/cm^3
Reynolds number based on length and free stream: 24,400

The heat transfer data taken from the test model is plotted on the developed surface map of the lower surface of one of the paraglider wings, as shown in Figure 23. The lettered contour lines correspond to surface element lines as coded in Figure 24.

The numbers in parentheses in Figure 23 are color-calibration code numbers. Code number 1.0, corrected for full-scale conditions, corresponds to 5.62 Btu/ft^2 sec. The number preceding the code numbers is the corresponding heat transfer rate for the full-scale vehicle at the specified flight conditions (h = 280,000 ft, v = 19,000 fps). The stagnation point surface color code number at the apex equals 1.9; the temperature increase along the boom "stagnation lines" to 2.2 is due to the small diameter of the boom at the aft end.

Normal flat-plate theory would indicate that the temperatures at line "N" would be approximately 30 percent of the apex stagnation point. However, due to the shock interaction with the boundary layer, the temperature on the model at line "N" is 84 percent of apex stagnation temperature. The surface temperatures on an actual vehicle depend on the materials of construction.

Although local hot spots (with temperature levels several times higher than stagnation temperatures) were anticipated, heating rates actually experienced during the test were much lower than expected. As a result, the high-temperature paint used did not go through the typical rainbow spectrum of colors but did show obvious color changes in shades of grey, blue, and silver.

The test indicated that the maximum shock-interference temperatures would occur on the trailing edge of the uppermost element of the wing membrane. While the test predicts a maximum heat flux at the trailing edge of the uppermost element of the semi-conical wing of 9.0 Btu/ft^2 sec, it also predicts a maximum heat flux at the aft boom tip of 12.4 Btu/ft^2 sec. As may be noted from Figure 18, the maximum heat flux predicted for the proposed paraglider in the computer trajectory analysis is 12 Btu/ft^2 sec, at the aft boom tip. Although this is an excellent agreement, the test data cannot be compared directly with the Space-General calculations on the proposed paraglider because the latter assumed an ablating surface material. The test indicated, however, that the heat flux at the wing trailing edge may be four to five times greater than predicted by calculations which neglected shock interaction.

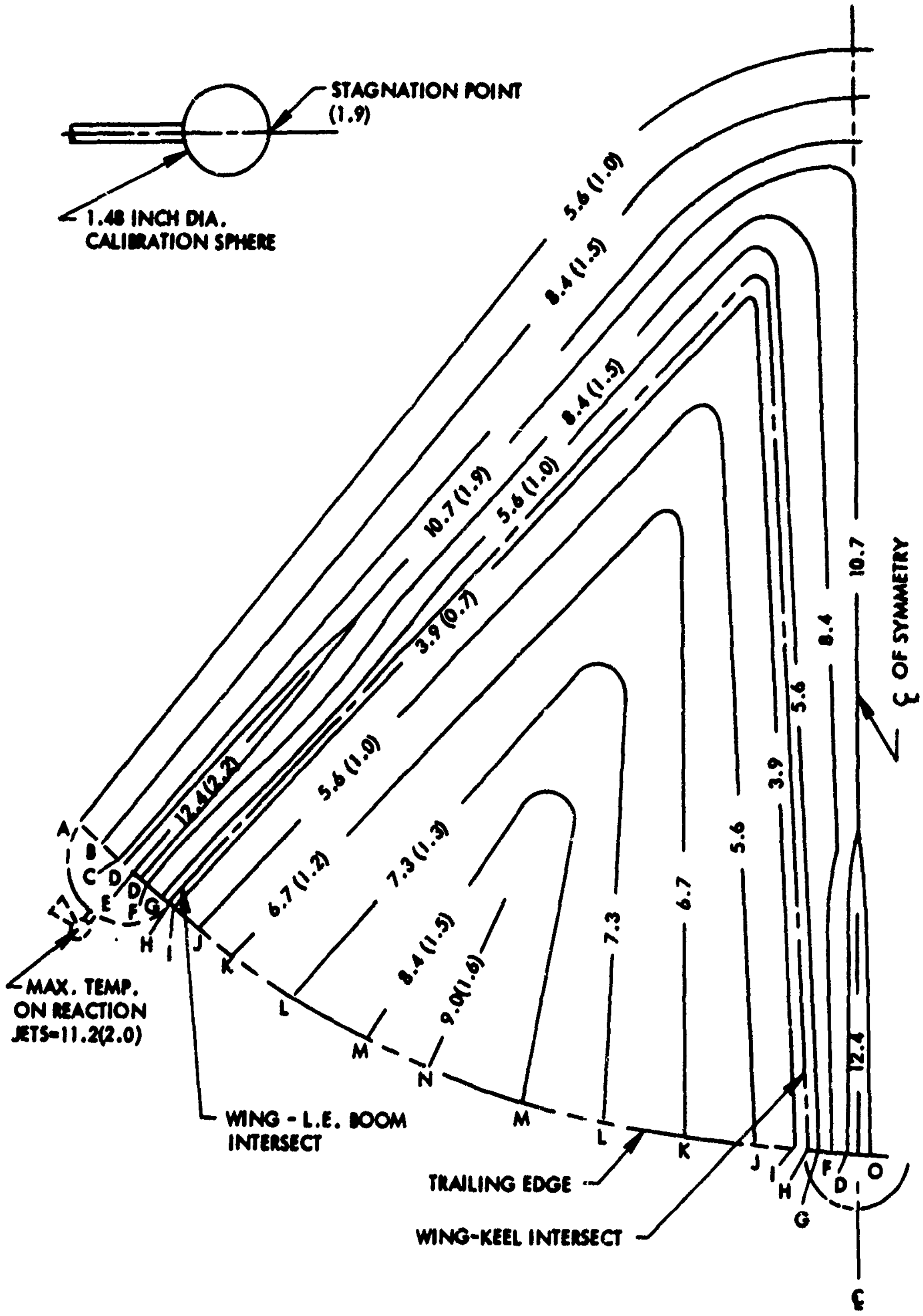

Figure 23. Heat Transfer Rate Contour Map

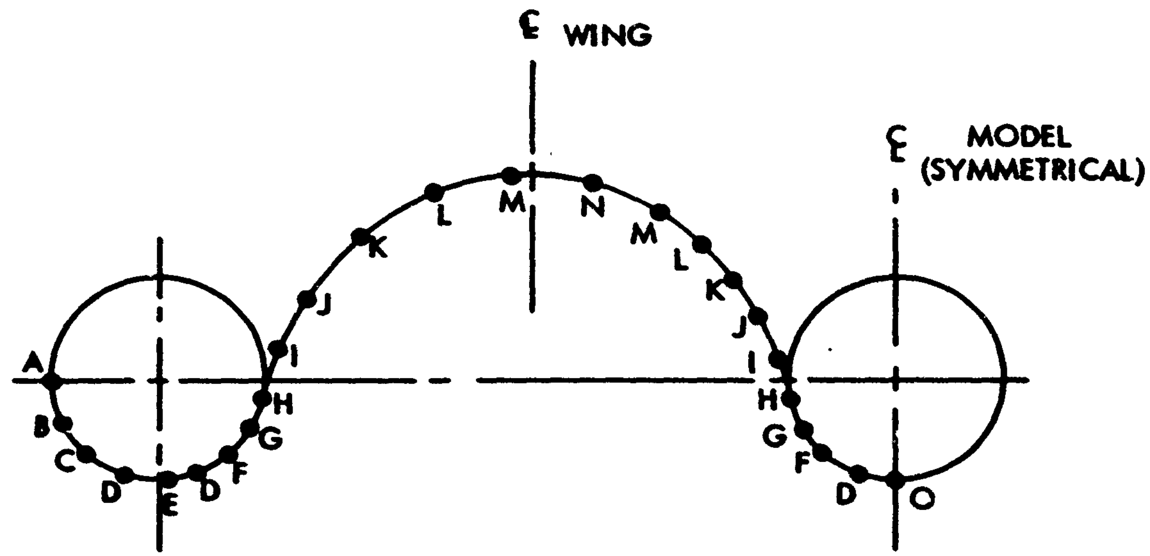

Figure 24. Test Model Heat Transfer Rate Contours

Conclusions drawn from these tests were as follows:

a. Shock interactions must be considered in evaluating the heating and temperature of the wing membrane.

b. For the proposed configuration, the wing membrane should remain somewhat cooler with considerably less ablation than the underside of the boom and apex structure.

c. Shallow concave surface defects on the model did not produce high local heating as might be expected.

d. The particular configuration chosen for the proposed paraglider shows much lower heating effects than anticipated as based on previous experience with other models at similar conditions.

e. Caution should be exercised in using this empirical data in that flight perturbations, such as small angles of yaw, usually increase shock-interaction heating effects. Also, other points on the trajectory may show higher local heating rates, although the point tested is predicted to be the most critical.

3.4 STRUCTURAL ANALYSIS

3.4.1 GENERAL CONSIDERATIONS

Pressurization of inflatable sections provides structural stability during bending and column loading. By utilizing internal pressure to maintain a tensile stress equal to or greater than the applied compression stress, buckling is prevented and deflections are kept small such that they are a direct function of the modulus of elasticity. Similarly, shear compression buckling may be prevented by pressure stabilization.

It is desirable to keep shear stresses small since the shear modulus of the fabric-elastomer composites being considered is low. Factors which enhance flexibility for compact packaging may result in low shear modulus. In the apex area of a paraglider vehicle the shear modulus becomes a major consideration. Deceleration inertia of the keel is reacted by aerodynamic loads on the wings and booms. The aerodynamic loads transferred to the boom must be carried around the apex to the keel resulting in significant shear stresses in the apex area.

3.4.2 BOOM LOADS

Based on the maximum aerodynamic load factors determined for the proposed trajectory (Section 3.2.4) the air loads normal to the plane of the vehicle were computed (see Figure 25) in which spanwise load distribution is shown for various longitudinal keel stations. For this purpose a wing membrane-to-boom attachment angle of 73° was used.

The horizontal and vertical components of the air load directly on the boom were determined from the boom air loads of Figure 25 and a maximum dynamic pressure (q) of 5.3 lbs/ft^2. The components of boom loading due to membrane and direct air loads are shown in Figures 26 and 27.

The inertial loads based on a boom weight of 42.3 pounds and a maximum acceleration of 1.54 g's are shown in Figure 28. The assumption of boom weight was made early in the program before the exact mass of the materials of construction was known. It is now known that the boom, as eventually constructed in this program, weighed about 100 pounds. However, optimizing some of the ablative coating thicknesses and eliminating reinforcement required for test mounting would reduce the weight to about 85 pounds total. After ablation, the estimated weight would be about 75 pounds. Furthermore, both plies of all the 2-ply structures constructed in this program were of the same metal fabric, whereas it would be possible to optimize the weight of the structure by making the inner bias ply of a lighter weight fabric. This would reduce the weight approximately another 10 pounds, to about 65 pounds total. Considering the fact that the inertial loads assumed during early structural analysis were too low and that they are of the opposite sign to the air loads, the resulting combined loads utilized for design and testing of the boom would be conservatively high.

The inertial loads attributable to the wing membrane are also shown in Figure 28.

Finally, the combined boom loads for vertical and horizontal components are presented in Figure 29.

From the above figure, the shear loads may be computed using the following formula:

$$V = \sum_{n=0}^{1} F_{n_T} \Delta \ell \qquad (15)$$

where

n = Station No. as a function of boom length, i.e., x/ℓ

F_{n_T} = Mean combined unit load over station n

$\Delta\ell$ = Length over which mean combined load is assumed to act.

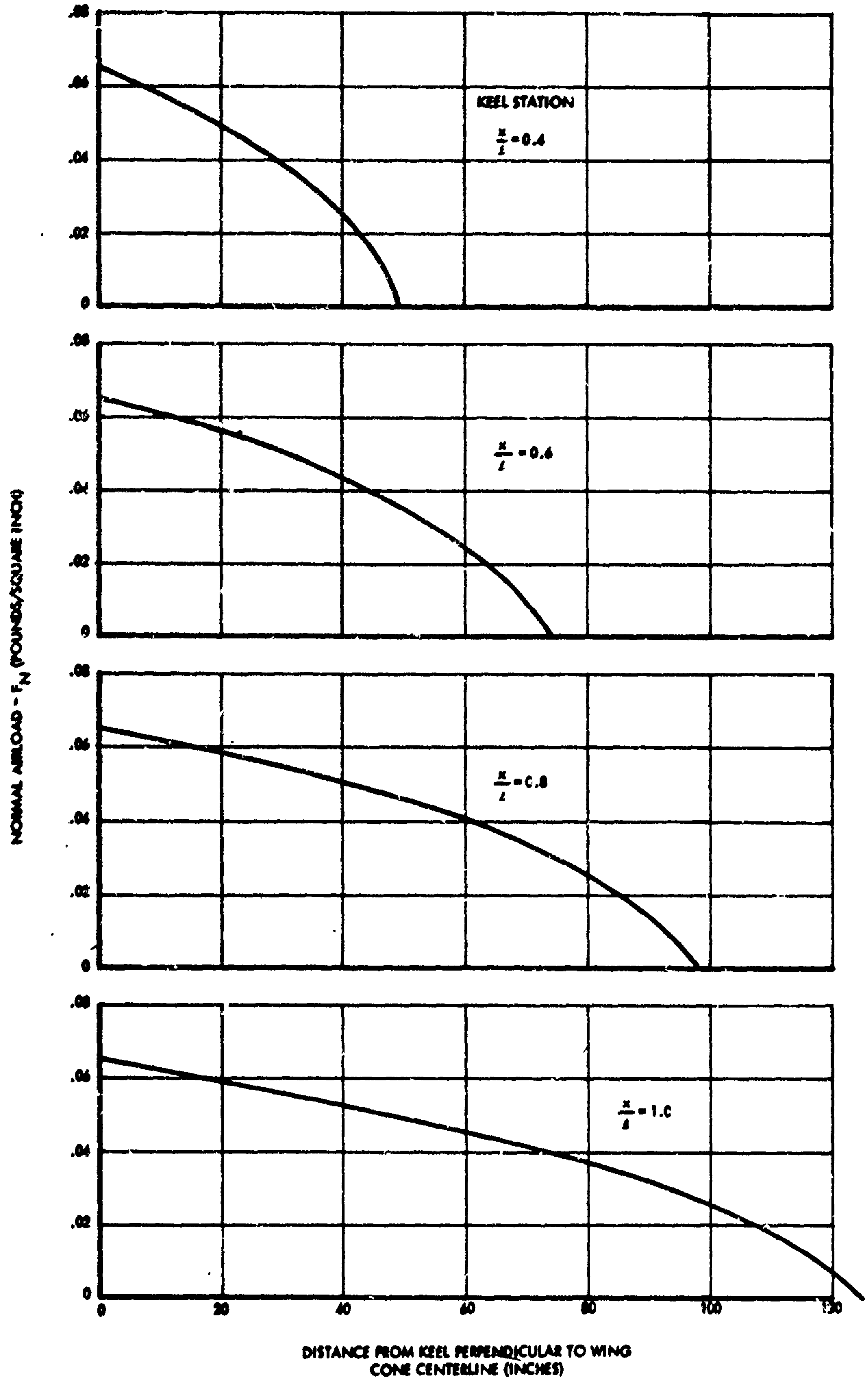

Figure 25. Membrane Normal (Vertical) Airloads Skewed Spanwise Distribution

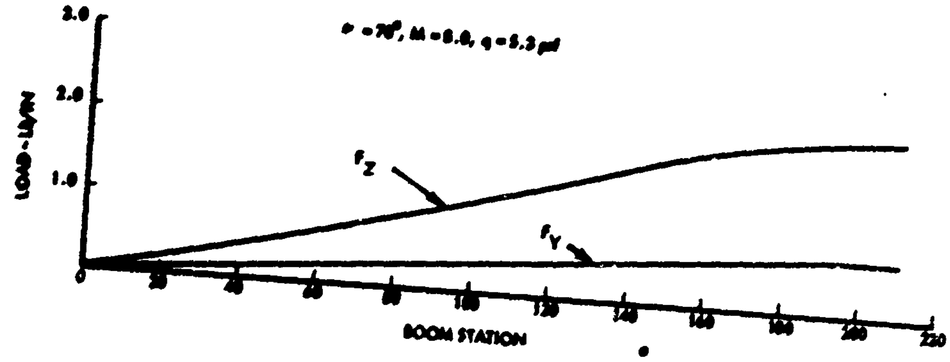

Figure 26. Boom Loading Due to Membrane Airloads

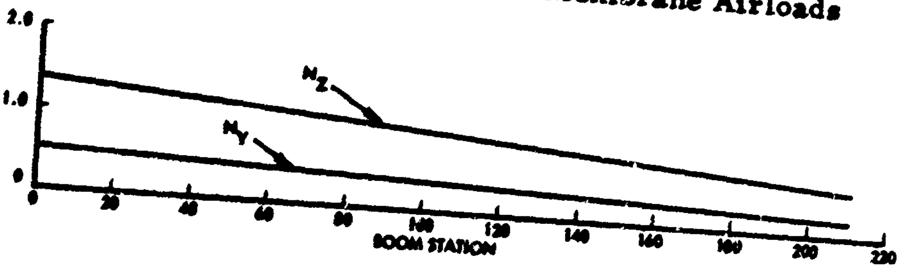

Figure 27. Boom Loading Due to Direct Airloads

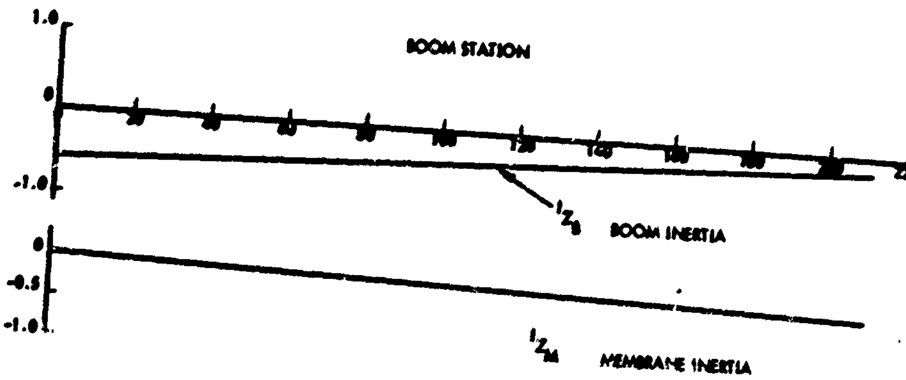

Figure 28. Loading Due to Inertia (1.54 g's)

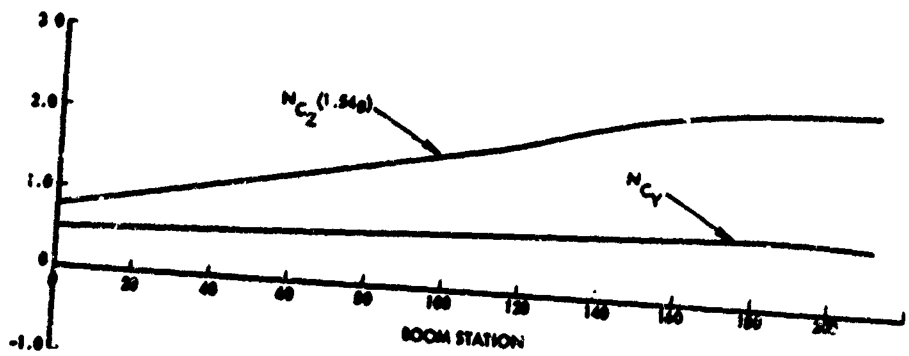

Figure 29. Combined Boom Loads (1.54 g's)

Therefore, the boom horizontal shear load is: $V_{y_o} = 146.7$ pounds and boom vertical shear load is: $V_{z_o} = 307.7$ pounds.

The resultant shear load and angle with the plane of the vehicle are as follows:

$$R = \sqrt{\Sigma N_{cz}^2 + \Sigma N_{cy}^2} = \sqrt{(307.7)^2 + (146.7)^2} \tag{16}$$
$$= 340 \text{ pounds}$$

$$\theta = \tan^{-1} \frac{146.7}{307.7} = 25^\circ\ 30' \tag{17}$$

To account for the membrane axial (drag) load acting on the boom, it may be conservatively assumed that one-half of the 100-pound axial load (in accordance with Figure 30), or 50 pounds, is reacted by one boom:

$$\phi = \tan^{-1} \frac{50}{340} = 8^\circ\ 22' \tag{18}$$

This is a resultant angle from the vertical from which a concentrated load would have to be applied to the boom to simulate the drag effect.

Vertical and horizontal bending moments may also be computed from the data in Figure 29. The total horizontal moment, M_x, equals 16,925 inch-pounds, the vertical moment, M_z, equals 39,075 inch-pounds, and the resultant moment, M_R, equals 42,500 inch-pounds.

Integrating the wing membrane vertical air loads on the boom from Figure 26, the total vertical membrane load is found to be 218 pounds.

Integrating the torsional loads on the boom due to the wing being tangentially attached to the inside of the boom, the total torsional load on the boom is found to be 2,084 inch-pounds.

The use of these calculated loads and load vectors will be shown in this report under the section dealing with component testing.

3.4.3 BOOM KEEL LOADS

The corresponding loads on the center boom or keel due to air load on the wing membranes is shown in Figure 31. Similarly, the load on the keel due to directly applied aerodynamic effects is shown in Figure 32.

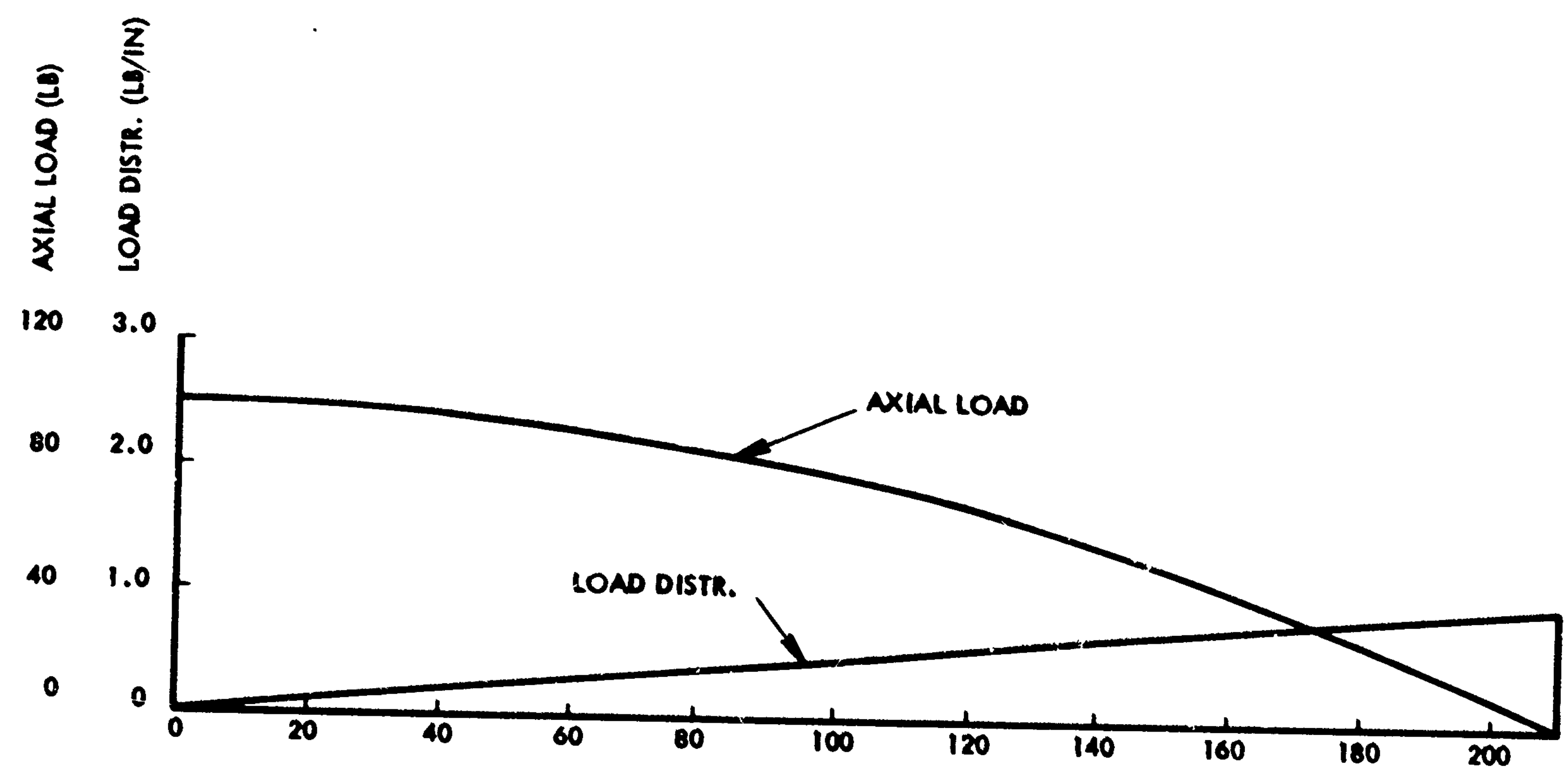

Figure 30. Axial Membrane Loads

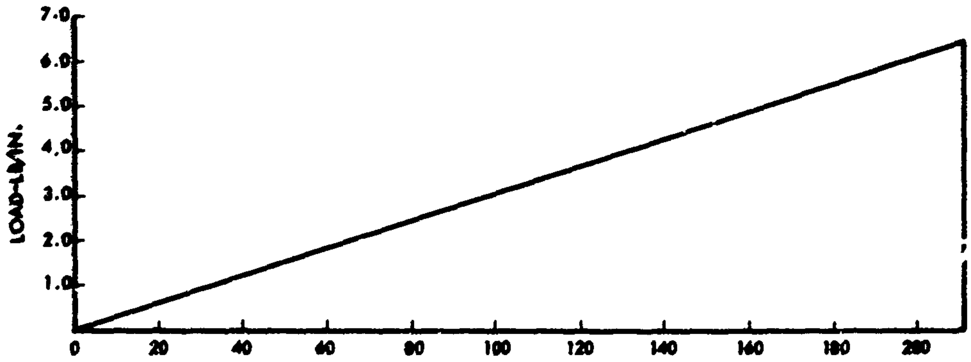

Figure 31. Keel Loads Due to Membranes (2)

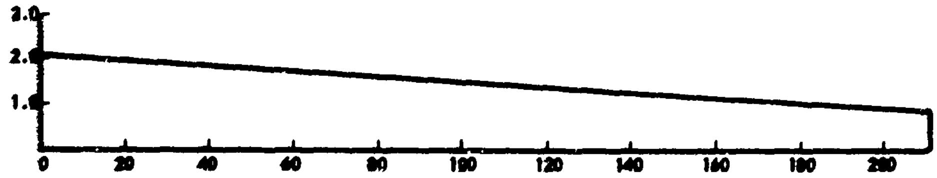

Figure 32. Keel Loads Due to Direct Airloads

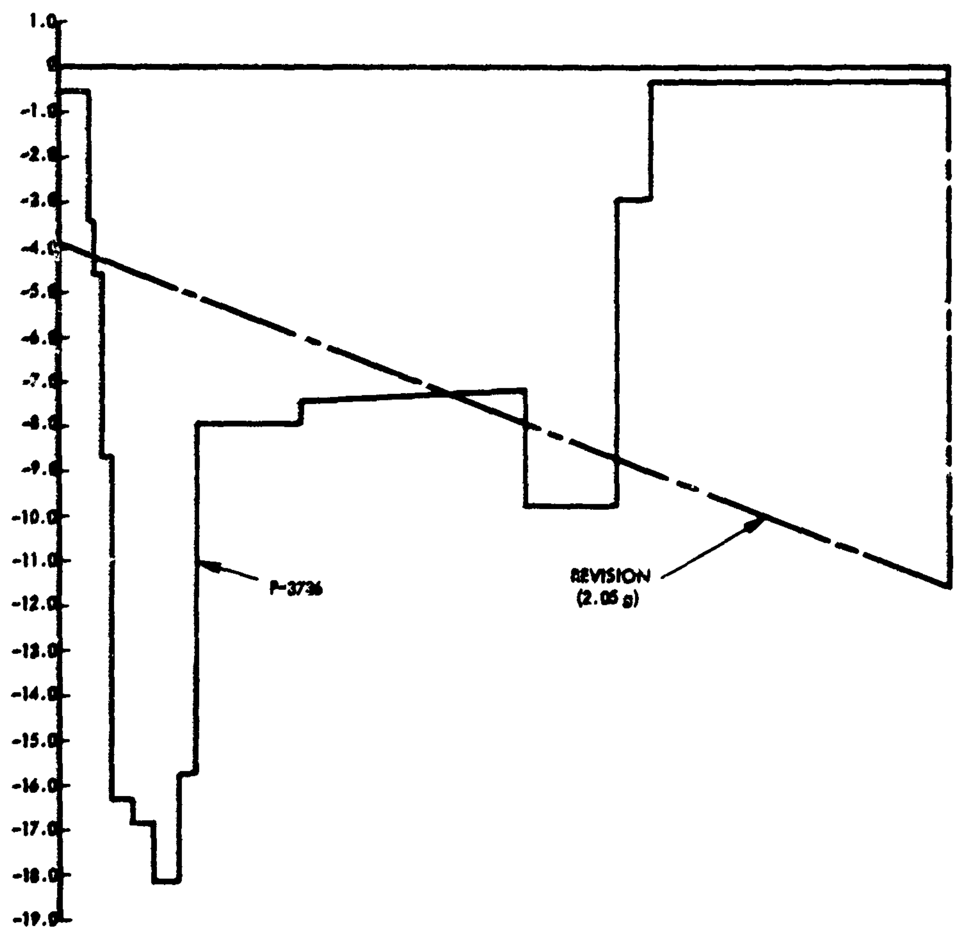

Figure 33. Keel Loads Due to Inertia

The distribution of inertial loads at a maximum of 2.0 g's in the keel was studied in some depth with respect to the weights of actual components and the man in the crew capsule of the keel. The fact that the crew capsule, including life support and flight control equipment, was not the subject of intensive study in this program precluded accurate analysis. The studies did indicate, however, that the assumption of linear weight distribution, as shown in Figure 33, would be reasonable and within sufficient accuracy to establish conservative design parameters.

The combined loads for the keel are shown in Figure 34 which presents curves for load distribution, shear loads, and bending moments versus keel length.

3.4.4 BOOM INTERNAL STABILIZING PRESSURE

The keel bending moment exceeds the leading edge boom bending moment; therefore, the following discussion establishes the internal pressure required to stabilize the keel boom.

The establishment of the internal pressurization requirement was based on the following assumptions:

a. There is to be no evidence of buckling at the boom due to bending compression, under the application of 120 percent of limit loads.

b. Buckling due to shear is not critical.

c. Stress concentrations, bending discontinuities, and gross effects of deflections are difficult to determine analytically and were, therefore, neglected pending results of testing.

d. Bending and buckling effects will be computed from hypersonic air loads only.

The aerodynamic load on the apex, under hypersonic re-entry conditions, is computed as follows:

$$C_p \, dA = 1.76 \quad (19)$$

$$N' = 1.76\,q = 1.76 \times 5.3 = 9.34 \text{ lb/ft}^2 \text{ or } 0.065 \text{ lb/in}^2 \quad (20)$$

$$N = N'D = 0.065 \times 32 = 2.08 \text{ lb/in} \quad (21)$$

The length of arc which the apex covers is

$$L = R\,\theta = 40.6 \frac{2\,(55)}{57.3} = 78.0 \text{ inches} \quad (22)$$

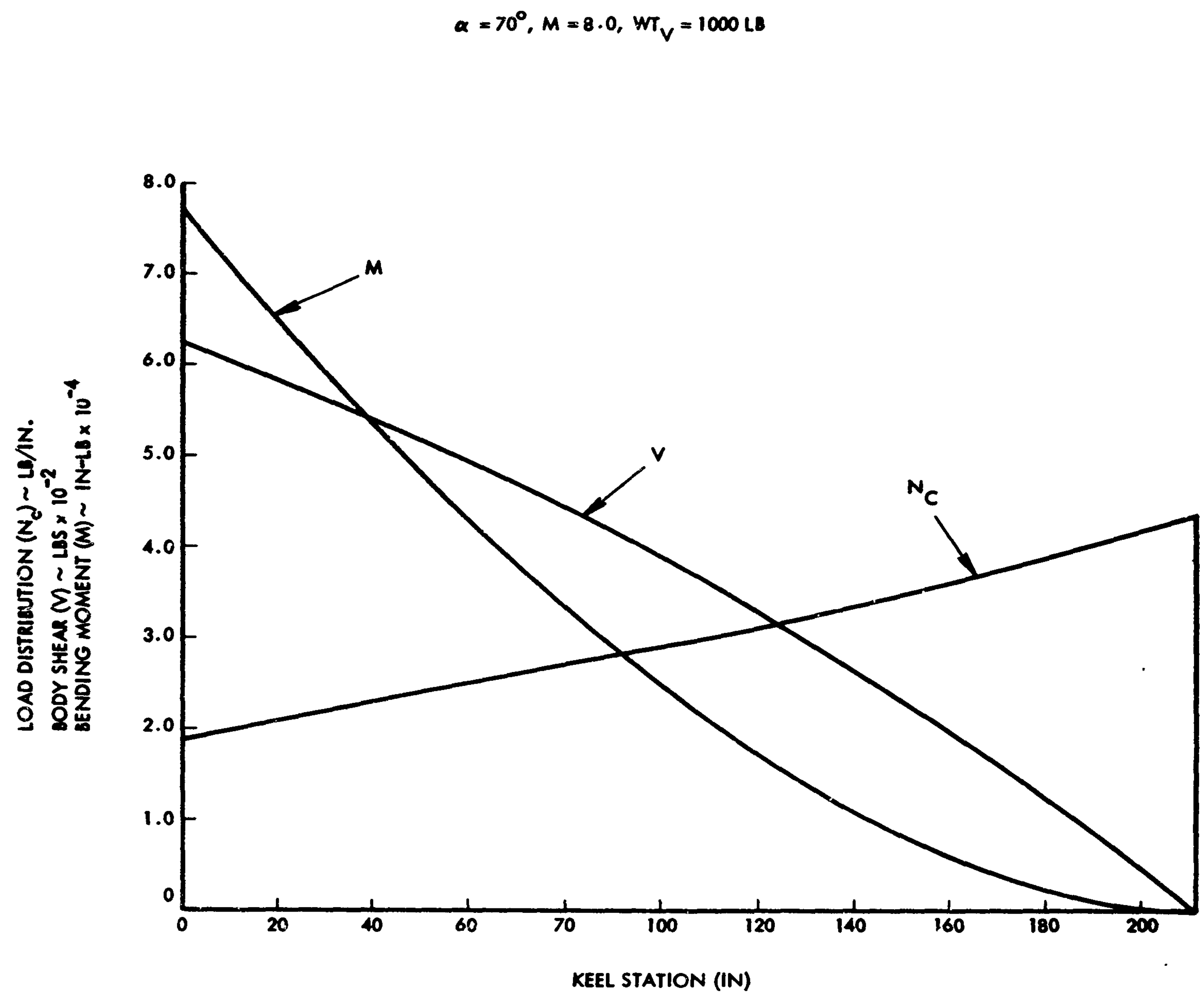

Figure 34. Keel Combined Loads (Revised)

therefore, the vertical shear load at the apex due to air loads directly is:

$$V_{z_o} = F_{z_o} L = 2.08\,(78.0) = 162.2 \text{ lbs} \tag{23}$$

and the moment about the horizontal axis through the apex due to air loads directly is:

$$M'_{y_o} = V_{z_o} \ell = 162.2\,(23.2) = 3760 \text{ inch-lbs} \tag{24}$$

The keel moment is the resultant of the two boom moments minus the apex moment:

$$M'_v = 2\,M_{y_o} \cos 35^\circ - M'_{y_o} \tag{25}$$

Therefore:

$$M'_v = 2\,(39{,}075) \cos 35^\circ - 3760$$

$$\cong 60{,}000 \text{ inch-lbs}$$

At a design moment of 120 percent of limit, or 1.2 (60,000) equals 72,000 inch-pounds, the longitudinal bending load in the cylindrical keel due to hypersonic air loads is:

$$N_{\phi_B} = \frac{M'}{\pi R^2} = \frac{72000}{\pi (16)^2} = 89 \text{ lb/in of circumference} \tag{26}$$

The longitudinal force required to resist this bending load is provided by the internal pressure, i.e.,

$$N_{\phi_P} = \frac{PR}{2} \tag{27}$$

Therefore, the internal pressure required is

$$P = \frac{2\,N_{\phi_B}}{R} = \frac{2\,(89)}{16} \cong 11 \text{ lb/sq in} \tag{28}$$

It will be noted that the internal pressure is based on stabilizing the keel boom with a bending moment of approximately 60,000 inch-pounds. Since the leading edge booms have a bending moment at the apex of about 39,000 inch-pounds, a leading edge boom with 11 psig internal pressure would have a safety factor of 1.85 rather than 1.20. As will be shown later in this report, incipient buckling of the full-scale boom at 11 psig was noted at approximately 250 percent of limit loads.

3.4.5 DESIGN LOADS FOR SELECTION OF STRUCTURAL REINFORCEMENT

Based on linear distribution of the air loads the maximum design longitudinal load per inch of circumference is:

$$N_{\phi_{max}} = \frac{PR}{2} + \frac{M}{\pi R^2} \tag{29}$$

$$= \frac{176}{2} + \frac{60,000}{\pi (16)^2}$$

$$= 88 + 89 = 159 \text{ lb/in}$$

In a cylinder, the unit hoop load per inch of length is:

$$N_\theta = PR$$

at the design internal pressure:

$$N_\theta = 11\,(16) = 176 \text{ lb/in}$$

3.5 VEHICLE DESIGN

In the design of vehicle components, the geometry involved and the orientation of the cloth weave must be considered. Since the mechanical properties of the fabric (as determined from coupon tests only) indicate approximate behavior of inflated component, additional testing is required on small cylinders or other shapes to establish material behavior under complex loading conditions. Even tests on small-scale components leave much doubt as to final strength, deflections and flexibility of a large, complex, inflated vehicle.

Unfortunately, materials for inflatable structures cannot be precisely scaled for both strength and stiffness (conversely flexibility) simultaneously. Changes in thickness of the elastomer and changes in weight of reinforcing fabric or in number of layers of fabric result in disproportionate changes in strength and flexibility for inflated objects of different sizes. These phenomena are common to reinforced plastics in general but are magnified in reinforced elastomers. Since this particular program did not provide for extensive theoretical investigation and development of empirical relationships, vehicle design was based on calculations, such as are presented in this report, with the provision for design changes as testing of prototype components proceeded.

The basic structural geometry of the inflatable paraglider is shown in Figure 35. The apex, to which the leading edge booms and keel boom are attached, is a toroidal section. The booms are conical frustums closed by hemispherical caps at the aft ends.

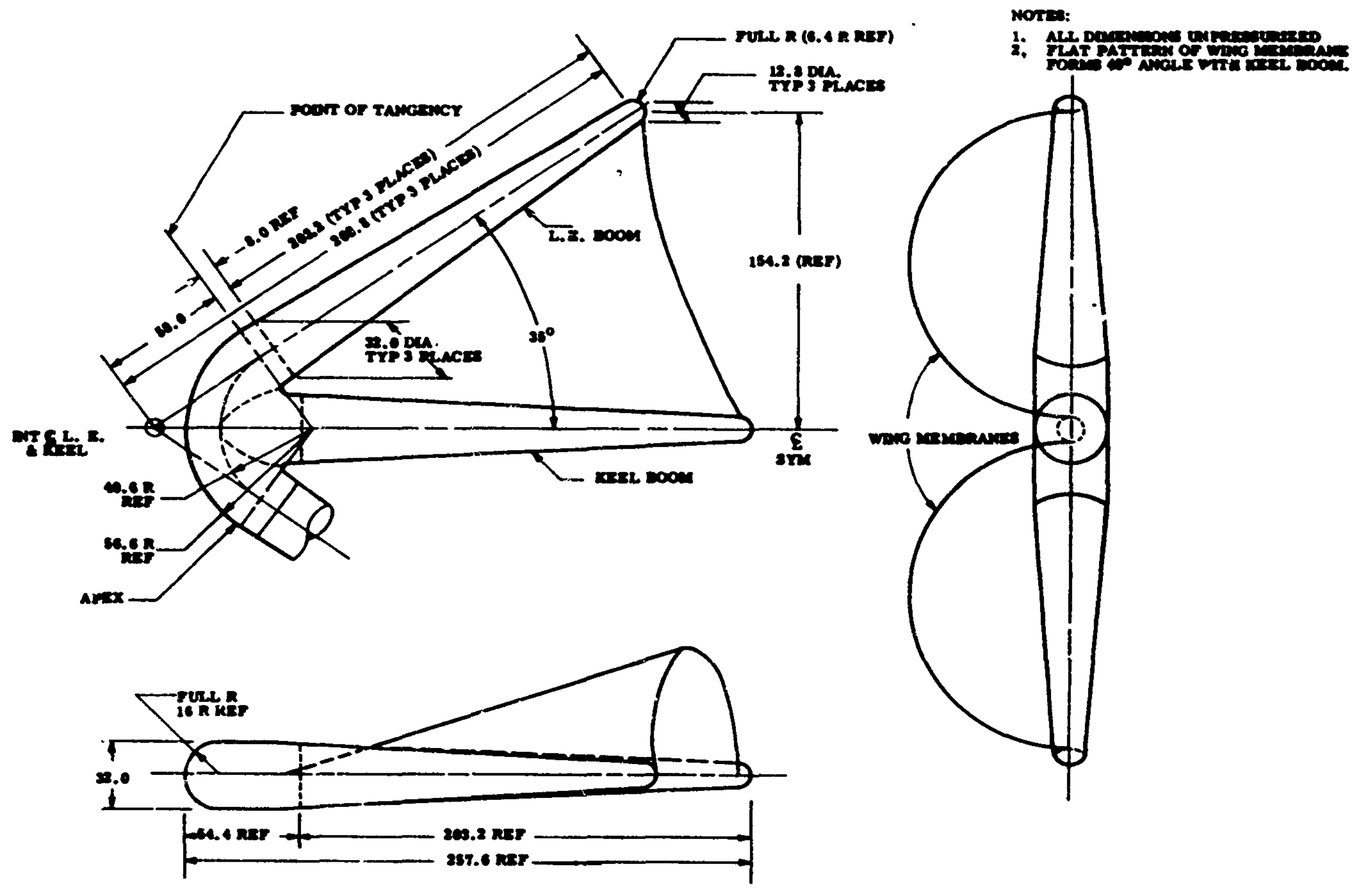

Figure 35. Re-Entry Paraglider - Project FIRST

3.5.1 STRUCTURAL REINFORCEMENT

Since an inflated elastomeric, balloon-like structure would be incapable of carrying the necessary bending, shear, and torsional loads required of a re-entry paraglider, a metal fabric reinforcement approach was selected. The selection and development of the actual metal fabric is presented in Section 3.6.2.

Stress analysis of a fabric structure is complicated. The strength of the structure is derived from the filaments which have a degree of individual freedom of motion. Therefore, a fabric composite cannot be analyzed by the simplified methods used for homogeneous materials. In addition, a fabric normally woven with a warp and fill yarns is anisotropic and the directional properties must be taken into account.

A plain weave or basket weave fabric (as shown in Figure 36) may be assumed to have ability to carry loads only as tension in the filaments; that is, bending stiffness of the filaments is negligible and, if subjected to compression, the filaments will buckle. There are only two coplanar primary directions of load carrying capability. If loads are applied to the fabric in other directions, or out of the plane of the fabric, the strands will reorient into the directions and/or plane of the loads. Impregnating, filling, or coating the fabric with other materials can increase the fabric's capability to carry loads in secondary directions but, to maintain flexibility, the elastomeric coating used with the fabric for an inflatable structure must allow the individual filaments to continue to move to some extent. Therefore, it was assumed that the composite will behave more similarly to a bare fabric than to a rigid, plastic-reinforced structure.

Used as the skin of a pressure vessel, the elastomeric-coated fabric is stretched in tension by internal pressure forces. In a cylinder, with the fabric strands placed parallel and perpendicular to the cylinder axis, i.e., cross-plied, changes in internal pressure do not cause changes in direction of the strands. Compression and tension loads as may be associated with beam bending cause only linear changes in the strands. Such changes include not only elongation of the filaments, but increases and decreases in the amount of crimp inherent in the yarns of the woven fabric. The shear loads associated with beam bending must be resolved into axial components of strand loads with a resulting angular reorientation of the longitudinal strands and an increase in longitudinal strand load, as shown in Figure 37. The angular change (θ) may be roughly approximated as the arc tangent of the unit shear load divided by the unit tension load. Similarly, torsional shear loads are resolved into resultant tension loads in the strand.

Reorientation of the strands due to torsional shear loads also causes a curvature of the strand as the strand traces a helix on the cylindrical surface. A cross-section cut through the cylinder parallel to a segment of the reoriented strand would be elliptical with the instantaneous radius at the minor axis being the radius of curvature of the strand, as indicated in Figure 38. To maintain the curvature, tension in the strand must be balanced

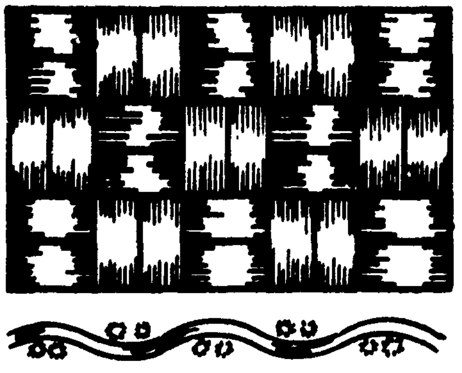

Basket Weave

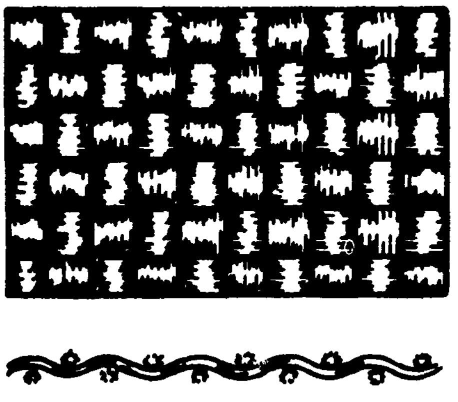

Plain Weave

Figure 36. Symmetrical Cloth Weaves

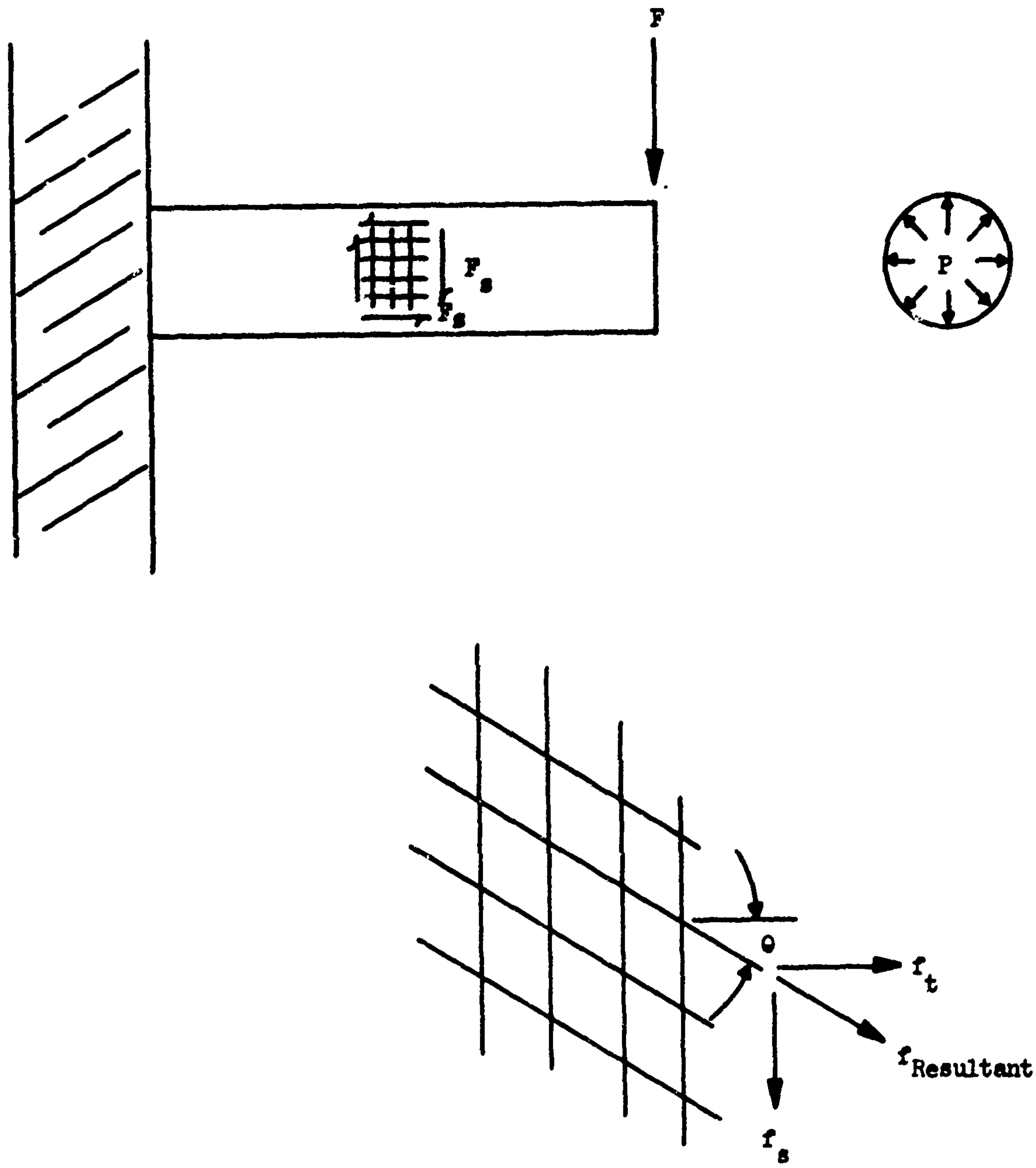

Enlargement Showing Deflection at Centerline

Figure 37. Shear Loading Shear Deformation Due to Lateral Load

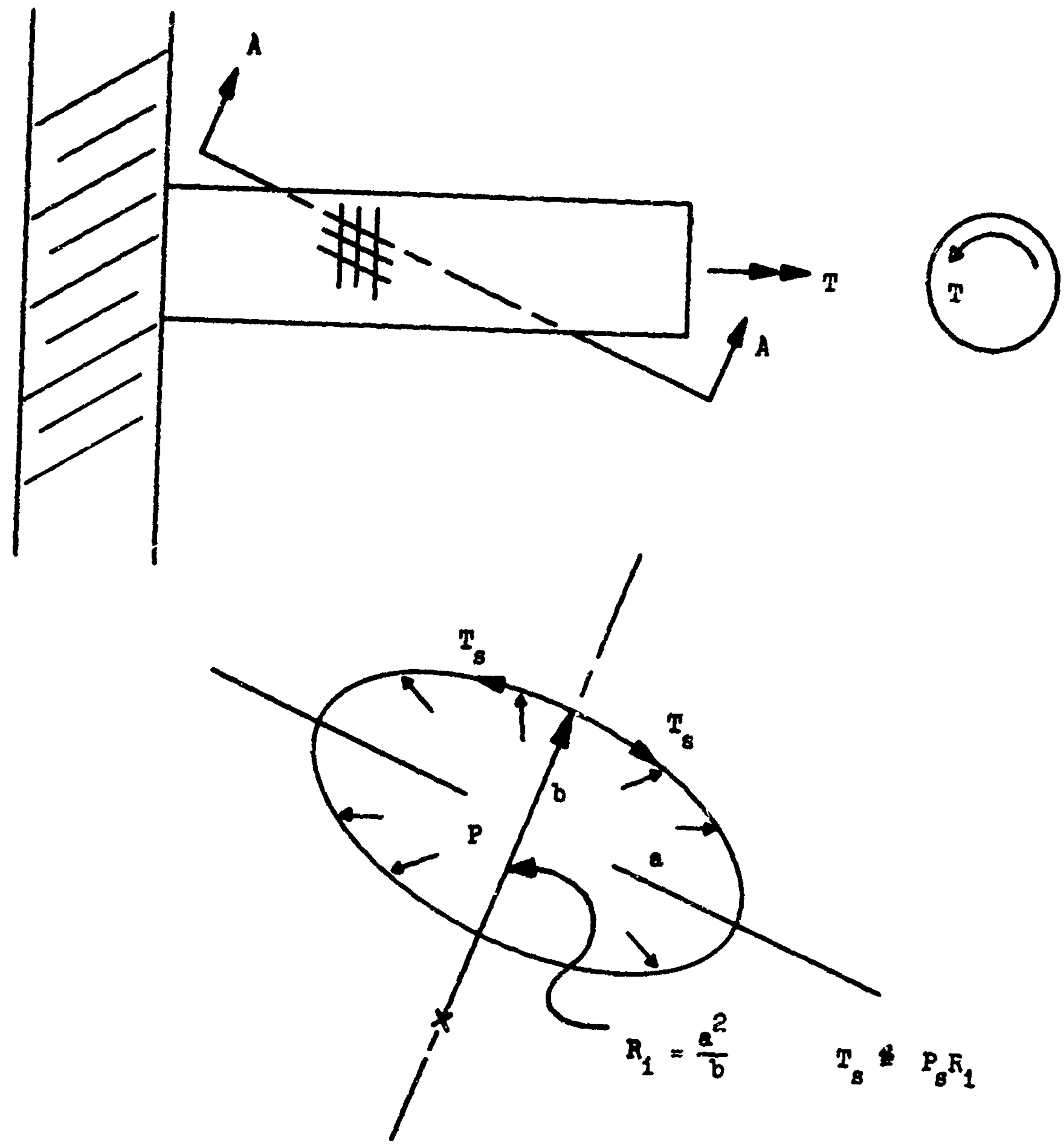

View A-A

Figure 38. Shear Deformation Due to Torsional Load

by an increment of internal pressure applied to the strand ($T_s \leq P_s R_i$). Since part of the internal pressure force is then balanced by the reoriented longitudinal strands, there will be a reduction in the forces in the hoop strands: $T_H = (P - P_s)R$.

As the shear force increases, the angle θ increases and the load in the hoop strands decreases to a limit of zero. When the longitudinal strands have been so loaded as to completely balance the internal pressure, the buckling shear load has been reached (since at this time any addition to the shear load would cause a radial inward pressure in excess of the nominal outward pressure).

The preceding discussion is obviously an extreme simplification of the phenomena because it ignores interaction between the strands, distortion of the hoop strands, changes in volumes, local effects, etc. The behavior of the hoop and longitudinal fibers is not truly independent due to the crossover and crimping of the woven yarns as well as the effect of the impregnant or coating material. It is recognized that bending stresses in the fibers and stress concentrations might have large magnitudes.

Since for a single layer of fabric, small shear loads create large deformations and increases in stresses, it has become standard practice to use multiple layers of fabric. By placing one of the layers of fabric on a bias (with yarns at 45° with respect to the adjacent layer), a truss is formed with the strands. In the case of wire fabric, the two layers of fabric may be bonded together by brazing or welding to cause the structure to behave more like a homogeneous material. Such bonding would drastically reduce flexibility and introduce serious stress concentrations, however.

Under loading in a direction parallel to the strands, the modulus is a function of the strain in the wire and the crimp effect. When loaded at 45° to the strands, the strands undergo angular reorientation, in addition to the strain, despite the effect of crimping.

The contribution of a 45° bias ply of fabric to the membrane strength of a structure is dependent on a biaxiality of the stresses. In a uniaxial stress field, a 45° bias ply fabric may contribute less than 50 percent of the strength of a similar cross-ply fabric. On the other hand, in a 1-to-1 biaxial stress field, a 45° bias ply fabric would contribute equal strength to an equivalent cross ply fabric.

Because of the variation in deflection and strength with changes in the biaxial stress field, it is difficult to predict the behavior of a pressurized structure based on coupon tests. It is, therefore, necessary to test scaled components for proper evaluation of materials and design parameters.

For a fabric to be flexible, the individual fibers must be of an extremely small diameter so as to have negligible resistance to bending and compression. In the stranding process, excessive twisting of yarns must be avoided to prevent frictional forces and high angularity of the filaments with the longitudinal load-carrying direction.

The elastomeric coating which may be used as an ablator, insulation, and gas barrier, must also be very flexible. It has a thickness which can act as a beam in bending if the elastic modulus is significant. Also, if the elastomer is impregnated into the fabric between the filaments and bonded thereto, it will act as an adhesive creating a lamination of the filaments whereupon the bending stiffness of the fabric becomes a function of the shear modulus of the elastomer. Also, the elastomer, if properly impregnated, supports the filaments in compression, increasing the buckling resistance of the fibers with increased bending stiffness of the fabric.

If the coated or impregnated fabric has low bending stiffness, it will also have low in-plane shear stiffness.

When the coated fabric is made into a structural member (such as a pressurized cylindrical boom) it is inherently capable of carrying the tension stresses due to pressurization. Lateral loads applied to the boom create beam bending and shear stresses in the fabric. Since the shear stresses in the fabric may be carried only by tension in the fibers, deformations must occur to reorient the fibers so that tension due to shear and tension due to pressure are components of the fibers stress.

With sufficiently high pressures and low shear stresses, deflections may be within allowable limits for the structure. However, with large shear stresses, the deformation of the single-ply fabric may be excessive and, to prevent formation of shear wrinkles, increased pressure may be required. Therefore, for high shear stress conditions, a second ply of fabric is required, oriented on a 45° bias to the first ply.

To effectively form a shear resistant truss between the cross ply and the bias ply, there must be a bond between the two. This bond is best obtained by use of an elastomeric impregnant. Fortunately, the unit shear loads between the two plies are relatively small and only modest strength is required for the elastomer. Similarly, with essentially intimate contact between the two plies, the low modulus of the elastomer may be tolerated.

3.5.2 DESIGN OF BOOMS

The leading edge booms are a basic design element in the configuration selected. Being cantilevered from the apex, they are subjected to bending, shear, and torsion due to location of the wing membrane attachment, as well as internal pressure to stabilize against compression buckling. The keel boom is a similar inflatable structure except as modified by the integral, rigid crew compartment.

Figure 39 shows the basic boom design concept. To carry hoop and longitudinal loads, the outer ply of fabric ("cross ply") is laid with the warp yarns parallel to the boom centerline and the fill yarns in the hoop direction. To carry shear loads, the inner ply of fabric ("bias ply") is laid with yarns at 45° to the boom's centerline, forming a "truss" as described in Section 3.5.1.

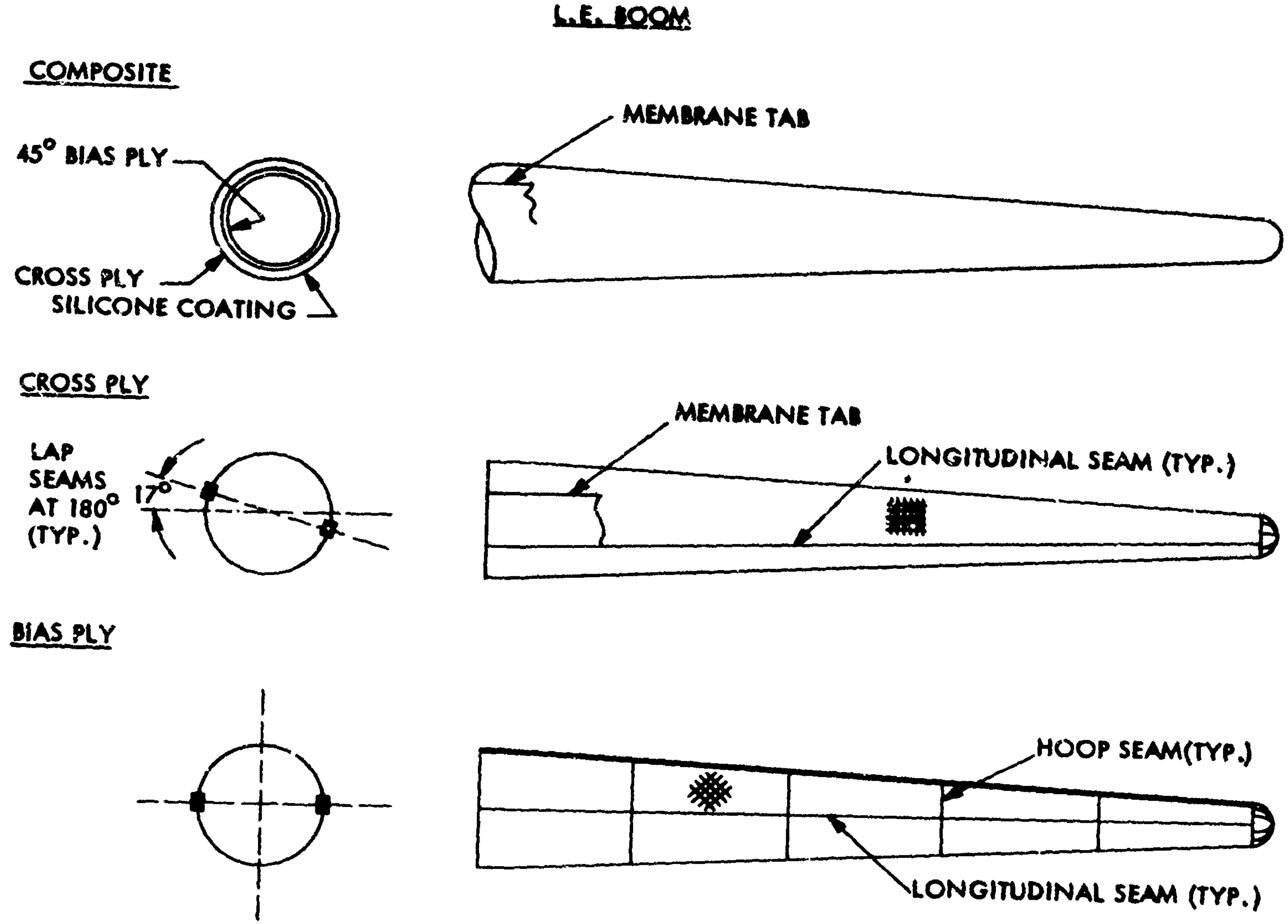

Figure 39. Design of Meta' Fabric Lay-Up for Booms

The number of longitudinal and hoop joints in the fabric is a function of the fabric size availability. Since 60-inch-wide metal fabric was woven for this program, two longitudinal joints of approximately 100-inch maximum circumference were required for the boom.

Circumferential seams are required in the bias ply since the fabric must be cut 45° to the warp yarns. These circumferential seams must be perpendicular to the boom longitudinal axis since a helix seam would cause bending and twisting when the boom is pressurized. Also, to maintain symmetry, two longitudinal seams are used in the bias ply. To reduce the magnitude of load transfer at the seam, the seams in the bias ply are staggered with respect to the cross ply. This also minimizes stiffness and thickness in the seam area.

Circumferential seams are required in both plies to attach the apex and the end caps to the boom. The wing membrane would be attached to a flap which is a continuation of the outer cross ply beyond the longitudinal closure seam.

3.5.3 DESIGN OF APEX

Since one of the goals of this program was to design, develop, and fabricate an integral apex which would be completely flexible and inflatable (without interior reinforcing structure), considerable analytical and experimental development effort was applied to this complex design problem.

The apex geometry involves the intersection of a cylinder and a torus, as shown in Figure 40. Under internal pressure the membrane stresses, σ_t and σ_c, at the intersection line of such a basic geometry, are not under static equilibrium. It is, therefore, necessary for large deformations to occur, reorienting the stress direction until equilibrium is achieved. If the intersection line was in the form of a large forging capable of taking significant bending and torsional loads in addition to tension, the membrane forces would be essentially in equilibrium with only small deflections as normally experienced in pressure vessels at flanges, bosses, etc. In constructing a completely flexible apex, considerable fabric material must be used in the intersection area. Additional reinforcing fabric is required at "A" and "B" to balance the hoop tension at the leading edge cross-section "C". See Figure 40. Additional material is required to balance a portion of the keel cylinder loads and to overcome distortion and concentration of stresses.

The design which was established is defined in Figure 41. Two plies of fabric, in 45° bias relationship, are cut to required pattern sizes and joined to form the apex shape. Again, the seams are staggered in the inner and outer plies so as to minimize thickness and stiffness. Tapes are added, fanning out from areas "A" and "B" to header strips. The tape wraps

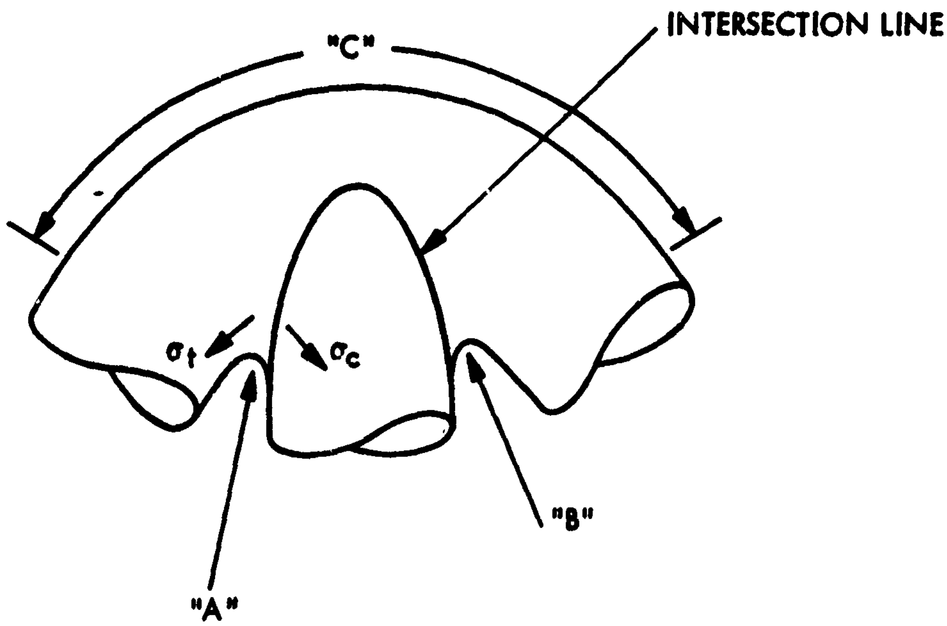

Figure 40. Intersection Membrane Stresses

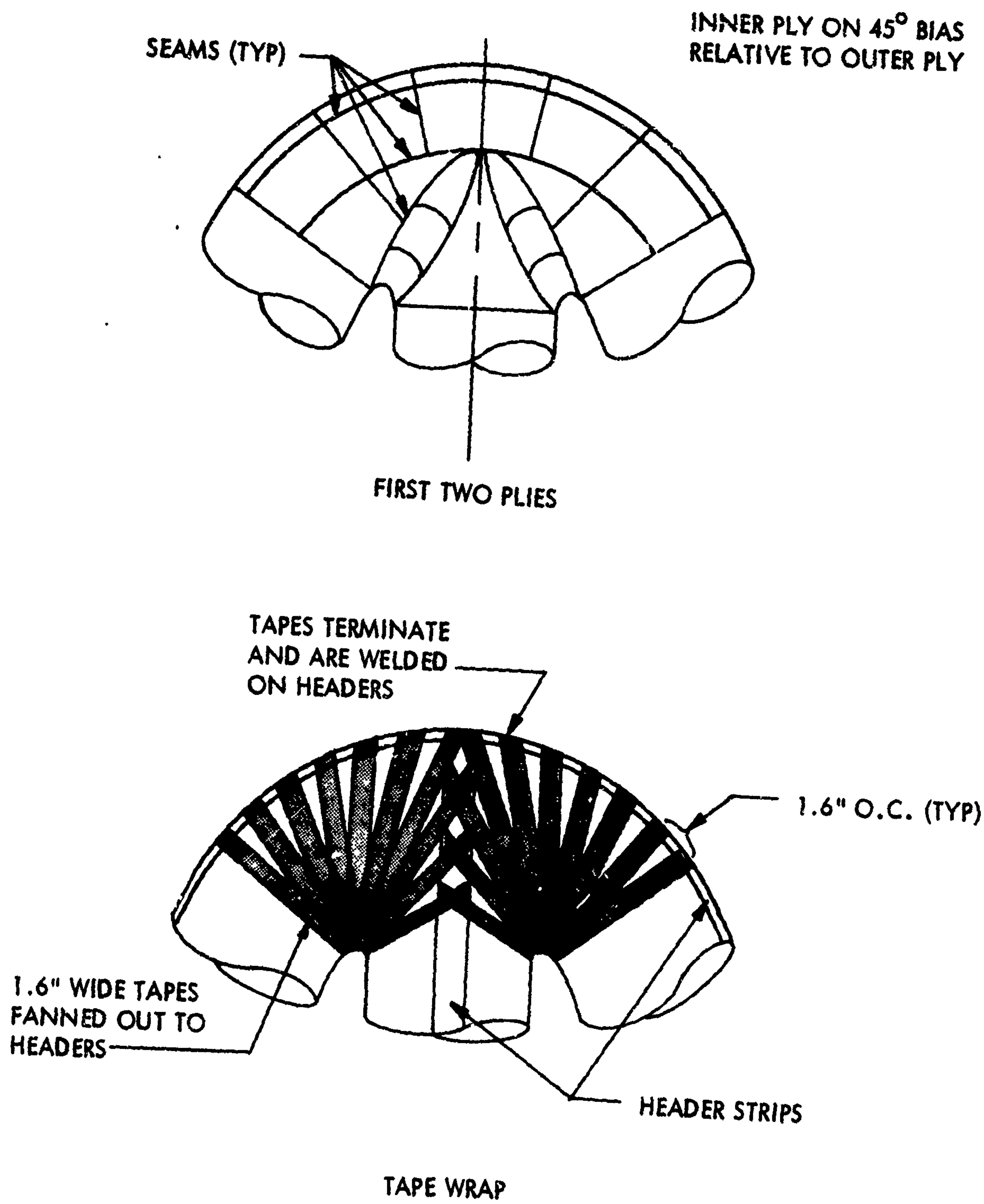

Figure 41. Design of Metal Fabric Lay-Up for Integral Apex

carry a portion of the hoop stresses due to internal pressure, providing the additional reinforcement required at "A" and "B".

The primary two plies (cross and bias) are capable of carrying the bending and shear loads due to aerodynamic forces as well as the longitudinal tension loads due to internal pressure.

3.6 MATERIALS EVALUATION

The two major areas of investigation of materials in this program were devoted to evaluation of silicone elastomer coatings and fabric reinforcing materials. The silicone elastomers were desirable because of their retention of elastomeric properties at higher temperatures than other known elastomers while they also appeared to have reasonably low ablation rates under the moderate heat fluxes encountered by the re-entry vehicle. Metal fabrics appeared to be likely candidates for the reinforcing material since they could be woven from ultra-fine filaments of high-temperature, high-tensile alloys. Metal fabric was chosen in favor of glass fabric early in the program due to the freedom from abrasion during handling, fabrication, and actual use (which tended to drastically lower the strength of known glass fabrics) and, more important, the potential ability to join the metal fabrics by metallurgical techniques producing joints or seams capable of resisting temperatures as high as the parent metal fabric itself.

It was found that the effective ablation temperature of silicone rubber is not likely to exceed 1100-1500°F. Although this effective ablation temperature might be increased through the addition of metamorphic-type frits, this would appear undesirable unless these additives decreased the ablation rate or the total amount of material ablated. Since the heat transfer is from the outer heated surface toward the inner surface of the fabric matrix, it is desirable to keep the outer surface temperature as low as possible because the substrate reinforcing fabric will always be at a lower temperature than the outer surface. It may, therefore, be concluded that the heat of ablation (Btu/lb) should be as high as possible to keep the amount of material ablated at a minimum and absorb as much heat as possible through the chemical ablation process, without allowing the temperature to rise unnecessarily high. This permits the use of less exotic and more available alloys for the metal fabric reinforcing material.

3.6.1 SILICONE ELASTOMERS

To expedite the survey of candidate silicone elastomers, a Silicone Materials Requirement was sent to the four major suppliers of silicone rubber materials: General Electric Co., Dow-Corning Corporation, Union Carbide Corporation, and Minnesota Mining and Manufacturing Co. This requirement outlined the objectives, requirements, and the information required for materials to coat the paraglider reinforcing fabric.

In addition to the testing of standard silicone elastomer products, a number of modified silicone compositions were formulated and tested. Additives evaluated included ceramic frits, micro balloons, and flame retardants. Many of these additives, however, caused significant decrease in flexibility and some, while minimizing cracking and spalling under ablative conditions, formed a molten surface which re-solidified to a glass-like, brittle composition upon cooling. In the case of the proposed re-entry vehicle, this loss of flexibility and formation of brittle surface was unacceptable since the vehicle must be capable of maneuvering and flying to a safe landing after cooling to normal temperatures from the high temperature re-entry regime.

Investigation of the many different types, methods of compounding, and quantity of additives would have been an extensive research project and efforts were directed toward obtaining the simplest impregnated and coated fabric system consistent with the philosophy that "available" materials be used. Among the silicone compounds which were evaluated were S-6510 (Dow-Corning), Y-3350 and K-1305 (Union Carbide), SE-5517 (General Electric), and ME-100 (Aerojet-General).

An acetylene torch, screening test apparatus was assembled and calibrated. This was used for screening the candidate silicone elastomers and modified silicone materials because such tests could be run inexpensively with relatively small set-up time as compared to the more expensive plasma arc tests.

Air arc plasma jet tests were run on each of the materials which appeared attractive as a result of the acetylene torch test. The plasma jet was calibrated to expose the specimens at heat fluxes simulating the re-entry conditions described in Section 3.6.1.2.

3.6.1.1 ACETYLENE TORCH TEST

To reduce the time and expense involved in running plasma arc tests, an acetylene torch test was set-up to screen candidate ablation materials. Specimens one-quarter inch thick by five-inch diameter were prepared and clamped in a holding fixture. An acetylene torch was directed perpendicularly onto the center of the specimen. The torch was previously calibrated on an alloy metal plate to produce a continuous temperature of 2000°F on the plate. The details of the torch test procedure are given in Appendix I, "Torch Test Procedure."

The silicone rubber specimens were weighed and calipered before and after the test. Evaluation of this quantitative data along with the appearance of the char layer, etc., permitted comparison of the ablation performance of the candidate materials. A photograph of the test set-up is shown in Figure 42.

SG/26

Figure 42. Test Apparatus - Torch Tests

In general, torch tests indicated the same order of preference of materials tested as the plasma arc test. The magnitude of the ablation velocity was also similar to that determined in the plasma arc tests, although this fact is believed to be a coincidence. Although both methods tend to oxidize and degrade the specimen, many significant differences, such as the atmospheric pressure and partial pressure of oxygen, the temperature and nature of the impinging jet, and the physical position and shape of the sample, could cause the results to be quite different. The results of torch tests are shown in Table I.

It will be noted that the specimens which were loaded with frit and other additives tended to have much higher backside temperature rise in addition to their decreased flexibility. This is one reason that such additive-type mixtures were discarded.

3.6.1.2 PLASMA-JET TESTS

Air arc plasma jet tests were conducted in an 80 kW supersonic plasma arc facility to provide data which would permit computation of the temperature of the reinforcing fabric and to give a quantitative evaluation of the rate of ablation exposure to heating effects simulating those of the re-entry regime.

Specimens used were one-half inch diameter by two inches long. These were inserted in a hypersonic jet of air heated to approximately 5800°F (depending on test conditions) by passing it through a high-voltage electric arc. The entire process takes place in a vacuum chamber and the heat flux to the specimen is regulated by adjustment of the voltage, gas flow, and distance of the specimen from the jet nozzle. The silicone rubber specimens were prepared by mounting three thermocouples at various distances along the longitudinal axes. Each specimen was insulated around the cylindrical surface with approximately one-half inch of a standard RTV silicone rubber used for this purpose. Pyrometric temperatures were monitored optically to calculate the corresponding effective surface temperature.

The ablation velocity was obtained from dimensional changes as well as mass loss of the specimens. Recorded temperature traces of the thermocouples mounted in the specimens permitted evaluation of thermal conductivity and heat capacity effects. By extrapolation of the temperature curve through these three known points within the specimen at any instant, the temperature at the base of the char layer ("ablation temperature") was determined for given conditions. Similarly, knowledge of the thermal conductivity permits the temperature of the reinforcing fabric substrate to be computed at given conditions.

Color movies were taken of the ablation process through a window in the side of the vacuum chamber. The plasma jet test apparatus is shown in Figure 43. Table II presents the plasma jet test data obtained from the three major candidate ablation materials. Corresponding ablation velocity versus cold wall heat flux for these materials is presented in Figure 44.

Table I

RESULTS OF MATERIALS TORCH TESTS
TEST DATE: 5-3-63

Material	Weight, Grams			Thickness, in.			Temp., °F			Ablation Velocity in/sec	Test Time sec.	Remarks
	Orig.	Aged	Loss	Orig.	Aged	Loss	T_1	T_2	ΔT			
Y3350	79.647	78.647	1.120	.242	.168	.074	70	120	50	.00164	45	Good char adhesion
	81.482	80.000	1.482	.245	.175	.070	70	140	70	.00175	40	Hard char layer
												Specimen shrunk from 5 to 4-5/8" during curing.
												Specimen continued burning from 5-7 sec after flame was removed.
S6510	92.202	91.560	0.642	.250	.172	.078	74	124	50	.00130	60	Poor char adhesion
	92.107	90.075	1.032	.250	.173	.077	74	124	50	.00128	60	Soft flaky char. Specimen shrunk from 5 to 4-7/8" during curing.
												Specimen continued burning from 5-7 sec after flame was removed.
SI-5010	109.877	108.545	1.332	.250	.170	.080	74	144	70	.00133	60	Fair char adhesion
(80% S6510 20% $3304 FRIT)	109.877	108.523	1.354	.250	.170	.080	74	144	70	.00133	60	Soft flaky char

Table I (Continued)

RESULTS OF MATERIALS TORCH TESTS
TEST DATE: 5-3-63

Material	Weight, Grams			Thickness, In.			Temp., °F			Ablation	Test	Remarks
	Orig.	Aged	Loss	Orig.	Aged	Loss	T_1	T_1	ΔT	Velocity In/Sec.	Time Sec.	
SI-5010 (con'td)												Specimen continued burning from 5-7 sec after flame was removed.
SI-5015	93.092	92.865	0.227	.240	.170	.070	74	189	115	.00116	60	Fair char adhesion
(80% Y3350 20% No. 3304 FRIT)	92.287	92.010	0.227	.235	.168	.067	74	189	115	.00115	60	Medium hard flaky char. Specimen continued burning from 5-7 sec after flame was removed.
ME100	90.080	88.760	1.320	.250	.165	.085			168	.00142	60	Poor char adhesion-flaky char specimen continued burning 25 sec after flame removed.
EC1667	121.450	120.048	1.402	.275	.210	.065			128	.00083	60	Hard char. Poor adhesion. Did not flame.
SE5517	96.510	95.310	1.200	.265	.130	.135			118	.00276	60	Soft char. Poor adhesion. Specimen continued burning 13 sec after flame was removed.

Table I (Continued)

RESULTS OF MATERIALS TORCH TESTS
TEST DATE: 5-3-63

Material	Weight, Grams			Thickness, in.			Temp., °F			Ablation Velocity in/sec	Test Time sec.	Remarks
	Orig.	Aged	Loss	Orig.	Aged	Loss	T_1	T_2	ΔT			
SE4606	102.115	100.653	1.462	.250	.165	.085			154	.00142	60	Two layers of char: top soft and flaky, second leather-like. Good adhesion. Specimen continued burning 12 sec after flame was removed.
SE5517	96.315	93.770	2.545	.270	.155	.115	77	90	167	.00192	60	Soft flaky char. Poor adhesion. Burned 12 sec.
S325	73.420	71.995	1.425	.250	.174	.076	77	77	154	.00127	60	Very hard char.
	72.200	70.600	1.600	.250	.150	.100	77	91	168	.00167	60	Very good adhesion.
	72.885	71.320	1.565	.255	.165	.090	77	121	198	.00150	60	Burned 12 sec.
Q2-0103	122.425	120.500	1.925	.250	.155	.095	77	150	227	.001585	60	Fair char.
	120.765	116.795	3.870	.255	.157	.098	77	156	233	.00163	60	Poor adhesion.
	123.635	122.220	1.415	.255	.156	.099	77	143	220	.00165	60	Burned 26 sec.
Q90006	122.450	120.180	2.270	.260	.164	.096	77	121	198	.00160	60	Fair char.
	117.620	115.500	2.120	.255	.161	.094	77	132	209	.00157	60	Medium adhesion.
	116.940	114.300	2.640	.260	.151	.109	77	143	220	.00182	60	Burned 13 sec. Gas bubbles under char.
Y3350	81.120	79.220	1.900	.235	.165	.070	75	165	240	.00117	60	Hard char.
	80.625	78.330	2.295	.235	.167	.068	75	208	283	.00113	60	Good adhesion.
	80.985	78.830	2.115	.240	.170	.070	75	208	283	.00117	60	Burned 20 sec.
S6510	93.190	91.220	1.970	.250	.168	.082	75	143	218	.00137	60	Flaky char.
	92.830	90.890	1.940	.235	.167	.068	75	121	196	.00113	60	Fair adhesion.
	91.995	89.535	2.460	.240	.179	.061	75	113	188	.00102	60	Burned 16 sec.

Table II

PLASMA-JET ABLATION DATA

Specimen	Density (lb/ft^3)	Stagnation Enthalpy (But/lb.)	Pressure (Atm.)	Cold Wall Heat Flux (Btu/ft^2 sec)	Brightness Temp. (°F)	Wt. Loss Rate (gms/sec)	Mass Ablation Rate (lbs/ft^2 sec)	Ablation Vel. (Mils/sec)	Avg Abl. Vel. (Mils/sec)	Cold Wall Avg Eff. Heat of Ablation (Btu/lb)
Union Carbide Y-3350	74.9	716	.045	10.35	1560	0.000900	.00161	.298		
		716	.045	10.35	-	0.000518	.000965	.155	.172	9650
		716	.045	10.35	-	0.000375	.000704	.113		
		716	.045	10.35	-	0.000544	.00101	.162		
		1420	.045	15.25	1860	0.00319	.00544	.874		
		1420	.045	15.25	1955	0.00274	.00475	.764	.813	3010
		1420	.045	15.25	1920	0.00270	.00500	.803		
		1770	.045	25.40	2100	0.00394	.00718	1.152		
		1770	.045	25.40	1960	0.00387	.00737	1.183	1.176	3470
		1770	.045	25.40	2080	0.00421	.00743	1.192		
Union Carbide K-1305W	77.8	716	.045	10.35	1670	0.001225	.00177	.277	.277	5830
		1420	.045	15.25	1940	0.00322	.00465	.727	.727	3350
		1770	.045	25.40	2100	0.00815	.0123	1.92	1.92	2070
Dow Corning S-6810	75.5	1420	.045	15.25	1840	0.00311	.00465	.740	.665	3740
		1420	.045	15.25	1870	0.00242	.00369	.587		
		1770	.045	25.4	2050	0.00407	.00611	.973	1.009	4000
		1770	.045	25.4	2100	0.00455	.00657	1.046		

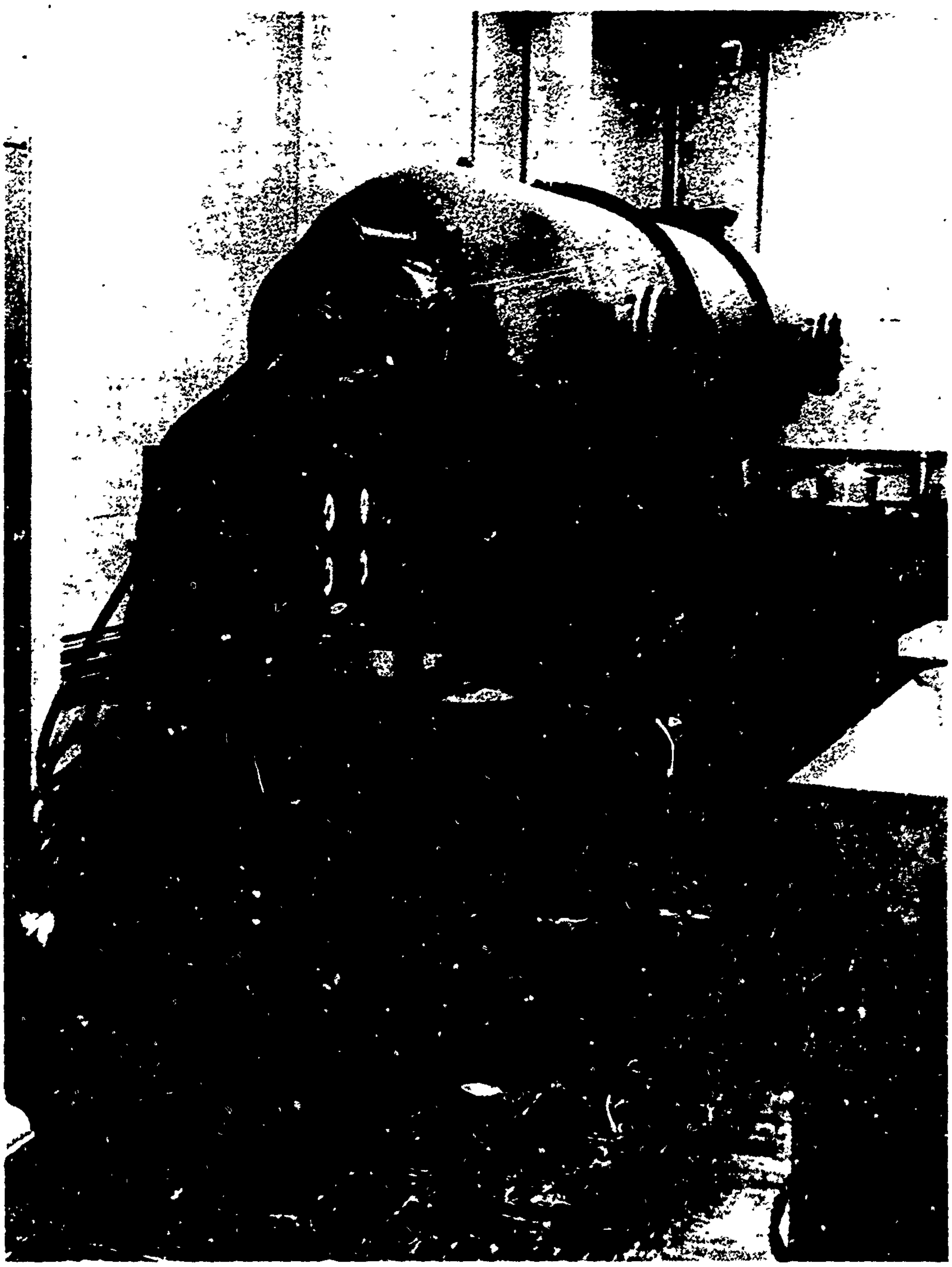

335/045

Figure 43. Plasma-Jet Test Apparatus

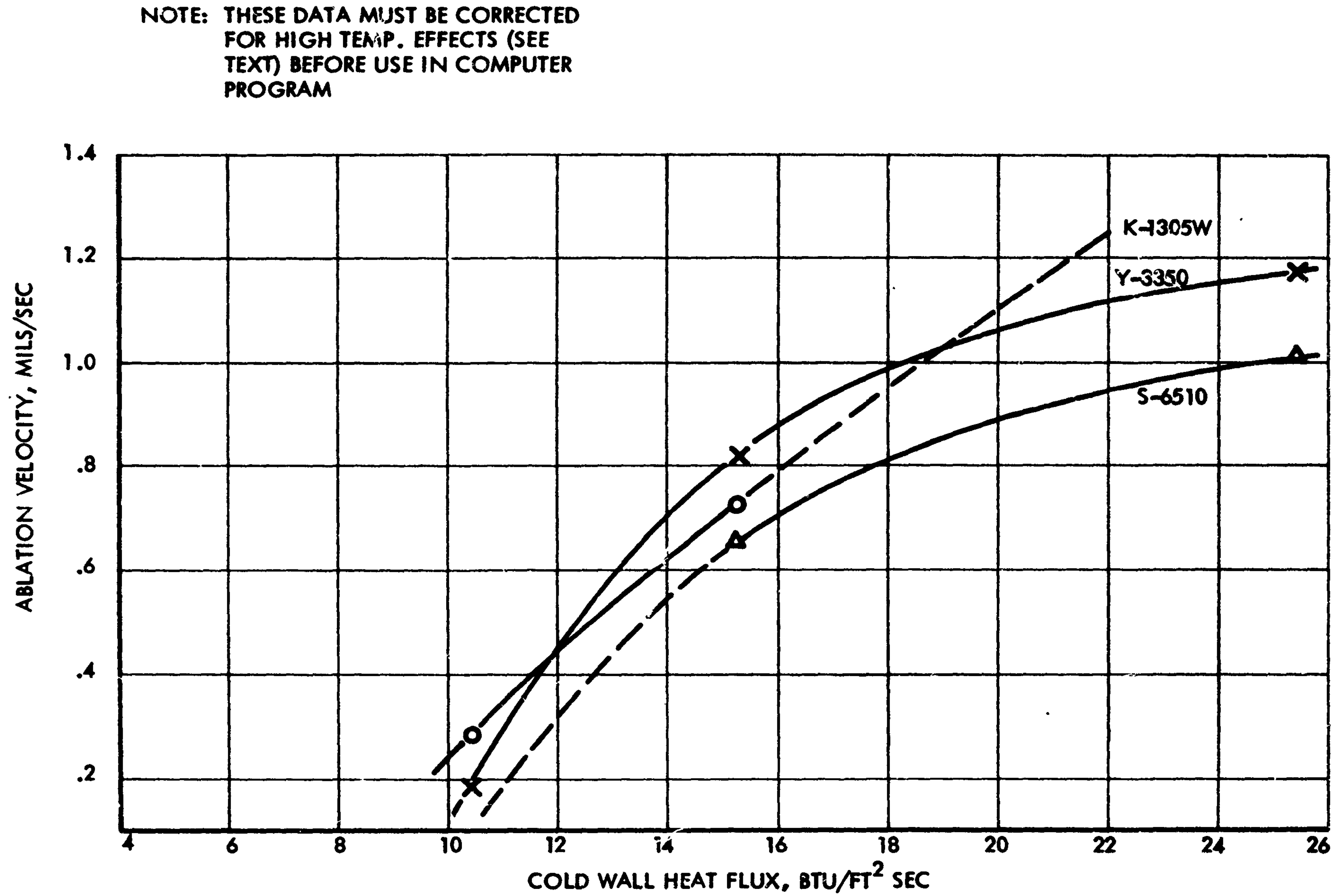

Figure 44. Ablation Velocity Versus Cold Wall Heat Flux

Table III summarizes the computations to generate the corrected effective heat of ablation for use in the digital computer thermodynamic analysis. Figure 45 shows these data plotted as curves relating corrected hot wall effective heat of ablation to cold wall heat flux. Some extrapolation of the S-6510 data was necessary in the low heat flux range. Since the basic chemical structure of S-6510 is similar to Y-3350 and K-1305W, it is expected that performance of the materials will allow the same trend. The average heat flux selected for evaluating the effective heat of ablation in computer analysis was 8.5 Btu/sq ft, sec. However, the minimum heat flux for which plasma-jet data could be obtained was 10.4 Btu sq ft/sec. The trend of the data indicates that the corrected effective heat of ablation will be above 10,000 Btu/lb at a heat flux of 8.5 Btu/sq ft/sec. For computer analysis it was assumed that the maximum value was that obtained at a heat flux of 10.4 Btu/sq ft/sec. This approach will cause the computed thickness ablated to be conservative or slightly higher than would have been obtained from rigorous extrapolation of the test data. Material properties used in these analyses are shown in Table IV.

The results of the thermodynamic analysis performed by the computer are shown in Figure 18 for the S-6510 silicone rubber which was selected because it had the lowest total material ablated and also showed the lowest temperatures at the metal fabric substrate. Some of the test specimens exposed to the plasma arc are shown in Figure 46. Close-up photographs of the SE-5517 and K-1305W are shown in Figure 47. In these photomacrographs, the end of the specimens exposed to the arc jet is sectioned so as to show the extent of charring and swelling. The S-6510 finally selected as the ablative coating material, showed a charring and swelling effect similar to the K-1305W.

3.6.1.3 HIGH TEMPERATURE GAS RETENTION PROPERTIES OF SILICONE RUBBER COATINGS

The test fixture shown in Figure 48 is 4 inches in diameter with a 1-inch diameter cavity, 1/4-inch deep, in the center of each flange. The two flanges were bolted together with a circular specimen of silicone rubber coated "tensil bolting" cloth (light weight monofilament stainless steel screen) sandwiched between them. The metal cloth side of the specimen was pressurized with air or nitrogen to 10 psig. The entire fixture was placed in an oven and allowed to come to equilibrium temperature during "soak" periods at temperature increments of approximately 100°F. The effectiveness of the soak periods was checked by the use of a thermocouple inserted into the outlet tube of the cavity in a position adjacent to the rubber coated specimens surface. The outlet tube was immersed in a shallow beaker of water so that any leakage was immediately revealed by bubbles. The oven temperature was raised and held at each temperature increment for approximately 10 minutes. Data for these tests are presented in Table V.

It will be noted that the first test run on S-6510, with air as a pressurizing gas, failed at a lower temperature than subsequent tests which were run using nitrogen. In the nitrogen pressurizing tests, the outer periphery of the silicone specimen was sealed with a high temperature copper base adhesive to prevent oxidization. In general, it will be noted that the silicone rubber candidate materials can withstand the average reinforcing fabric temperature of

Table III

CORRECTED EFFECTIVE HEAT OF ABLATION

	Cold Wall Heat Flux $\dot{q}_{cw}$ Btu/ft^2 sec	Radiation Correction Δq_{rr} Btu/ft^2 sec	Heat Flux Contribution To Ablation Assumed $\dot{q}_{chem}$ Btu/ft^2 sec	Ablation Velocity $\dot{V}$ Mils/sec	Corrected Effective Heat of Ablation $\dot{Q}_c$ Btu/lb.
Y3350					
	10.35	6.19	2.30	.172	7930
	15.25	11.19	3.40	.813	2880
	25.4	14.64	5.60	1.176	2760
K1305W					
	10.35	6.26	2.30	.277	4850
	15.25	13.09	3.40	.727	2540
	25.4	16.09	5.60	1.92	1760
S6510					
	11.0	6.49	2.44	.18	7900
	15.25	9.64	3.40	.663	3130
	25.4	15.24	5.60	1.009	3280

Table IV

MATERIAL PROPERTIES SELECTED FOR COMPUTER ANALYSIS

Union Carbide Y3350	
Density, lbs/ft^3,	74.9
Thermal Conductivity, Btu/hr ft^2 $^\circ$F/ft,	.0916
Specific Heat, Btu/lb $^\circ$F,	.363
Emissivity,	.90
Ablation Temperature, $^\circ$F	1100
Effective Heat of Ablation, Btu/lb.	7400
Dow Corning S6510	
Density, lbs/ft^3	75.5
Thermal Conductivity, Btu/hr ft^2 $^\circ$F/ft,	.129
Specific Heat, Btu/lb $^\circ$F	.37
Emissivity,	.90
Ablation Temperature, $^\circ$F,	1100
Effective Heat of Ablation, Btu/lb,	8800
Karma Wire	
Density, lbs/ft^3	505
Thermal Conductivity, Btu/hr ft^2 $^\circ$F/ft	7.51
Specific Heat, Btu/lb $^\circ$F	.104

Table V

GAS RETENTION RESULTS

Material	Pressurizing Gas	Maximum Temperature at Which Significant Leakage Occurred (°F)	Time at Maximum Temperature Level Before Significant Leakage Occurred (Minutes)	Remarks
S-6510	Air	870	5	Specimen started smoking after 5 minutes at 870°F.
S-6510	N_2	915	0	Specimen was held for 12 minutes at 870°F and failed when temperature was increased to 915°F.
K-1305	N_2	985	30	Test fixture seal failed at this time.
Y-3350	N_2	1030	10	Gradual increase in leakage when temperature was increased to 1070°F at which time fixture seal failed.
SE-5517 (two-ply fabric)	N_2	870	10	Gradual increase in leakage to specimen failure at 1070°F
SE-5517	N_2	--	--	Specimen withstood a pressure of 30 psig at 980°F for approximately 2 min. at which time test fixture seal failed.

NOTE: 1. Test Pressure 10 psig except as noted.
2. All specimens single ply metal cloth except as noted.

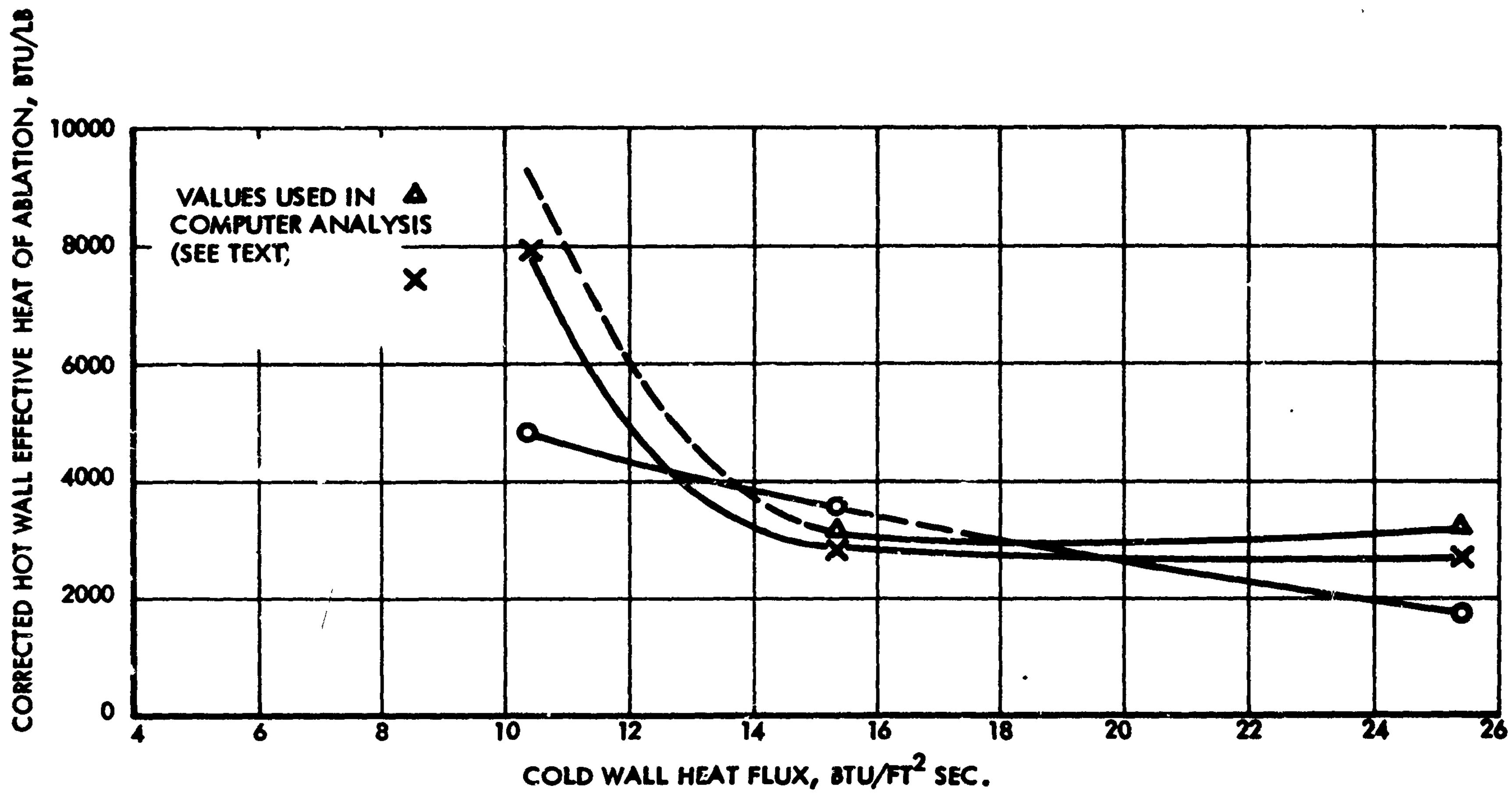

Figure 45. Corrected Hot Wall Effective Heat of Ablation Versus Cold Wall Heat Flux

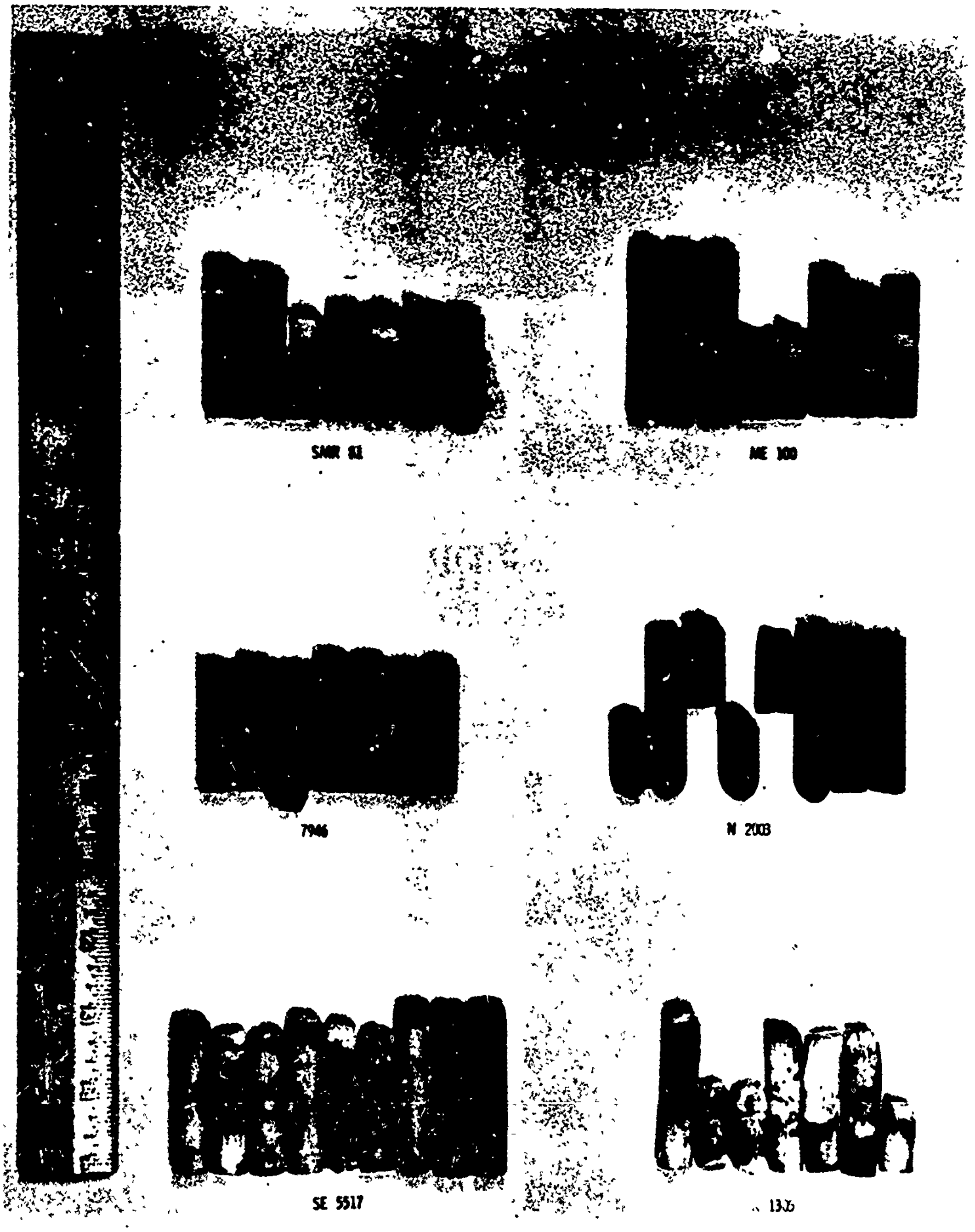

335/036

Figure 46. Plasma-Jet Test Specimens

SE 5517

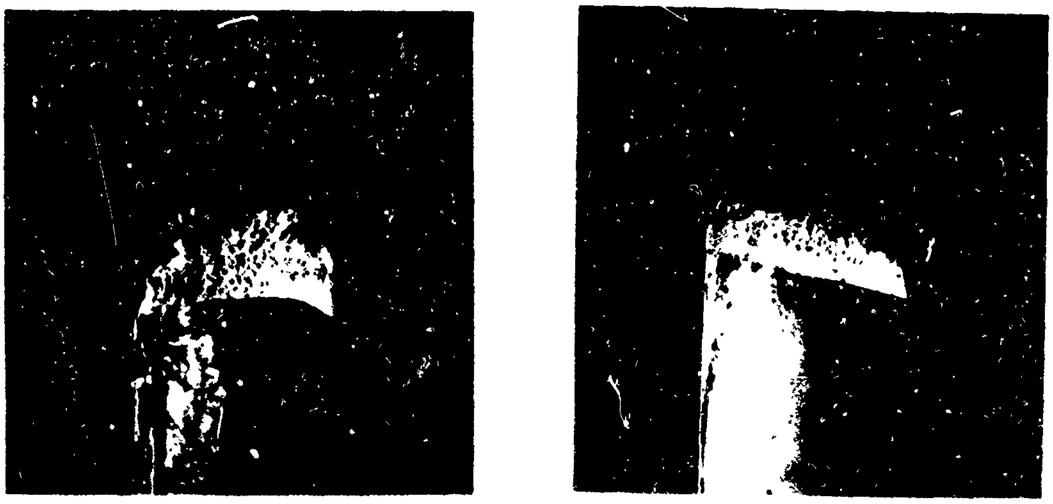

SG/27

K 1305

Figure 47. Sectioned Plasma-Jet Test Specimens

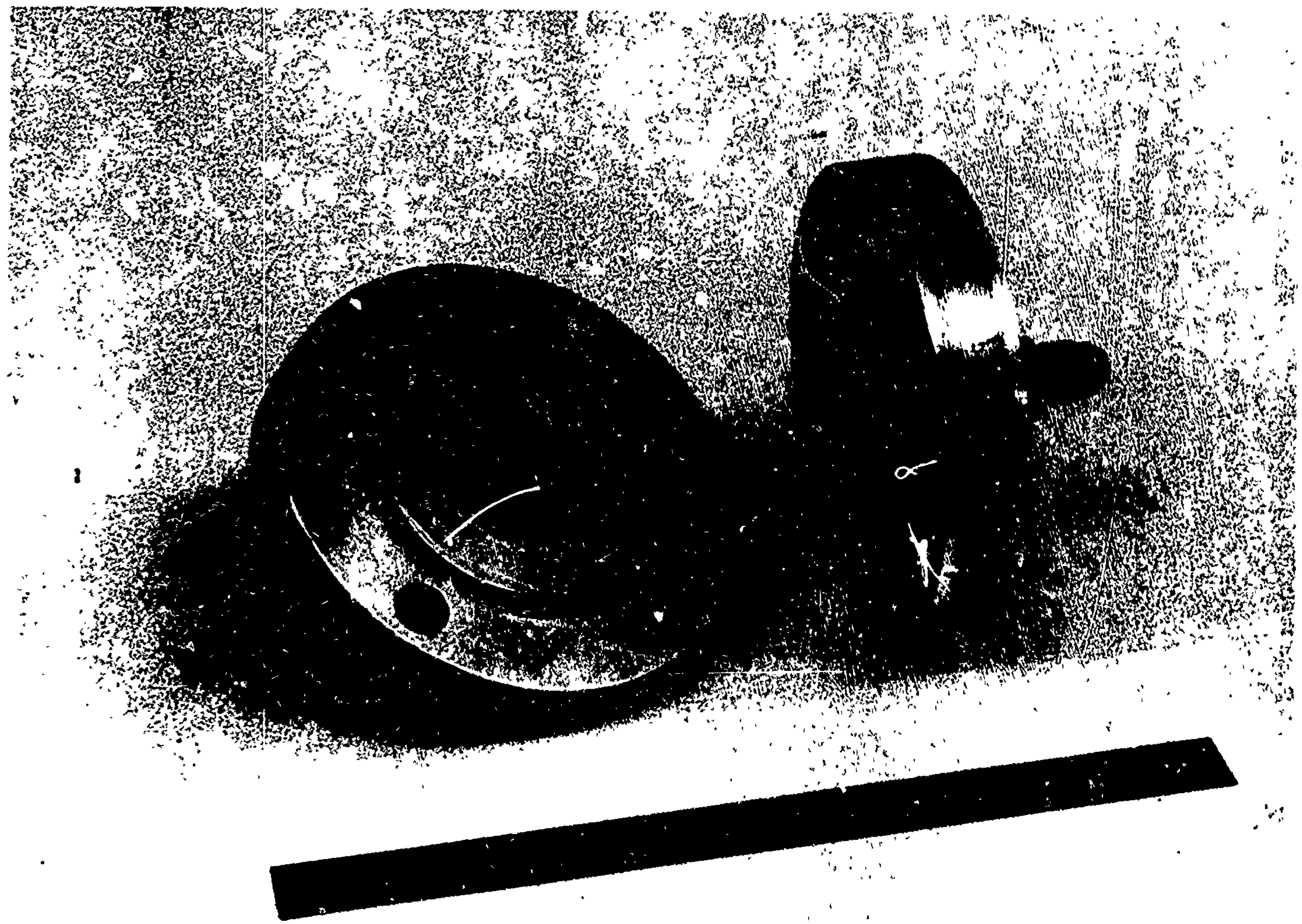

335/009

Figure 48. Permeability Test Fixture

850-900°F for at least 10 minutes without failure. This is in spite of the fact that the presence of oxygen cannot be precluded, and it is likely that there was more oxygen present than there will be during the re-entry maneuver of the paraglider at high altitude. If the partial pressure of oxygen in an "inert" nitrogen gas chamber at one atmosphere total pressure were to be the same as the 260,000-foot altitude at which maximum materials temperatures are reached during re-entry, the concentration of oxygen in the nitrogen would be 7.8 PPM.

In appearance some of the silicone rubber specimens behaved much better during this test than others. It will be noted in Figure 49, that the specimens of S-6510, SE-5517, and Y-3350 tended to melt and flow somewhat, and did not give any indication of surface cracking and crazing which are the major deterents to the use of silicone elastomers for ablation and sealing coatings. The K-1305 tended to chalk and flake more than the other specimens mentioned above. For this reason, emphasis was placed on testing the S-6510 and Y-3350 in final plasma arc tests discussed in Section 3.6.1.2.

3.6.2 REINFORCING FABRIC

In addition to the Silicone Materials Requirement (See Section 3.6.1), a materials Requirement for Reinforcing Fabrics was prepared and sent to 40 potential suppliers of reinforcing fabrics. A copy of this requirement, No. 335-R2, is reproduced in Appendix II.

Fabric Research Laboratories, Dedham, Massachusetts, was retained as consultant to: (a) evaluate samples of metal fabric and assist in obtaining such samples, (b) assist Space-General in the design of a fabric meeting Space-General's Fabric Reinforcing Requirement, (c) evaluate final fabric when woven, and (d) prepare consultation reports of findings and recommendations. Fabric Research Laboratories very ably performed these functions (in addition to twisting the yarn for the final fabric) and the results of their work are included in this report.

3.6.2.1 GLASS FABRICS

Since regular type E fiber glass is inadequate as a structural reinforcing material at temperatures approaching 1000°F, the new high strength S-994 (Owens Corning) fabric was evaluated by Space-General as soon as samples became available early in 1963. This glass fabric had the conventional HTS, epoxy compatible finish. After a number of exploratory tensile tests, with no particular coupon edge preparation, a more formalized set of tests was run using the grab method, cut strip method, and ravel strip method of Federal Specification CCC-T-191b. These results are presented in Table VI. It will be noted that the maximum strengths ranged from 810 pounds/inch to 643 pounds/inch depending on the method of test.

Comparative tests were then run on standard type E, 181 glass fabric and maximum loads on standard test specimens, per method 5110 of the

Table VI

RESULTS OF EXPLORATORY ROOM TEMPERATURE TENSILE TESTS OF S-994 181 GLASS FABRIC USING FEDERAL TEST METHODS; ALL SPECIMENS ORIENTED PARALLEL WITH WARP DIRECTION

Specimen Number	Federal Test Method (1)	Specimen Width in.	Jaw Width in.	Maximum Load (2) lbs./in	Elongation at Max. Load (3) % in. 3 in.
1 GC	5100:	4.0	1.0	-	-
2 GC	Grab			740	9.2
3 GC	Method			810	10.4
4 GC				785	10.0
5 GC				765	10.0
6 GC				808	10.8
1 GR	5100:	4.0	1.0	772	9.7
2 GR	Grab			731	9.6
3 GR	Method			681	8.0
4 GR				747	9.4
5 GR				755	9.6
6 GR				767	10.4
1 C	5102:	1.0	1.0	696	9.2
2 C	Cut Strip			643	9.1
3 C	Method			730	8.6
4 C				660	8.0
5 C				735	9.6
6 C				725	10.0
1 R	5104:	1.0	1.0	653	8.8
2 R	Ravel Strip			800	10.4
3 R	Method			689	9.2
4 R				808	10.4
5 R				700	10.0
6 R				680	9.6

(1) Federal Specification CCC-T-191b, "Textile Test Methods," 15 May 1951.
(2) Crosshead speed 12.0 in/min.
(3) Gage length: 3.0 in.

335/048

SE-5517

335/049

Y-3380

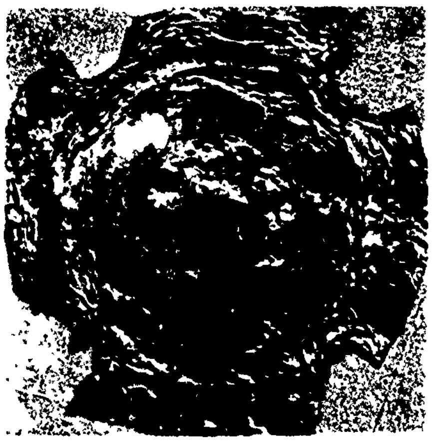

335/046

K-1305

335/047

DC-6510

Figure 49. Permeability Test Specimens

above federal specification, ranged from 118 to 212 pounds/inch. The same material with a special stitched joint, prepared by Kirby Fiberglass Company, was tested according to the same federal specification method. It will be noted from Table VII that the maximum strength of the seamed specimens ranged from 30 to 65 pounds per inch or approximately 30% of the strength of the parent material. Failure, as shown in Figure 50 was adjacent to the seam.

Table VIII illustrates the results of tests on heat cleaned type S-994, 181 glass fabric. Since it appeared that heat cleaning might be necessary to remove the HTS finish in order to make the fabric compatible with silicone coatings, these tests were performed to illustrate the possible effect of heat cleaning on the handling and fabrication operations. It will be noted that the decrease in maximum load from 675-759 pounds/inch to 76-104 pounds/inch indicated about 1/8 the original strength after heat cleaning. Even though subsequent coating with silicone rubber might increase the glass strength, it is apparent that the fabric would be more susceptible to damage after heat cleaning and it is doubtful whether all of its strength would be re-gained after coating. Samples of S-994 glass fabric with a silicone compatible finish were subsequently obtained but not tested due to the fact that the manufacturer could not recommend glass fabric for this application in which severe folding and packaging followed by high temperature flexing would be encountered. Representatives of Owen Corning stated that the high temperature application would require S type glass while the packaging and in-flight flexing would require a fabric with beta (small diameter) filaments, which was not available in S glass at the time (1963) that a selection of the reinforcing fabric had to be made. Beta filament S glass is becoming available now in 1967.

3.6.2.2 MONOFILAMENT METAL CLOTH

Because of the more attractive qualifications of woven metal fabric, efforts were turned to testing of coated and uncoated monofilament stainless steel cloths. Mult filament alloy fabrics were being produced in 1963 on essentially a laboratory basis but they were not immediately available at the beginning of this material evaluation phase. Table IX illustrates some of the results obtained on four different finely woven stainless steel monofilament fabrics. It will be noted that maximum strength ranges from about 38 pounds/inch to 69 pounds/inch depending upon the fabric mesh and filament diameter as well as the direction of tensile pull. The specimens under (b) in Table IX for 2.1 mil filament diameter, 200 mesh fabric, ruptured at maximum strengths about 30% below the value of 64 pounds/inch which had been published by other investigators (Reference 5).

3.6.2.3 MULTIFILAMENT METAL FABRIC

The first multifilament metal fabric sample was obtained from Unique Wire Weaving Company. This sample was woven 100 x 100 mesh with cabled yarns consisting of seven 0.0015-inch diameter filaments. It was a relatively dense but reasonably flexible fabric. The yarns were twisted fairly

Table VII

RESULTS OF ROOM TEMPERATURE TENSILE TESTS OF STITCHED TYPE E, 181 GLASS FABRIC

Specimen Number	Specimen Width in.	Jaw Width in.	Maximum Load lbs/in.
*			
1 CS	4.0	1.0	65
2 CS	4.0	1.0	43
3 CS	4.0	1.0	45
4 CS	4.0	1.0	30
5 CS	4.0	1.0	60
(1)			
RB 1	4.0	1.0	212
RB 2	4.0	1.0	118
RB 3	4.0	1.0	194
RB 4	4.0	1.0	177

* Seamed Specimens

(1) Parent Material Specimens

Table VIII

RESULTS OF ROOM TEMPERATURE TENSILE TESTS OF HEAT CLEANED S 994, 181 GLASS FABRIC

Specimen Number	Specimen Width in.	Jaw Width in.	Maximum Load lbs/in.
(1)			
R-1	4.0	1.0	718
R-2	4.0	1.0	759
R-3	4.0	1.0	675
R-4	4.0	1.0	740
(2)			
H-1	4.0	1.0	98
H-2	4.0	1.0	99
H-3	4.0	1.0	104
H-4	4.0	1.0	103
H-5	4.0	1.0	76

(1) As received material specimens

(2) Heat cleaned material specimens

Table IX

RESULTS OF ROOM TEMPERATURE MECHANICAL TESTS PERFORMED ON TYPE 316 STAINLESS STEEL FABRIC (MONOFILAMENT)

Specimen Number	Federal Test Method	Direction Of Specimen Taken	Specimen Size In Inches	Maximum Load To Rupture lbs/in.
(a)	*			
SS-1	5102	Fill	1x6	40.0
SS-2	5102	Fill	1x6	40.0
SS-3	5102	Fill	1x6	38.0
SS-4	5102	Warp	1x6	41.0
(b)				
SS-7	5102	Fill	1x6	39.0
SS-8	5102	Fill	1x6	40.0
SS-10	5102	Warp	1x6	48.0
SS-11	5102	Warp	1x6	46.0
SS-12	5102	Warp	1x6	49.0
(c)				
SS-13	5102	Fill	1x6	48.0
SS-14	5102	Fill	1x6	50.0
SS-15	5102	Fill	1x6	49.0
SS-16	5102	Warp	1x6	56.0
SS-17	5102	Warp	1x6	61.0
SS-18	5102	Warp	1x6	60.0
(d)				
SS-19	5102	Fill	1x6	55.0
SS-20	5102	Fill	1x6	55.0
SS-21	5102	Fill	1x6	52.0
SS-22	5102	Warp	1x6	65.0
SS-23	5102	Warp	1x6	68.0
SS-24	5102	Warp	1x6	69.0

* Specimens were loaded at a rate of 0.5" per minute
(a) 200 mesh-filament diameters 1.6 mils
(b) 200 mesh-filament diameters 2.1 mils
(c) 170 x 120 mesh-filament diameters 2.4 mils
(d) 150 x 120 mesh-filament diameters 2.6 mils

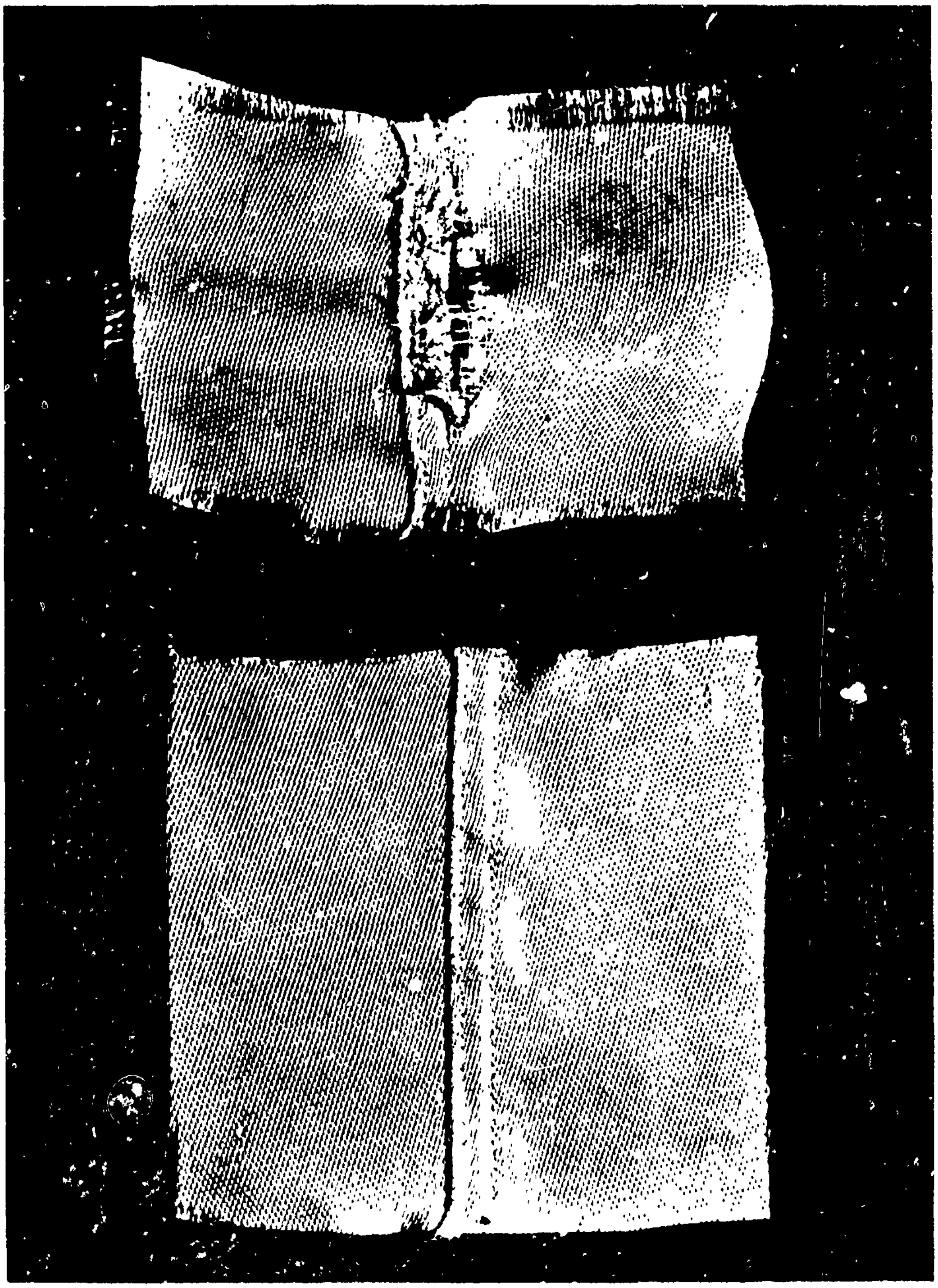

Figure 50. Sewed Fiberglass Specimens

tightly, at 10.7 turns per inch, consistent with the wire industry's "lay twist" custom while the textile industry generally uses a more limp yarn in which the fibers are only twisted two to three turns per inch.

Testing of the stainless steel fabric from Unique Wire Weaving Co. produced the strength and elongation characteristics presented in Table X. In general, the results indicated that this material was not sufficiently strong or flexible and had inadequate crease resistance and crease recovery for purposes of this program. However, these tests provided definite indications of the qualities to look for in a multifilament metal fabric. As a result of this testing of this early version of multifilament metal fabric, recommendations were prepared for the selection of a final fabric.

Investigations by Fabric Research Laboratories indicated that since the escape vehicle must be packed into a small container prior to deployment, a fabric with flexibility and crease recovery, as comparable as possible to typical organic filament fabric, was desired.

Flexibility implies low bending rigidity. Metallic filaments, as a class, are ten to twenty times stiffer than organic filaments of equal tensile strengths. This difficulty can be overcome by decreasing the diameter of metal filaments and increasing their number in the yarn to maintain the total tensile strength of the yarn. Such a structural design results in the yarn rigidity being proportional to the square of the filament diameter. This indicates that metallic filaments would have to be drawn to less than 1/4 the diameter of organic filaments to achieve equal yarn rigidity at equal strength, assuming complete freedom of filaments to bend individually.

The diameter of typical organic filaments is approximately 0.5 to 1.0 mil. The diameter of metallic filaments necessary to achieve equal yarn rigidity at equal strength would therefore be in the order of 0.1 to 0.25 mil. Also, in yarns of comparable strength and stiffness, there would be about 700 to 1400 metal filaments per yarn compared to 50 to 100 organic filaments. At the time of the material selection in this program (1963), 0.5 mil wire was the finest commercially available in quantity, and today (1967) this is still largely true.

Since poor fabric flexibility and wrinkle recovery would be detrimental to the performance of a paraglider or any other space structure requiring flexibility, wire larger than 1.0 mil diameter for the reinforcing fabric would not be desirable. Of course, fabric woven from 0.5 mil wire would be the most suitable. However the high price of that material made it unattractive compared to 1.0 mil wire which presents a compromise between fabric performance and wire price.

The three alloys listed in Table XI were evaluated as candidates for the multifilament metal fabric. The particular alloys listed are products of the Hoskins Manufacturing Company, Detroit, Michigan but similar alloys are produced in ultrafine wire by other manufacturers. The nominal analysis, specific gravity and approximate price per pound for 1.0 mil wire are shown in the table.

Table X

TENSILE STRENGTH AND ELONGATION CHARACTERISTICS OF UNIQUE'S 304 STAINLESS STEEL CLOTH*

Direction	70°F Rupture		1000°F Clam-Shell Rupture		1000°F Hot Box Rupture		Translation** (%)
	Elongation (%)	Load (lb/in)	Load (lb/in)	Translation (%)	Elongation (%)	Load (lb/in)	
Warp	38.8	154.9	-	-	17.5	84.5	54.6
Filling	20.9	151.4	92.2	60.9	8.2	92.5	61.1

Wire Diameter (Mils)	Yarn Construction	Weave Pattern	Ends/Inch (Warp Ends/Inch)	Picks/Inch (Filling Ends/Inch)	Thickness (Mils)	Weight (oz/yd^2)
1.5	7/1, 10.7 tpi	Plain	99.8	95.1	9.3	16.7

*Plain weave. Yarns composed of seven 0.0015 inch diameter type 304 stainless steel wires twisted together approximately 10.7 turns per inch.

**Translation of load from room temperature strength, $\frac{1000^\circ F \text{ tensile strength}}{70^\circ F \text{ tensile strength}}$

Table XI

COMPARISON OF 1.0 MIL CHROMEL WIRE

Wire	Nominal Analysis	Specific Gravity	Approximate Price
Chromel A	80 Ni, 20 Cr	8.41	$220 per pound
Chromel D	35 Ni, 20 Cr, 1.5 Si, 0.5 Mn, 0.1 C, balance Fe	7.94	180 per pound
Chromel R	73 Ni, 20 Cr, 3 Al, 3 Fe, 0.5Si, < 0.05 C	8.10	260 per pound

Chromel D is an alloy Hoskins markets instead of stainless steel. The price per pound is about the same as stainless steel and its elevated temperature properties are claimed to be somewhat superior to those of the various types of stainless steel.

Hoskins supplied 50 feet of fully annealed 1.0 mil wire of each of the three alloys to Fabric Research Laboratories for evaluation. Although considerably greater yield and rupture stresses are obtained with hard temper wire, the increased elongation that is characteristic of fully annealed wire is probably advantageous in the application contemplated. It will not only facilitate twisting and weaving the wire, but also should enhance the performance of a space vehicle by allowing greater opportunity for crease recovery, elongation balance, and load distribution.

A stress-strain diagram for each alloy at 70°F is shown in Figure 51, and at 1000°F in Figure 52. At both 70°F and 1000°F, Chromel R exhibits the highest yield stress and rupture stress and Chromel D the lowest.

The translations of the yield and rupture stresses of the wires from 70° to 1000°F, i.e., the rupture stress at 1000°F as a percent of the stress at 70°F, are given in Table XII. As shown, Chromel R exhibits the highest translation and Chromel D the lowest.

The rupture stress per dollar and the yield stress per dollar at 1000°F are also given in Table XII. As shown, the values are very close, with the yield stress per dollar of Chromel R being slightly greater than that of the other alloys. The ratio of yield stress at 1000°F to the specific gravity is given also in Table XII for the three alloys. This ratio is proportional to the ratio of fabric strength to fabric weight. As shown Chromel R exhibits the largest and Chromel D the smallest.

On the basis of the above information, Chromel R alloy or equivalent was selected for the purposes of this project.

Table XII

TRANSLATIONS OF YIELD AND RUPTURE STRESSES OF 1.0 MIL CHROMEL WIRES

Wire	Stress Translation (%) from 70°F to 1000°F		Rupture Stress/Dollar at 1000°F (PSI/$)	Yield Stress/Dollar at 1000°F (PSI/$)	Yield Stress at 1000°F/Specific Gravity (PSI)
	Yield	Rupture			
Chromel A	81.1	8.13	480.0	332.1	8,750
Chromel D	70.2	73.1	481.7	317.8	7,280
Chromel R	83.8	83.7	479.5	343.5	11,100

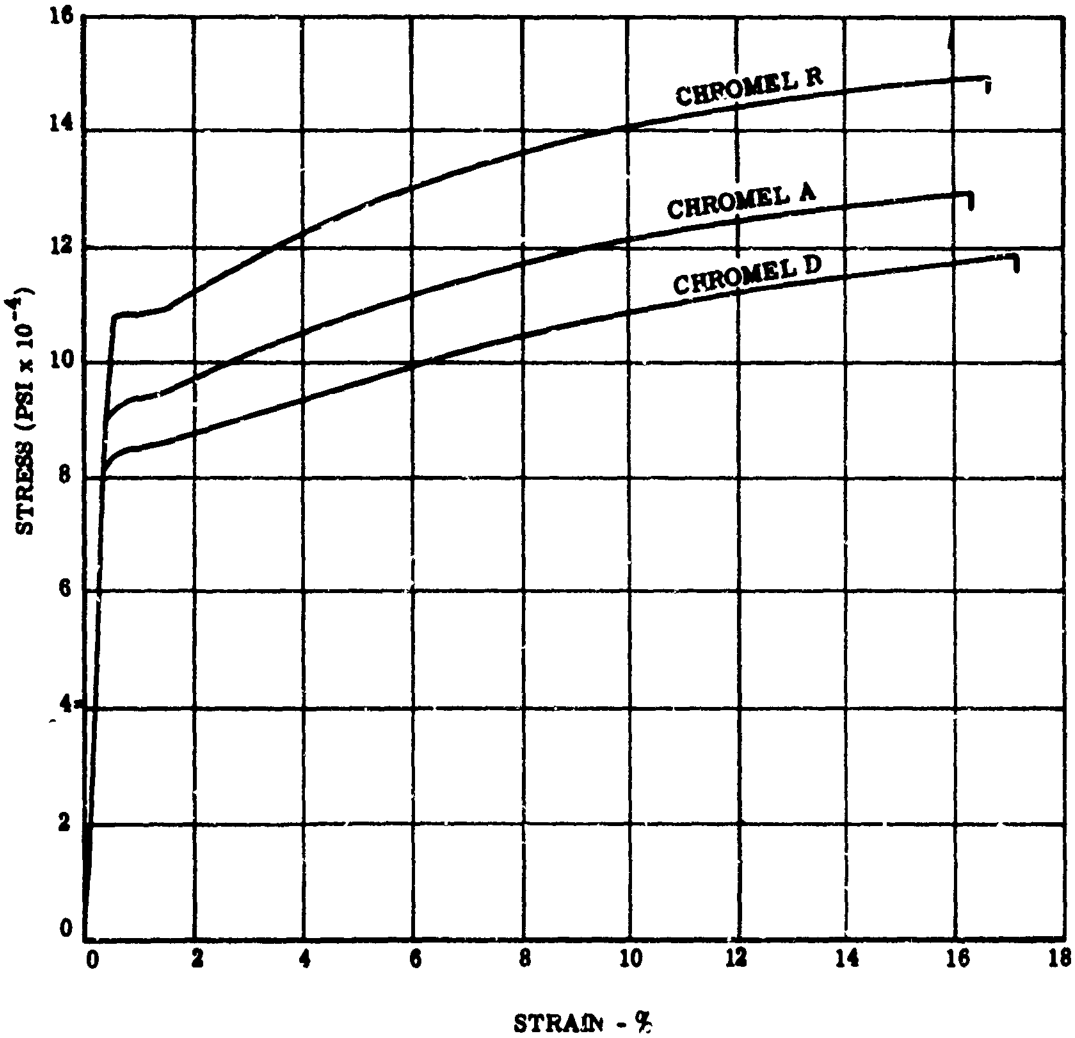

Figure 51. Stress-Strain Diagrams of 1.0 Mil Chromel Wires at 70°F

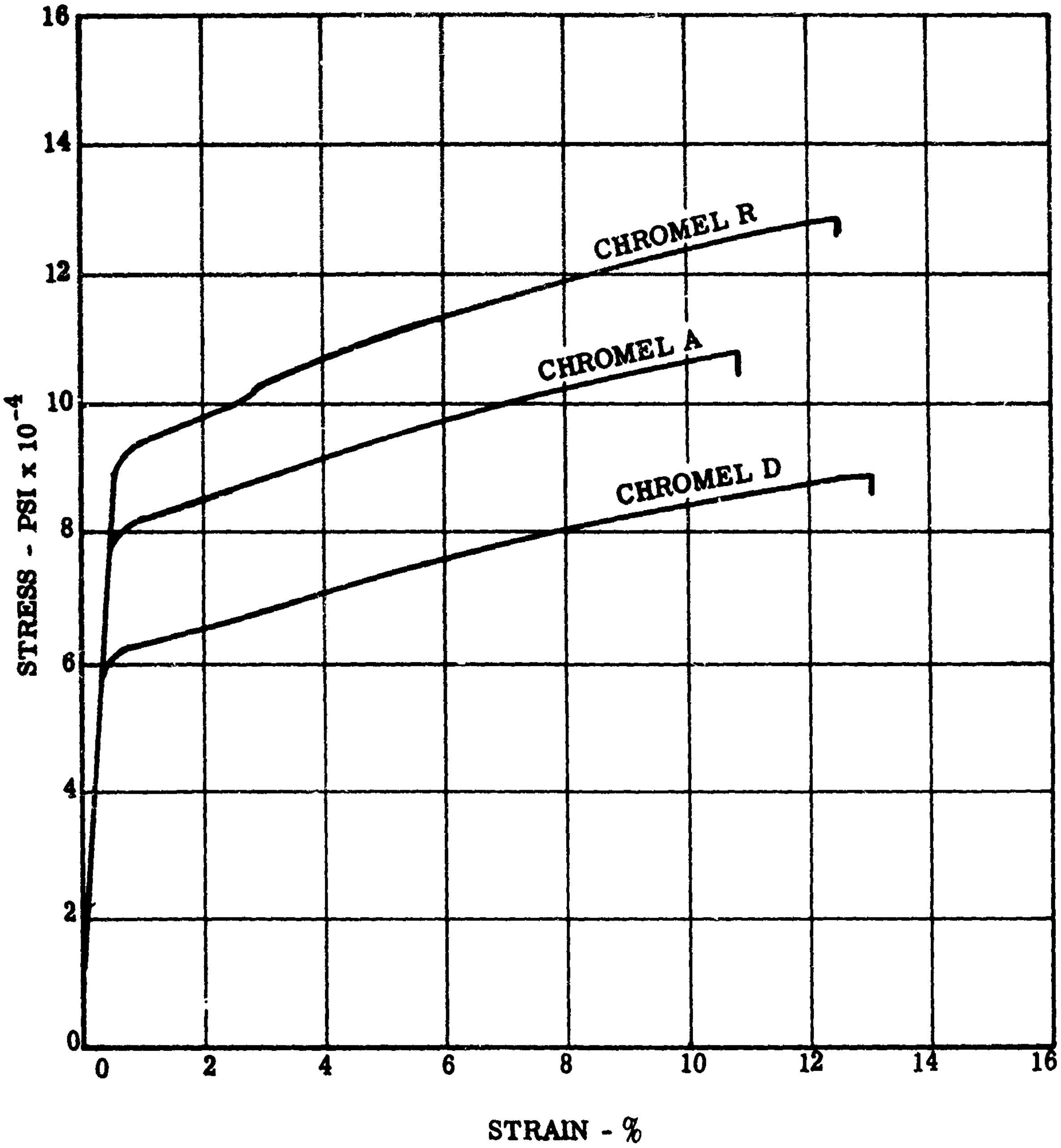

Figure 52. Stress-Strain Diagrams of 1.0 Mil Chromel Wires at 1000°F

A 2 x 2 basket weave fabric was chosen as the most suitable fabric construction. A more tightly interwoven fabric such as a plain weave would result in greater fabric shear strength but lower tear strength, wrinkle recovery, fold endurance, and tensile strength (due to greater crimp). A longer float weave such as a 3 x 5 twill will result in somewhat greater fabric tear strength, wrinkle recovery, fold endurance, and tensile strength but considerably less shear strength.

In order to obtain the highest fabric fold endurance, wrinkle recovery, and tensile strength with multifilament yarns composed of 1.0 mil wire, a low yarn twist of 2 to 4 turns per inch was recommended.

To facilitate yarn handling during weaving, the yarn should be torque-free, i.e., the yarn should exhibit no twist unbalance. This can be accomplished by twisting the filaments together and then annealing the yarn. A balanced yarn can also be obtained by twisting filaments together into a plied yarn and then twisting a group of the plied yarns together into a cabled yarn. If a cable twist of the correct magnitude and opposite direction to that of the plied twist is used, a balanced yarn can be obtained.

Tensile strength tests of fabrics woven from Chromel A were run at 70° and 1000°F to evaluate the performance of fabric under tension relative to single wire filaments.

It appeared from a study of several different alloys and types of fabrics that were available, that Chromel R (trademark of Hoskins Manufacturing Company, Detroit, Michigan) or equivalent alloy with a nominal analysis of 73 Ni, 20 Cr, 3 Al, 3 Fe, 0.5 Si, would be the most desirable material. The final fabric was made from 1.0 mil wires of the above alloy and consisted of 7 filaments twisted 3.0 Z (left hand) and 7 of these plied yarns twisted 2.0 S (right hand) to give a 49 filament yarn. This yarn was woven 58 picks and 58 ends per inch in a 2 x 2 basket weave. Two plies of this fabric were used in 45° relationship for the basic structure of all of the test components in this program.

3.7 PROCESS DEVELOPMENT

The two major areas of process development were joining of the metal fabric with high strength/high temperature seams and the impregnation and coating of the metal fabric with silicone rubber compounds. The development of the metal fabric joining process included the necessary development of an applicable metal fabric cleaning process, design and fabrication of a semi-automatic metal fabric seam welder, and planning and fabrication work having to do with ancillary operations such as form tool design and construction, handling and storage aids for metal fabric, and instrumentation and auxiliary equipment for control and interpretation of all process variables.

The impregnation and coating development program included theoretical and laboratory study of the silicone rubber chemistry applicable to the required processes; engineering development of unit operations such as mixing, milling, calendering, vacuum bagging, and autoclaving; as well as the scaling up of laboratory techniques to semiproduction operations.

3.7.1 METAL FABRIC JOINING INVESTIGATIONS

Numerous joining methods for making high-efficiency seams in the metal fabric were studied and most of these methods were experimentally evaluated. Included in the methods studied were sewing, exobrazing, microspot welding, interrupted seam welding, continuous seam welding, infra-red brazing, induction brazing, resistance brazing, electron beam welding, adhesive bonding, and, although not strictly a joining process, integral weaving of compound shapes. Table XIII presents a digest of some of the investigations conducted during the six-month period during which miscellaneous joining techniques were evaluated. The X-marked spaces and corresponding data in a vertical column show the combination of variables used in each of 20 different tests.

The various techniques which have been evaluated will be discussed briefly along with conclusions resulting from investigations.

3.7.1.1 SEWING

In addition to the unsuccessful attempts to obtain high-efficiency seams in fiber glass, discussed in Section 3.6.2.1, consideration was given to the use of sewing as a means of joining metal fabric. At the time of the investigation on this program in 1963, consultation with the Singer Sewing Machine Co. led to the conclusion that sewing of ultra-fine filament metal fabric would not be practical using existing sewing equipment. Attempts to make sewn joints resulted in maximum joint efficiencies, relative to parent fabric strength, of less than 60 percent. Since that time, Fabric Research Laboratories has developed sewing techniques for metal fabrics, using metal yarn, which demonstrate joint efficiencies in excess of 90 percent, and this is comparable with the efficiencies finally obtained in this program, by welding. Limitations still exist today in sewing techniques, however. A double-fold seam must be used which results in four layers of fabric to join two pieces. Also, maximum efficiencies are only obtained with four parallel rows of stitches. Crossing or intersecting seams present complications which have not been solved to date; that is, it has not been practical to sew more than two pieces of fabric together in the same seam.

As will be discussed subsequently in this report, the final welding technique developed in this program permits joining of up to six pieces or layers of fabric with efficiencies of 90 percent or better, and thickness is considerably less than the sewn seam since double-fold seams are not required. Even with present state-of-the-art it would be impossible to fabricate a complex structure of many separate patterns (such as the paraglider apex) using the sewing technique.

Table XIII

TABULATION OF METAL CLOTH JOINING DATA

15 Sept through 15 Oct 1963

TEST COMBINATIONS

GROUP	VARIABLE	1	2	3	4	5	6	7	8	9	10	11	12	13	14	15	16	17	18	19	20
I. Materials	1. Metal Cloth																				
	a. Chromel "A"	X					X									X	X	X	X	X	X
	b. Tomil Bolting		X	X	X	X		X	X	X	X	X	X	X	X						
	2. Brazing Alloy																				
	a. Lithobraze "BT"	X	X	X	X	X															X
	b. Stoflo 761*																				
	c. None						X	X	X	X	X	X	X	X	X	X	X	X	X	X	
II. Methods	1. Joining																				
	a. Aeroray Braze		X																		
	b. Spot Braze	X		X	X																
	c. Roll Seam Braze*																				X
	d. Spot Weld					X			X	X	X	X	X	X	X	X	X	X	X	X	
	e. Roll Seam Weld						X	X													
	2. Precleaning																				
	a. None					X	X	X	X	X	X										X
	b. Degrease & Deoxidize	X	X	X	X							X	X	X	X	X	X	X	X	X	
	3. Atmosphere Control																				
	a. Standard Atmosphere	X			X	X	X	X	X	X	X	X	X	X	X	X	X	X	X	X	X
	b. Enclosed Chamber } A or N_2		X																		
	c. Local Purging			X																	
	d. Reducing Gas (6% H_2)		X	X																	
III. Configuration	1. Tensile Test																				
	a. Gauge Length, in.	1.13	2	2	2	2	2	2	2	2	2	2	2	2	2	2	2	2	2	2	2
	b. Specimen width, in.	1	1	1	1	1	.75	.5	1	1	1	1	1	1	1	1	1	1	1	1	1
	2. Single Seam Lap		X				X	X				X									X
	3. Double Seam Lap	X		X	X	X			X	X	X		X	X	X	X	X	X	X	X	
	4. Number of Spots/Inch	20		20	20	20			40	40	40	40	40	40	40	30	67	40/60	200	100	
	5. Seam Spacing, mils	125		125	125	.25			125	125	125	none	125	125	125	60	60	125	60	60	
	6. Reused Specimen															X	X	X	X	X	
IV. Results	1. Number tested	1	17	12	29	6	1	2	15	8	6	10	12	6	6	3	3	6	7	7	2
	2. Avg. Joint Efficiency, %	62	58	77	60	86	18	66	63	34	75	58	90	83	80	67	61	56	82	60	78
	3. Min. Joint Efficiency, %	62	56	67	27	75	18	60	22	19	66	36	80	80	75	50	61	45	71	32	72
	4. Max. Joint Efficiency, %	62	72	89	92	96	18	60	89	66	88	72	94	89	87	84	67	62	89	72	80
V. Remarks	1. Footnote number	2		2	2	2	8	8	2,7	2,6	2,5	2	2,9	2,4	2,3	1	1	2	1	1	10

1. Spot weld seam spacing of 60 mils and spot spacings were controlled by use of graduated machine tool holder.

2. Spotweld seam spacing is approximate. Spot spacing estimated from counting as spotwelds were made.

3. Post-cleaning time lapse experiment; joints were made in early morning with material which had been cleaned and deoxidized late the previous afternoon. Tape was used to secure the cloth sections, with paper inserted at joint area to prevent contamination by the tape adhesive.

4. Joint contamination experiment; joints were made with material which had been secured with masking tape passing over joint areas immediately following precleaning. Tape removed just before joining. Joints made within one-half hour after precleaning.

5. Joints made by Unitek during a visit to their Monrovia, Calif. facility, using 1085C welding head set at 7.25 pounds tripping pressure and a 1057 power supply set at 2.5 watt-seconds.

6. Joints made with guided hand probe at energy settings of 9 to 12 watt-seconds, with 100 watt-second scale of Unitek 1048B power supply.

7. Initial experiments at SOC with Unitek pulse welder using Unitek model 1032B commercial bench type welding head.

8. Joints roll seam welded by Sciaky Bros. Co.; failure loads extrapolated to one inch width.

9. This combination is the one selected for fabrication of test cylinders.

10. Joints made by Alloy Spotwelders, Los Angeles.

Considering the difficulties encountered by Space-General and other investigators with sewing techniques several years ago, the recent significant accomplishments by Fabric Research Laboratories are noteworthy, nevertheless.

3.7.1.2 ADHESIVE BONDING

Although non-metallic methods of joining the metal fabric did not appear encouraging, a high-temperature adhesive known as "Imidite," manufactured by Narmco Materials Division of Telecomputing (Whittaker) Corp., was reported to withstand temperatures in excess of 1000°F with substantial strength. The chemical name for the material is "polybenzimidazole." At the time Narmco advised that Imidite was available coated on fiber glass fabric only, there was a significant charge for samples and it was their opinion that the material would be unsatisfactory for joining metal fabric. As a result of this information it was not investigated further.

3.7.1.3 SILICONE RUBBER BONDED JOINTS

The principal object of the tests on silicone rubber-bonded metal fabric was to determine the strength of this type of joint under simulated re-entry environmental conditions. Although it was not anticipated that this type of joint would have sufficient strength, previous Space-General work with the micrometeoroid paraglider (which reentered from a lower altitude at about Mach 6) showed this type of joint to be satisfactory.

A radiant heating method was used to produce high temperatures in specimens mounted in the jaws of the tensile test machine. The entire specimen and both jaws were enclosed in a quartz tube. Relative movement of the tensile machine jaws was permitted by sealing the tube to the pull rods of the tensile machine with a bellows-type diaphragm at one end. To take advantage of the test setup, high-temperature tensile tests were also run on stainless steel monofilament tensile bolting cloth with and without welded joints.

Prior to heating, the enclosure was purged with argon gas for 30 minutes to eliminate oxygen. This is consistent with the fact that the concentration of oxygen at the re-entry altitude is very small. Iron-constantan thermocouples were affixed to the metal fabric in each test specimen and the average thermocouple temperature was maintained at $\pm$ 10°F of the desired test temperature. The tensile failure loads of the metal cloth with silicone rubber bonded joint, with welded joint, and as parent fabric, are given in Table XIV. It will be noted that the silicone rubber bonded joint is completely unreliable since each of the three one-inch overlap by one-inch-wide joints failed at a tensile load of approximately three pounds or less.

Good correlation and precision is indicated in the data for all three types of specimens. The high strength of the welded joints relative to the parent fabric strength at the same temperature gave further encouragement for proceeding with the welded joint technology.

Table XIV

TENSILE FAILURE LOADS OF METAL CLOTH

Specimen Identification	Test Temperature (^oF)	Failure Load (lbs)
Tensil Bolting Cloth, Silicone Coated, Bonded Joint		
1	1000	3.0
2	900	18.3
3	800	22.4
4	1000	2.3
5	R.T.	55.25
6	1000	3.0
Tensil Bolting Cloth, Welded Joint, No Coating		
1	1000	28.9
2	1000	29.6
3	900	32.0
4	900	27.3
5	800	33.7
6	800	33.4
Tensil Bolting Cloth, Parent Fabric, No Coating		
1	1000	30.4
2	900	32.4
3	800	26.6
4	R.T.	56.5

3.7.1.4 CONTINUOUS WEAVING

Continuous weaving of metal fabric into closed bodies of revolution and shapes of compound curvature can be accomplished on special looms programmed by punched card systems. The programming controls the number of warp threads which are picked up for each pass of the shuttle. One pass of the shuttle is required for the top or bottom of a body of revolution, which, while on the loom, appears as a flat shape. The length of the fill thread at any point is approximately equal to one-half of the circumference of the body of revolution.

This technique offers many obvious advantages in that it would eliminate the need for longitudinal seams in long tubular shapes. It would also make possible the continuous weaving of the hemispherical end caps as an integral part of the boom. One company, Raymond Development Industries, Los Angeles, who possessed this type of capability, indicated that it would actually be more complicated to weave the toroidal apex than the tapered boom since fewer punched cards would be required. Considerable cost would be involved in making the punched cards.

The greatest deterrent to using this type of construction was that the entire paraglider could not be woven and some joints would be required. As long as it would be necessary to develop a joining technique for some locations, it appeared uneconomical to go to the expense of continuously weaving sections of the paraglider. Furthermore, the vehicle would be no stronger than the seams joining the woven sections. It was not certain that the continuously woven section would be of uniform strength since the points or lines where yarns are dropped off to change contour are physical discontinuities in the structure and have the appearance of a kind of seam.

Another major disadvantage to continuous weaving was that two plies of a complex shape could not be woven with the yarns in bias relationship to each other. For a given shape, the yarns always would run in given directions. The advantages of combining two plies in bias relationship, giving a truss structure, could not be realized. It is doubtful that a double-ply structure, with both plies identically oriented, could adequately carry torsional and shear loads of the type imposed on the paraglider.

3.7.1.5 EXOTHERMIC BRAZING

At the time of this investigation in 1963, a process called "Exobraze" was under development by the Narmco Research and Development Division of Telecomputing (Whittaker) Corporation and samples of joints made by this method were obtained from Narmco. Figure 53 shows a typical joint in monofilament stainless steel cloth using this technique.

In principle the Exobraze system is quite simple and may offer significant potential for some applications. A strip of brazing alloy is applied to the joint area and an exothermic material is also overlaid. The exotherm is then

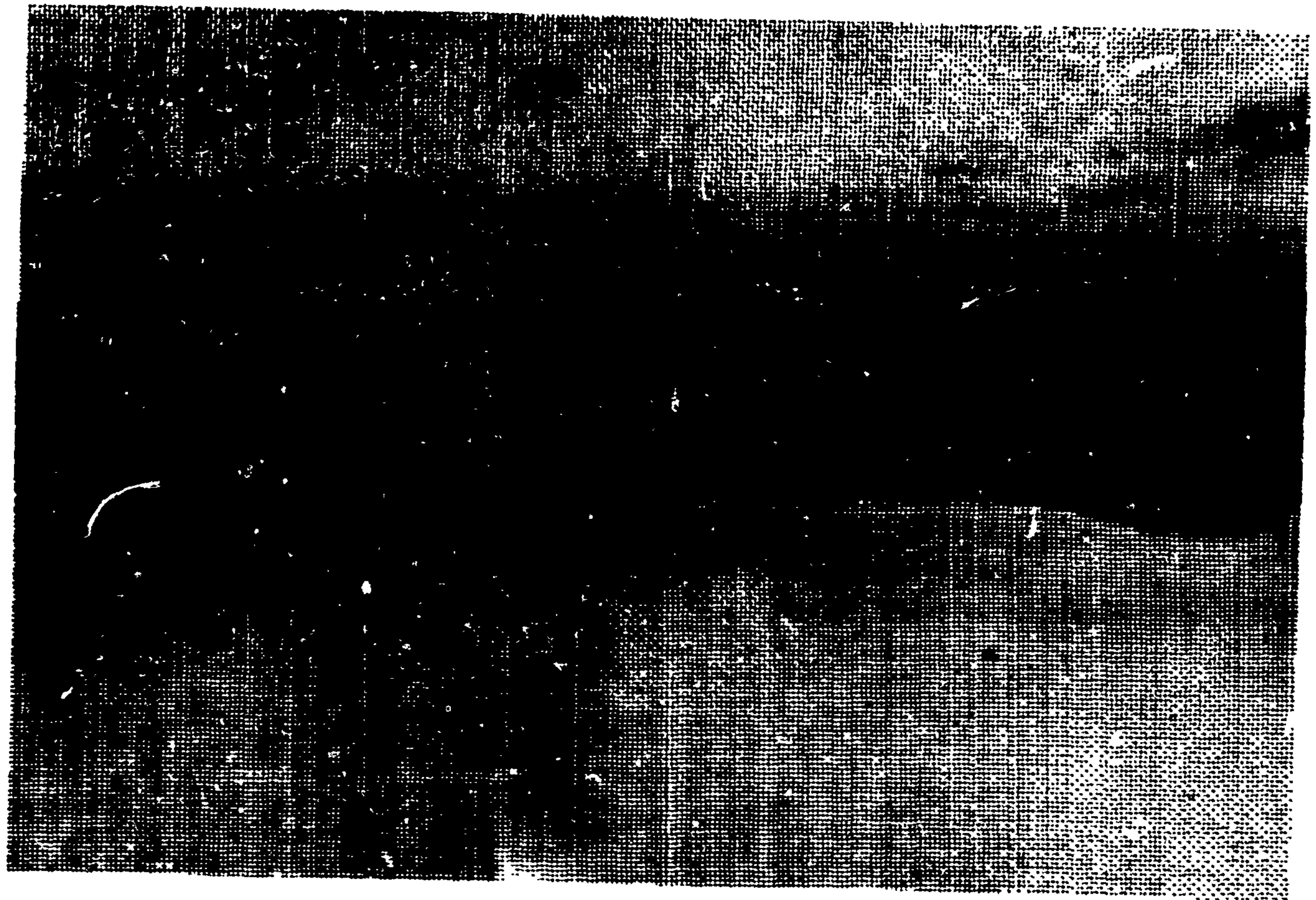

Figure 53. Exobrase Joint

ignited and produces sufficient heat to melt the brazing alloy and increase the temperature of the materials to be brazed to effect a brazed joint. Since the exothermic material contains its own oxidizing agent and organic carriers, the brazed joint becomes oxidized and discolored during the process. Since the wire filaments in the fabric material which Space-General planned to use were 0.001 inches in diameter, the loss of strength in individual filaments due to oxidation was of concern.

Probably the greatest deterrent to this process was the joint rigidity due to a continuous strip of brazing alloy being formed. With multifilament fabrics utilizing close packed yarns, the stiffness of the joint would be completely unsatisfactory for flexible structures. Attempts to sharply crease such joints indicated significant cracking.

3.7.1.6 INFRA-RED BRAZING

A new development, which had become available in 1963, was the Aeroray Braze Gun manufactured by Aerojet-General Corporation. Figure 54 shows the gun in use brazing a joint in a metal cloth tubular section. The gun is basically a heat source utilizing a quartz lamp and a highly polished and focussed parabolic reflector which concentrates the energy on a line on the work piece. The area being heated is enclosed by the gun and provision is made for the introduction of inert gases to preclude oxidation during brazing. A timer is also furnished as part of the standard equipment, to shut off power after a preset interval.

Considerable experimentation was devoted to this process since it showed some promise. Figure 55 shows samples of joints produced on monofilament metal cloth by this means. These were strong joints of reasonable flexibility, especially with light application of brazing alloy. Tensile tests on these joints did not indicate any significant degradation of the parent cloth and the joints had nearly 100 percent efficiency relative to parent cloth strength.

The most satisfactory brazing material found for this purpose was Wall-Colmony 50, a high-nickel alloy which is suspended in a liquid to form a slurry and then applied with a small nozzle from a pressure applicator.

The greatest drawback to this process was the fact that the joints were still not as flexible as desired and attempts to braze the thicker multi-filament woven fabrics resulted in the molten brazing alloy spreading through the fabric due to capillarity, thus making a very rigid seam. Attempts to use various "stop-braze" materials were also unsuccessful because these also tended to saturate the fabric in an irregular fashion and actually interferred with the brazing in the desired areas.

3.7.1.7 INDUCTION BRAZING

Another method of providing the heat necessary to braze would be an induction coil. An induction brazing coil about the size of a paper clip and

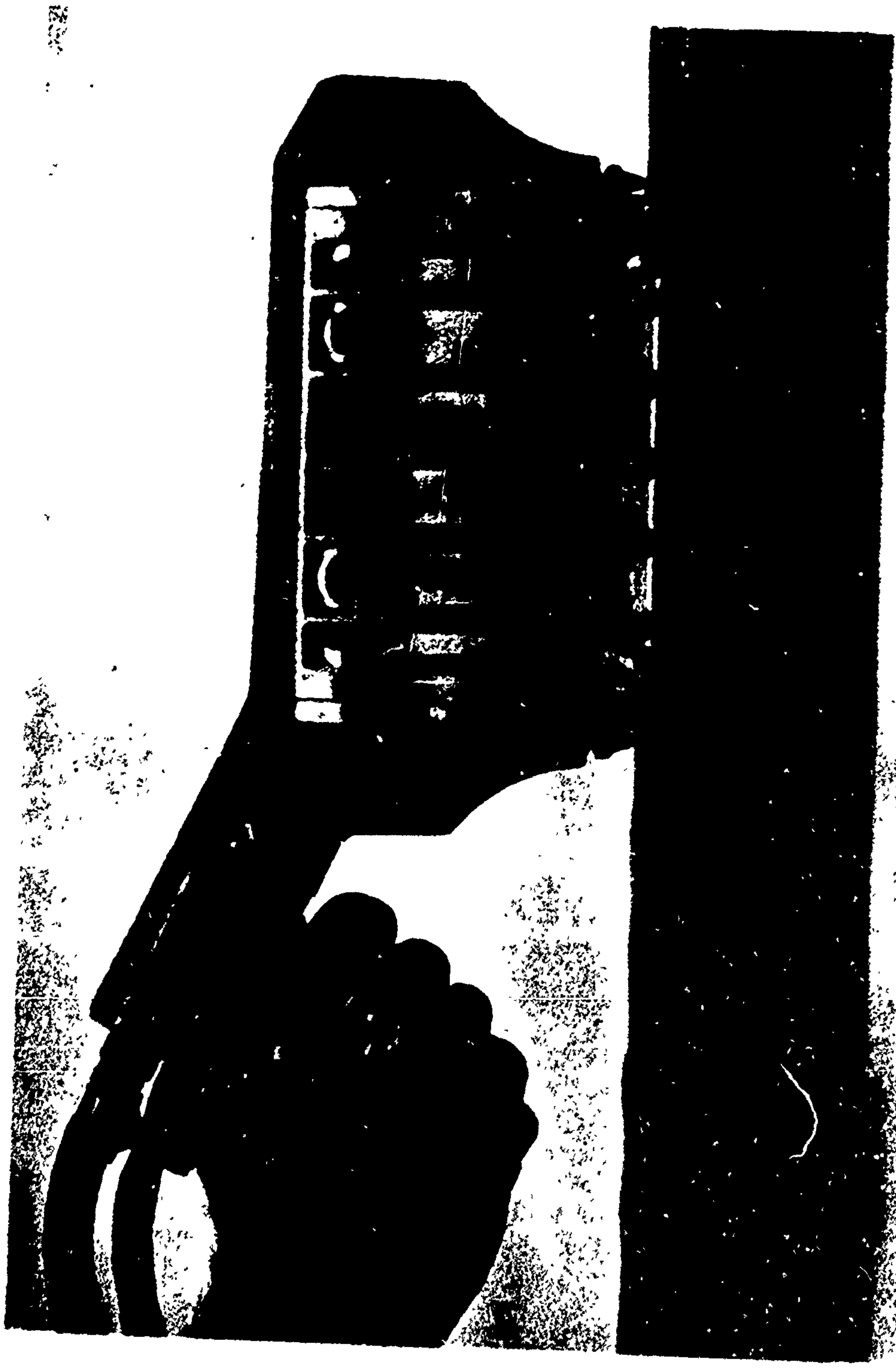

335-3/001

Figure 54. Aeroray Braze Gun

a. Light Application of Brazing Alloy

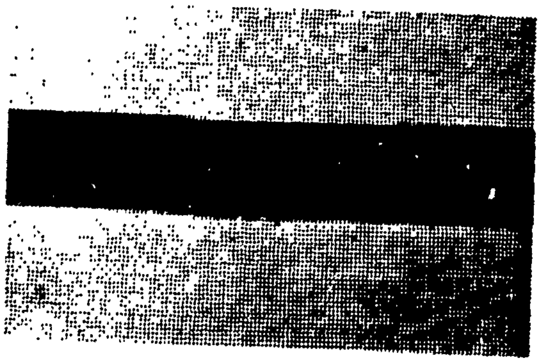

b. Medium Application of Brazing Alloy

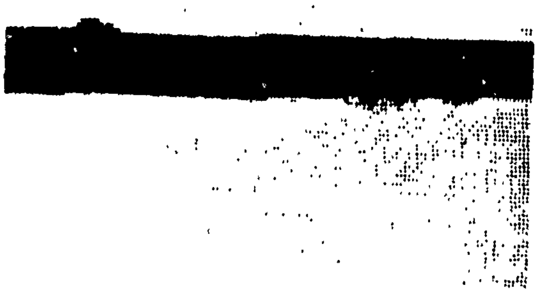

c. Heavy Application of Brazing Alloy

Figure 55. Infrared (Aerobraze) Braze

mounted like a small soldering iron would permit brazing in confined a. long compound curves. Such a coil could be made portable by using a coaxial cable to deliver the necessary power. However, joints made with such a tool also require an inert atmosphere. A number of such joints were made with induction brazing coil, as illustrated in Figure 56. This heating coil was somewhat larger than the one ideally described above but demonstrated the fact that the inert atmosphere was necessary and obtaining it in a confined area adjacent to the heated joint would be somewhat difficult. Again, as with other brazed joints, the seam was rigid and the method was abandoned.

3.7.1.8 RESISTANCE BRAZING

Spot and seam brazing using conventional resistance welding equipment showed the most promise of all the brazing techniques. The resistance welding equipment was used in the conventional manner but with molybdenum electrodes to discourage the braze alloy from adhering to them. The electrode pressure, current level, and pulse time were carefully controlled so that the individual fibers were not damaged or actually welded together. Only the brazing alloy was melted. Reasonably good brazed joints with both individual spots as well as continuous seams were produced. Photographs of these brazed joints are shown in Figure 57 illustrating a staggered spot braze on monofilament stainless steel cloth and a continuous seam braze in multi-filament Chromel-R fabric. A cross-section of seam braze is compared with a cross-section of a seam weld in Figure 58. The retention of the identity of individual filaments may be noted in the photomicrograph of the brazed joint as compared to the solid nugget produced by the weld. The brazing alloy was Lithobraze-BT alloy and was preplaced between the metal fabric layers. Joint efficiencies in excess of 85 percent were produced by the resistance spot brazing technique and an inert atmosphere was not required.

During the development of this resistance brazing method it became apparent that cleaning methods formerly employed were not adequate. New techniques involving pickling in a hydrochloric acid solution and degreasing and drying in acetone or methyl ethyl ketone were developed. As a result of this, it was decided to revert to the spot welding techniques (earlier investigated with monofilament metal cloth) to see if the improved cleaning techniques might improve the spot welding efficiencies.

3.7.1.9 INTERRUPTED SEAM WELDING

Test coupons were fabricated by the Arrowhead Products Co. using an available stainless steel, monofilament wire cloth and continuous contact welding equipment with an interrupted seam. This type of seam was obtained by intermittently applying power to rolling electrode wheels. A sample of this joint is shown in Figure 59. A quantative evaluation was made of the joint and revealed the peel strength was very low and also indicated severe weakening of the fibers adjacent to the weld. The existing resistance seam welding equipment did not have sufficient throat depth to accommodate the large complex fabric sections which had to be constructed in this program.

335/025

Figure 56. Induction Brazing Coil

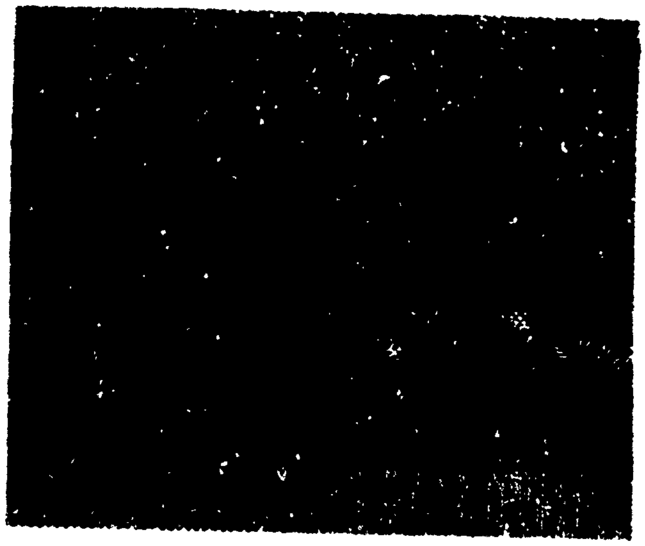

Spot Braze - Stainless Steel Bolting Cloth

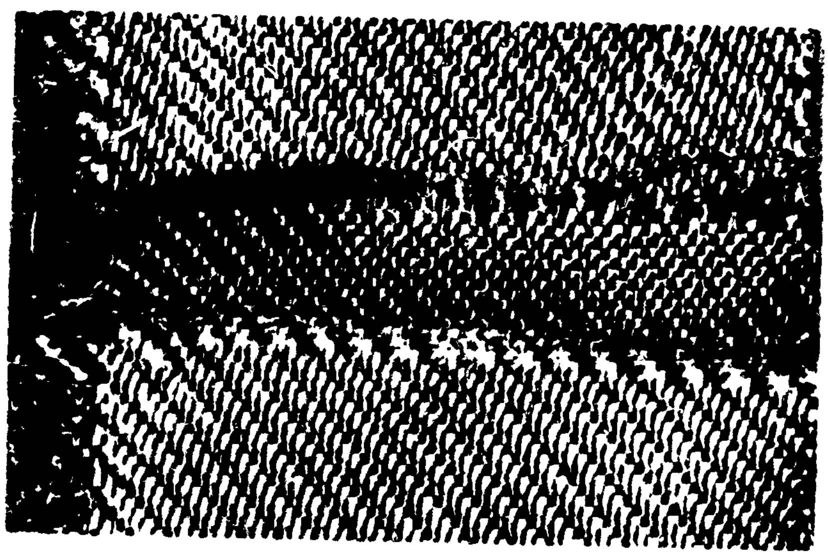

Seam Braze - Chromel-R Metal Cloth

Figure 57. Spot and Seam Brazed Specimens

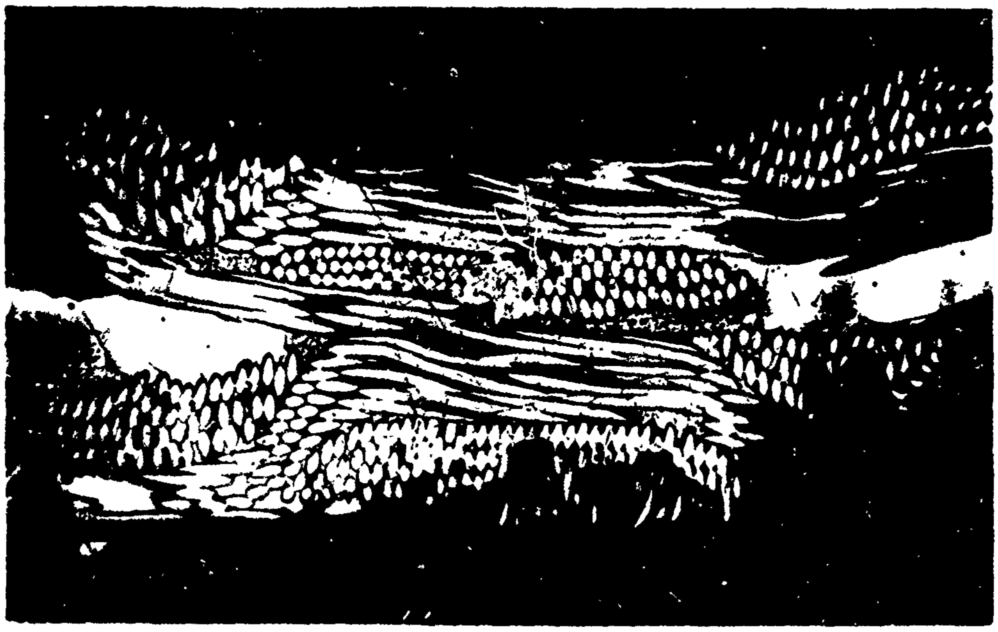

Rolled Seam Braze

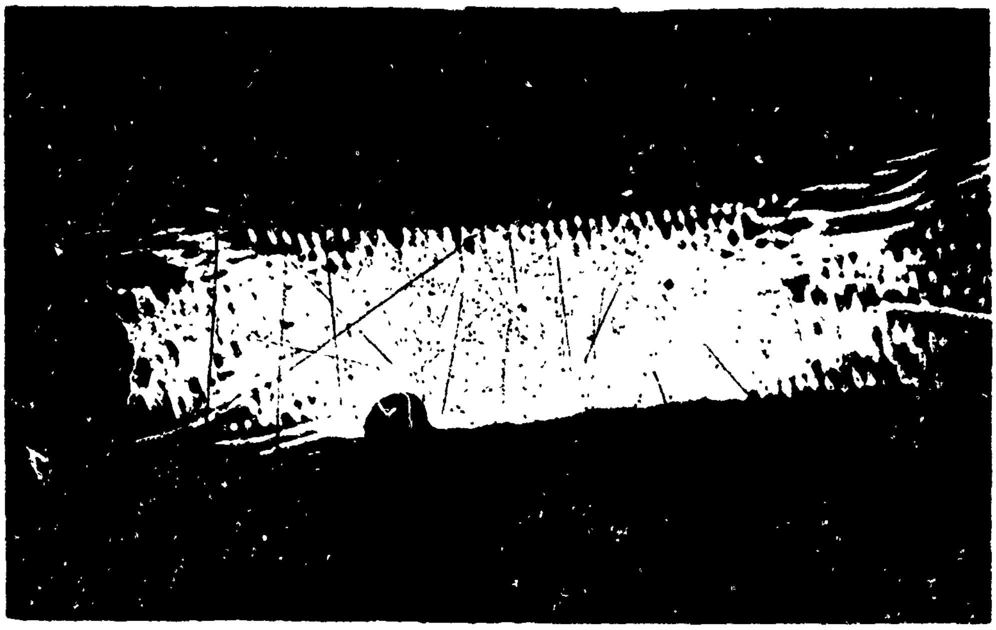

SGC/1150

Rolled Seam Weld

Figure 58. Cross-Sections of Seam Braze and Weld Joints

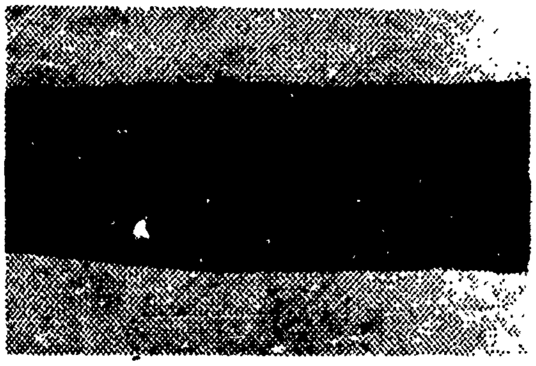

a. Interrupted Seam Resistance Weld

b. Interrupted Seam Resistance Weld - Staggered

Figure 59. Seam Resistance Weld

3.7.1.10 CONTINUOUS SEAM WELDING

Test coupons were obtained from the Arrowhead Products Co. using an available stainless steel, monofilament wire cloth and conventional continuous seam resistance welding equipment. The evaluation made for interrupted seam welding (Section 3.7.1.9) is also considered applicable for continuous seam welding except that the weakening adjacent to the weld was more pronounced and the stiffness of the seam greatly increased. Figure 60 illustrates this type of joint.

3.7.1.11 EDGE WELDING

This method required that one piece of metal cloth be placed on top of the other piece of metal cloth with the edges to be welded being perfectly aligned. The edges were held tightly together and torch-welded so that a tiny bead was formed. It was suggested that inert gas shielding could be used. The two pieces of fabric were then opened up but this 180° creasing of the weld joint tended to overstress and weaken the fibers. Joint efficiencies of only 20-40 percent relative to parent material were obtained.

3.7.1.12 BUTT-WELDING OF WIRES

A method of butt-welding the individual wires in a wire cloth has been developed by the wire cloth industry in the manufacture of Fourdriner "wires" or screens. This operation, which requires the precise alignment of each and every wire, is time consuming and has proprietary aspects with the companies that have developed it. Alternate methods of making Fourdrinier wires involved butt-brazing techniques. In addition to the painstaking effort required for this operation (which is performed under a microscope by skilled craftsmen), it does not lend itself to intersecting seams, joining of multiple layers in objects of complex curvature, or joining of multi-filament yarns.

3.7.1.13 ULTRASONIC WELDING

The possibility of using ultrasonic welding for metal fabric joining was investigated through contact with Sonobond Corp., Westchester, Pennsylvania. They reported that ultrasonic welding had been attempted for very simiiar joining applications on several occasions and that the process had proven unsatisfactory in each instance. It was stated that the difficulty arising with such woven materials was that, because of their hardness, the nickel chromium filaments require very high ultrasonic welding energy levels to obtain satisfactory joints. While single filament-to-metal joints were possible, attempts to weld woven fabric resulted in each of the small wires cutting into its neighbor wire without welding, and the only result was severe damage to the fabric.

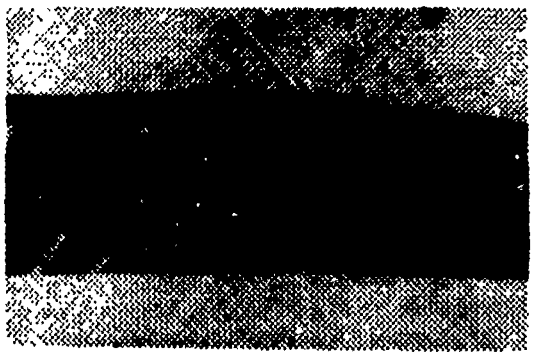

Figure 60. Continuous Seam Resistance Weld

3.7.1.14 ELECTRON BEAM WELDING

A very low absolute pressure of 10^{-4} or 10^{-5} mm Hg is required for electron beam welding and no work had been reported on metal fabric by this method as of the date this investigation took place. Information obtained from Sciaky Brothers, Inc. indicated that the expense and bulk of the equipment, plus the required development effort, would preclude this approach.

Subsequently, some multi-filament metal fabric of the Chromel-R type was subjected to an electron beam welding experiment. Although it is not known what settings were used, it was reported that the ultra-fine metal filaments simply "disappeared" rather than forming a weld nugget.

3.7.1.15 SPOT WELDING BY MICROWELDER

The Aerojet Model AD120 was used to prepare the spot welded samples shown in Figure 61. This device produces miniature spot welds using a tiny dual-electrode on one side of the material. Some damage to the fibers has been observed when using this method on ultra-fine filament wire fabric. Because the equipment is a bench-top precision welding device with the work piece being manually positioned for one spot at a time, it was not applicable to large-scale fabrication. Unknown at the time of this investigation was the fact that a through-type spot welding technique would eventually be the most successful method of making joints in metal fabric but the characteristics (including wave shape, position of electrodes, forging pressure, etc.) are quite different from the microwelder approach.

3.7.1.16 REVIEW OF BRAZING VERSUS WELDING TECHNIQUES

After approximately six months of investigation in 1963 it became apparent that adequate high-temperature joint strengths in the metal fabric reinforcing materials could only be obtained by welding or brazing. Regardless of the method of welding or brazing, several basic procedures had to be followed. First, all materials (both metal fabric and brazing alloy when used) had to be cleaned of foreign contamination and as much oxidation as possible. Second, the two pieces of fabric to be joined must be held tightly together during the brazing or welding operation. This is particularly important when joining metal fabric since the heat applied causes the metal to expand and the joint to separate or slip before or/and during solidification of the molten metal. Third, any application of heat external to the joint must be accompanied by an inert atmosphere. This is necessary not only to prevent oxidation of the materials in the joint area before the materials are fused but, perhaps more important, to prevent oxidation and degradation of the metal fabric fibers adjacent to the joint. Failure of the test specimens appeared to occur adjacent to the joint in all cases and at significantly reduced strength when the fabric was scorched. Reductions in material strength from 10-35 percent were found depending on the degree of apparent scorching (discoloration).

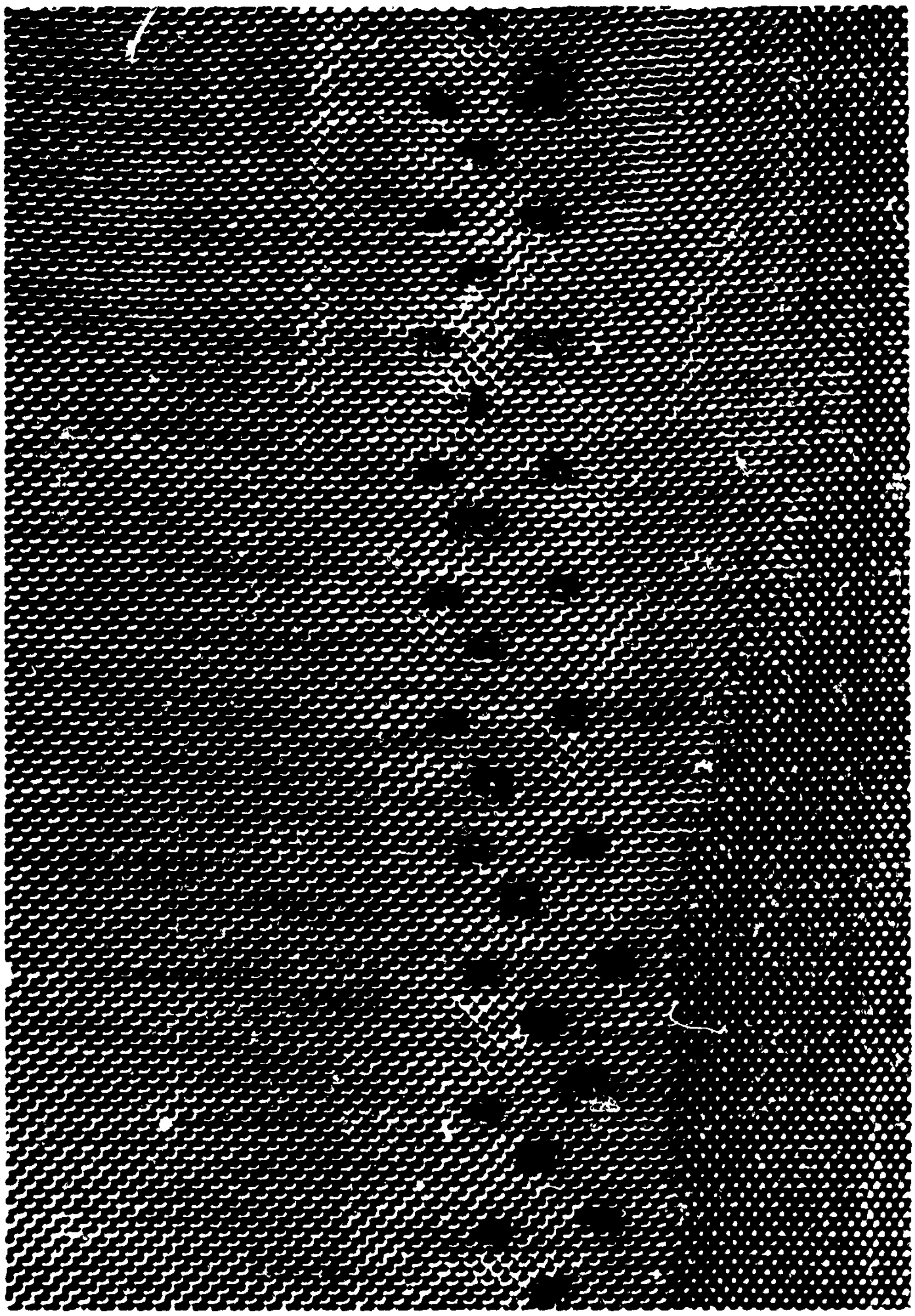

Figure 61. Spot Welding by Microwelder

Although a silver alloy known as Lithobraze-BT (manufactured by Handy & Harman) proved most satisfactory for the experimental brazing work with monofilament, stainless steel cloth, difficulty was experienced with it in attempts at brazing multifilament Chromel-A cloth when heat was applied externally as with infra-red or induction coil heating. Through capillary action the molten alloy would tend to diffuse through the weave of the fabric. This effect was so pronounced that most of the alloy was attracted into a broad band in the hotter upper layer of fabric and thus lost from the interface of the intended joint. Two approaches were utilized in an attempt to overcome this problem, both of which proved not unsuccessful. One approach was to use an alloy with low capillarity. This was Handy & Harman's Staflo-761. This alloy is a combination of Lithobraze-925 and nickel and is furnished in three-layer laminated sheets having a dispersion of 20 percent nickel and 80 percent Lithobraze-965 as a center layer with outer layers of Lithobraze-925 on either side of the center. This alloy reportedly had been used successfully for furnace brazing stainless steel honeycomb structures. Its lack of capillarity when molten was so pronounced that, in brazing Chromel cloth, it could not be made to penetrate into the cooler layer of the fabric opposite the side from which heat was applied.

The other approach was to use a "stop-braze" material (Rinshed-Mason S-51Z805) applied to the fabric adjacent to the joint area to keep the brazing alloy from spreading. Lithobraze-BT brazing alloy was then used. As reported in Section 3.7.1.6, this approach was unsuccessful due to the excessive capillarity of the stop-braze in the metal fabric, making it impossible to keep the joint area free of it.

Although attempts to braze the multi-filament Chromel fabric were not sufficiently successful, it was noted that no scorching took place using only the normal purging system of the Aeroray gun and the 6 percent hydrogen and 94 percent argon mixture. Four different purging gases were tried in an attempt to circumvent the scorching problem when brazing mono-filament stainless steel cloth with the Aeroray infra-red gun. These gases were 94 percent argon plus 6 percent hydrogen; 94 percent high purity nitrogen plus 6 percent hydrogen; pure argon; and cryogenic nitrogen. The cryogenic nitrogen was obtained from a permanently installed liquid nitrogen vaporization and distribution system in the Space-General laboratories. All other gases were "cylinder gases" obtained from normal commercial sources. Visible improvement was realized when using the reducing gases (those containing hydrogen) but adequate confidence was never obtained in the ability to avoid scorching of metal fabric with any gas. Continued efforts to avoid scorching led to the construction of 2-1/2 cubic foot transparent vinyl plastic bag for use as a brazing enclosure. This bag was equipped with sleeves which could be tightly fitted to the operator's arms and provided openings for inlet connections for the infra-red heating device and electric cord, as well as inlet and outlet purge connections. Although some success was noted with the use of this bag, results were not consistent in spite of diligent attempts to eliminate all oxygen by purging prior to brazing. It is probable that the cloth mesh is fine enough to enable some oxygen to be retained within the interstices.

Similarly, joints which were made by the induction brazing approach showed considerable scorching, and it was apparent that simply blasting the purging gas on the joint area from above and below was unsatisfactory due to induction of air from the surrounding atmosphere. An enclosed chamber (such as a Lucite sleeve placed in close contact with the fabric) containing inert or reducing gas might have proved satisfactory but it is doubtful.

As a result of these investigations it became apparent that resistance braz' g (besides spot welding) was the only feasible method of joining multi-filament metal fabric since all methods of brazing using external heat (infra-red and induction) were so badly scorched that tensile testing of most of the specimens was not warranted. Although brazing with externally applied heat caused very rigid joints, even resistance spot brazing produced stiffer joints than spot welding because of the need for pre-placed brazing alloy strips.

Wh never a reasonable coupon was obtained by any of the joining techniques, tensile tests were made on the coupon. All joints tested were simple lap joints. In every case the specimens failed in the filaments adjacent to the joint at less than the strength of the basic material. This was attributed to degradation of the filaments due to the high brazing or welding temperatures and bending in the filaments adjacent to the braze or weld zone during loading of the specimen. Results of typical tests are presented in Table XV. Prior to each of these tests, except for those involving the Heliarc welded specimens, the materials were cleaned with a degreasing agent such as acetone or MEK solvent, rinsed in distilled water, treated in 10 percent solution of HCl to remove oxidation, rinsed in distilled water and finally washed again in acetone or MEK to permit rapid air drying.

The tensile bolting cloth used in these tests consisted of 2.2 mil, 316 stainless steel wire woven in a plain-weave 145 x 145 mesh. The Chromel-A fabric consisted of 0.7 mil filaments, standard 7/7/1, 2.7 S/3.1 Z, and woven as 2x2 twill.

Because of the fact that spot welding produced a highly flexible joint without the need of an inert atmosphere, efforts were directed to improving the efficiency of spot welded joints with the result that the final joining technique, as described in the next section, proved very successful. Reference to Table XIII, Section 3.7.1, indicates the rather encouraging average joint efficiencies obtained with spot welded coupons in test combinations 5, and 8 through 19.

3.7.2 DEVELOPMENT OF THE SPOT WELDING PROCESS

Early experiments with spot welding are summarized in Table XIII, ection 3.7.1. Experiments denoted by combinations 5, and 8 through 14 of this table represent typical tests performed with mono-filament stainless steel cloth and resistance spot welding. These early experiments were not considered to be exhaustive, since several parameters, such as seam spacing and electrode size, were not independently studied in sufficient detail to optimize. It was established, however, that two adjacent seams were stronger than a single one, as compared in test combinations 11 and 12. Welding within 5 or 10 minutes after cleaning appeared to produce stronger joints than when welding was postponed overnight as compared by test combinations 12 and 14. It will be noted that 12 coupons welded immediately after cleaning in test 12 produced an average joint

Table XV

RESULTS OF TENSILE TESTS OF BRAZED AND WELDED JOINTS

Brazing or Welding Process	Material and Specimen Configuration	Number of Specimens Tested	Ultimate Load (lb)			Average Joint Efficiency (%)
			Least	Greatest	Average	
Basic Cloth; No Joint	Tensil Bolting Cloth 4" Width; 1" Grab	3	72	90	81.0	--
	Tensil Bolting Cloth 1" Width; 1" Grab	8	55	60	57.1	--
	Chromel Cloth 1" Width; 1" Grab	1	184	184	184.0	--
Heliarc Weld; Edge Resistance Weld	Tensil Bolting Cloth 4" Width; 1" Grab	2	16	32	24.0	30
Spot Weld; Double Row of Welds	Tensil Bolting Cloth 4" Width; 1" Grab	2	41	60	50.0	62
Aeroray Braze Gun; Nicrobraze "LM" Alloy; Poor Purging	Tensil Bolting Cloth 4" Width; 1" Grab	2	50	52	51.0	63
Aeroray Braze Gun; Lithobraze "BT" Alloy; Good Purging	Tensil Bolting Cloth 4" Width; 1" Grab	2	34	42	38.0	47

Table XV (Continued)

RESULTS OF TENSILE TESTS OF BRAZED AND WELDED JOINTS

Brazing or Welding Process	Material and Specimen Configuration	Number of Specimens Tested	Ultimate Load (lb)			Average Joint Efficiency (%)
			Least	Greatest	Average	
Aeroray Braze Gun; Coast 62 Alloy Good Purging	Tensil Bolting Cloth 4" Width; 1" Grab	1	55	55	55.0	68
Spot Braze Nicrobraze "LM" Single Row Spot Braze	Tensil Bolting Cloth 4" Width; 1" Grab 2" Gage Length	1	16	16	16.0	20
Spot Braze Nicrobraze "LM" Alloy - Two Rows Staggered Spot Braze	Tensil Bolting Cloth 4" Width; 1" Grab 2" Gage Length	1	45	45	45.0	56
Spot Braze; Nicrobraze "LM" Alloy - Two Rows Staggered Spot Braze	Tensil Bolting Cloth 4" Width; 1" Grab 3" Gage Length	1	73	73	73.0	90
Spot Braze; Lithobraze "BT" Alloy - Two Pows Staggered Spot Braze	Tensil Bolting Cloth 4" Width; 1" Grab 3" Gage Length	1	97	97	97.0	100

efficiency of 90 percent, while 6 coupons in test 14, welded the day after cleaning, produced a joint efficiency of only 80 percent. Essentially, all other test conditions remained constant.

Test combinations 15 through 19 represent most of the significant spot welding experiments performed on multi-filament (Chromel-A) fabric. These tests were not more extensive because of the very limited amount of this fabric available at the time. For this reason, a "reused specimen" category is shown, indicating the fact that such specimen joints were made from coupons previously tensile tested, with tested joints cut off prior to making the new joints. Undoubtedly, the joint efficiencies obtained would have been improved if it had not been necessary to reuse the materials.

A photomicrograph, Figure 62, was made of a spot welded joint in Chromel-A fabric which proved to have a joint efficiency of 67 percent. Photomicrographs of higher magnification in Figure 63 show cross-sections of spot welded joints in Chromel-A fabric.

Considerable joint fabrication test work was done during the fabrication of four 7-inch-diameter by 15-inch-long cylinders made of mono-filament stainless steel cloth.

A Unitek Model 1048-B capacitance discharge-type spot welder was used for these cylinders as well as many of the early coupons. This equipment consisted of an adjustable power supply capable of a maximum of 300 Watt-seconds and a variety of hand-held, probe-style electrodes and foot-operated, bench-mounted welding heads. The power supply and a welding head are shown in Figure 64 performing the welding of one of the mono-filament cylinders which are also depicted.

The energy and forging pressure settings finally decided upon for mono-filament stainless steel fabric were 2.75 Watt-seconds for two-layer lap seam joints and 3.75 Watt-seconds for four-layer lap seam joints with an electrode force setting of 14.5 pounds for each. The electrodes used were a 1/16-inch-diameter copper movable tip and a 1/16-inch-thick copper stationary platen. No difficulty was experienced in obtaining joint efficiencies as high as 88 percent.

A discussion of the manufacturing aspects in the fabrication of these cylinders is presented in the section of this report entitled "Fabrication of Test Components."

A small hand-held welder with a motor-driven wheel was evaluated. This welder, manufactured by Microdot, Inc., was primarily intended for affixing metallic strain gages to metallic surfaces; it had no provision for adjusting and controlling forging pressure, the speed, or the spot spacing. It was designed for use with the same Unitek capacitance discharge power supply which had been used for earlier spot welding tests.

In the meantime, the pilot run of multi-filament Karma fabric was woven for Space-General. This was the first quantity of the fabric which was to be used for fabricating the main test components in this program.

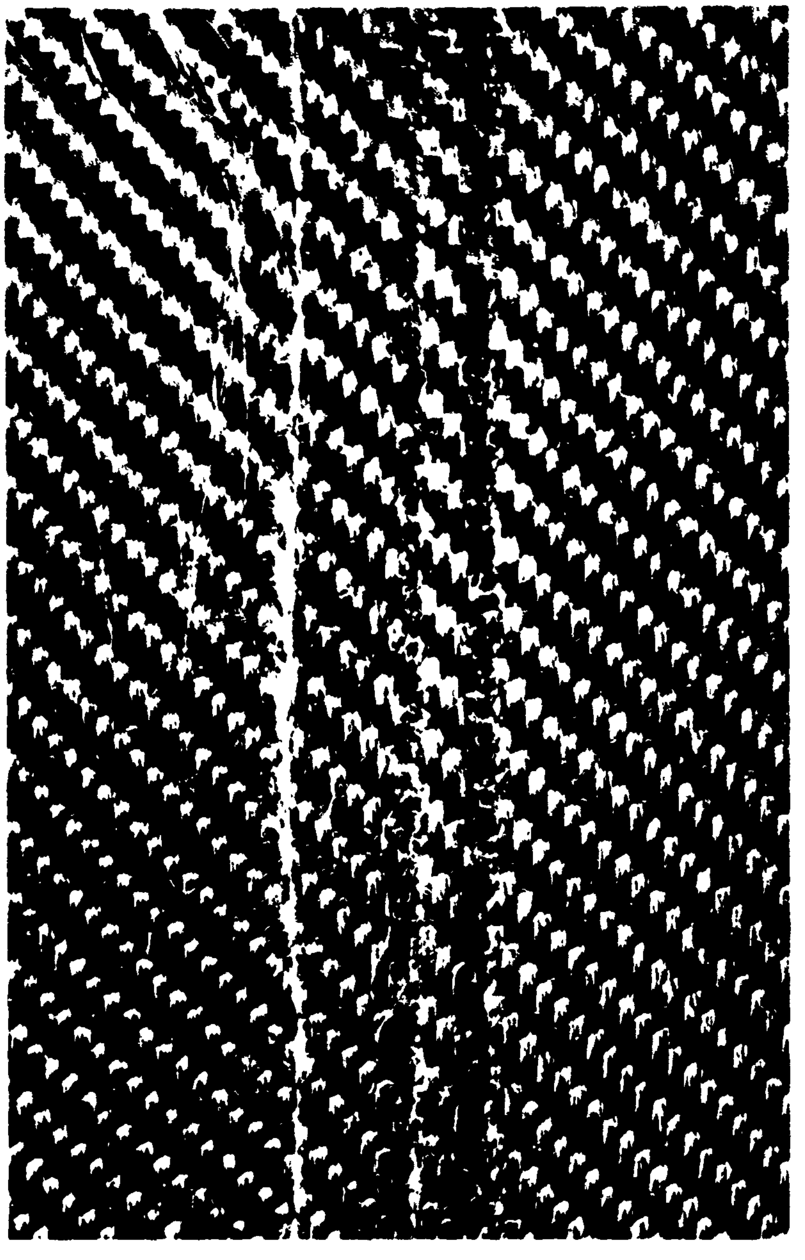

(Enlarged Approx. 6.5 Times)

Figure 62. Metal Fabric - Resistance Spot Welded Joint

A. Joint sectioned transverse to line of weld spots (Joint rupture load was 156 lb/in).

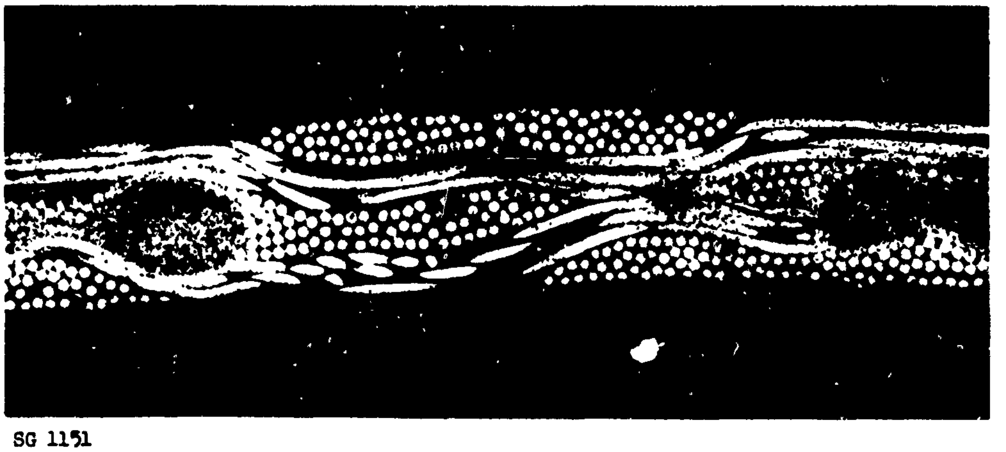

SG 1151

Figure 63. Photo-Micrographs of Spot Welded Joints (80-20 Nickel Chromium)

Welding Operation

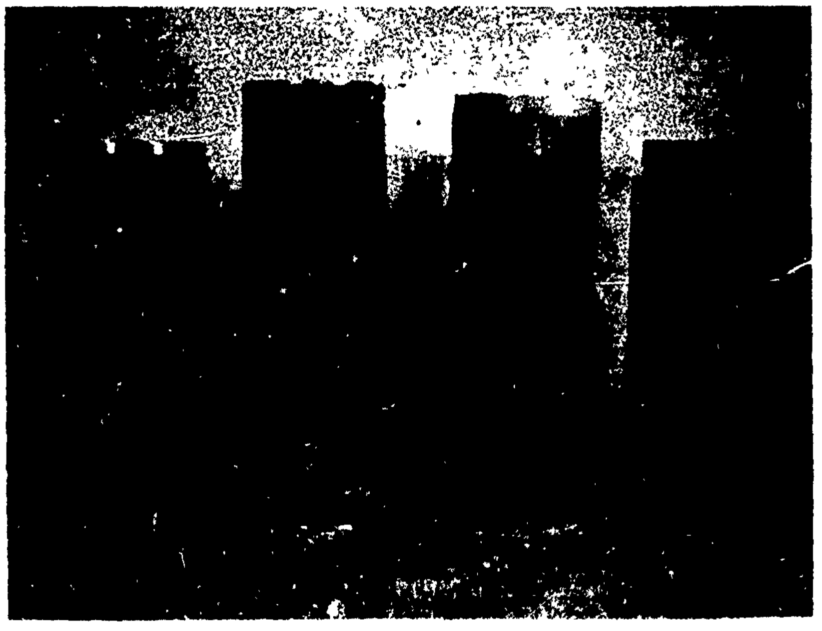

335/054

Cylinders Made for Project FIRST

Figure 64. Spot Welded Metal Cloth Cylinders

Some welds which were quite satisfactory in appearance were made in the multi-filament Karma fabric using the Microdot welder, but it was recognized that they would be far from optimum because of the lack of control of the above variables. Of the total of 14 one-half-inch wide joints made and tested, the average joint efficiency was 49 percent and the maximum was 73 percent. This device did demonstrate, however, that a hand-held welding tool might possibly be developed which would be simple, lightweight, and self-powered.

At this time in the program, early 1964, the encouraging results with resistance welding prompted Space-General to seek a welding equipment concern who would undertake a subcontract to develop and build a metal fabric resistance welder. The B. F. Goodrich Co., Akron, Ohio, had bid on a proposed subcontract from Space-General for the fabrication of the test components in this program as well as the development of a silicone rubber impregnating and coating technology. Since they wished to be responsible for the welding process as well, they were also permitted to bid on the welding tool work statement issued by Space-General. A major subcontract was subsequently awarded to the B. F. Goodrich Co. for the development of the welding equipment and the silicone rubber process, and the fabrication of all test components. B. F. Goodrich agreed to subcontract the welding tool development to a welding equipment concern and short-term evaluation contracts were awarded to Battelle Memorial Institute, Columbus, Ohio, and Sciaky Bros. Inc., Chicago, Illinois.

The results of the Sciaky investigation is reproduced as B. F. Goodrich Co. LC-1249 in Appendix III. The overall object of their evaluation was to study and recommend the best resistance weld method for the metal fabric. Using the 1-mil filament, nickel-chromium metal fabric which Space-General had obtained for this program, Sciaky experimented with probe (about 1/8-inch-diameter) and wheel (2-inch-diameter by 1/8-inch-wide) type electrodes (RWMA CL-2) making 40 to 68 spots per inch in single and double rows. The significant conclusions reported are that joint strength efficiencies of 85 percent on two-ply and 80 percent on three- and four-ply fabric could be achieved. Four- and five-ply welds were not recommended for high-strength joints. Double-row direct (through) welding was preferred over double-row series welding.

Two types of welding tools were used by Battelle in their development work. One type was the Hughes Aircraft Co. bench welding head with two such welding heads set up side by side for series welding. The other type of tool was a hand-held welding gun designed and developed by Battelle. The power supply recommended by Battelle and used in most of their experimentation was a "breadboard" prototype, size 3 square-pulse welding power supply on loan from General Electric Co. The power supply and the Hughes VTA-42 welding head setup for through welding, rather than series welding, is shown in Figure 65.

The weld seams were prepared by making a series of spot welds centered on each pair of warp yarns of the fabric, as nearly as possible, resulting in seams having about 30 spot welds per inch. Early work was with 1/8-inch-diameter flat-end electrodes but these were replaced with 1/4-inch-diameter domed electrodes. Both sets of electrodes were made of RWMA Class-2 copper base alloy.

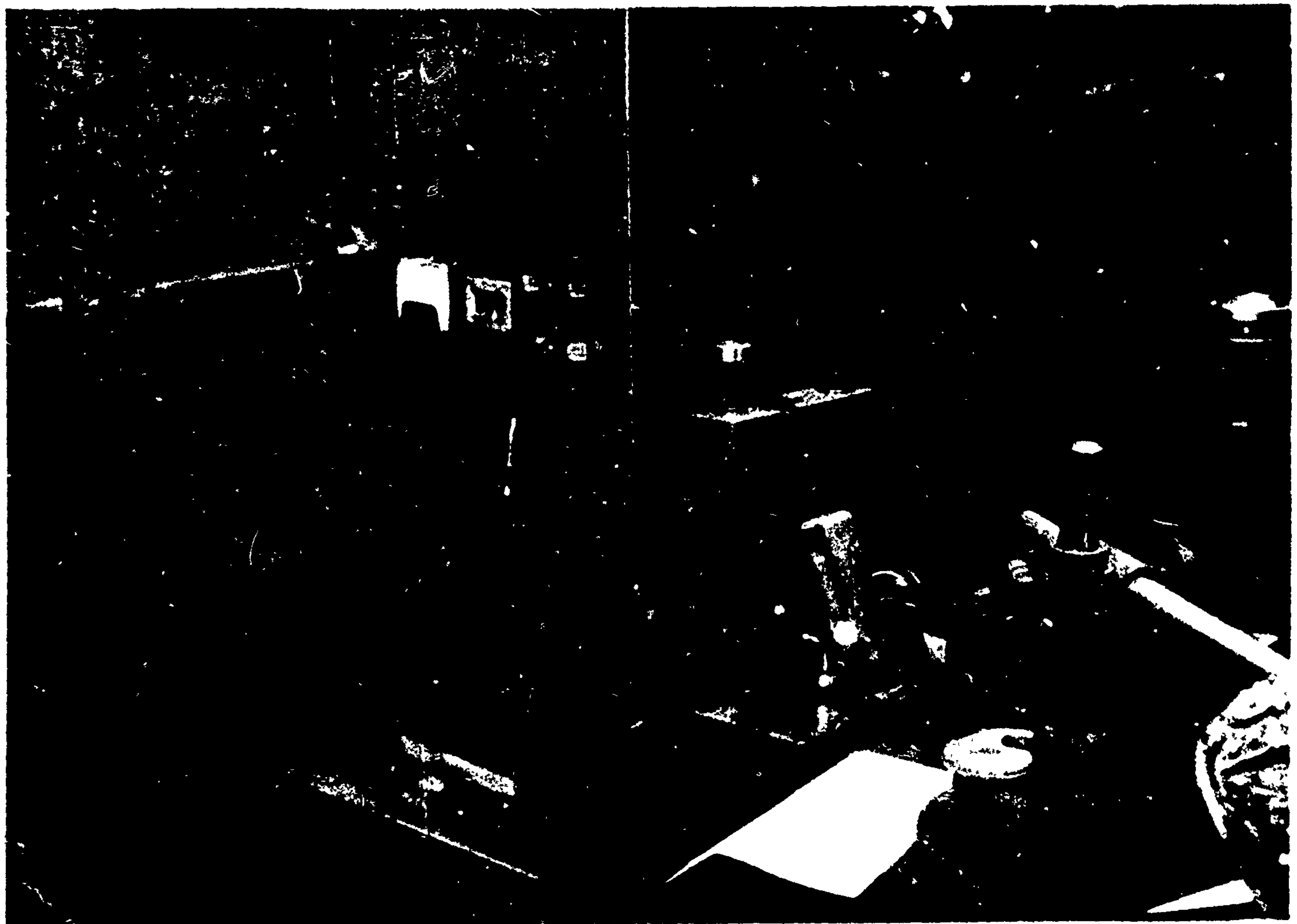

SGC/343

Figure 65. General Electric Size 3 Breadboard Square Pulse Welding Power Supply and Hughes VTA 42b Welding Head Setup for Single-Seam Through Welding

Current pulses of 3 to 10 milliseconds duration with a single pulse per spot weld were used. Measured weld currents were between 900 and 1200 Amperes. Delivered energy per spot weld was varied between 2.2 and 6.3 Watt-seconds or Joules. All but the last two welds were made using the lowest output transformer tap of the eight taps available. Electrode pressure was not measured directly but it was kept constant at a setting of 5, which corresponded to 50 pounds force, during most of the tests. At this pressure, there was no sparking or expulsion and there was very little marking of the fabric surface. Some electrode sticking was noticed at 1200 Amperes.

Strengths of multiple (more than two) layer joints appeared to be somewhat inferior to the general level of strengths obtained with two-layer specimens. Joint efficiencies ranged up to 63 percent relative to a parent fabric strength of 408 pounds per inch and with all specimens pulled in the fill direction. The weld joint efficiency goal established by Space-General was 85 percent; this was not obtained although there was encouragement in the fact that the better specimens failed in the fabric near or adjacent to the weld seam and not in the weld itself.

No systematic attempt was made to examine the effects of seam spacing in double-seam welds. The spacing was kept approximately constant at about 1/8-inch.

Since the damage to the fabric by this process was obviously much less than by other processes previously investigated, the square pulse power supply and small area electrode technique appeared to be very promising. As a result of these studies, Battelle Memorial Institute was given an additional subcontract by B. F. Goodrich who, in turn, were under subcontract to Space-General. Battelle's new task was to develop the proposed resistance welding technique and to design and build a portable welding tool.

In carrying on their work on a "bench scale" basis, Battelle set up two single-electrode Hughes Model VTA-42B welding heads side by side for series welding - that is, welding with both electrodes on the same side of the fabric. Electrode movement and pressure on the heads were controlled mechanically by foot pressure. An oscilloscope was used to measure the current during welding, and a microscope was used to predetermine the weld locations. Welding attempts on two layers of fabric were unsuccessful even with the highest rated output transformer tap. This was unexpected since the lowest rated output transformer tap of the size 3 power supply was adequate for welds made in the evaluation studies with through-type welds (one electrode on each side of the fabric). It had been judged, therefore, that the size 2 power supply would meet the requirement for series, double-seam welding.

Typical test results obtained with a size 2 power supply are given in Table XVI. The procedure was to check the circuit first by closing the electrodes and firing the welding circuit without fabric, then to apply the same conditions to two layers of fabric and finally to four layers. Four pulses were used, with 9 milliseconds total per pulse, 3 milliseconds for welding and 6 milliseconds for cooling. The latter period was needed by the capacitor bank in the power supply for recharging. Four such cycles constituted four welding pulses. As can be

Table XVI

CURRENT CHARACTERISTICS OF WELDS WITH SIZE 2 POWER SUPPLY

A. Single Head through weld

Tap H-4 - 3 millisecond pulse
6 millisecond cool
40 lb. force
4 pulse total

	Copper Shunt	2 Layer Fabric	4 Layer Fabric
1st Pulse	2400 amps	1200 amp	500 amp
4th Pulse	2400 amps	2000 amp	1400 amp

B. Two Heads - Series Weld

(Same settings and pulse count as in "A" above.)

	Copper Shunt	2 Layer Fabric	4 Layer Fabric
1st Pulse	2200 amps	400 amp	300 amp
4th Pulse	2200 amps	600 amp	500 amp

NOTE: Welding heads were Hughes VTA-42B

seen by comparing welding currents for fabric, both for two and four layers, the welding currents for series welding are 1-1/2 to 3 times those for through welds under the same initial conditions for both the first and fourth pulses. The 600-Ampere maximum noted for two layers with series welding was reported to be near the maximum available for the size 2 power supply and the tests showed that it was on the order of 1/2 to 1/3 of the necessary current for series welding. This directed the decision to return to the size 3 power supply (with a nominal rating of 3000 Amperes) for further work.

Using the welding heads previously described (fitted with pneumatic actuators to apply the necessary force to the electrodes), joint efficiencies as high as 84 percent were obtained during the experiments in which 22 tensile test specimens were welded and tested. All of these specimens were joined with series welds, pulse durations of 3.0 to 6.0 milliseconds, electrode force of 25 to 50 pounds, and 1000 to 1800 Amperes. Failure always occurred adjacent to the weld.

3.7.2.2 PORTABLE WELDING GUN

The proposed design of the apex portion of the paraglider required that four or five overlapping layers of the nickel-chromium fabric, differently oriented, each about 12 mils thick, be joined with at least 85 percent joint efficiency. Because of the complex curvature of the seams and the tolerances required, it would be necessary to lay up the fabric on a solid form, thus limiting access to one side while on the form. Assuming that welding was to be performed on the form, it appeared that a light, portable, resistance seam welding gun was required.

The single-sided access to the work dictated the use of series-type resistance welding in which both welding electrodes were "in parallel" on one side of the fabric seam. Considering that the gun might not have a constant rate of travel and the need to maintain maximum seam flexibility, a seam consisting of series of spot welds appeared to be more appropriate than one made using a constant rate of power delivery. To assure a preset number of spot welds per unit length of seam, the weld firing control would have to be actuated by an indexing mechanism connected to the wheels of the gun. Provision would have to be made to assure that welding pressure was in the proper range before a weld could be made and that this pressure was equally distributed between the electrodes. The problem of dissipation of pressure in deep layers of multi-layer layups, with consequent departure from proper welding conditions, was recognized as a potential problem. The use of electrode wheels having relatively small bearing surface was proposed to help maintain adequate welding pressure throughout the multiple layer construction. Furthermore it was agreed that well known principles of secondary circuit design, which are critical for the delivery of significant quantities of current at low voltage to a spot weld, could not be violated in the gun design, but the design should incorporate standard, easily obtainable parts.

Since alternating current and spike current power supplies had already been investigated by Space-General and the B. F. Goodrich Co., Battelle directed their effort to the use of the square pulse power supply. The circuit is described by D. L. Watrous of the General Electric Co. (Reference 6). In cases where the square pulse welder had been compared with other types of power supply, it had proved to give welds with higher strengths, less variability, and without the burning of metal under the electrodes which was often found to be associated with capacitor discharge power supplies.

The welding gun designed and constructed by Battelle is shown in Figure 66. The gun was a hand-held device using the principle of electrical resistance heating for welding and was designed specifically for production of double-seam, lap-type joints in the metal fabric.

The gun was designed to operate using power furnished by a General Electric square wave pulse power supply. A "kickless," low-inductance cable was provided to present the least possible secondary circuit impedance. Although the currents were of the order of 1200 Amperes, the water cooling feature of the cable was found to be unnecessary.

The kickless cable was electrically connected to two vertical bus bars seen at the left end of the gun in Figure 66. The bus bars were made of copper and electrically insulated from one another. Axles for the electrode wheels were inserted in the bus bars. These axles carried the current from the bus bars to electrode wheels and high-conductivity grease containing particles of pure silver was used.

Welding was done by moving the electrode wheels along an overlapped fabric seam which was resting on an electrically conductive surface. Vertical pressure was applied to the gun using the hand knob on top. Welding current would pass from one electrode wheel through the fabric, through the conductive backing under the fabric and up through the fabric to the other electrode wheel. Spot welds occurred directly beneath the electrode wheels.

Spot welds were spaced along the seam length under the control of the pulse triggering subassembly. This is seen mounted on the side of the gun in Figure 66. A microswitch in this subassembly was connected to the power supply triggering circuit so that a single spot weld pulse was initiated each time the microswitch closed. The microswitch arm was actuated by the motion of the rear wheels of the gun through a gear train. Approximately 33 double spot welds were made per inch of gun travel.

An adjustable, spring controlled, forging pressure system was used to assure the correct force on the electrodes. The springs for this system were mounted in the top of the bus bars, under the hardwood top to which the hand knob was attached. The micrometer, which may be seen on the side of the gun in Figure 66, was used for adjustment of desired spring compression, and was the device that actuated the microswitch. To prevent damaging the microswitch by applying too much pressure on the gun, the force on the switch was limited by the

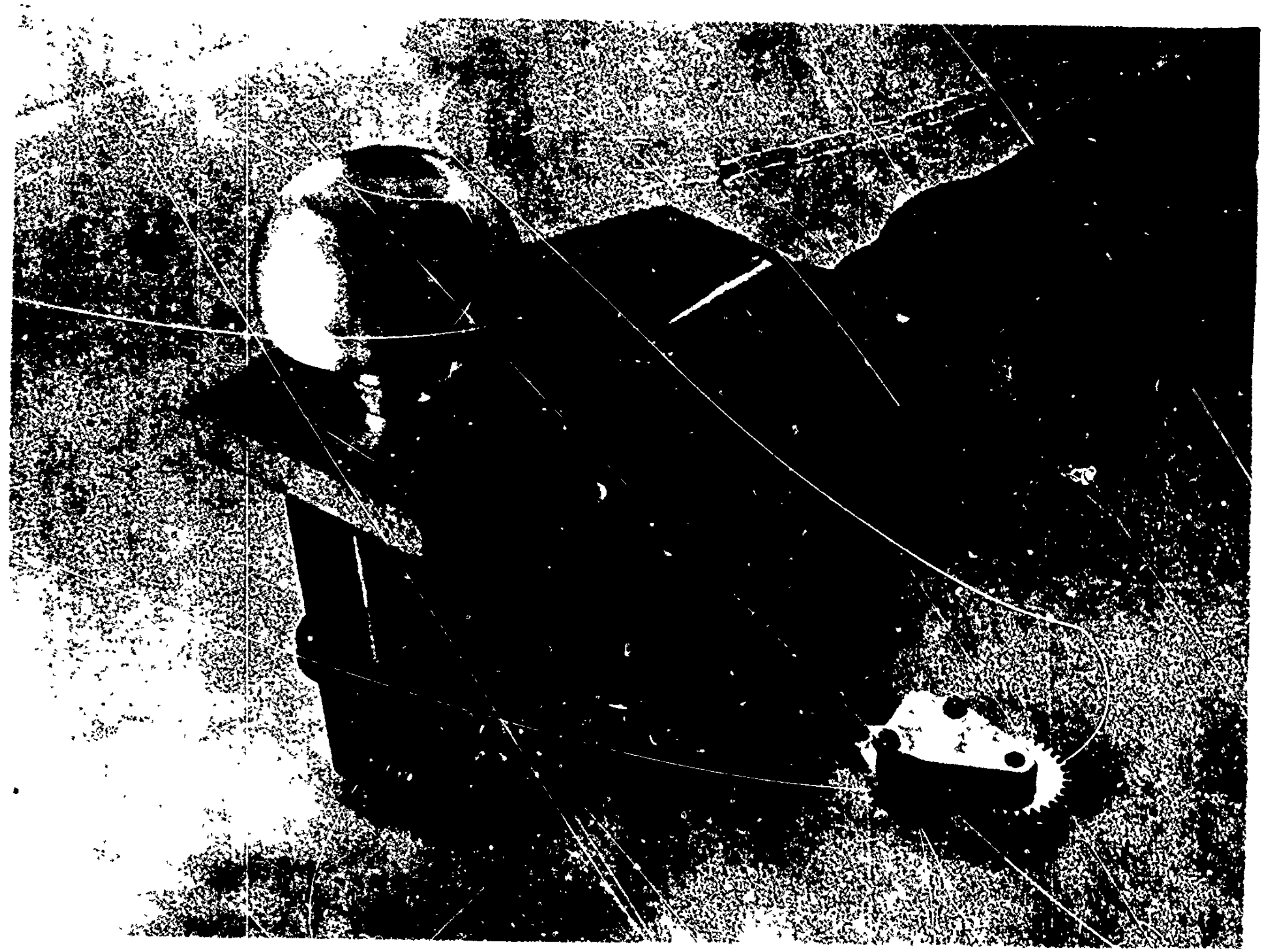

SGC/419

Figure 66. Assembled Welding Gun with Alternate Pulse Triggering Subassembly

coil spring attached to the micrometer. The springs were selected so as to require a total force of approximately 66 pounds (33 pounds per wheel) to actuate the microswitch at nominal adjustment of the micrometer.

The weld seam spacing was variable from a minimum of 9/64-inch to a maximum of 3/8-inch centerline distance, by interposing insulating discs of different thicknesses between the electrode wheels and readjusting the electrode axles.

The welding gun performed with the promising results shown in the data presented in Table XVII, the maximum joint efficiency being 93 percent. It was felt that the evaluation of the welding gun did not require consideration of the entire range of joint efficiencies obtained, from best to worst, since the worst joint efficiency represented only a development effort and was unreasonably unfavorable. However, a computation was performed to find the minimum statistical level of joint efficiency for a group of specimens welded intentionally to determine the welding quality. This was the group identified as specimens 1112-6A through 10B. These 10 specimens should qualify for statistical purposes since they were made consecutively and were tested by the acceptable method using leather-faced, serrated grips in the test machine. The lower confidence limit of joint efficiency was 71.8 percent, as calculated for 90 percent confidence level.

Problems encountered during development of the welding gun led to changes in the original concept. One such change was required since the necessary electrode loading was increased and prohibited complete manual operation as originally intended. Ultimately, it was necessary to apply the electrode loading by an external system of weights, as shown in Figure 67, and to furnish motive power for the gun with an electric motor drive attached to the gun.

The gun appeared to have a limitation of welding no more than 3 layers of fabric, whereas the original design concept for the paraglider structure and the welding gun set forth the objective of welding up to 5 layers of fabric. The obtainable joint efficiency decreased with increasing numbers of fabric layers. For 2-layer joints, the maximum joint efficiency obtained was 93 percent for 3 layers the maximum was 85 percent, as shown in specimens 1110-3A (Table XVII) and 11106-5A1 (Table XVIII), respectively. The apparent reason for the inability to weld increasingly thick layers of fabric was that the electrode pressure was dissipated as layers of fabric were added, a phenomenon which effectively reduces the welding current density as the area of applied pressure increases in depths of the fabric and shunting of current through the fabric increases. This was one of the problems of considerable concern at the onset of the gun development.

The welding gun program presented many other problems. Since the square pulse power supply required a time for recharging approximately three times the weld pulse period, and the weld pulse time for most of the work was 3 milliseconds, manually pushing the gun too rapidly resulted in inadequate recharging time. Inadequate recharging time resulted in increasingly large power

Table XVII

WELDING GUN DATA, TWO-LAYER JOINTS

Weld No.	Voltage	Maximum Current, amperes	Force per Electrode, lb	Spot Welds per Inch	Joint Efficiency, percent
930-1	185	1400	35	48	57
101-1B	185	1450	35	48	42
-2A	185	1400	35	48	51
-3A	185	1675	50	48	53
-3B	185	1675	50	48	42
-4	175	1400	50	48	69
-5	170	1375	50	48	48
102-1	165	1000	35	48	44
-2A	175	1350	35	48	63
-2B	175	1350	35	48	41
106-1A	180	1500	53	48	68
-1B	180	1500	53	48	48
107-1A	180	1450	53	48	68
-1B	180	1450	53	48	67
-2A	180	1400	53	48	69
-2B	180	1400	53	48	57
-3A	180	1175	53	48	56
-3B	180	1175	53	48	59
-3C	180	1175	53	48	45
109-1A	135	1160	53	48	75
-1B	135	1160	53	48	71
-2A	140	1250	53	48	71
-2B	140	1250	53	48	68
-4A	175	2050	53	48	61
-4B	175	2050	53	48	53
-5A	125	1150	83	48	27
-5B	125	1150	83	48	58
-7A	150	2100	83	48	76
-7B	150	2100	83	48	72
1028-3A	170	-	50	48	64
-3B	170	-	50	48	56
1030-1B	175	-	50	48	71
-2A	150	-	50	48	78
-2B	150	-	50	48	58
1102-2A	145	-	50	48	66
-2B	145	-	50	48	54
-3A	145	1140	50	48	66
1102-3B	145	1140	50	48	49
-4A	175	1200	50	48	59
-4B	175	1200	50	48	67
1103-5A	155	1525	50	48	65
-5B	155	1525	50	48	75
-6A	160	1750	50	48	45
-6B	160	1750	50	48	58
-7A	155	1550	50	48	75
-7B	155	1550	50	48	86
-8A	155	1550	50	48	83
-8B	155	1550	50	48	78
1104-1A	155	2075	75	48	75
-1B	150	1975	75	48	72
-2A	155	1700	50	48	64
-2B	150	1625	50	48	62
-3A	140	1675	75	48	83
-3B	140	1675	75	48	81
-4A	135	1350	75	48	77
-4B	135	1325	75	48	70
1105-5A	140	1475	84	48	75
-5B	140	1475	84	48	80
-6A	145	1600	84	48	72
1106-1A	145	1525	59	48	73
-1B	145	1525	59	48	80
1109-1A	140	1525	84	48	86
-1B	140	1525	84	48	78
1110-2A	140	1575	84	48	79
-2B	140	1575	84	48	78
-3A	140	1525	84	48	93
-3B	140	1525	84	48	74
-4A	140	1525	84	48	70
-4B	140	1525	84	48	67
-5A	140	1520	84	48	88
-5B	140	1520	84	48	83
-6A	140	1500	84	48	58
-6B	140	1500	84	48	75
-7A	140	1575	84	48	50

Table XVII (Continued)

WELDING GUN DATA, TWO-LAYER JOINTS

Weld No.	Voltage	Maximum Current, amperes	Force per Electrode, lb	Spot Welds per Inch	Joint Efficiency, percent	Weld No.	Voltage	Maximum Current, amperes	Force per Electrode, lb	Spot Welds per Inch	Joint Efficiency, percent
1110-7B	140	1575	84	48	66	1116-4B	140	1450	84	48	78
-8A	140	1350	84	48	54	-5A	140	1500	84	48	76
-8B	140	1350	84	48	39	-5B	140	1500	84	48	75
-9A	140	1425	84	48	58	-6A	140	1750	84	48	80
-9B	140	1425	84	48	38	-6B	140	1750	84	48	79
-10A	140	1500	84	48	37	-7A	140	1800	84	48	75
-10B	140	1500	84	48	27	-7B	140	1800	84	48	72
1112-1A	140	1325	84	48	72	-8A	140	1850	84	48	81
-1B	140	1325	84	48	71	-8B	140	1850	84	48	81
-2A	140	1475	84	48	55	-9A	135	1700	84	48	78
-2B	140	1475	84	48	53	-9B	135	1700	84	48	75
-3A	140	1575	84	48	55	-10A	135	1750	84	48	84
-3B	140	1575	84	48	58	-10B	135	1750	84	48	78
-4A	140	1610	84	48	62	1210-1A	150	1450	84	46	71
-4B	140	1610	84	48	61	-1B	150	1450	84	46	84
-5A	140	1380	84	48	61	-2A	155	1775	84	46	72
-5B	140	1380	84	48	60	-2B	155	1775	84	46	58
-6A	140	1300	84	48	70	-3A	153	1600	84	46	59
-6B	140	1300	84	48	72	-3B	153	1600	84	46	57
-7A	140	1475	84	48	67	-4A	153	1550	84	46	50
-7B	140	1475	84	48	70	-4B	153	1550	84	46	65
-8A	140	1500	84	48	70	-5A	153	1500	84	46	87
-8B	140	1500	84	48	81	-5B	153	1500	84	46	56
-9A	140	1525	84	48	75	-6A	155	1700	84	46	76
-9B	140	1525	84	48	82	-6B	155	1700	84	46	71
-10A	140	1490	84	48	78	-7A	154	1600	84	46	66
-10B	140	1490	84	48	87	-7B	154	1600	84	46	74
1116-1A	140	1625	84	48	72	-8A	154	1650	84	46	79
-1B	140	1625	84	48	52	-8B	154	1650	84	46	69
-2A	140	1450	84	48	65	-9A	154	1800	84	46	68
-2B	140	1450	84	48	70	-9B	154	1800	84	46	43
-3A	140	1450	84	48	67	-10A	154	1850	84	46	56
-3B	140	1450	84	48	75	-10B	153	1750	84	46	55
-4A	140	1450	84	48	63	-11A	153	1750	84	46	53
						-11B	153	1750	84	46	53

Table XVIII

WELDING GUN DATA, THREE-LAYER JOINTS AND OTHER TESTS

Weld No.	Voltage	Maximum Current, amperes	Force per Electrode, lb	Spot Welds per Inch	Joint Efficiency, percent
Three-layer joint data					
109-3A1	175	1475	53	48	58
-3A2	175	1475	53	48	53
-3B1	175	1475	53	48	66
1106-3A1	175	1900	84	48	60
-3A2	175	1900	84	48	72
-3B1	175	1900	84	48	59
-5A1	175	2075	109	48	85
-5B1	175	2075	109	48	73
-5B2	175	2075	109	48	59
1110-1A1	170	2000	109	48	75
-1B1	170	2000	109	48	79
1112-11A1	170	1900	109	48	57
-11B1	170	1900	109	48	75
-11B2	170	1900	109	48	79
1116-11A1	165	2000	109	48	67
-11A2	165	2000	109	48	33
-11B2	165	2000	109	48	33
-12A1	160	1825	109	48	35
-12A2	160	1825	109	48	23
-12B1	160	1825	109	48	28
-12B2	160	1825	109	48	35
Three-layer joint data, continued					
1116-13A1	160	1600	109	48	37
-13A2	160	1600	109	48	8
-13B1	160	1600	109	48	32
-13B2	160	1600	109	48	14
Bias welded two-layer joint					
1117-1	140	1700	84	48	74
Tests for contamination of joint area with primer					
No primer:					
1117-2A	138	1700	84	48	50
-2B	138	1700	84	48	74
-3A	138	1650	84	48	82
-3B	138	1650	84	48	76
Primer (Chemlok 607) brushed to 1-inch from edge of fabric:					
1117-4A	138	1575	84	48	50
-4B	138	1575	84	48	69
-5A	138	1500	84	48	56
-5B	138	1900	84	48	54
Primer brushed all over fabric:					
1117-6A	138	950	84	48	0
-6B	138	950	84	48	0

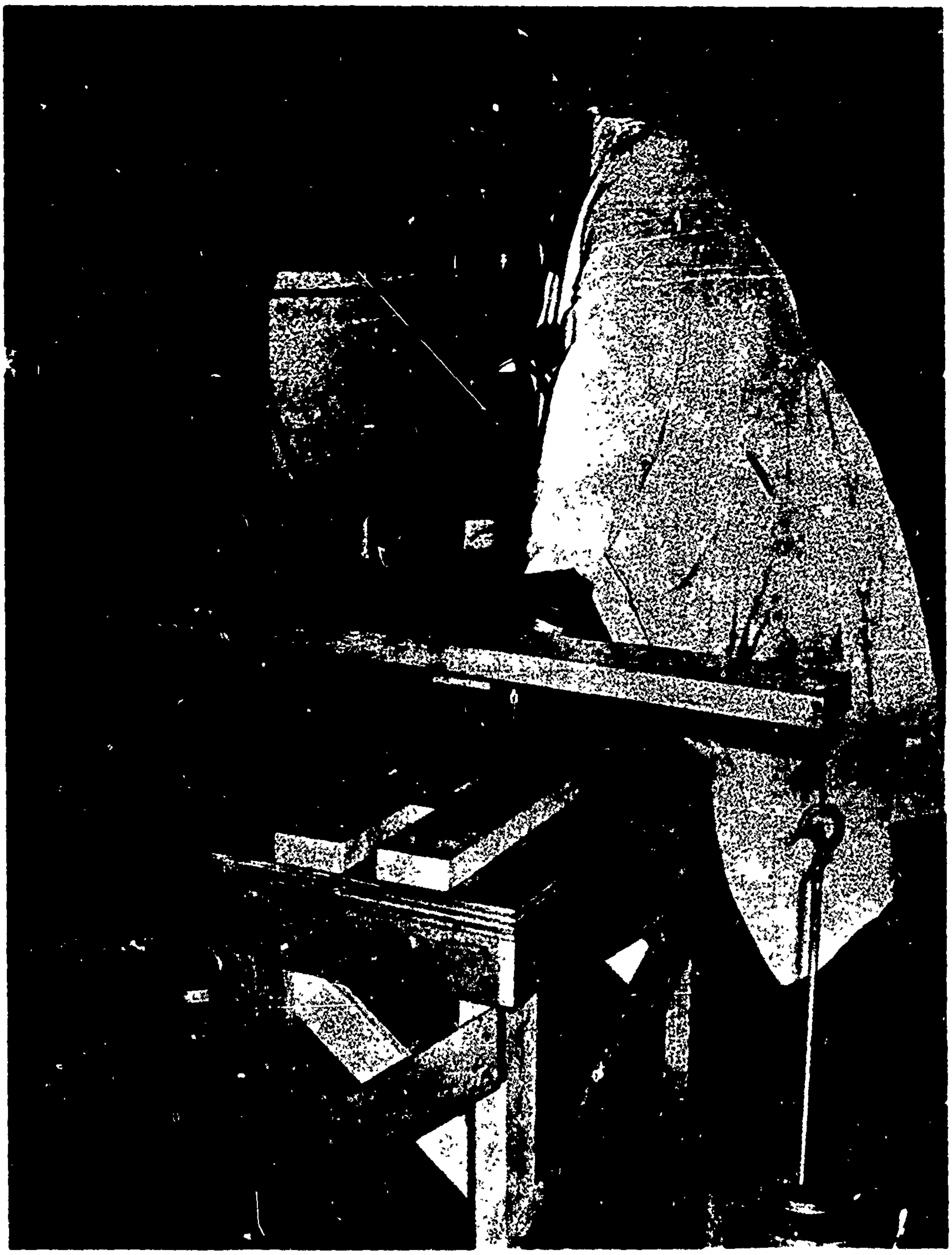

SGC/529

Figure 67. Welding Gun and Weight Loading System

consumption in the output circuit and fuses were blown. A motor with a chain drive attached to the gun, was successful but it later became desirable to increase the power of the motor due to the increasing weight loading.

The first welds made with the welding gun, while manual loading was still being used, presented obvious welding process defects, indicated by expulsion of molten metal and poor welding. The cause of this was determined to be due to grossly unequal electrode wheel pressures. To overcome this certain clearances were introduced to permit a small amount of freedom of movement between the axes of the wheels. This produced serious problems in maintaining the electrical connections between the kickless cable and the electrode bus bars.

The subcontract work by Battelle was eventually concluded and the gun was taken to the B. F. Goodrich Co., Akron, Ohio, for continuation of the development effort.

Problems continued to occur due to the increasingly heavy weight loading required to provide electrode force and obtain reasonably high efficiency welds. Because the weight loading was applied on the vertical centerline of the electrode wheels, additional vertical force had to be applied downward to the rear of the gun to insure that the rear wheels obtained traction and propelled the gun properly. As the electrode loading force was increased the force on the rear wheels needed to increase also. This resulted in overloading of the rear axle and failure of the bushings. Subsequently it became impossible to use the microswitch actuating the mechanism with the high loading. The switch operating mechanism was changed to a ratchet-shaped tooth profile on an operating cam. It was reported that weld pulses were frequently missed, however, possibly due to the effect of tolerances in both gear and switch.

Eventually the rear axle bearings were replaced with needle bearings. Finally, due to the requirement for a larger propelling motor, the chain drive was replaced with a system of spur driving gears, and heavier electrode wheel loading springs were used. All of these additional loads finally caused cracking of the hardwood body of the welding gun and it was recognized that the gun would have to be completely redesigned and a new concept of applying force to the electrodes would have to be devised. The electrode wheels showed fabric pattern indentations caused by the high electrode forces and either harder alloy or smaller area wheels would have to be used.

Data on tests of 3-layer joint welding, bias-oriented welding, and welding of fabric which had been coated with Chemlok-607 (primer for silicone rubber) are given also in Table XVIII. It was concluded that application of primer prior to welding would be impractical even if the immediate area of the joint was not primed.

3.7.2.3 FABRIC RESISTANCE MEASUREMENTS

An interesting experiment to measure change of resistance of the one-mil filament "Karma" nickel-chromium fabric was performed in August 1964.

The fabric was cleaned and deoxidized with 10 percent HCl, rinsed in distilled water and dried. The size 3 General Electric power supply was set up with 180 Volts across the primary. The H-1 secondary tap and a single pulse of 5.5 milliseconds duration were used for three specimens having different periods of elapsed time since cleaning. A specimen cleaned the same day conducted 2000 Amperes; one cleaned 9 days previously conducted 1800 Amperes; and one which had never been cleaned conducted 1500 Amperes. Obviously, there was increasing workpiece resistance caused by increase in time since the cleaning.

A test was performed at Battelle to determine the electrical resistance of the fabric. The data obtained are presented in Table XIX. One of the major variables in resistance was suspected to be the time for reoxidation of the fabric after cleaning. It was concluded that the surface resistance does increase with the time from cleaning by factors of about 1.5 to 3.0 during a five-day period of exposure to air after cleaning. Also, increased electrode loading force not only decreased the workpiece resistance due to lower contact resistance and possibly breaking down the oxide film but it also tended to minimize the effect of the time of exposure to air since cleaning.

3.7.2.4 DEEP-THROATED SEMI-AUTOMATIC WELDER CONCEPT

The rolling-wheel electrode welding gun for "series" welding required electrode loading in excess of what was considered a reasonable structural capability for such a device as well as for the form tool supporting the workpiece, in order to obtain high strength welds. Although some joint efficiencies above 90 percent were obtained on two layers of material, the repeatable weld strength was not able to meet the 70 percent minimum target efficiency temporarily established during the contract work carried out by the B. F. Goodrich Co. In addition, welds in three or more layers of fabric were of doubtful characteristics. It was concluded that a considerable portion of the problem, especially with multi-layers, resulted from the effect of current shunting between the electrodes through the fabric, rather than passing all the way through the layers of fabric to the metal backing and back again to the other electrode wheel.

The program for development of a welding tool,under the cognizance the B.F. Goodrich Co. as subcontractor, was concluded, and Space-General undertook the task of developing a welding technique of a different concept. It was hoped to be able to reestablish the original goal of 85 percent joint efficiency.

Since the fabric pieces must be positioned on a form tool, especially in the case of the compound curvature paraglider apex, it was envisioned that the pieces could be basted together by sewing or by widely spaced spot welds produced with a hand-held probe. In the latter case, a thin sheet of copper as a second electrode would need to be inserted behind the fabric. The fabric, properly joined, could then be removed from the form, or the form removed from within the fabric (when fabric sections were completely closed), and taken to a separate welding unit. The fabric pieces, basted together, would then be

Table XIX

RELATIVE ELECTRICAL RESISTANCE DATA FOR VARYING ELECTRODE LOADING AND ELAPSED TIME FOR TWO LAYERS OF NICKEL CHROMIUM FABRIC

Time Since Deoxidation	Hydraulic Loading Pressure, psi 100	200	300	400	500	600	700	800
	Resistance, ohms x 10^{-4}							
	(Fabric in same position as loading increased)							
Untreated	15	7.0	5.0	2.0	3.3	-	-	-
5 days	10	5.0	3.0	2.8	2.3	2.0	1.7	1.5
24 hours	7.0	4.0	2.5	2.0	1.6	1.3	1.2	1.0
2 hours	6.0	3.0	2.0	1.0	1.6	1.4	1.7	1.1
	(Fabric moved after each reading)							
Untreated	13	7.0	6.0	4.0	3.4	-	-	-
5 days	9.0	-	3.2	-	2.2	-	-	-
24 hours	-	4.0	-	2.0	-	1.5	-	-
2 hours	-	3.0	-	2.0	-	1.4	-	-

welded with high-strength structural seams by passing between the heads of a deep-throated welding machine. The machine could use electrode wheels or, more likely, reciprocating electrode probes of small diameter to reduce the electrode footprint area and increase the forging pressure. It was recognized that the unsupported fabric assembly would have to be properly positioned in the welding machine but simple handling fixtures could be used to prevent creasing or other damage.

A major technical question existed in the application of such a device in that many authorities considered it unlikely that sufficient power could be transmitted to the weld head because of secondary circuit inductance losses with a welder throat which would have to be seven feet or more in depth. To evaluate this, a test was run at Space-General using a 45-Watt-second capacitance discharge machine connected to a spot welding head through flat copper plate conductors nine feet long, as shown in Figure 68. Separation between these conductors was varied from 6 inches to 36 inches. The results were encouraging in that the current rise versus time characteristics for this setup and for the normal close-coupled arrangement were nearly identical, indicating that inductive losses would not be a problem with the deep-throated concept provided that flat copper plate conductors of proper dimensions were used. Oscilliscope traces of the voltage at the welding heads for both cases are shown in Figure 69.

The breadboard size 3 General Electric power supply originally used by Battelle was replaced with the first size 3 regular "production" unit manufactured by General Electric. This unit was equipped with adjustable controls and overload safety features.

Space-General subsequently performed the deep-throat test using the Hughes welding heads and the General Electric size 3 power supply shown in Figure 70.

In addition to the Hughes VTA 42-B pneumatically-actuated weld head electrically connected to the General Electric size 3 square pulse power supply with 5-inch-wide by 9-foot-long flat copper conductors, RWMA Class 2 electrodes were used. Instrumentation consisted of a Duffers current meter, Tektronix oscilloscope with chopped display for current and voltage versus time wave shape, and a machine cross-slide for controlled indexing of spot and seam spacing.

The usual metal fabric cleaning procedure consisted of:

a. Wash in acetone

b. Wash in deionized water

c. Acid deoxidize in 10 percent HCl for 1 minute ± 5 seconds

d. Wash in deionized water

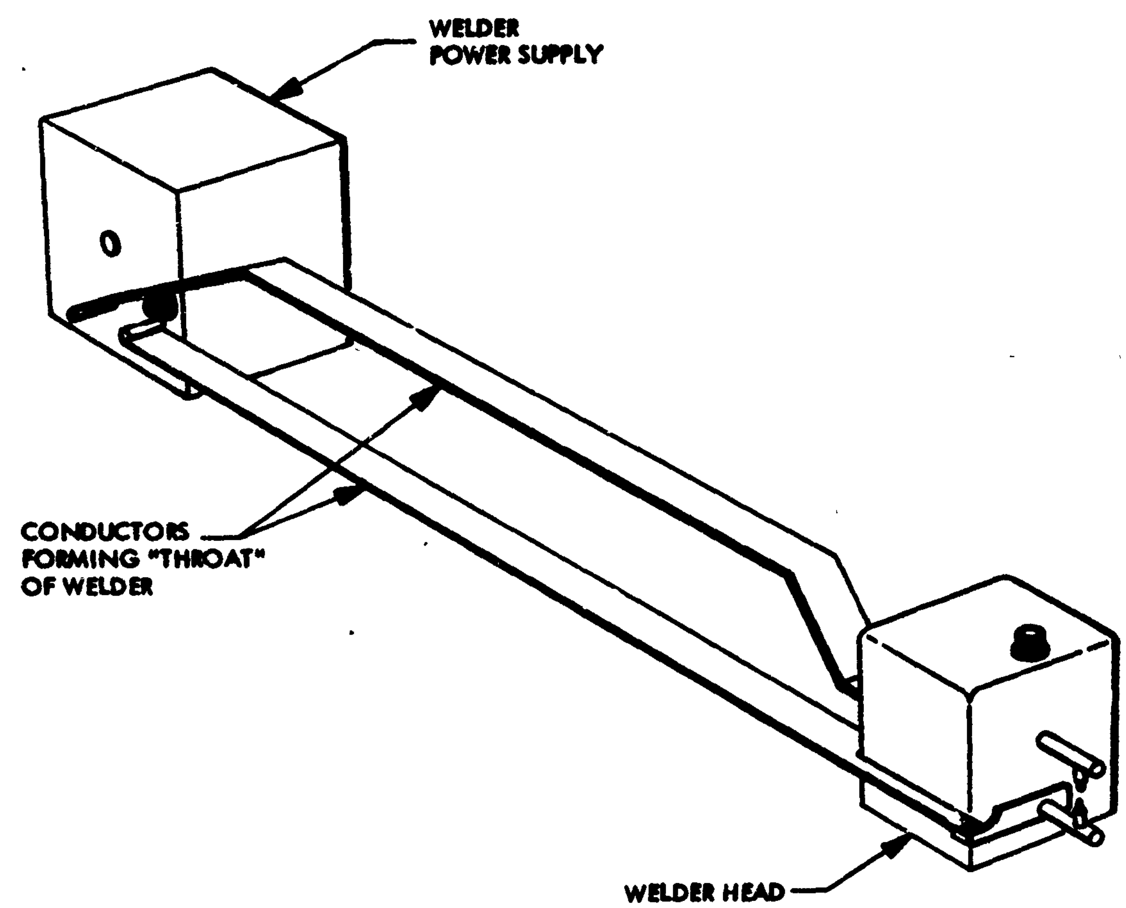

Figure 68. Induction Loss Test, Nine-Foot Throat Fabric Welder

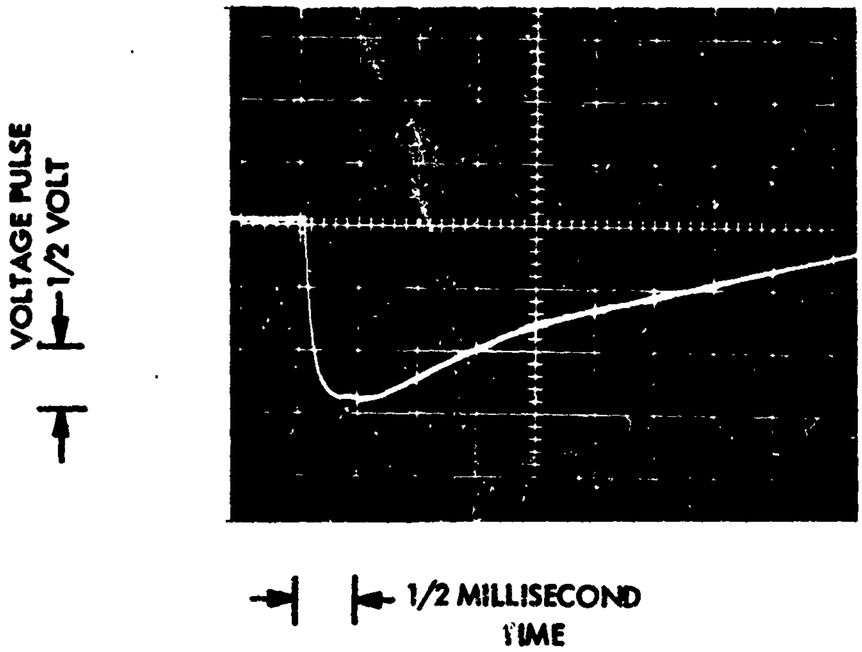

a. Close Coupled Welder

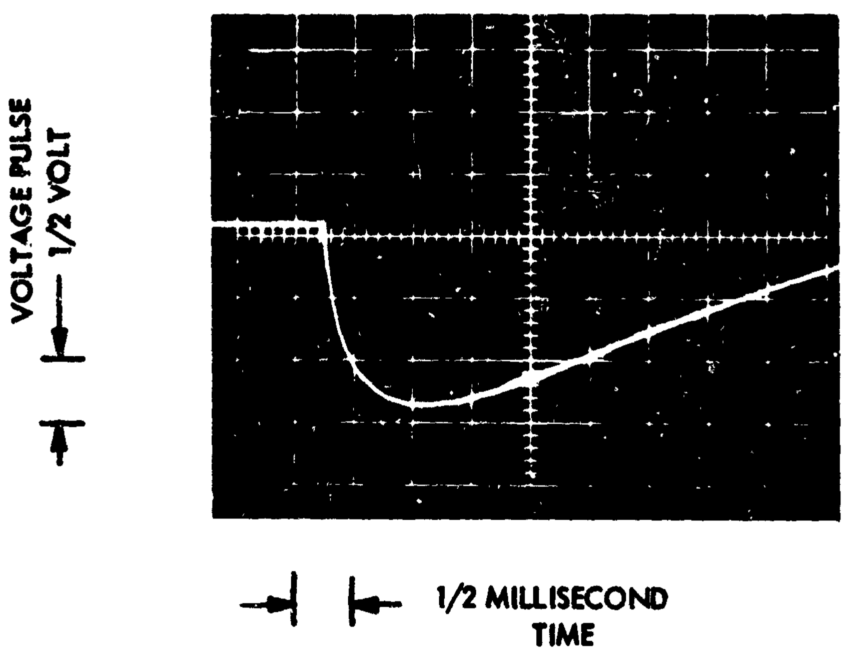

b. Nine Foot Throat Welder

Figure 69. Voltage Versus Time Comparison for Deep-Throated and Close-Coupled Welders

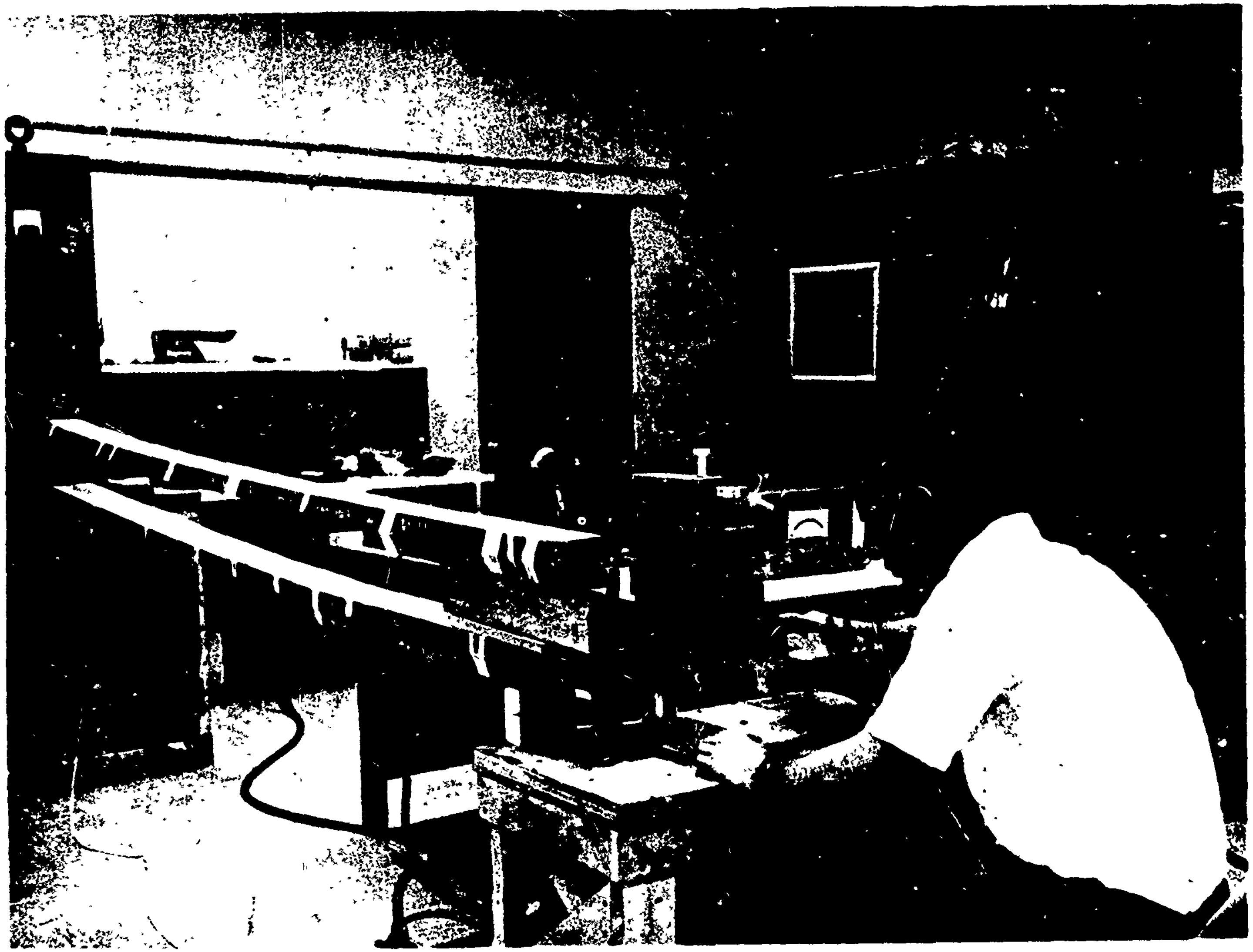

335/110

Figure 70. Deep-Throat Welder Test Set-Up with Square Pulse Power Supply and Nine-Foot Throat

e. Rinse in acetone

f. Air dry for 5 minutes minimum

A group of tests was performed for coarse optimization of the welding parameters with the object of determining trends corresponding to large deviations in the variables which would affect the design of a semi-automatic welder. The results are shown in Table XX. In the last column of this table the task identification letters indicate the type of variable being evaluated as follows:

Task A — Spot spacing was varied between 15 and 60 mils using the 125-mil-diameter electrodes. The results indicate that the larger spot spacing produces a stronger seam, possibly due to the elimination of the overlap of heat affected zones.

Task B — The electrode force was changed from 20 to 40 pounds and the results indicate that the lower force was better for the 125-mil-diameter probes. Increased strength with greater spot spacing was verified.

Task C — Using 35-mil-diameter electrodes, the force was varied at the maximum current setting that could be used without expulsion of metal. A stronger weld was obtained with smaller electrodes but there was little difference in joint strength with change in electrode force from 6 to 12 pounds.

Task D — This was an attempt to determine the effect of drastically varying the weld current from 540 to 400 Amperes. The joint strength appeared to be relatively insensitive to current variations under these conditions.

Task E — Weld pulse duration was varied from 2 milliseconds to 4 milliseconds. The longer pulse duration gave stronger joints, with efficiencies increasing to 87 percent at the longer pulse period.

Task F — Voltage rise time at the heads was varied by changing the inductance of the 9-foot-long conductor circuit. When the rise time of 0.6 milliseconds, used in previous experiments, was reduced to 0.3 milliseconds, the weld joint strength decreased from 85 to 74 percent indicating that the slower rise rate gave a stronger seam. This may be due to increased ability of the electrode to follow the melting nugget down without arcing and resultant metal expulsion.

Table XX

SPACE-GENERAL WELDING DATA - BENCH TOOL

Specimen Ident.	Electrode Dia. Mils	Electrode Force Lbs	Power Supply Primary Volts	Welding Data Average Current, Amps	Welding Data Spot Spacing, Mils	Rupture Data Joint Efficiency %	Notes (1)
319-1	125	6	180	1670	25	51	
319-2	125	6	180	1670	25	51	
322-4	125	40	180	1700	25	61	
-5	125	40	180	1700	25	64	
323-2	125	40	180	1700	25	59	
-3	125	40	180	1700	25	47	
325-4	125	20	160	1600	15	32	A
326-1	125	20	160	1600	15	29	A
-2	125	20	160	1600	60	41	A
-3	125	20	160	1600	60	42	A
329-1	125	40	171	2000	15	57	B
-2	125	40	171	2000	15	52	B
-4	125	40	180	2000	60	64	B
-5	125	40	180	2000	60	22	B
330-2	35	6	180	580	25	65	C
-3	35	6	180	580	25	71	C
331-2	35	12	180	700	25	61	C
-3	35	12	180	700	25	72	C
-5	35	12	160	540	25	77	D
-6	35	12	160	540	25	82	D
41-2	35	12	147.5	400	25	80	D
-3	35	12	147.5	400	25	78	D
-5	35	12	190	650	25	71	E
-6	35	12	190	650	25	53	E
42-2	35	12	155	590	25	87	E
-3	35	12	155	590	25	76	E
-4	35	12	160	540	25	82	F
-5	35	12	160	540	25	85	F
45-2	35	12	176	540	25	80	F
-3	35	12	176	540	25	74	F
-4	35	12	160	600	25	90	(2)
46-1	35	12	171	540	30	74	G(2)
-2	35	12	171	540	30	82	G(2)
-3	35	12	171	540	30	89	G(2)
-4	35	12	171	540	30	72	G
-5	35	12	160	600	15	71	G
-6	35	12	160	600	15	80	G
-7	35	12	165	600	45	62	G
-8	35	12	165	600	45	71	G
48-1	35	12	155	500	30	84	(5)
-2	35	12	155	500	30	78	(5)
412-1	35	12	152	430	25	80	H(3)
-2	35	12	152	430	25	82	H(3)
-3	35	12	152	430	25	76	H(3)
-4	35	12	152	430	25	84	H(3)
413-1	35	12	152	430	25	80	H(6)(4)
-2	35	12	152	430	25	74	H(6)(4)
416-1	35	12	152	520	25	76	(6)
-2	35	12	152	420	25	80	(6)
-4	35	12	150	470	25	75	(7)
						72	(7)

NOTES:

(1) Capital letters indicate "Task" identification and are used in the accompanying analysis.
(2) Yarn basted sample.
(3) Hot detergent cleaning followed by ultrasonic cleaning then standard cleaning.
(4) Same as (3) except ultrasonic cleaning followed only by acetone wash.
(5) Staggered spot orientation.
(6) Pre-evacuated and helium purged.
(7) 5 layer joint, 2 tensile tests.

Task G	Spot spacing variation was evaluated using spacings of 15, 30 and 45 mils. The 30-mil spacing appeared to be best for these conditions.
Task H	Alternate cleaning methods were evaluated using hot detergent, ultra-sonic washing, and acetone rinse in various combinations as noted, in addition to two tests with a helium-purged chamber around the weld heads. Welding efficiencies were consistently in the 74-84 percent range, but no conclusions could be drawn as to the specific effects of these techniques.

3.7.? 5 BASTING TECHNIQUE

Some basting experiments were made with a 3/4-inch-radius curved needle and the Karma yarn, some of which remained on bobbins forwarded to Space-General following completion of the fabric weaving. This type of yarn basting can be done successfully but it is cumbersome, time consuming, and would require considerable refinement to achieve a desirable degree of success. Various methods were used, including a double stitch technique wherein one line of stitches was in the approximate middle of the lap joint and another row of stitches was used to tie the edge of the upper lap to the lower edge of the fabric by overcasting the edge. One of the difficulties encountered in this type of basting was that the fabric would lift away from the form tool while the needle was being forced through from stitch to stitch. The yarn would become kinked and snag easily when being pulled through successive stitches. The metal yarn was desirable in that it could be left in place while a non-metallic yarn would have to be removed. It was difficult to stitch the two pieces of metal fabric together tightly enough to insure that the entire assembly would conform to the shaping tool when it was finished.

The type of basting which proved most practical was made with a single, hand-held electrode probe and a Unitek spot welder power supply. The technique is illustrated in Figure 71. A thin copper strip is pre-placed or a copper shoe is positioned behind the fabric and acts as the second electrode. In the case of the copper shoe-type, it is bent in such a manner that it slides between and behind the overlapped fabric as the spots are made without disturbing the lap joint positioning. With this method, a single row of spot welds is made with the hand probe at relatively low-level power. The spot welds are approximately 0.5-inch apart and positioned in the middle of the lap joint.

Tensile tests were made on the various types of basted joints. Test results showed the double-yarn basted joint was the strongest, the single yarn was next in strength and the spot welded basted joint was the weakest, although the difference between the last two was not significant. The average failure loads were 72, 30 and 29 pounds each, respectively, for four joints of each type in which the seam length in each coupon was three inches. The lower strength of the spot weld basted joints was attributed to the fact that the fabric specimens were not acid-cleaned prior to fabrication.

Figure 71. Spot Weld Basting

The spot weld basted joints were quickly fabricated, taking approximately one-half-minute each (for 3 inches), while the yarn basted joints were time consuming, taking approximately 10 minutes each. One of the factors in favor of the yarn basting was that errors could be corrected with little or no damage to the fabric, whereas errors which occur in the spot weld bastings are usually irreversible. However, it was felt that the facility of doing the spot weld basting outweighed the disadvantages. This technique was developed into a very satisfactory method in which the spots were made down the middle of the lap joint and the final double-row weld produced by the semi-automatic welder straddled the basted weld spots.

It was later found that the weld spots could be cut apart with an X-acto knife and if care was taken minimal damage to the fabric occurred.

3.7.3 SILICONE RUBBER IMPREGNATION AND COATING

Since the S-6510 silicone rubber, manufactured by Dow Corning, proved to be the best elastomer to use as a result of ablation tests (including plasma-arc testing), early investigations were directed to impregnating the metal fabric with solvent disbursed solutions of S-6510. The investigation eventually showed that a void-free and gas-tight sealant could not be impregnated into the metal fabric by this method. Subsequent work with liquid, room-temperature-vulcanizing silicone rubber proved satisfactory and a vacuum impregnation process was developed. The impregnated metal fabric was then overlaid with calendered sheets of the S-6510 ablative material and the entire matrix of impregnated metal fabric and overlaid coating was laminated together using autoclaving techniques. The following sections discuss the development work in each area of investigation.

3.7.3.1 IMPREGNATION WITH SOLVENT DISPERSED SILICONE RUBBER

Four 7-inch-diameter by 15-inch-long cylinders were fabricated from mono-filament stainless steel cloth. Each of these cylinders consisted of two layers: one inner bias ply and one outer cross ply. The cylinders were equipped with reinforcing cuffs at either end in accordance with the detailed description in the section of this report entitled "Fabrication of Components."

Three of these cylinders were sent to Arrowhead Products, Los Alamitos, California, for impregnation and coating with silicone rubber.

Five general process steps were used in the application of silicone rubber to the cylinders: degreasing, priming, impregnation, coating, and curing. Each of the three cylinders was given identical degreasing treatment: vapor degreasing in trichlorethylene, and rinsing with distilled water and acetone. The cylinders were then dip-primed, using a solution of equal parts of Chemlock 607 and methyl alcohol, and then allowed to air dry. Following dip-priming, the cylinders were ready for impregnation.

Three impregnation methods were tried: dipping, vacuum, and brushing. For dip impregnation, 5%K-1305W (similar to the S-6510 silicone rubber) solids cement in toluene was used. The solution incorporated a 2, 4 dichlorobenzoyl peroxide catalyst. The primed cylinder was soaked in this solution and then forced-air dried in an oven at 120°F to evaporate the solvent. After six dip and dry cycles, followed by three brush coatings of the same 5% solution, the final, uncured K-1305W silicone rubber slab was applied to the exterior of the cylinder and then rolled down on a mandel to assure a satisfactory bond. The assembly was placed over an inflatable mandrel which was then pressurized to 3 psig to eliminate any clearance existing between the plies of the wire cloth. Unfortunately, this resulted in weld joint failures which prevented further work on the cylinder. However, the rupture due to weld joint failure showed that the impregnation had not been thorough, in spite of the six dips and brushing. It was concluded that a different impregnation process was required.

With the other two cylinders, a vacuum impregnation technique was tried. The primed cylinder was sandwiched between inner and outer nylon film liners and the liners sealed at the ends, forming a vacuum bag. A 10 percent solids solution, using the benzoyl peroxide catalyst, was introduced into the vacuum bag forcing entrapped air from between the metal fabric plies. Since a relatively low boiling solvent, toluene, was being used, the vacuum could not be too great because excessive boiling would occur in the vacuum bag. The first of the two cylinders processed this way suffered weld seam failures. The second showed negligible impregnation after evaporation of the solvent. Repeated vacuum impregnation simply washed the previous rubber deposit from the fabric.

Impregnation finally was carried out on this cylinder with brush application of a 10 percent solids solution with the cylinder on a sheet metal mandrel. Ten cycles of brush application and drying were applied from the exterior of the cylinder; three more were applied from the interior.

Slab coating of the silicone was carried out by successive applications of 0.030-inch calendered thicknesses of rubber. The calendered stock was applied while the cylinder was on the expandable mandrel, the final coating thickness varying from 0.120-inch-thick at one side of the cylinder to 0.030-inch-thick at the opposite side as a result of selective placement of the 0.030-inch-thick sections. This was in accordance with the desire to have a thicker surface of ablative material on one side of the component to simulate the proposed construction of the paraglider boom. The cylinder was fitted with a nylon bleeder cloth on the exterior surface with a nylon film vacuum bag being placed over this for the curing process.

Curing consisted of evacuation of the vacuum bag, hot air autoclaving of the assembly for 2 hours at 300°F and 90 psig, after which the vacuum bag and bleeder cloth were removed. A few areas of the inner surface were recoated with silicone rubber solution and the cylinder was recured for two hours at 275°F in a hot air oven. The cylinder was then post-cured in a hot air oven in the following steps: 2 hours at 300°F, 2 hours at 350°F, and 16 hours at 400°F. Final inspection of this cylinder showed wrinkles in the inner ply presumably resulting from inadequate fit between the outer and inner plies of metal cloth. Other observations were that the inner surface coating peeled in a few places when the vacuum bag was stripped and the original white color of the silicone had discolored to a light tan, possibly due to inadequate degassing during curing. The completed cylinder is shown in Figure 72. It was used in the preliminary tests for setting up the heating and loads combination tests for the 7- and 10-inch components.

It was concluded that impregnation of the final multi-filament fabric would be difficult by this method, and investigation of other techniques was required. Regarding the weld failures, the welding process was far from reaching its final high level of development. It was performed one spot at a time as shown in Figure 64 and only a limited amount of experimental welding work was undertaken with mono-filament fabric since it was not the actual reinforcing material to be used for the final paraglider components.

Very simple tests were conducted on the tendency of the solvent-cut silicone rubber solutions to wet the multi-filament metal fabric. The approximate diameter of the area moistened by five drops of toluene-silicone elastomer solution was noted. The area into which the solution soaked was measured after a period of about 15 to 20 minutes when the toluene had evaporated. The specimens were cut through the treated area to study the wetting effects from the edge.

In general, the silicone rubber tended to stay on top of the fabric without soaking in, even when wetting agents were added. Solutions of 2.5, 5, and 10 percent solids, using both S-6510 and Y-3350 silicone elastomers in toluene, were used.

During the investigations conducted by the B. F. Goodrich Co., under subcontract to Space-General, many combinations of various concentrations of solids in toluene, numbers of coats of solution, and different methods of evaporating the solvent were tried. For example, one process which Goodrich tried involved six solution coats of S-6510 solution, including three coats of 2.6%, two coats of 5.4%, and one coat of 11.2% solids solutions. Penetration of the multi-filament fabric was obtained but some void areas were apparent when the sample was cross-sectioned and photomicrographed.

The multi-coating process was very time consuming. As many as 24 coats were applied in some experiments. It was finally decided that brush coating of the more dense multi-filament fabric with low solids solutions did not appear practical, due to the large number of coating operations required and the erratic results obtained, with inadequate adhesion between multiple plies of fabric.

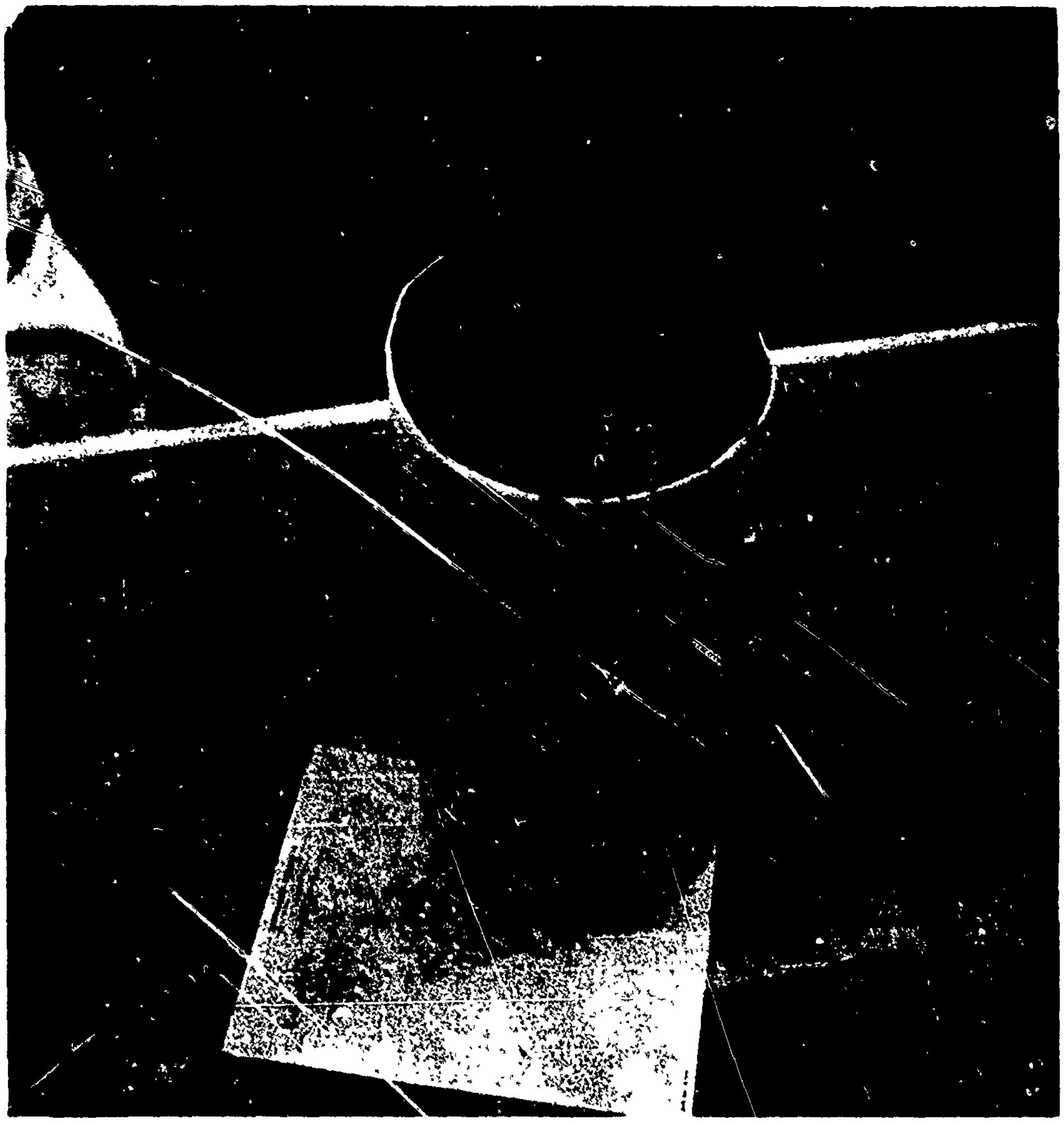

SG/249

Figure 72. Silicone Coated Cylinder

3.7.3.2 ALTERNATE IMPREGNATION TECHNIQUES

Although the work performed by Arrowhead Products (under subcontract to Space-General) on impregnation with solvent-cut silicone rubber solutions did not appear too promising due to the delaminations and presence of voids, the rupture of the weld seams in those monofilament cylinders made it difficult to properly evaluate the impregnation.

Altogether, three methods were tried with the S-6510 silicone rubber and a fourth method was tried with liquid, RTV silicone rubber.

One of the techniques tried with the S-6510 involved brush coating of solvent cut solutions, evaporating the solvent, and stitching or pressing the calendered sheets to the impregnated metal fabric. As a result of experimentation with this method by Arrowhead Products, brush coating of 5% solutions appeared somewhat promising when used in coating the monofilament metal cloth cylinders earlier in the program. During the investigations conducted by the B. F. Goodrich Aerospace and Defense Products Division, under subcontract to Space-General, many combinations of various concentrations of solids in toluene, numbers of coats of solutions, and different methods of drying the solvent rich coatings were tried. Both primed and unprimed, multi-filament fabric was tried. Cross-sectional photomicrographs, while indicating some degree of penetration of the filaments, always showed some void areas. Figure 73 shows a magnified cross-sectional view of a pair of yarns, consisting of 49 - one mil filaments each, in a sample of unprimed metal fabric with six solution coats of S-6510, including three coats of 2.6%, two coats of 5.4%, and one coat of 11.2% solids. The impregnated matrix was dried overnight and then 1 thin layer of S-6510 stitched to the surface. Figure 73 also shows a side view, of the same magnification, of the filaments spread apart. The degree of impregnation and attachment of the rubber to the filaments does not appear to be very uniform.

The multi-coating process is very time consuming. As many as 24 coats were applied in some experiments. Brush coating of the more dense multifilament fabric with low-solids solutions does not appear practical due to the large number of coating operations required and the erratic results obtained, usually with inadequate adhesion between multiple plies of the fabric.

The second method, calendering the silicone rubber directly into the fabric, was considered but was rejected because tests indicated that although the rubber was squeezed between yarns there was practically no penetration of the interstitial areas between the filaments. Furthermore, the large size equipment required might possibly damage the expensive, irreplaceable fabric. It would be impossible to calender previously welded shapes of compound curvature, and it appears impractical to attempt to pre-coat flat segments of fabric while leaving the areas to be welded free of impregnant and primer.

The third method of impregnation involved a lamination technique using metal fabric and S-6510 calendered stock. This method used a diaphragm press to exert sufficient pressure to actually force the raw gum stock into the fabric. On a large scale basis this might be accomplished by using vacuum

SGC/411

Figure 73a. Cross Sectional View of Solution Impregnated Fabric (150X)

SGC/447

Figure 73b. Side View of Filaments Spread Apart to Slow Adhesion of Silicone Rubber (150X) bagging and autoclaving techniques, but it is doubtful whether adequate pressure could be obtained in large autoclaves to push the S-6510 gum into the yarns of the fabric. However, this method gave good adhesion, assured a continuous uniform film of silicone between the metal fabric plies, and also eliminated the waste and damage factor present in the calendering method.

It was suggested that multiple construction might be made using the laminating method described above by building one ply at a time using thin copper strips placed directly under the joint areas so that they could be welded. Experiments on small specimens showed the copper strip could be removed easily after the welding, if a parting agent were used. This method presented problems with respect to possible contamination of the weld area and the need to apply high force with the welding tool which would possibly cause extruding of the uncured rubber from under the copper strips. It did not appear that a suitable fabrication procedure could be easily developed for large components.

Because of the difficulties involved in impregnation of high temperature curing gums, further investigations of liquid room-temperature-vulcanizing type silicone rubber compounds was undertaken with the ultimate objective of complete impregnation between all filaments of every yarn of the metal fabric.

3.7.3.3 IMPREGNATION WITH LIQUID RTV SILICONE RUBBER

An exploratory attempt was made at Space-General to demonstrate the impregnability of metal fabric with fluid pre-polymeric silicone rubber by use of differential pressure. Two candidate RTV silicone rubber pre-polymers, RTV 511 and RTV 615 (General Electric), were investigated. Of the two, the impregnation with RTV 615 proved to be the most satisfactory since it was considerably lower viscosity. The candidate materials were selected on the basis of their relatively low pre-catalyzed viscosities and their reputedly favorable post-cure physical properties at elevated temperatures. The technique of using a primer to promote high bonding strengths between rubber and metallic yarns was not used for this study, because communication with General Electric established the fact that the primer had comparatively poor temperature characteristics with respect to bonding with the metal in excess of 500°F.

The exploratory impregnation technique consisted of simply using atmospheric pressure to force the fluid pre-polymer into an evacuated sample of the metal fabric. A critical phase of this operation, the thorough cleaning of the cloth specimen, consisted of:

a. Washing in hot aqueous non-ionic detergent solution.

b. Thorough distilled water rinsing.

c. Treatment for 1 minute in 10% solution of hydrochloric acid.

d. Repeat thorough distilled water rinsing.

e. Rinsing in successive portions of clean acetone until all the water was removed.

The wet acetone soaked fabric sample and the freshly catalyzed polymer were placed in separate portions of a chamber and the system was evacuated until a reasonably good vacuum was obtained (approaching 100 microns), the acetone obviously evaporated. The polymer was then allowed to flow over and around the fabric sample. After approximately 45 minutes, air was admitted to the chamber and the system was left undisturbed for another 45 minutes. The specimen was then removed, the excess polymer scraped off both sides with a wooden spatula and the impregnated fabric was cured for 2 hours at 150°F.

The complete impregnation with the RTV 615 proceeded easily and produced a very homogeneous appearing specimen. Photomicrography established the fact that the fabric was completely impregnated with penetration of the RTV 615 rubber between every individual filament.

Complete impregnation with the RTV 511, however, did not occur. Apparently, the catalyzed RTV 511, a relatively viscous material which contains a significant amount of disbursed solid filler, was not able to flow freely around and subsequently through the metal yarns. A fairly large area of the lower surface of the specimen did not appear to be wetted by the rubber. Also examination of the edges confirmed the lack of penetration. In fact, there appeared to be only a top and partial bottom layer of rubber surrounding the cloth specimen with essentially no interstitial penetration.

The different behavior of the two rubber materials can probably be ascribed predominantly to two facts:

a. The viscosity of the RTV 615 pre-polymer was approximately 1/10 that of the RTV 511 pre-polymer.

b. The RTV 615 pre-polymer is clear and free of solids, whereas the RTV 511 material has a significant amount of filler solids and has a white, paste-like appearance.

Attention was then directed toward the problem of joining or laminating the ablative S-6510 rubber to the RTV 615 impregnating rubber. The manufacturer indicated that the peroxide catalyzed S-6510 could be directly bonded to the platinum derivative catalyzed RTV 615. Catalytic poisoning and subsequent bond failure would occur only if the S-6510 catalyst were an amine or a metallic soap. It was suggested that a "barrier layer" cement of RTV 108 could be tested between the two materials if direct bonding did not occur.

Subsequently samples of a new liquid silicone rubber, RTV 655, were obtained from the General Electric Co. This silicone polymer has better high temperature properties due to the addition of a phenyl side-chain and is a transparent, low viscosity liquid that cures with the addition of a curing agent. It is a pourable material with a viscosity (77°F) of 5000 centipoise, specific gravity of 1.07, shelf life (77°F) of six months minimum, and a pot life (77°F) of about four hours after adding the curing agent. After curing, the material is claimed to have a Shore A Durometer of 35, specific gravity 1.07, tensile strength of 850 - 1000 psi, and elongation of 150%. Since it contains no solvents, i.e., it is 100% solids, it will cure in deep sections, in closed assemblies without air, without exothermic effects, and with low shrinkage. Its weight loss after 1000 hours at 392°F is claimed to be about 3.0%. It also remains flexible to -100°F.

The primer recommended for bonding this silicone rubber to metal was General Electric's SE-4120. Although this primer was recommended for high temperature use, the manufacturer advised that the thermal stability of this primer would be relatively low above 500°F and might deleteriously affect the rubber to metal bond strength at the maximum potential exposure temperature of 850°F. In the interest of bonding strength at ambient conditions, it was recommended, neverthele ·, that the primer be used. To minimize the anticipated high temperature weakness, it was further suggested that the primer be applied in very dilute solution so that a minimum thickness of primer would adhere to the metal.

Evaluation of impregnation test results indicates that the vacuum technique completely impregnates the yarns and encapsulates the individual filaments. Using a solution of 1 part of the SE-4120 methanol primer solution to 10 parts of additional methanol, specimens of multi-filament fabric were primed and dried prior to impregnation. Good wetting was obvious during impregnation with the RTV 655. Samples containing two layers of metal fabric were cured under pressure at 250°F overnight and a thin layer of S-6510 gum was then cemented to the specimen with fresh RTV 655. The final laminates were again cured at 250°F overnight and finally post-cured at 475°F for 8 hours. The resultant material matrix was quite flexible and non-tacky. When subjected to a peel test, these specimens failed at about 4 to 6 pounds per inch at the rubber-to-rubber interface between the fabric layers. This indicated that the inherent tensile properties of the RTV 655 determined the limiting strength. Attempts to peel the S-6510 from the samples failed. The S-6510 layer tore rather than peeling from the impregnated metal fabric. The fact that impregnation occurred completely down between the individual filaments was indicated by studying polished cross-sections with a binoncular microscope attachment to the metallograph and with the aid of polarized light and color filters. Although many black and white photos of these cross-sections were obtained, they do not permit easy distinguishing of transparent rubber and void areas. The cross-section samples were prepared by sandwiching the impregnated fabric between thin aluminum strips and potting in transoptic mounting compound. The mounted samples were initially hand ground on wet grinding paper down to 600 grit and then polished with one micron diamond-polishing compound.

3.7.3.4 PRIMER CONCENTRATION

As previously discussed it was felt desirable to minimize the microscopic coating of primer which would be applied, in order to improve the high temperature adhesion of the silicone rubber. The SS-4120 primer is available in 6.0% methanol solution as a proprietary product of General Electric. The supplier's instructions state that unless the material is applied very sparingly, poor adhesion may result. It was recognized that the closely woven nature of the metal fabric would encourage the primer to deposit too thickly. A study was carried out to determine the optimum concentration of primer to be applied, as described below.

A series of pairs of metal fabric coupons were prepared in which each member of a given pair was primed by dipping into a different concentration of primer. The primer consisted of stock solution diluted with methanol. The two coupons, constituting a pair, were placed together and vacumm impregnated with RTV 655. After suitable curing, the specimens were subjected to peel tests and visual observations were made of the freshly peeled surfaces at the interface. Evidence of adhesive versus cohesive failure provided a means of bracketing the concentration at which a minimum prime coat was provided. It may be seen from the results in Table XXI that the most promising concentration appeared to be between a 10 and 20% dilution of the stock primer solution. This was subsequently confirmed by a series of tests made at a 15% dilution where all the layers demonstrated cohesive failure. The latter tests also included specimens which were primed by brushing as well as dipping of the metal fabric specimens.

When the "Phos-It" cleaning procedure, discussed in Paragraph 3.7.3.5 below, replaced the solvent-acid cleaning procedure the selection of the proper SS-4120 primer solution concentration required to provide maximum adhesion of the RTV 655 to the metal fabric, was re-examined. The effect of primer concentrations between 10 and 25% of the stock solution dissolved in methanol was studied by tensile testing peel specimens impregnated with RTV 655, as before. Although all the specimens demonstrated a similar peel strength in excess of 2.0 pounds/inch, the appearance of the specimens after testing indicated that the amount of adhesive relative to cohesive failure was minimized at about 20% stock solution in methanol. Previous observations indicated that 15% might be optimum but the figure was changed to 20% as a result of these studies.

3.7.3.5 FABRIC CLEANLINESS REQUIREMENT

Since the adhesion characteristics of the RTV 655 to the Karma fabric using the S-4120 primer, could conceivably be affected by surface cleanliness, a study of the effect of intentional contamination was made. A number of metal fabric specimen pairs were prepared which had been scrupulously cleaned, in sequence, with: (1) detergent, (2) water, (3) dilute hydrochloric acid, (4) water, and (5) methyl ethyl ketone, followed by final drying with nitrogen gas. Specimens were then dipped in various concentrations of mineral oil dissolved in methanol, ranging from 0.001 to 0.1%, allowed to dry, primed with 15% stock solution primer, then vacuum impregnated with RTV 655 and cured. Cross-sections through the cured impregnated specimen pairs, observed under a high power microscope with polarized light, indicated that the impregnation had been accomplished completely in all cases. Further, peel tests indicated that for the range of contamination study, no significant differences existed. However, later specimens with large amounts of oil or other contamination showed poor adhesion even though the impregnation still appears to be complete.

It appears that the degree of impregnation of multi-filament fabric by RTV 655 is relatively insensitive to fabric cleanliness, but the fabric should be as clean as possible for maximum adhesion.

Table XXI

PRIMER CONCENTRATION EVALUATION

Pair No.	Primer Concentration (% Stock Solution) Layer 1	Layer 2	Peel Strength lb/in	Failure Mode* Layer 1	Layer 2
1	0	2	0.9	adh.	coh.
2	2	10	1.5	adh.	coh.
3	2	10	1.5	adh.	coh.
4	10	20	2.4	coh.	coh.
5	10	20	1.8	adh.	coh.
6	20	50	1.7	coh.	adh.

*adh - adhesive failure
coh - cohesive failure

Subsequent to this study, a commercial metal cleaning agent, "Phos-It", supplied by the Wyandotte Chemical Co., was found to be much more effective than the previous acetone or MEK and hydrochloric acid cleaning procedures. Using the Phos-It solution as discussed under "Fabrication of Components", increased the weld efficiency significantly.

It was then necessary to assure that this cleaning procedure would provide a satisfactory surface for impregnation as the previous solvent and acid procedure. A number of tensile peel specimens were fabricated from the metal fabric, cleaned with Phos-It or the solvent-acid procedure and subsequently primed, impregnated with RTV 655 and peel tested. Table XXII shows the superiority of the Phos-It cleaning procedure over the one originally used.

In general it was concluded that the Phos-It technique provides at least twice the peel strength compared to the original cleaning technique. It also appeared that the dip primer application method was more effective than the brushing technique, however, subsequent examination indicated that the brush technique could be improved in order to provide adequate priming.

Table XXII

EFFECT OF CLEANING PROCEDURES AND PRIMING METHODS ON ADHESION OF RTV 655 IMPREGNANT TO METAL FABRIC

Cleaning Procedure	Primer	Peel Strength (lb/in) Max.	avg.**
Original method*	15% solv. (dip)	1.1	0.9
Phos-It wash	15% solv. (dip)	4.4	3.3
Phos-It wash	15% solv. (brush)	3.0	2.3

* Degreasing with methyl ethyl ketone, water rinse, deoxidation with 10% hydrochloric acid, water rinse.

** Data are mean values for three specimens.

3.7.3.6 VACUUM BAGGING MATERIAL

An 8-mil thick standard polyvinyl chloride film material was investigated for vacuum bagging purposes. This material, which is reasonably transparent, was found to maintain its impermeability to air with a 29-inch Hg vacuum even after exposure to 250°F for approximately 16 hours. Since the curing of the S-6510 required only about 1 hour at 250°F, it was concluded that a 8 mil PVC film would adequately meet the requirement.

Vacuum impregnation with the RTV 655 however, requires the use of a vacuum bag at room temperature and although the first shipment of PVC film worked quite satisfactory for this purpose, a second quantity of PVC film (possibly procured from a different source) poisoned the RTV 655 during impregnation of the boom and apex, such that it was difficult to get the impregnant to completely polymerize. At the time that it was used, it was not known that the PVC was the cause of the trouble, but in later investigations it was found that the RTV 655 would not cure in contact with this particular batch of PVC film. Since the RTV 655 is sensitive to poisoning by many substances, it is recommended that every material with which it comes in contact, such as vacuum bagging, be tested in advance for poisoning effects. This is further discussed in Paragraph 3.7.3.8 below.

3.7.3.7 CURING SCHEDULE

Optimization of RTV 655 to S-6510 adhesion was of obvious importance requiring evaluation, in terms of curing temperatures and times. A series of specimen pairs of primed metal fabric were impregnated with RTV 655 and overlaid with freshly calendered, catalyzed S-6510 gum silicone rubber using different techniques. The different types of fabrication process studied were as follows:

a. Freshly impregnated specimens were overlaid immediately with two layers of fresh S-6510 and vacuum bagged. The cure was one hour at 150°F, one hour at 250°F, followed by removal of the vacuum bag, and a final cure of eight hours at 450°F at atmospheric pressure.

b. The impregnated specimens were allowed to cure at room temperature overnight and then painted with fresh RTV 655. They were immediately overlaid with two layers of fresh S-6510 and vacuum bagged. The cure included overnight at room temperature followed by one hour at 250°F after which the vacuum bag was removed. Final cure was for eight hours at 450°F.

c. Impregnated specimens cured at room temperature for about eight hours still had tacky surfaces. These were overlaid with two layers of S-6510 and vacuum bagged, followed by cure for one hour at 250°F after which the bag was removed. Final cure was for eight hours at 450°F.

d. Impregnated specimens were cured at room temperature overnight and then painted with fresh RTV 655. One layer of S-6510 was immediately overlaid, vacuum bagged, and the assembly was cured overnight at room temperature. The bag was removed, a second layer of S-6510 was overlaid and re-vacuum bagged. This was followed by cure for one hour at 250°F, removal of vacuum bag, and final cure for eight hours at 450°F.

In all cases, peel tests for strength between the RTV 655 and the S-6510 failed cohesively in the RTV 655 near the interface. Furthermore, peel tests attempted between the S-6510 pairs failed by tearing of the S-6510 rather than in peel. This indicated that the adhesive strengths were greater than the inherent strength of the materials regardless of the sequence of the fabrication and variations in cure.

3.7.3.8 LABORATORY DEMONSTRATION OF IMPREGNATION CAPABILITY

Although two layers of metal fabric had been easily impregnated on many occasions, it was desirable to demonstrate that both spot welded and multi-layered specimens could be impregnated satisfactorily. The process was easy and troublefree as had been experienced with simple two layer specimens. The samples were mounted, cross-sectioned, polished, and prepared for metallographic analysis as described in Section 3.7.3.3 above. A photomicrograph of a cross-section through a weld is shown in Figure 74 in which the silicone rubber may be seen as the lighter colored material surrounding

Figure 74. Two-Layer Welded Karma Fabric Joint Impregnated with RTV 655 (Approximately 100X)

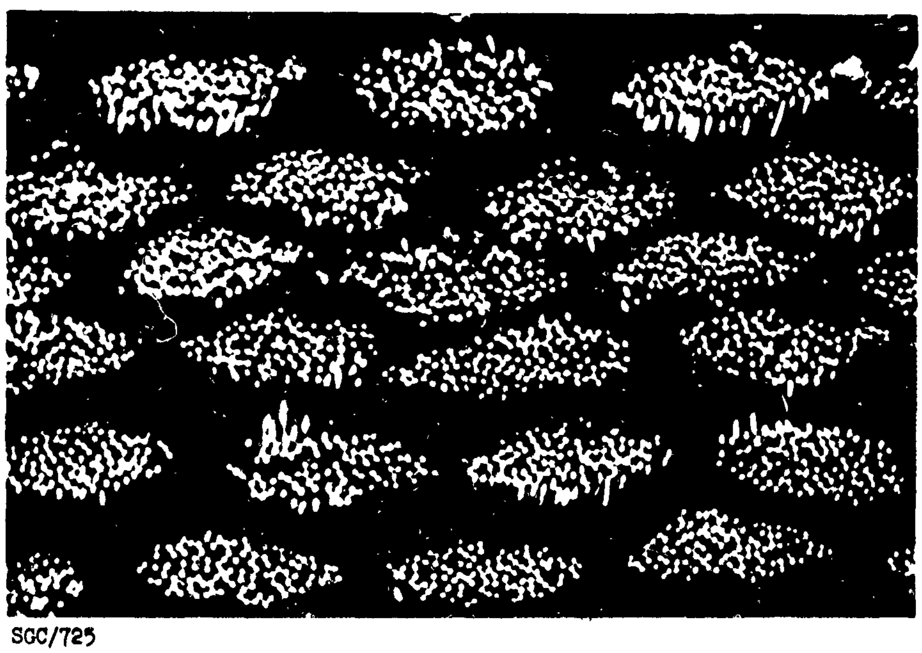

SGC/725

Figure 75. Six Karma Fabric Layers

the filaments and the central weld nugget. Another photomicrograph of a cross-section of six layers of fabric impregnated with RTV 655 is shown in Figure 75. Due to different lighting conditions the silicone rubber is shown as the darker material with the wire filaments as light spots in this photo. Study of each of these specimens under polarized light gave assurance that complete, void-free impregnation had occurred in each case.

3.7.3.9 VACUUM EFFECTS ON IMPREGNATED AND COATED METAL FABRIC

Although vacuum bagging techniques were to be used for the impregnating and coating of the metal fabrics, a question still existed concerning the possible behavior of the final product in a space vacuum. To explore this question, a small composite specimen impregnated with RTV 655 and coated S-6510 was prepared and exposed to a pressure of less than 10^{-5} mm Hg for a period of one hour at ambient temperature. Careful dimensional measurements were made and the specimen cross-sectioned for photomicrographic analysis. The results indicated that no significant effects on the composite should be expected as a result of the exposure to high vacuum. A small entrapped air bubble was intentionally allowed to exist under the S-6510 coating, and under vacuum this bubble expanded although no significant delamination occurred.

3.7.3.10 AUTOCLAVING PROCESS STUDIES

In each of five separate tests, two layers of metal fabric were impregnated with RTV 655 and allowed to cure at room temperature before being overlaid with fiberglass reinforced S-6510. The specimens were then cured as shown in Table XXIII it can be seen that a clear case cannot be made for a pressure autoclaving versus simple vacuum bagging. In the actual curing of the 10-inch-diameter frustums later, it was found that autoclave pressure did perform the function of smoothing out irregularities and filling cracks between laid up slabs of S-6510. The higher pressure autoclaving coupled with the use of the vacuum bag seemed to more homogenously bond the entire multi-layer fabric structure together. It is obvious that the vacuum bag should be evacuated first, followed by raising of the pressure in the autoclave, before the temperature is raised. This permits the matrix to become laminated and the silicone rubber to be forced into a uniform composite before curing is accelerated.

It is noteworthy that the specimens shown in Table XXIII were prepared with the new "Phos-It" cleaning procedure and show the relatively high peel strengths compared to those previously prepared by the solvent-acid cleaning procedure.

Table XXIII

AUTOCLAVE REQUIREMENTS STUDY

Test No.	(Cure History)* Initial	Intermediate	Final	Peel Tests, lb/in.** 655/655	655/6510
1	Vac. bag 4 hr @ 150°F	Vac. bag only, 0.5 hr @ 250°F	4 hr @ 400°F	4.7	3.5
2	Vac. bag 4 hr @ 150°F	Vac. bag & Autoclave (100 psig), 0.5 hr @ 250°F	4 hr @ 400°F	4.1	-
3	None	Vac. bag only, 0.5 hr @ 250°F	4 hr @ 400°F	4.5	3.3
4	None	Vac. bag & Autoclave (100 psig), 0.5 hr @ 250°F	4 hr @ 250°F	3.6	3.9
5	None	None	4 hr @ 400°F under 100 psig	3.6	3.5

* In all cases, two layers of metal fabric were impregnated first with RTV 655 and allowed to room temperature cure approximately 16 hrs. before overlaying fiberglass reinforced S-6510

** Data are mean values for three specimens. Cohesive strength between reinforced laminated silicone rubber materials as shown (i.e., RTV 655 to RTV 655, or RTV 655 to S-6510)

3.8 MANUFACTURING OF METAL FABRIC

In the Fall of 1963, preliminary specifications for ultra-fine wire, twisted yarn, and weaving of metal fabric were submitted to a number of vendors, together with requests for quotation and for comments on the preliminary specifications. The responses to this solicitation were very useful and helped to prepare the final specifications which were used for the procurements. It was discovered that the processes of wire production, metal yarn twisting, and metal fabric weaving were so specialized that there was no one vendor in this country whose capabilities clearly enabled him to excel in performance of more than one of these operations. Space-General decided to specify each of the processes and purchase the ultra-fine wire, yarn twisting operation, and fabric weaving as separate entities.

Personal visits were made by the Space-General Project Engineer to the plants of six potential vendors of products and services which were required for the wire, twisting, and weaving. Discussions with the manufacturers centered around steps which had to be taken regarding quality control, product cleanliness and tolerances, the effects of die wear and construction on out of round tolerances, the problems involved in specifying chemical composition of the chromium-nickel alloy, twisting of multi-filament yarn from ultra-fine wire without introducing extensive work hardening and unbalanced stresses in the wire, and the quantities needed at each production stage to insure a given final amount of reinforcing fabric.

3.8.1 PRODUCTION OF ULTRA-FINE WIRE

A Space-General component specification was issued to establish the requirements for the ultra-fine, nickel-chromium alloy wire. This specification contained the following elements.

a. Tolerances for an alloy with the following nominal composition were specified: chromium 20%, aluminum 3%, iron 3%, silicon 0.5%, carbon 0.05% max, and nickel balance.

b. Dimensional requirements included a wire diameter of 1.0 $\pm$ 0.1 mil and out-of-round not to exceed 0.1 mil.

c. Mechanical properties were specified as follows:

Yield stress at 0.2% offset	110,000 psi min.
Yield load at 0.2% offset	39.0 grams min.
Rupture stress	150,000 psi min.
Rupture load	53.0 grams min.
Elongation at rupture	12.0% min.

d. The wire was to be continuous filament and uniformly wound on spools. This was later changed in a revised specification to the winding of seven separate wire filaments layed on a spool in parallel to expedite the twisting of seven filaments and avoid unequal runout.

e. The size, weight, and shape of spools were specified to permit maximum economy, assure uniformity, and prevent snagging etc.

f. The wire was to be fully annealed.

g. Spool identification and quality of workmanship were established.

h. The supplier was to inspect and certify the wire in accordance with MIL-STD-105, Double Sampling Plan, Inspection Level II with an Acceptance Quality Level (AQL) of 2.5.

i. Methods of testing and certification were specified.

j. Packing, packaging, and marking for shipment were specified.

The Driver Harris Company, Harrison, New Jersey was awarded the contract for both the pilot run and production run of wire. Approximately 28 pounds of the one-mil wire were procured for the pilot run and 340 pounds were procured for the production run of metal fabric.

In the manufacture of ultra-fine wire such as produced by Driver Harris, raw materials such as nickel, chromium, iron, and aluminum are received in batch lots from suppliers. These are checked chemically and spectrographically to insure that they meet the chemical analysis standards required by the wire manufacturer. The proper mixture weights are carefully made up and recorded by melt number. For Karma, the trade name of the alloy supplied by Driver Harris, the melt charge is placed in a 600-pound vacuum induction melting furnace and melted under approximately five microns total pressure. A sample of the melt taken from the resulting ingots is sent to the laboratory and a chemical analysis is run to assure that the material meets the required range of chemical analysis specified. Ingots are then released to production to be reduced to 1/4-inch wire rod in the standard hot working practice of cogging and rolling on a looping merchant mill.

Both ends of the hot rolled rod are metallographically inspected for cleanliness and surface imperfections. The 1/4-inch rod is then released to be cold drawn.

Following routine standard practice, the 1/4-inch rod is reduced on multiple role carbide die wire drawing equipment with appropriate intermediate anneals to a semi-finished wire size. At the semi-finished or "breakdown" size, both ends of each coil are again metallographically inspected and released for finished drawing. The finer size wire drawing is accomplished with standard equipment through diamond wire drawing dies. The finished hard drawn wire is then continuously annealed through dry hydrogen (from disassociated ammonia) and is re-spooled on appropriate equipment to produce a finished spool of the required 0.001-inch wire.

During the pilot run for Space-General, it was determined that the process of twisting yarn with the wires ballooning off the end of each spool, caused considerable difficulty due to individual wires catching on one or more of the seven spools feeding into the twister. The usual waste was also encountered due to unequal runout, wherein one spool would be finished before the others and the small amount remaining on the other spools would be wasted.

While working on this contract for Space-General with the cooperation of Fabric Research Laboratories (FRL) and suggestions from Space-General, Driver Harris developed the idea of seven strands of 0.001 inch, on a single spool. Through tests run at FRL it was determined that this gave greater efficiency in the twisting operation because the spools could now be de-reeled rather than ballooning the wire over the end of the spool. Not only did this completely new concept of spooling produce better resultant yarn, it also allowed improved tension control. Seven ends on a spool simplified the set-up time and reduced down time in the twisting operation.

Probably the most important gain from the development of seven ends per spool was the reduction of wire waste in the twisting operation. Previous to this development, seven spools were shipped as a group matched in weight to $\pm$ 10%. The probability was that this would give an average of 10% of the wire wasted due to one of the seven matched spools running out before the others were finished. The other six spools would then be too short to produce an economical run. Theoretically, seven ends per spool should reduce the wire waste to zero in the twisting operation. In practice this actually turned out to be approximately 2 to 3% waste. In theory (and in practice on small diameters) there is no limit to the wire size which could be utilized for multiple ends per spool.

Driver Harris was encouraged by Space-General to perform some selection of wire prior to winding the seven ends on a given spool as well as in the combining of spools in the shipment, so that the average diameter of wire twisted into 49 filament yarn would be 1.0 mil. This was necessary since the specification permitted the wire diameter to vary from 0.9 to 1.1 mils. If the yarn averages significantly under or over 1.0 mil diameter, the strength, weight, and density of the fabric are affected by approximately the square of the discrepancy. The amount of fabric that can be woven is similarly affected because usage of yarn during weaving is only dependent on the length and not the size.

The combined efforts of Driver Harris, Space-General, and Fabric Research Laboratories led to a very successful and economical production of high quality wire for use in this program.

3.8.2 YARN TWISTING

The following discussion of the yarn twisting equipment and methods used in preparation of the pilot run yarn was taken from a report furnished by Fabric Research Laboratories, Inc., who were both the vendor of the yarn twisting and Space-General's consultants on reinforcing fabric and weaving.

The 28 pounds of 1.0 mil Karma wire received from Driver-Harris were processed on a Model 10B ring-twister manufactured by the Leesona Corporation, Providence, Rhode Island. This 6-inch gauge unit is equipped with 3-1/2 inch by 3/8 inch Eadie rings, and an 8-inch tapered top builder motion. The spindle speed is 5200 rpm.

The seven ends of 1.0 mil wire were plied 3.0 Z* tpi (turns per inch) using an E-29-D nylon traveler (manufactured by Coates and Clark, Newark, New Jersey) at a feed roll speed of 143 feet per minute.

The seven plied ends of 1.0 mil wire were cabled 2.33 S* tpi using an E-131-D nylon traveler at a feed roll speed of 185 feet per minute.

The resultant 25 pounds of cabled yarn, 7/7/1.0 mil/3.0 Z/2.3 S, was balanced; the yarn tendency to twist on itself when relaxed was minimal. Three pounds of wire were not used because of unequal run-off among spools. The purpose and objectives were to ply** and cable*** 1.0 mil wire into a 49-filament textile-like yarn for subsequent weaving into fabric.

The two most common textile methods for twisting are "uptwisting" and "downtwisting". The uptwister utilizes a vertical supply bobbin on a spindle rotating at high speed. The yarn is led up over the end of the bobbin and wound on a take-up spool. The ratio of the spindle speed to the take-up speed determines the number of turns of twist per unit length inserted in the yarn.

The downtwister utilizes a vertical take-up bobbin on a spindle rotating at high speed, a ring and a traveler. The ring is a circular track on which the traveler rides. It moves vertically up and down the length of the take-up bobbin. The yarn passes around positively-driven feed rolls, through the traveler to the take-up bobbin. The ratio of the spindle speed to the feed roll speed determines the yarn twist. A downtwister can be used to ply and cable; however, an uptwister can only twist one end.

A photograph of a close-up of the spindle, ring and feed rolls of a downtwister (ring-twister†) is shown in Figure 76. Figure 77 is a sketch of the major functional components of one position of the ring-twister. As shown, the ring is a circular track on which the traveler rides. The ring moves vertically up and down the length of the take-up bobbin. The yarn passes around the positively driven feed rolls, through the traveler to the rotating take-up bobbin.

Yarn twist in turns per inch is usually taken as the ratio of the spindle speed in revolutions per minute to the feed roll surface speed in inches

---

* S and Z denote twist direction; S clockwise and Z counterclockwise.

** Fine wire was supplied on spools, one end to a spool. The operation of grouping the single wires into a yarn is referred to herein as plying and the resultant yarn is called a plied yarn.

***The operation of grouping the plied yarns into a yarn is referred to herein as cabling, and the resultant yarn is called a cabled yarn.

† The terms ring-twister and downtwister are synonymous and are used interchangeably.

SG/241

Figure 76. Downtwister, Spindles, Ring, and Feed Rolls

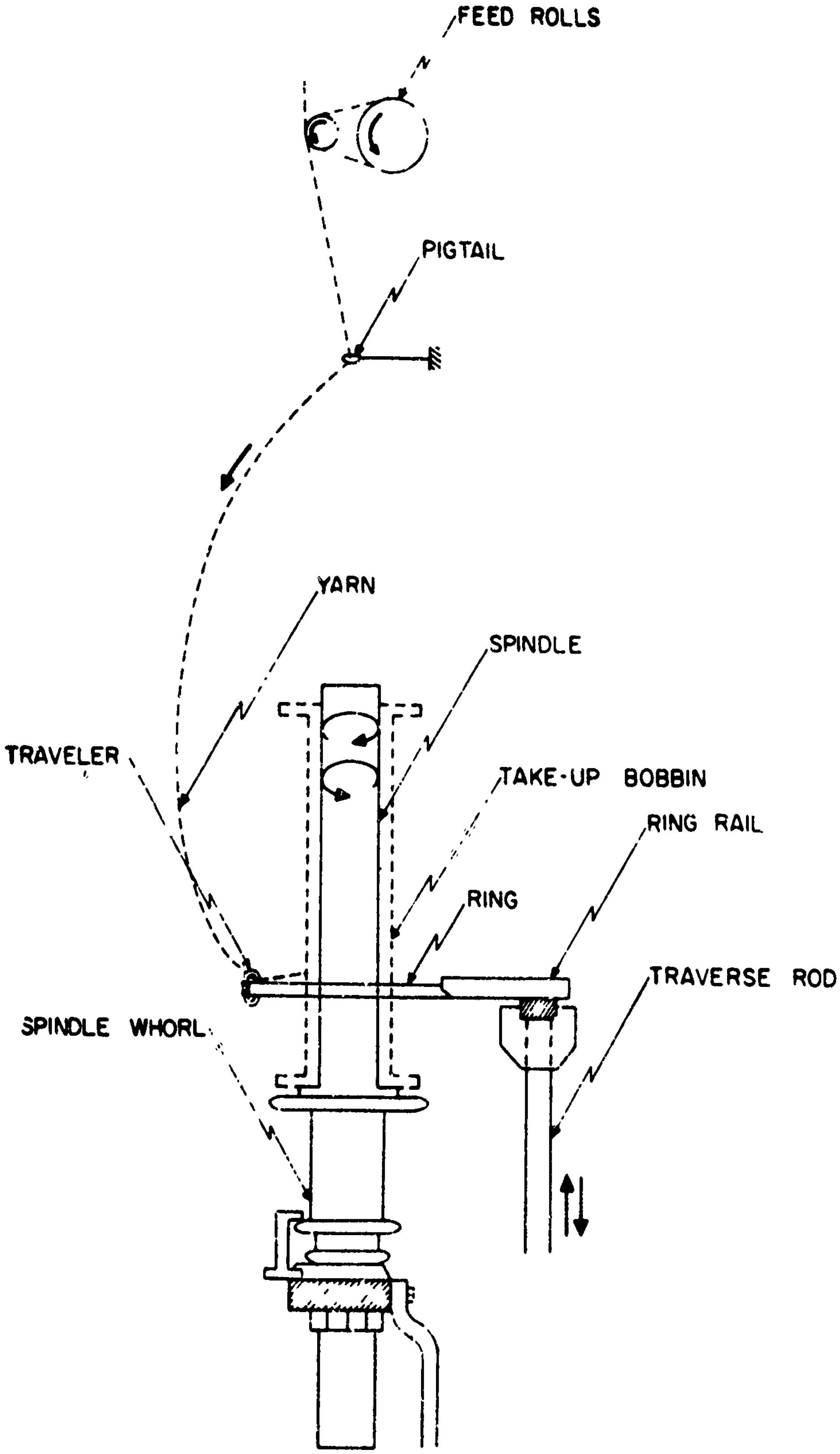

Figure 77. Ring Twister

per minute. However, the yarn twist as it lies on the take-up bobbin is actually given by the ratio of the traveler speed in revolutions per minute to the feed roll surface speed in inches per minute, and, as the analysis of ring-twisting outlined below shows, this ratio is not identical to the ratio of the spindle speed to the feed roll surface speed.

Letting S_f = feed roll speed in rpm
S_t = traveler speed in rpm
S_s = spindle speed in rpm
d_f = feed roll diameter in inches
d_p = take-up yarn package diameter in inches

it can be shown that

$$\pi d_p (S_s - S_t) = \pi d_f S_f \tag{19}$$

Yarn twist T in turns per inch is given by

$$T = \frac{S_t}{\pi d_f S_f} \tag{20}$$

where $\pi d_f S_f$ is the feed roll surface speed or yarn speed in inches per minute. Solving Equation (1) for S_t and substituting into Equation (2)

$$T = \frac{S_s}{\left(\pi d_f S_f\right)} - \frac{1}{\pi d_p} \tag{21}$$

As Equation (3) shows, the yarn twist is given by the ratio of the spindle speed to the feed roll surface speed minus the reciprocal of the take-up package circumference. The take-up package diameter varies with the amount of yarn that has been wound on the bobbin. Thus, the twist of the yarn as it lies on the take-up bobbin varies from the inside of the package to the outside, increasing from the inside to the outside.

In most textile processes the yarn is removed from the take-up bobbin by pulling the yarn over the top end of the package. This increases the yarn twist by the amount

$$T = \frac{1}{\pi d_p} \text{ tpi} \tag{22}$$

Adding Equations (3) and (4), it is seen that the twist in a yarn processed on a downtwister and removed from the package over end would be given simply by the ratio of the spindle speed to the feed roll surface speed. It is constant along the yarn length, independent of whether the yarn was on the inside or outside of the take-up bobbin package.

One of the most important variables in ring-twisting is the weight of the traveler used. A photograph of a typical traveler is shown in Figure 78. The required traveler weight varies with the yarn weight per unit length (denier) and traveler speed. The traveler speed is a function of the spindle speed, twist being inserted and ring diameter. The traveler weight must be such that the yarn balloons out between the pigtail and the traveler. If the traveler is too heavy, the balloon tension becomes too high and the yarn breaks; if it is too light, the balloon diameter becomes excessive, with the yarn possibly catching on the twister frame.

The manner in which the wire is pulled off the supply spools is an extremely important consideration. Pulling the wire off the side of the package by allowing the spools to rotate is not satisfactory due to the inertia of the spools and possible variable bearing friction. However, pulling the wire over the end of the spool in conjunction with a wisker disk* has been found to be completely satisfactory. A wisker disk consists of radially-oriented nylon monofilaments glued between paper disks. It is held on the end of the spool over which the wire is pulled. The nylong monofilaments provide the correct amount of back tension on the wire, minimize wire contact with the spool flange and trap the wire (between filaments) upon rapid take-up decelerations, thereby preventing the wire from sloughing off the end of the spool. The back tension can be varied appropriately with wire diameter by taking a wisker disk with a large number of filaments and cutting out every third or fourth filament until a suitable tension is achieved. The tension can also be varied by using a disk made with different diameter monofilaments.

FRL also found that the plied yarn can be pulled over the end of the take-up bobbin during cabling without any difficulty by utilizing wisker disks.

In order to accommodate the wire supply spools on the twister at FRL, the conventional creel supplied with commercial ring-twisters was replaced by a creel similar to a pegboard, Figure 79. Each of the spools (or bobbins) is mounted on a metal rod with a wisker disk held against the end of the spool (or bobbin) by a circular metal plate and screw threaded into the end of the rod.

The standard stop-motions on ring-twisters are adequate for cabling and plying large diameter wires. However, the twister at Fabric Research Laboratories, Inc., is equipped with only a five-end per position stop motion and since the plying operation for the subject work required plying seven ends, the stop motion was not utilized. This necessitated continuous patrolling of all twisting positions.

Ideally, a plying doff** should be completed without a break in the supply yarn. This is essentially impossible due to unequal spool run-outs and filament trapping on the supply spool. Therefore, a method of knotting the plied yarn after a supply yarn break was established.

---

*Manufactured by Azonic Products, Inc., Palos Heights, Illinois.
**Doff is a term used for denoting a predetermined running time and/or yardage.

SG/242

Figure 78. Traveler

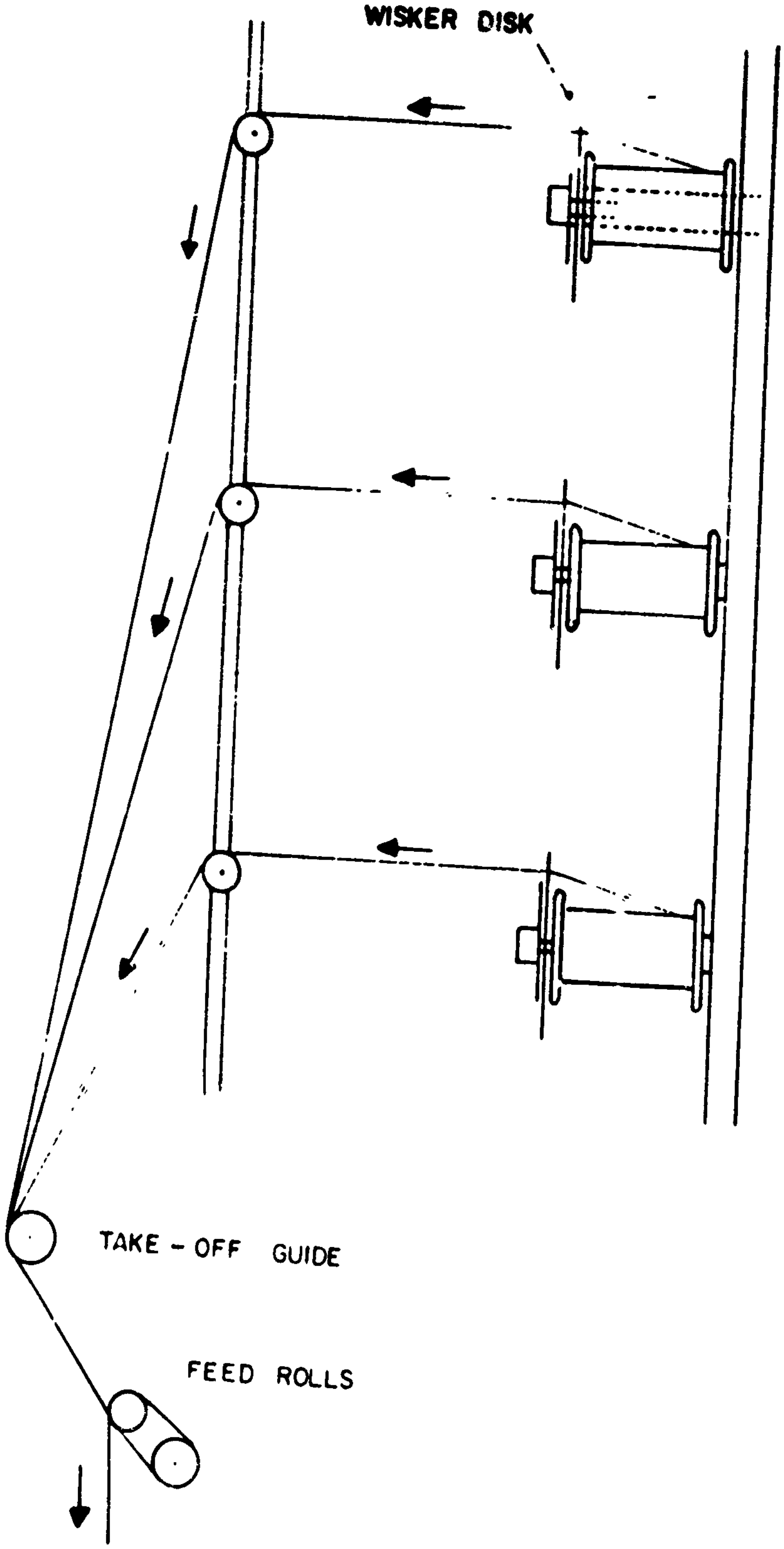

Figure 79. Wire Supply Creel

Upon observing a supply or plied yarn break the position is immediately stopped by the operator. The cause of the break is determined and rectified. the plied yarn is then tied in a simple overhand knot and the tails waxed with a water-soluble wax (S-52*). The knot is then laid at the extreme top of the traverse, against the top flange of the bobbin, and the position restarted. It is extremely important to place the knot at the top flange as this minimizes the plucking that occurs when pulling the yarn from the ply bobbin. When the knot is left on the traverse** of the bobbin, filaments are sometimes broken as the leading end is dragged over the knot.

The plied yarn bobbins are creeled in exactly the same manner as the wire spools described above. The cabling operation is different from the plying only by the fact that the twist is changed and a water-soluble wax (S-52) is applied to the cabled yarn. This is accomplished by installing a felt pad saturated with S-52 wax on the take-off guide, Figure 79, just prior to the feedrolls.

The yarn twisting for the production run, utilizing 340 pounds of wire, was similar to the above technique except that the process was simplified and the waste was prevented due to having seven ends of wire on a supply spool.

The yarn which was twisted met specifications which included the following conditions:

a. The yarn was plied and cabled to produce a 49 filament final yarn which was torque-free.

b. The final yarn was to exhibit a minimum of 92% strength translation from filament to yarn, i.e., the rupture load required to break the final yarn had to be at least 92% of the sum of the minimum rupture loads of the individual filaments.

c. The coating applied during twisting had to be easily and economically removable, and coatings had to be approved by Space-General.

d. Knots in final (cabled) yarn had to be marked with a slip of paper so that locations of knots could be identified and cut out during unwinding of the spooled yarn for weaving.

e. Workmanship and package identification were specified.

f. The supplier was to perform tests for twist balance, tensile strength, spooling quality, etc.

---

* Manufactured by Specialty Products Co., Jersey City, New Jersey. Polyethylene glycol 300 condensed with stearic acid.

** Traverse is the distance between top and bottom flanges of the take-up bobbin.

g. The yarn was tested in accordance with MIL-STD-105, Double Sampling Plan, Inspection Level II with an Acceptable Quality Level (AQL) of 2.5.

h. Tensile tests demonstrated that the 92% strength translation was realized when a 10 inch gage length of yarn was tested at a strain rate of 1.0 ± 0.1 inch per minute Acceptance of the yarn was based on conformance with a rupture load of 2389 grams minimum.

i. Packing and packaging techniques were specified.

All 340 pounds of wire for the production run were supplied with seven ends on a spool. The seven ends of wire could not be taken off the spools in the twisting operation by ballooning over the end of the spool; they had to be taken off by de-reeling, for which spindles were specially arranged. The resulting twister creel arrangement used on the production run is shown in Figure 80.

In the production run an actual total of 341.088 pounds of wire were used to produce 336.075 pounds of yarn indicating only 1.47% waste in the twisting operation. However solvent extraction showed the wire as received contained 1-2% by weight of oil and the yarn shipped contained 2-3% of wax (applied during twisting).

The yarn was tensile tested to insure conformance with Space-General's process specification. In accordance with MIL-STD-105 D, a batch size of over 280 bobbins was anticipated resulting in General Inspection Level H and a sample size of at least 32. Actually, every ninth bobbin was tested giving a total of 34 samples. All the yarn exhibited a strength greater than the 2545 grams minimum required, with the minimum sample giving a strength of 2718 grams and the maximum sample 3058 grams.

3.8.3 FABRIC WEAVING

As in the case of the ultra-fine wire and the twisting operation, a specification was written for the weaving of the metal fabric to meet the Space-General design requirements. This fabric specification including the following requirements for weaving both broad goods, five feet wide, and tape, 1.6 inches wide:

a. The fabric would be woven using a 2 x 2 basket weave with the broad goods having 58 picks and 58 ends per inch, and the tape having 40 picks and 80 ends per inch.

b. The warp and filling crimp in the broad goods were to be approximately equal with essentially the same tensile strength and elongation in both directions.

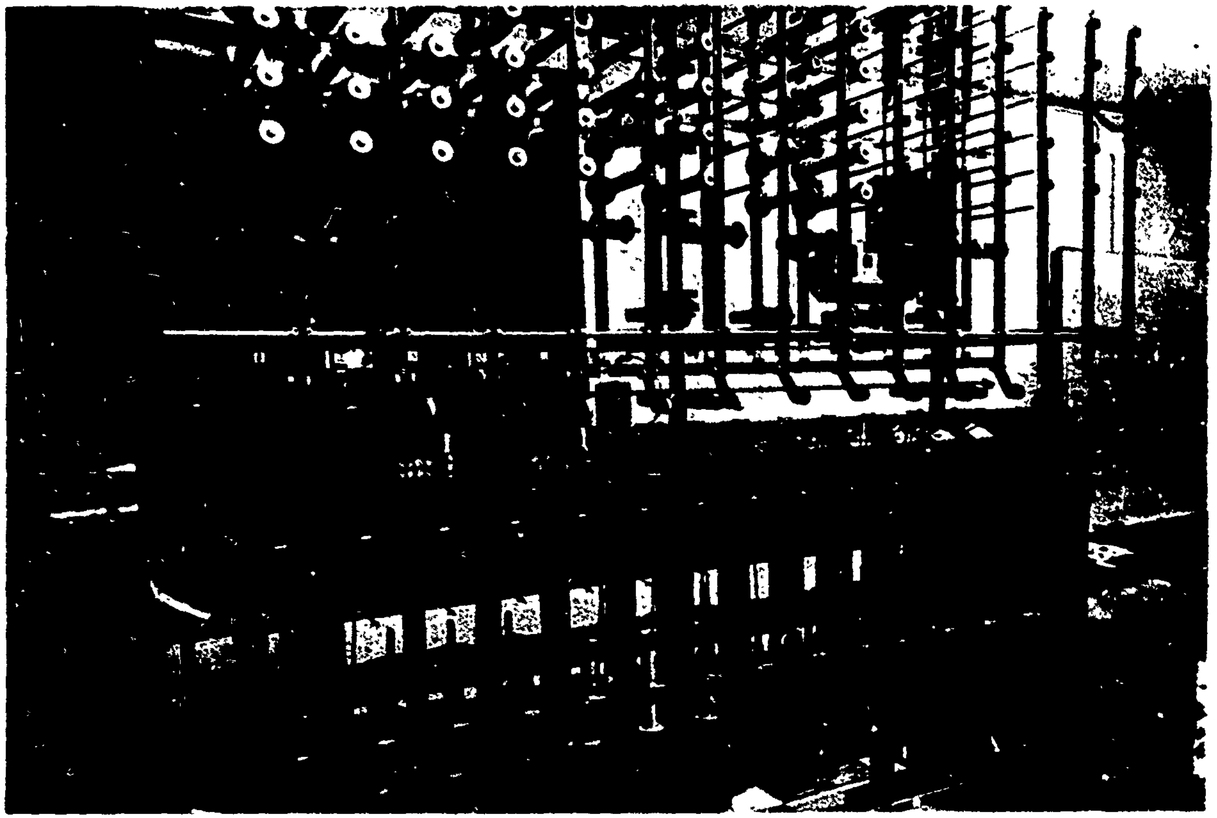

SGC/444

Figure 80. Ring Twister

c. The selvage edges were to contain only the metal yarn used in weaving.

d. Space-General had to approve all coatings used during the weaving process.

e. The final fabric was to be scoured to remove all coatings, sizings, lubricants, or other impurities.

f. The quality of workmanship was specified with specific tests being outlined to demonstrate the quality.

g. The warp and filling count were to be within ± 3% of the specified values.

h. Packing and packaging and shipment marking were specified.

Prodesco, Incorporated, Perkasie, Pennsylvania, was awarded the contract for weaving both the pilot run and production run of metal fabric. For the pilot run, 80 square feet of fabric, 25 inches wide (not including selvage edges) was ordered. For the production run, 1185 square feet of metal fabric was ordered 60 inches wide (plus 1/2 inch selvage on each edge).

3.8.3.1 PILOT RUN OF FABRIC

The two warps of the pilot run totalling 90.0 square feet of usable fabric were prepared on a single end warper and woven on a Crompton and Knolls silk loom with a 36-inch reed space. The fabric was woven 26 inches wide.

The single end warper is used in the preparation of warps where minimal amount of yarn to be utilized for a small quantity of woven material. The waste factor of this machine averages one to two percent of the total warp. The single end warper consists basically of a large rotating wheel with a circumference of 9 yards, 14 inches. This wheel is made up of twelve equally spaced bars upon which the yarn is laid during the warping process. The yarn guide is carried on a worm gear which is controlled directly by the rotation of the warp wheel. The action of the yarn guide is to cause the yarns to lay next to each other across the entire width of the warper as it rotates. This may be seen in the photograph of the partially filled warper, Figure 81. The worm gear was adjusted so that the yarn guide would travel one inch every 58 revolutions of the warp wheel. The yarn was wound 1,542 times around the circumference of the warping wheel, giving a warp width of approximately 26.6 inches. The limitations of this warper are that warps can be made no wider than 28 inches, no longer than 9 yards 14 inches, and the speed is constant at approximately 94 yards of yarn per minute.

Slightly less than seven pounds of yarn were used in preparing the first warp (two warps were made for the pilot run). The circumference of the creel is 9 yards 14 inches and 1,542 warps of yarn were wound on the

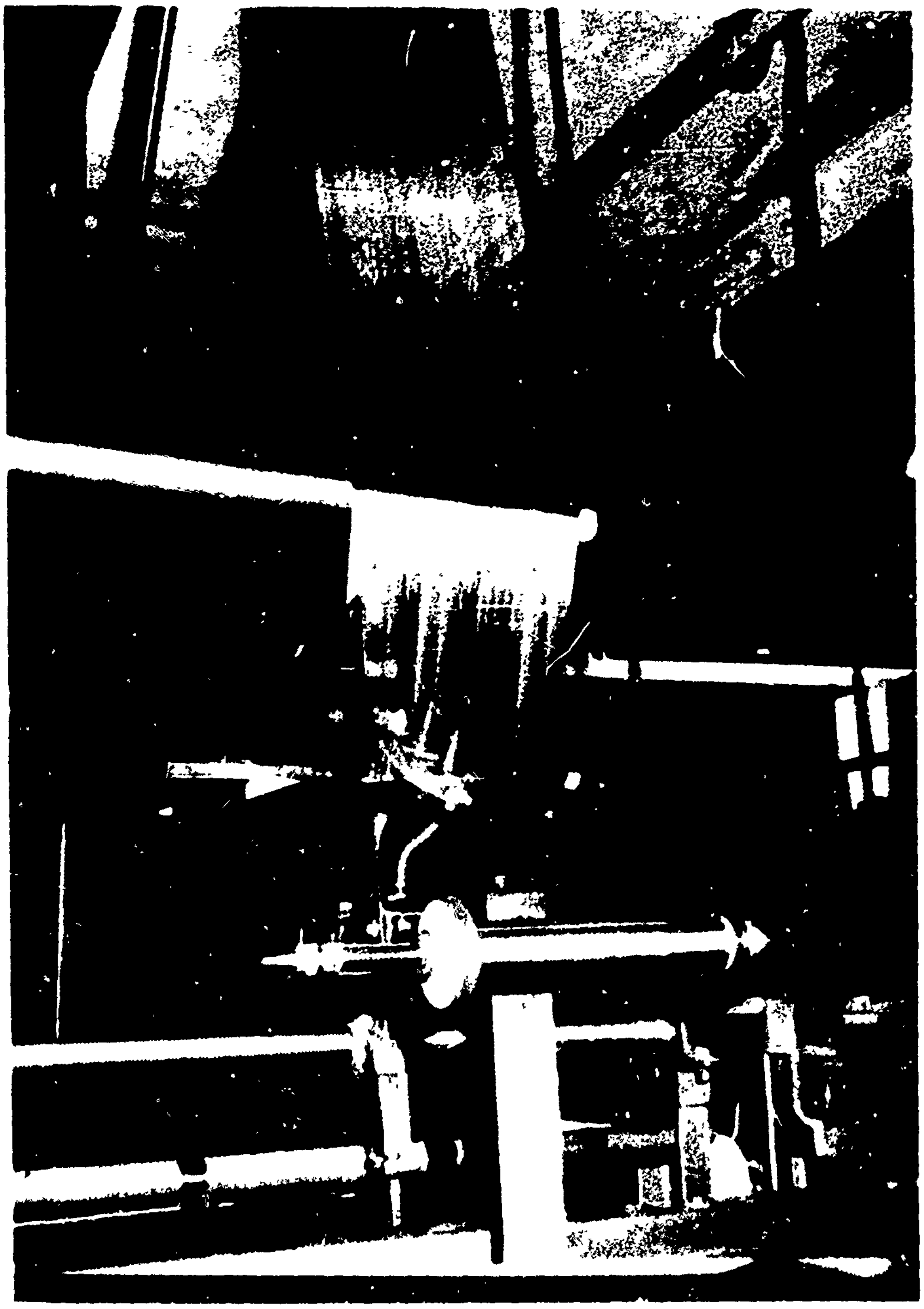

SG/27L

Figure 81. Single End Warper, Partially Filled

creel. This indicated that a pound of yarn was 2,087 yards. A pound of zero twist wire yarn containing 49 ends of 1.0 mil wire would be 2,380 yards. A small portion of the difference between the 2,056 yards/pound and 2,380 yards/pound figures is due to twist. However, the magnitude of the difference (14%) indicated that most, if not all, of the wire in the pilot quantity was over 1.0 mil in diameter. Although the wire was within specification between 0.9 and 1.1 mils, the likelihood of the wire being large in diameter was not anticipated since it was expected that the effect of diamond die wear would result in the wire starting out with the low diameter and gradually increasing to the high diameter, giving an average diameter of about 1.0 mil. Apparently the small size of the pilot run shipment did not encompass the full range of die wear and dies which were 1.0 mil or larger were used at the beginning of the drawing.

A 250 gram yarn tension was used in warping the wire yarn to help insure that the yarns were laid side by side on the creel with no crossovers.

It would have been desirable to pull the yarn off over the end of the bobbin in the warping operation in order to balance the yarn twist from the inside of the yarn package to the outside. However, it would then have been necessary to use yarn tension gates in order to get the 250 gram tension, which would have imposed excessive bending strains on the yarn and would have removed most of the waxed coating.

Certain modifications were made to the standard warper set-up so that metal yarn could be satisfactorily handled. A special bracket was made so that the supply bobbin could be dereeled (by rotating it) with a pretensioned coil spring producing a desired amount of drag on the rotation of the bobbin to give the necessary yarn tension. All guide surfaces were changed to "Alsimag", an American Lava Corp. brand of ceramic-type material, since the yarn would wear the normal guides excessively and be damaged. The wire yarn was delivered from the top side of the bobbin and guided between two posts and under a wheel to position it properly so that it would properly pass through an orifice of sufficiently small diameter to guide the yarn to its proper placement on the bars of the warping wheel.

Figure 82 shows the modified guide set-up. The light colored guide wheel in the center of the photograph was not in contact with the yarn when it was under tension.

A total of 6.936 pounds of wire yarn were used in making the first warp and 6.998 pounds on the second warp. The tension obtained by the spring pressure against the supply bobbin was kept at an average of 250 grams per end. Because of variations in the bobbins, the spring tension on each had to be adjusted differently to give the correct yarn tension as determined by a tensiometer.

In the beaming operation, two clamps were placed on two adjacent bars on the warping wheel. A length of pressure-sensitive tape was placed across the width of the warp above and below the yarns between the clamps. The tape was then cut in half lengthwise, severing all of the yarn ends. One portion of the cut tape was then attached to the warp beam and the upper clamp was removed

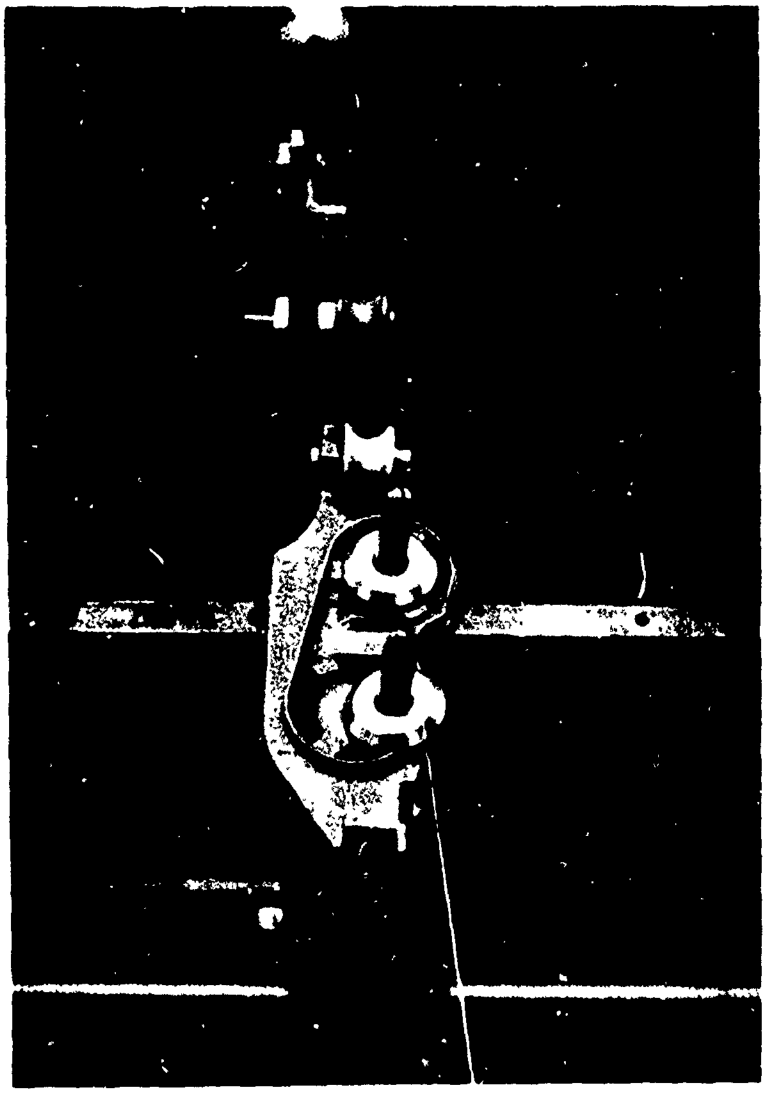

SG/287

Figure 82. Yarn Guide (with Alsimag Fittings)

so that the warp could be wrapped onto the beam. A continuous sheet of paper was rolled onto the beam with the warp to prevent the turns of yarn from snagging and assure more uniform tension across the warp while weaving.

During the wrapping of the beam, an adjustable brake on the axis of the warping wheel produced the desired tension in the warp yarns. The lower clamp, which was kept in place during the beaming of the entire warp, restricts the yarns from sliding or slipping and was removed when the nine yards had been warped onto the warp beam. In preparing this particular warp for the beaming operation, the wax on the yarn was removed with solvent so that the pressure-sensitive tape would adhere. A series of cords were tied to the warp directly above the tape to permit the warp to be completely woven out with a minimum of waste as shown in Figure 83. The cords act as auxiliary warp and must be attached to the beam very carefully as they directly affect the weaving of the last one to two yards of fabric.

The drawing-in operation, which must be performed completely by hand, places each individual warp end through a controlling heddle. The main body of the warp was drawn-in by eight harnesses using what is known as a straight draw. In this procedure, the first end is drawn in on harness No. 1, the second end on harness No. 2, and so on up to harness No. 8. Then the ninth end is drawn in on harness No. 1 and the steps repeated. No selvage as normally seen on textile fabrics was used. A metal yarn catch cord was put on the right side to catch the filling on every other pick.

During this manual drawing-in procedure, each individual end must be picked off a tape and handed to the operator who is drawing the ends through the heddle. Figure 84 shows the operator drawing the ends through the eye of the heddle with a hook.

After all of the ends have been placed through the proper heddles, they must be drawn through a reed which keeps them in proper alignment for weaving. In this case, a 29 dent per inch reed was used, drawing two ends through each dent (opening between wires of the reed). Figure 85 shows the operator drawing the yarn ends through the dents.

The handing in operation could not be facilitated by a comb-type reed which is normally used when handing in a single end warp. It was felt that a comb reed would disturb the filaments in the yarn and cause possible defects in the fabric. When a longer warp is made, drawing-in can be performed more easily because the ends are crossed in a lease so that they may be picked off individually.

Winding of the filling yarns was done on a Whitin-Schweiter automatic filling winder with a No. 4 winding motion and a stroke of one-half inch. The winding speed was slowed to approximately 100 yards per minute. A normal build and taper was used on all the quills. The average tension while winding was approximately 250 grams, but fluctuated much the same as it did during the warping process.

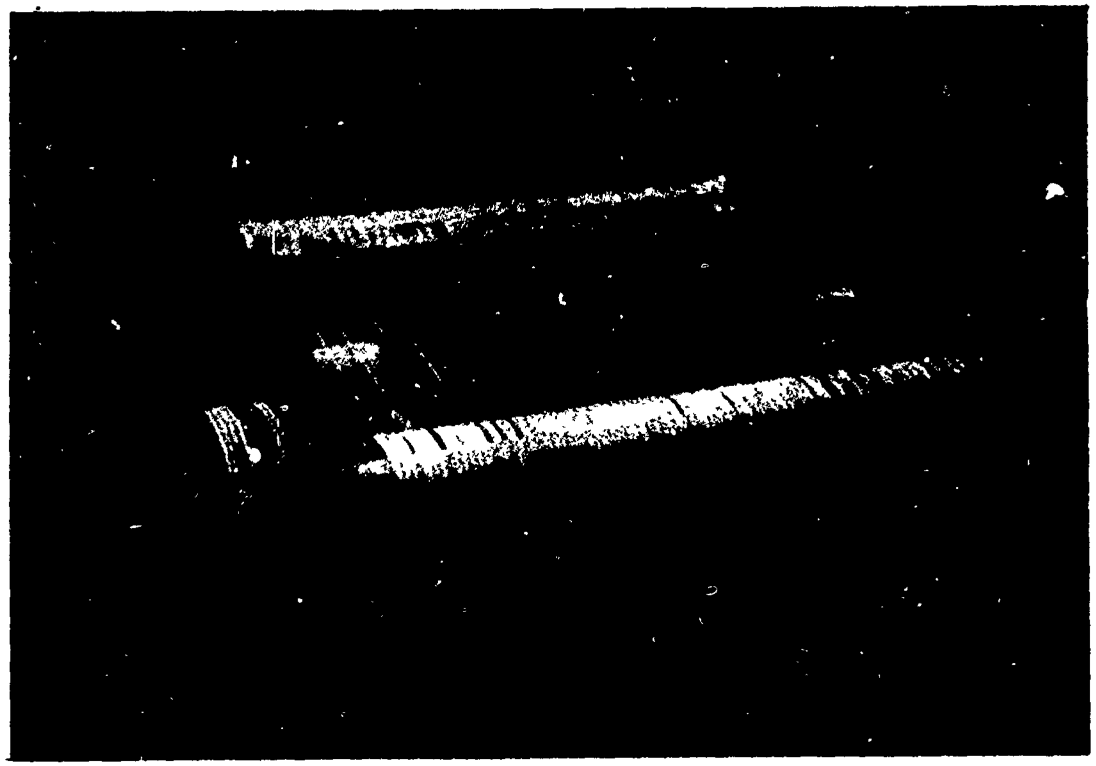

SG/292

Figure 83. Beaming Cords and Tension Weights (Near Completion of Weaving)

SG/283

Figure 84. Drawing Yarn Ends through Heddle

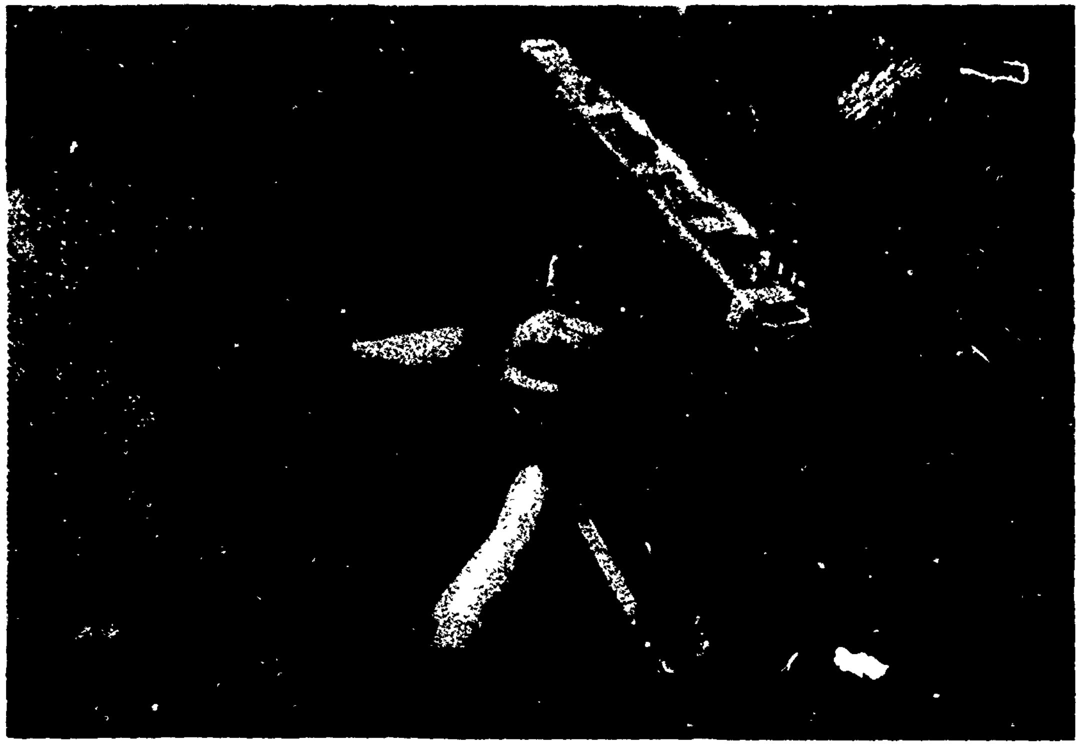

8G/284

Figure 85. Drawing Yarn Ends through Reed

The bobbin was mounted on the same type of bracket that was used in the single end warping and no other tensioning device was used except the pretension coil spring at the end of the bobbin. The yarn guide surfaces consisted of an Alsimag eye guiding over a freely rotating Heanium wheel, from Heany Industrial Ceramics.

The first few quills which were wound from each twister bobbin had to be waxed with additional S-52 aerosol spray wax (manufactured by Specialty Products Company). This is the same wax which was applied to the bobbins during the twisting operation.

The normal clockwise direction of winding was reversed so that twist would be added to the yarn when it is pulled over the end of the quill in the shuttle. The filling was wound on a prepared quill that had several hundred yards of stock cotton yarn wound on it first so that there would be a pre-built taper on the quill allowing as much metal yarn to be used as possible. Because of the experimental nature of the procedure and the cost of raw materials, the winder was not run automatically and an operator monitored the quill filling operation.

Prior to setting the drawn-in warp in the loom, a canvas leader was inserted so that the beginning of the warp could be tied to it and weaving could be started with a minimum of setup waste. A sheet of Teflon was installed above the breast beam to present minimum friction to the fabric in this area. The whip roll, which is normally set up in the back of the loom, was removed and the warp was set in its place. This was done to eliminate the right angle bend which normally takes place over the ship roll and to get the warp closer to the harness, eliminating additional waste.

The warp, which has been drawn into the harness and through the reed, was then set in the loom. The reed cap was then placed over the reed to reinforce it in the weaving operation. In addition to its function of aligning the ends into the proper fabric density, the reed also aids in beating the filling yarns into the construction. After installation of the reed cap, the warp was tied to the canvas leader with an even tension throughout the warp, as shown in Figure 86. The center warps were tied first, with remaining bundles being successively tied toward the edges.

While weaving, the warp must be held under tension so that the proper weaving action will occur. Figure 83 shows the method of tensioning the warp utilizing weights on cords wrapped around the warp beam. Increasing or decreasing the amount of weight applied to the warp can vary the number of picks per inch that can be woven. Weaving tension for this particular fabric averaged 26.5 grams for each end in the warp to obtain 58 picks per inch.

In future weaving on this type of loom, it may be desirable to wind the selvage yarns separately on selvage spools rather than on the same beam with the rest of the warp. This would permit the selvage yarns to be tensioned and let off independently of the warp beam.

SG/290

Figure 86. Tying Warp to Canvas Leader

During the beginning of the weaving operation on the first warp the first three or four inches of the warp was filled with a blue cotton cord rather than metal yarn. This equalized the tension on the warp yarns. Five 4-inch sections of metal yarn filling were then put in, each with a different experimental machine setting, resulting in 20 inches of "improperly" woven fabric at the lead end of the warp. This fabric was used for welding and silicone rubber impregnation experimentation even though it was not exactly the correct weave.

The timing of the loom was set so that the harnesses were level when the reed was fully forward, i.e., at front center. The loom was originally set up with selvage temples, but these were found to be unsatisfactory in holding the filling out to its proper width. An attachment known in the industry as a "crow picker" was installed and no temples were used during the remainder of the weaving. Figure 87 shows the crow picker holding the selvage of the fabric. The crow picker is a pointed shaft which catches the filling yarn to hold it out from the edge of the fabric, thereby, eliminating tight selvages. As the lay of the loom comes forward to beat the pick into the fabric, the crow picker is raised out of the way. Using crow pickers, it was possible to run a shuttle tension averaging 65 grams. In addition, the right side selvage was redrawn so that the last four ends on the outside of the fabric wove as a catch cord arrangement to catch the filling in every other pick.

Aside from the extreme precaution in leveling and timing of the harness and the care needed in making certain the selvages were properly tensioned, no outstanding difficulties were noted in the weaving of the pilot run fabric. Figure 88 shows the fabric being woven in the loom with the original "needle point" selvage temples.

The shuttle used in this particular loom had a double tension, preliminary tension being a gate spring and secondary tension being a series of prestressed loops. The final yarn delivery was made around two stainless steel posts of as large a diameter as the shuttle could accommodate.

The main observable defect in the fabric was the lack of crimp balance, i.e., the fact that the filling yarns were nearly straight while the warp yarns bend over and under the fill yarns. Improvement was made in this condition during the production run weaving.

After weaving the warp as far as possible, the remainder was cut loose from the cords and pulled through the reeds. The fabric was rolled onto a specially made roller which was placed on the front of the loom so as to eliminate any possibility of creasing or wrinkling.

This wooden roller with the fabric on it was placed in the sample jig used for both scouring and dyeing of fabrics, when they must be handled without wrinkling. Figure 89 shows the fabric in the jig ready to be scoured. The ends attached to the leader at the beginning of the warp were stapled onto the wooden beam of the jig. The fabric was rolled onto this beam from a wooden roller and the other end of the fabric was taken under the immersion roll and secured to the other beam.

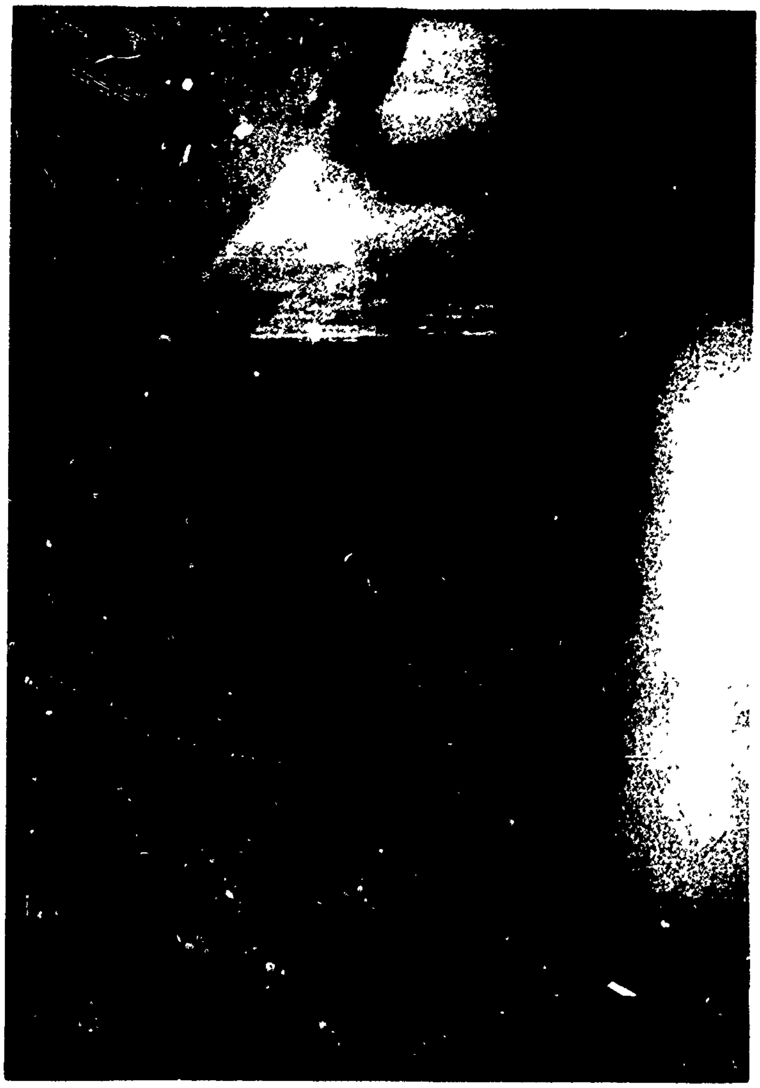

Figure 87. "Crow-Picker", Holding Selvage

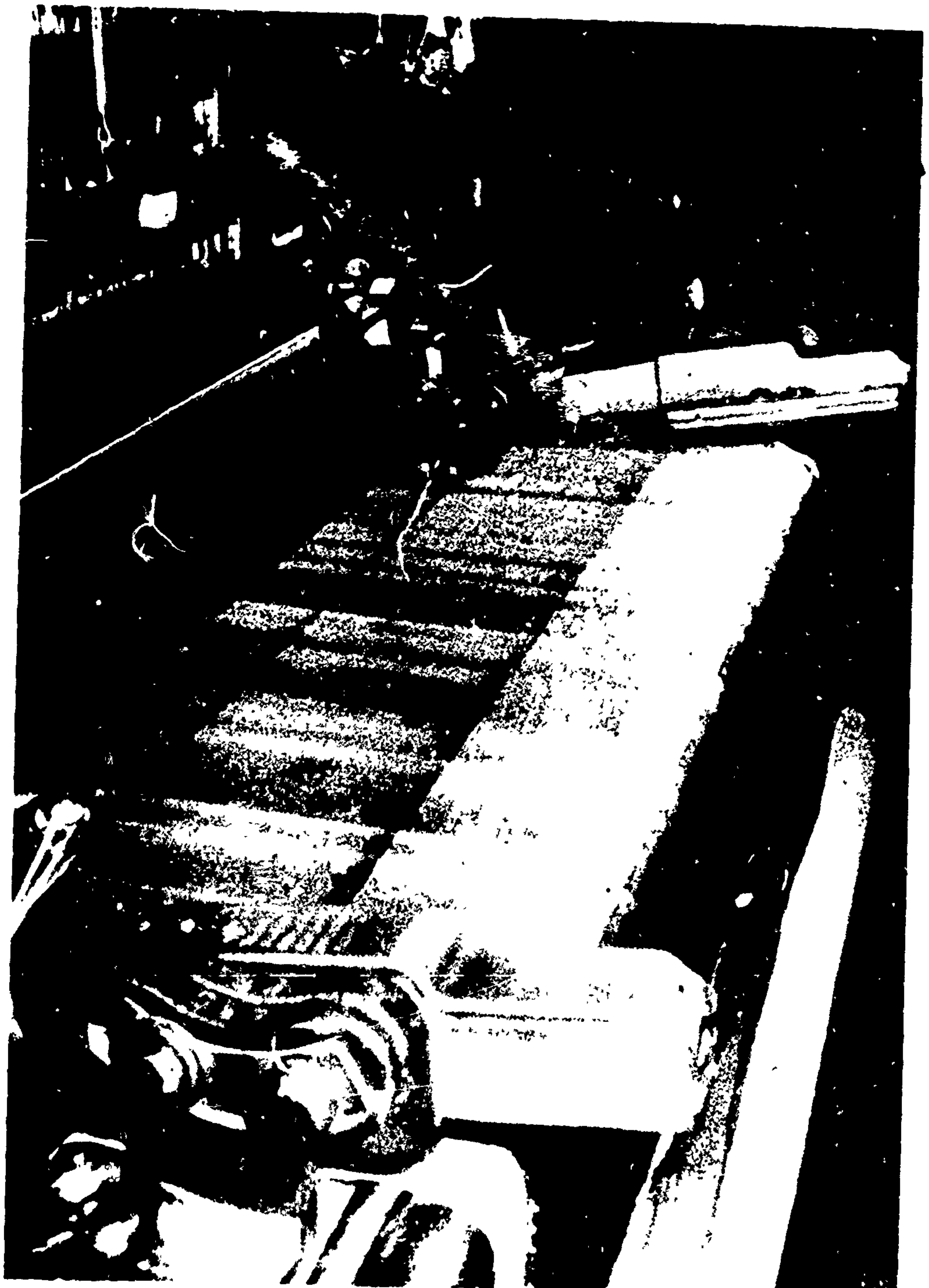

SG/280

Figure 88. Loom in Operation

80/289

Figure 89. Fabric in Scouring Jig

The fabric was scoured in a boiling solution of 1% Alkanol H.C.S. This is a non-ionic detergent manufactured by E.I. duPont de Nemours, Inc. Numerous passes were made through this boiling solution rolling the fabric up on either beam of the jig. This bath was dropped and a second bath of the same solution was used. A final rinse with cold water was made to remove any residual detergent or emulsified wax.

After the fabric had air dried, it was inspected over its full length and width in accordance with the Space-General specification.

The fabric was rolled on a specially fabricated wooden shipping shell to keep it as free from creases as possible. The shell was about 8 inches in diameter to keep the bending of the fabric to a minimum. After the fabric was secured on the shell, it was placed in a wooden shipping container and sealed for shipment to Space-General. The wooden shell on which the fabric was rolled was supported in a wooden yoke at either end of the crate so that the weight of the roll would not be carried by the fabric.

3.8.3.2 EVALUATION OF PILOT RUN FABRIC

The first warp of the pilot run laid out for inspection at Space-General is shown in Figure 90. It had a total length of 22 feet, with 20 feet 4 inches of usable material. There were some puckered effects 2 to 4 inches from one edge and approximately seven snicks and snags per square foot, but this quality was considered very good for the first trial run with a material which had never been woven before. In most respects the fabric essentially met the specification, except for crimp balance. It was found to be 0.0145 inches thick consistently.

The second warp (47.9 square feet) of pilot run fabric was inspected in May 1964 and was similar to the first warp.

As consultants to Space-General, Fabric Research Laboratories inspected samples of the completed fabric from the first and second warps of pilot run material and submitted a report. The main observations by both Space-General and FRL indicated some snicks and snags in the fabric which were possibly due to the additional twist put into the yarn when it was pulled off the filling quill, uneven selvage edges, and a distinctive lack of crimp balance. Actually, there was little difference between the first and second warps except that there was less wastage at the beginning of weaving of the second warp due to adjustments to the loom, and the second warp showed a lesser degree of non-uniform weaving, snicks and snags, and other minor discrepancies.

The lack of crimp balance was the most serious consideration. Since two plies of this fabric were to be used with one ply at a 45-degree angle to the other, lack of crimp balance could cause distortion of the vehicle on inflation and external loading. Lack of crimp balance causes the stress-strain curves in the warp and fill directions to assume significantly different shape with much more apparent elongation occurring in the warp direction due to the decrimping effect under load.

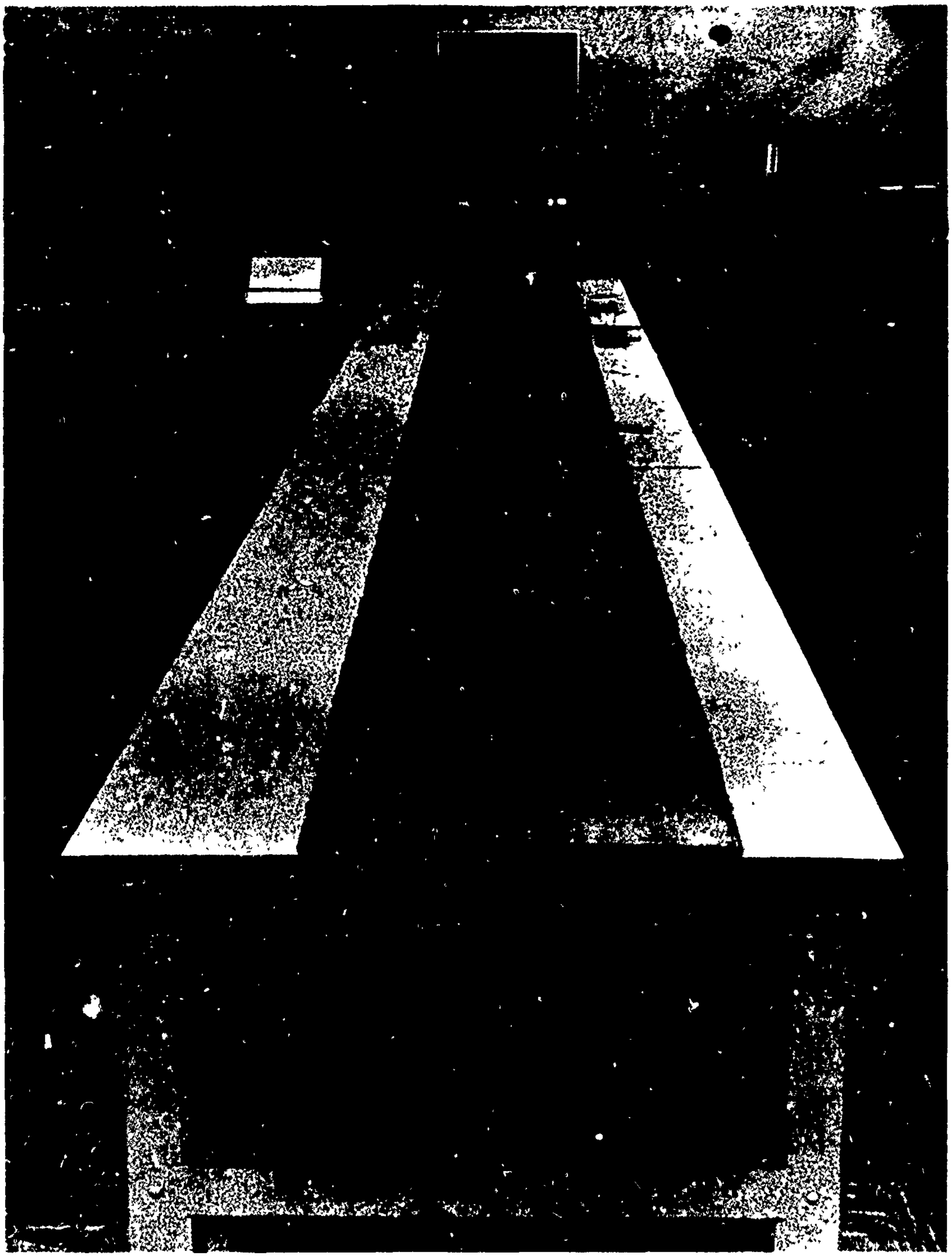

335/093

Figure 90. First Warp of Pilot Run Fabric Laid Out for Inspection

It appeared that a large portion of the snicks and snags in the fabric were caused by the filling yarn. Since this filling yarn was removed from the quill over the end, and the diameter of the quill was 0.5-to 1.0-inch, a twist of 0.3 to 0.7 turns per inch was inserted in the filling yarn. This twist unbalance was probably responsible for causing occasional filling yarn snicks in the fabric. Since the yarn was supplied to the weaver on sufficient packages or spools to permit warping the loom with one package per warp end, and all remaining yarn on each spool after warping was used for filling, it was possible to have a different twist in the filling yarn than in the warp yarn. Further attention was given to this problem during the weaving of the production run.

The following evaluation of the pilot run fabric was made by the Fabric Research Laboratories acting as consultants to Space-General.

The construction, weight, thickness and permeability of the pilot run multi-filament wire yarn fabric are given in Table XXIV. A photomicrograph of the fabric is shown in Figure 91. The magnification is approximately 13X.

The fabric thickness was measured using a pressure of 6 oz/in^2. The fabric air permeability was measured with a Frazier Permeometer using a 0.5-inch of water pressure drop across the fabric.

The fabric permeability was low due to yarn flattening during weaving. The weight of the fabric (34 oz/yd^2 was 24 percent greater than estimated (27.4 oz/yd^2) in the design study. This was probably due to the diameter of most of the wire in the early shipments being greater than 1.0 mil (average about 1.07 mil). The sample of fabric examined was woven from the wire in the first shipments.

The tensile strength of the fabric, 388 to 407 lb/in at 70°F and 331 to 343 lb/in at 1,000°F, was high due to the inherently high-strength metal filaments used. The strength translation from filament to fabric was excellent - 90 to 95 percent at 70°F and 77 to 80 percent at 1,000°F. The fabric tear strength, fold endurance and wrinkle recovery were also good. These properties were superior to those obtained in the past with 1.0-mil wire multifilament yarn fabrics (ASD-TDR-62-542, Part II) because of the greater number of filaments per yarn and fewer yarns per inch in the present fabric.

3.8.3.2.1 FABRIC TENSILE PROPERTIES

The tensile yield load, yield elongation, rupture load, rupture elongation and modulus in both the warp and filling directions of the fabric were measured with an Instron tensile tester. The results of the tests performed at 70°F are given in Table XXV and the results of the tests at 1,000°F in Table XXVI. The elevated temperature tests were performed in an environmental chamber mounted in the Instron. The air in this chamber is heated by six Calrod heaters and continuously circulated by a blower.

A one-inch fabric width, 3.5 inches gauge length, and 0.5-inch-per-minute jaw speed were used. The test specimens were actually cut to a width somewhat over an inch and several yarns were then ravelled from both sides of

335/107 (13X)

WARP FILL

Figure 91. Photomicrograph of Multi-Filament Karma Metal Fabric (Magnified 13X)

Table XXIV

FABRIC CONSTRUCTION AND PROPERTIES

Wire Diameter (mils)	Material	Yarn Construction	Weave Pattern	Ends per Inch	Picks per Inch	Weight (oz/yd^2)	Thickness (inches)	Permeability ($ft^3/min\text{-}ft^3$)
1.0	No. 331 Alloy, soft (Driver-Harris Company)	7/7/1, 2.33 S/3.0 Z tpi	2x2 basket	58	58	34	0.015	6

Table XXV

FABRIC TENSILE PROPERTIES AT 70°F

Yield Load (lb/in)		Yield Elongation (%)		Rupture Load (lb/in)		Rupture Elongation (%)		Tensile Modulus (lb/in)	
Warp	Fill	Warp	Fill	Warp	Fill	Warp	Fill	Warp	Fill
(First Warp - Average of 5 Samples)									
352	363	8.8	1.95	388	407	15.6	8.6	8,054	23,990
(Second Warp - Average of 5 Samples)									
361	361	8.8	2.1	403	400	13.7	7.6	9,689	28,300
(First & Second Warps - Average of 10 Samples)									
356	362	8.8	2.00	395	403	14.7	8.1	8,864	26,145

Table XXVI

FABRIC TENSILE PROPERTIES AT 1000°F

Yield Load (lb/in)		Yield Elongation (%)		Rupture Load (lb/in)		Rupture Elongation (%)		Tensile Modulus (lb/in)	
Warp	Fill	Warp	Fill	Warp	Fill	Warp	Fill	Warp	Fill
(Average of 5 Samples)									
303	306	7.8	2.9	331	343	12.6	10.1	4,948	9,672

the specimen until an inch width remained. Instron jaws with serrated faces were used. The faces were lined with leather for the 70°F tensile tests and with quartz fabric for the 1,000°F tests.

The yield load and yield elongation were taken from the load-elongation curve at the point where the bisector of the angle formed by the extrapolations of the pre- and post-yield portions of the load-elongation curve intersects the load-elongation curve. The tensile modulus was taken as the slope of the linear portion of the fabric load-elongation diagram prior to the yield.

All the breaks in the 70°F tensile tests of the fabric occurred about 1/8-inch from a jaw. Two 2-inch wide, 1-inch gage length specimens were tested with the same result. Since the quantity of fabric available was limited, long narrow specimens were not tried. Standard 1-inch wide 3.5-inch gage length specimens were used for all the tests reported in Tables XXV and XXVI.

In the 1,000°F tensile tests of the fabric, Table XXVI, three of the warp tests were jaw breaks. All the breaks in the filling direction were of the serigraph type; progressive failure of yarns from one portion of the fabric outward instead of complete rupture of all yarns at one time. The rupture elongations given for these tests are the values at the maximum load.

Typical load-elongation diagrams at 70°F and 1,000°F for both the warp and filling directions are given in Figure 92.

As indicated by Figure 92 and the data in Tables XXV and XXVI, the tensile modulus was much greater in the filling direction. This was due to more crimp in the warp yarns than in the filling yarns. This can be visually detected also in Figure 91.

From Driver-Harris Company data, the average properties of the 1.0-mil wire used were:

Yield load	- 57.5 gms
Rupture load	- 68.6 gms
Rupture elongation	- 14.5%

If the fabric exhibited 100 percent strength translation from filament to fabric, the fabric strength would be:

$$\frac{68.6 \text{ grams} \times 49 \text{ fils/yarn} \times 58 \text{ ends/inch}}{454 \text{ gms/lb}} = 429.4 \text{ lb/in}$$

The observed tensile strength translations from filament to fabric in the warp and filling directions at both 70°F and 1,000°F were 90 and 95 percent at 70°F and 77 and 80 percent at 1,000°F, for warp and fill directions, respectively. The strength translations were good and approximately the values that were anticipated. However, the actual level of fabric strength was much higher than was anticipated in the preliminary design due to the strength of the wire used in the pilot run being 28 percent greater than that of the wire on which the design calculations were based. Since the wire appeared to average 1.07 mils, however, approximately 14 percent of this increase in strength could be attributed to the larger diameter, while the remainder was due to the improved strength inherent in the alloy.

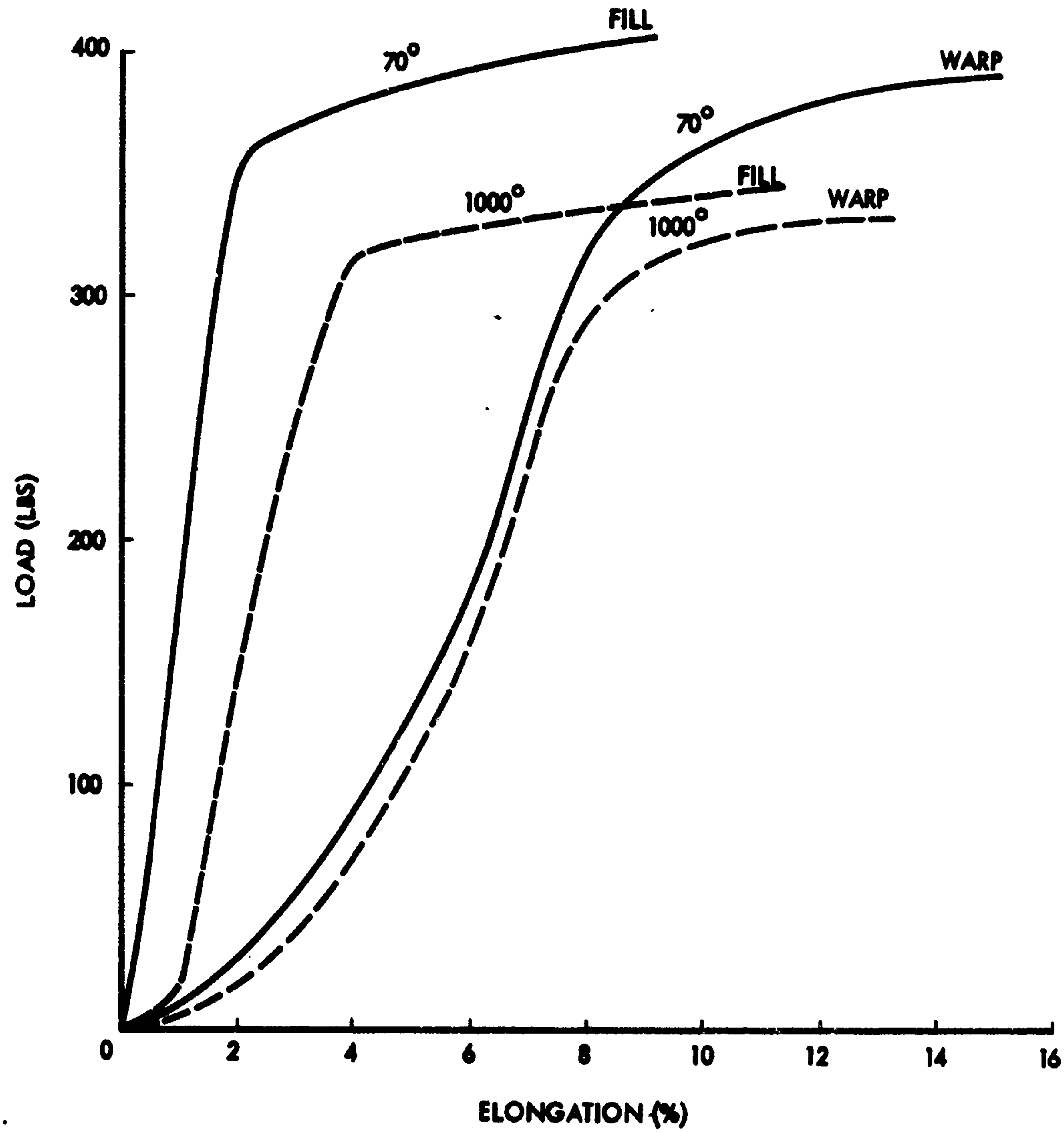

Figure 92. Typical Fabric Load - Elongation Diagram for Pilot Run of Metal Fabric

The strength translation was greater in the filling direction. This resulted from there being more crimp in the warp yarns than in the filling yarns. The yarn angulation to the plane of the fabric decreases the fabric strength.

The fabric elongation in the warp direction at 70°F was greater than the average filament elongation because of crimp. The elongation in the filling direction was lower than that of the wire. This probably resulted from the occurrence of work-hardening during twisting and weaving.

3.8.3.2.2 FABRIC TEAR STRENGTH

Specimens 3 inches wide and 4.5 inches long were used to determine tear strength. They were cut lengthwise along their centerline for a distance of approximately 2 inches. The two portions of the cut end were placed one inch into Instron jaws, one in the upper jaw and one in the lower (see Figure 93). The specimens were subjected to a constant rate of extension of 2 inches per minute for approximately 2 inches of tear, the load being recorded. Two specimens were used in both the warp and filling directions.

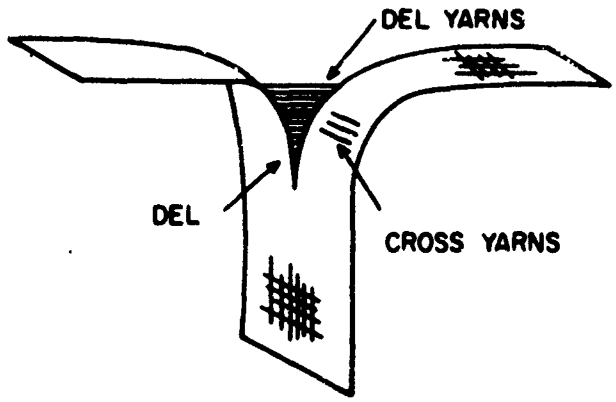

Figure 93. Fabric Tear Strength Set-up

The load-elongation curve obtained in a tear test is sawtoothed with each peak representing one or several yarn breaks. Tear strength values, as the average peak values of the two tests were 23 pounds in the warp direction and 29 pounds in the fill direction.

3.8.3.2.3 FABRIC FLEXURAL RIGIDITY

The bending length and flexural rigidity of the fabric in both the warp and filling directions were measured. The data were obtained by the cantilever beam test (ASTM D1388-55T, Method A). In this test, one end of a fabric sample one inch wide is clamped in a horizontal position. Then the free length, ℓ, of the sample is measured when the angle of the cord of the bent fabric sample with the horizontal is 41.5°. The bending length is $\ell/2$ and the flexural rigidity (EI) is

$$(EI) = w \left(\frac{\ell}{2}\right)^3$$

where w is the fabric weight per unit area.

Five measurements were made in both the warp and filling directions. The fabric samples exhibited a tendency to twist approximately 90° in 6 inches. The bending lengths were taken when the lower edge of the twisted sample touched the 41.5° plane. The average bending length in the warp direction was found to be 4.4 cm and in the filling direction 6.7 cm. The average flexural rigidity of the fabric in the warp direction was, therefore, 9.8 gm cm^2/cm and in the filling direction 34.7 gm cm^2/cm.

Yarn crimp decreases fabric rigidity. The fabric rigidity in the filling direction was, therefore, considerably greater than in the warp direction.

3.8.3.2.4 FABRIC FOLD ENDURANCE

The fold endurance of the fabric in both the warp and filling directions was measured with the MIT Folding Endurance Tester (ASTM D643-43, Method B). In this test both ends of the fabric are clamped in jaws. The lower jaw is subjected to a rotary oscillating movement such that the fabric is folded through an angle of 135 $\pm$ 5 degrees to both the right and left of the centerline position. The folding surface of the jaw has a radius of curvature of approximately 0.015-inch. A tension of 1.5 kg was applied to the test specimen at the upper jaw.

Test specimens 0.59-inch wide and 4.5 inches long were used. Five specimens were tested in both the warp and filling directions. The opening width of the jaw used was 0.01-inch.

All the specimen failures were of a progressive type. Therefore, both the number of cycles to when failure began (first noticeable yarn rupture) and the number of cycles to total rupture of the sample were noted. The average warp folding endurance for five samples was 303 and 448 cycles to first rupture and total rupture, respectively. The average fill folding endurance for five samples was 392 and 523 cycles for first rupture and final rupture, respectively.

3.8.3.2.5 FABRIC WRINKLE RECOVERY

The wrinkle recovery of the fabric was measured with the Monsanto Wrinkle Recovery Tester (ASTM D1295-53T). In this test, 1.5 by 4.0 centimeter test specimens are folded 180° with a 0.01-inch-thick metal shim between the two fabric surfaces. A load of 1.5 pounds applied for five minutes is used to crease the specimens. The recovered angle is measured after a five-minute free recovery time and its percentage of 180° is calculated, i.e., the percent wrinkle recovery equals (Recovered Angle/180°) x 100. Three measurements were made in both the warp and filling directions. Average results were 26 percent in the warp direction and 31 percent in the fill direction.

3.8.3.3 PRODUCTION RUN OF FABRIC

As with the pilot run of fabric, the most significant weaving problem was the inability to obtain completely balanced crimp between the warp and fill yarns. In attempting to obtain suitable crimp balance prior to commencing full-scale weaving, samples of the broad goods from the initial stages of weaving were sent to Fabric Research Laboratories for evaluation of physical properties. The data from these tests are given in Table XXVII. The best crimp balance achieved in these samples was with "Metal Fabric C," with the crimp percentage in the warp direction being 3.6 times that of the fill direction, but this loom arrangement caused breakage of warp yarns.

Consideration was given to a suggestion by Prodesco that a less dense weave, such as a 3 x 3, be tried since they felt this would more readily permit the achievement of equal crimp balance. Fabric Research Laboratories recommended the 2 x 2 basket weave be retained as the 3 x 3 weave would lack adequate lateral shear or would be too "sleazy." This reasoning was taken into account during the fabric selection phase. Observation of 3 x 3 weaves in other experimental metal fabric samples confirmed the decision to retain the 2 x 2 weave even if some crimp balance were to be sacrificed.

After five weeks of experimental effort to improve crimp balance and other weaving aspects, approval was given by Space-General for Prodesco to proceed with the production fabric weaving.

The best final ratio of warp-to-fill-crimp percentages, consistent with maintaining an otherwise high-quality fabric on this production run of wide goods, was 6.3. The corresponding ratio for the pilot run fabric was 19.0.

The following information has been taken from the report to Space-General by Prodesco, covering their work in weaving the production fabric and tapes.

3.8.3.3.1 WARPING

Both the wide warp and the tape warps were made on Prodesco's modified silk warper. This is essentially a section warper which wraps a given number of sections, containing a certain quantity of ends, from a creel onto a warp reel.

The bobbins of twisted and cabled yarn, as received from Fabric Research Laboratories, were placed on the creel. After some difficulties were encountered due to stuffing and kinking of yarn, Fabric Research Laboratories recommended that each bobbin be equipped with an H-2-1/2 whisker disk as shown in Figure 94(a). The yarn was then satisfactorily pulled over the end of these twister bobbins (198 bobbins on creel), through a pot eye, around one tension post, and through another eye to the condensing reed. Figure 94(b) shows the overall creel set-up and the path of the yarns from the bobbins to the reed.

Table XXVII

RESULTS OF TESTS ON MULTI-FILAMENT METAL FABRIC

Sample	Description	Yield Elongation %	Yield Load lbs	Rupture Elongation %	Rupture Load lbs	Modulus of Elasticity lbs x 10^{-4}	Crimp %	Remarks
A	Pilot Run (26 in. wide):							
	- Warp Direction	8.8	352	15.6	388	80	3.8	Avg. 5 samples
	- Fill Direction	1.95	363	8.6	407	240	0.2	Avg. 5 samples
	Production Run (61 in. wide)							
B	Two Stationary Steel Drag Rolls:							
	- Warp Direction	5.49	255	9.27	296.1	78	2.04	Avg. 4 samples
	- Fill Direction	1.85	274	10.99	346.5	209	0.23	Avg. 5 samples
C	One Stationary Steel Drag Roll With Increased Warp Tension; Crossing 1 5/16 Ahead:							Yarn breakage at reed.
	- Warp Direction	5.02	289	8.50	329	99	1.85	Avg. 5 samples
	- Fill Direction	2.55	317	9.30	380	183	0.51	Avg. 5 samples
D-1	Rubber Covered, Rotating Top Whip Roll:							
	- Warp Direction	5.40	292	12.79	359	96	2.07	Avg. 5 samples
	- Fill Direction	1.91	301	12.02	385	211	0.33	Avg. 5 samples
D-2	One Stationary Chrome Plated, Spring Loaded Top Drag Roll, Rotating Steel Bottom Roll; Crossing ½" Ahead; Selvage Temples; New 28.5 Dent Reed:							
	- Warp Direction	5.34	284	14.33	352	100	2.23	Avg. 4 samples
	- Fill Direction	2.12	273	11.85	363	183	0.25	Avg. 4 samples
E	Two Stationary Chrome Plated Rolls, Upper Spring Loaded; Crossing ½" Past Front Center:							
	- Warp Direction	5.10	280	14.21	350	105	2.12	Avg. 4 samples
	- Fill Direction	1.81	298	12.07	379	225	0.22	Avg. 4 samples
F	Final Setting - Same as E. Minimum 25 gms Shuttle Tension; Manual Quill Changing:							
	- Warp Direction	4.83	278	12.94	339	105	1.84	Avg. 4 samples
	- Fill Direction	2.05	300	11.67	375	205	0.29	Avg. 4 samples
	Tape (1.52 - 1.53 in. Wide)							
	- Warp Direction	3.55	580	9.18	683	230	0.78	Avg. 8 samples
D-2	Measurement of Crimp by Measuring Straightened Length of Yarn from Known Length of Fabric Sample:							
	- Warp Direction (Uncrimped Length: 10.31 Inches):						2.48	Avg. 3 samples
	- Fill Direction (Uncrimped Length: 6.10 Inches):						0.33	Avg. 3 samples

NOTES: (1) Tests performed by Fabric Research Laboratory, July & August, 1964 (Except Pilot Run - April 1964).
(2) Tensile specimens 1.0 inch wide except tape tested full width.
(3) Tests were run at room temperature.
(4) Each fabric specimen tested on Instron Machine at 3 inch gage length and 0.5 inch/minute jaw speed.

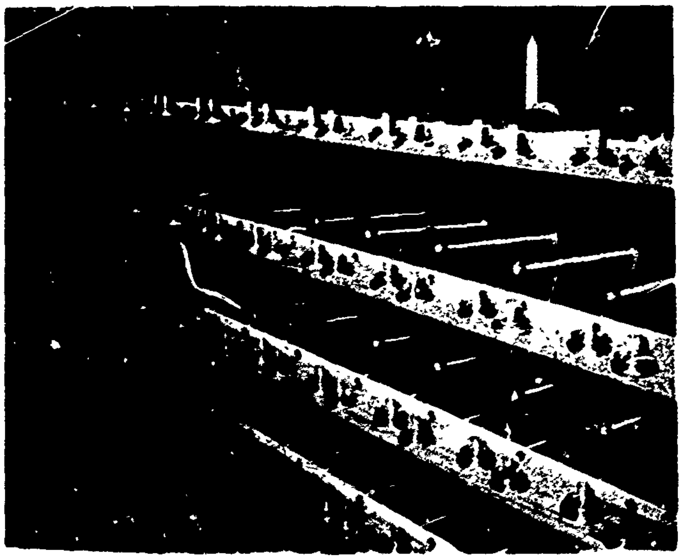

SGC/436

a. Close-Up of Twister Bobbins

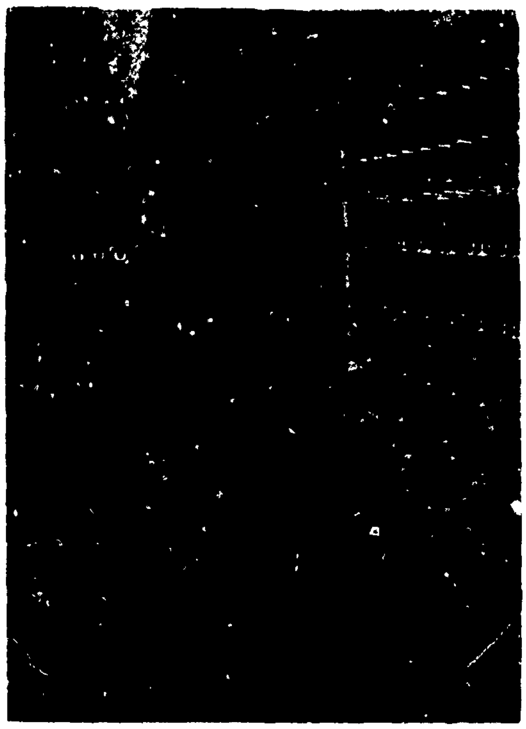

SGC/437

b Overall View

Figure 94. Creel Set-Up for Warping

The individual ends form what is commonly referred to as a "sheet" of yarn which passes over and under various snubbing rolls, as in Figure 95(a), to give it the proper tension before placing it upon the warper reel. The particular "sheet" of yarn which constituted a section of this warp was made up of 198 ends of wire which were wrapped on the reel for 101.75 yards. This was repeated 18 times for the total number of 3,564 ends in the wide warp.

Several changes had to be made in the standard warping equipment to accommodate the wire yarn. These changes included replacement of glass guide rods at the rear of the warper and all tensioning posts on the creel with Alsimag rods and posts. The locations of the Alsimag rods and guide posts on the warper and creel are shown in Figures 95(a) and 94(a), respectively.

Figure 95(b) shows the warp approximately one-half complete, the view being from the front of the warper. The tensions per end were 35 grams at the creel and 35 grams directly in front of the reel. The white lines seen in Figure 95(b) are the tie-down strings necessary to hold the sections of the warp in place during the process. String was utilized in place of the usual masking tape used in fabric working because the wire yarn was coated with a wax to which the tape would not stick.

After the entire warp, containing 18 bands or 3,564 ends, was wrapped onto the reel, it was then rewound onto the loom beam. The flanges on the loom beam were set at the exact width of the warp and the section ends were attached to the loom beam and wrapped.

The warps for weaving the tapes were made 3 inches wide to fit onto the beams properly. Each warp contained 132 ends and was wrapped onto the warping reel for the proper length, then beamed onto the tape loom beam.

After the warp was made and beamed, it was placed in a drawing-in frame so that the ends could be drawn through the heddle preparatory to weaving. Reference is made to Section 3.8.3.1 for a more complete description of the drawing-in operation. The difference between drawing-in a single end warp as described in that Section, and drawing in this warp, is that the yarns do not have to be picked from a tape. The ends are crossed in what is known as a "lease" and can be easily separated by insertion of two rods over which the yarns alternately cross. The drawing-in operation is shown in Figure 96, the view being from the back of the harness.

3.8.3.3.2 WINDING OF FILLING QUILLS

Winding of filling for the wide fabric was accomplished on a Whitin-Schweiter single spindle, filling winder with layer lock attachment (prevents sluffing). The direction of winding on the quills was reversed from normal and the speed slowed considerably below that used for standard production. The direction of winding was such that twist was added to the filling

SGC/435

(a) Warper Snubbing Roll

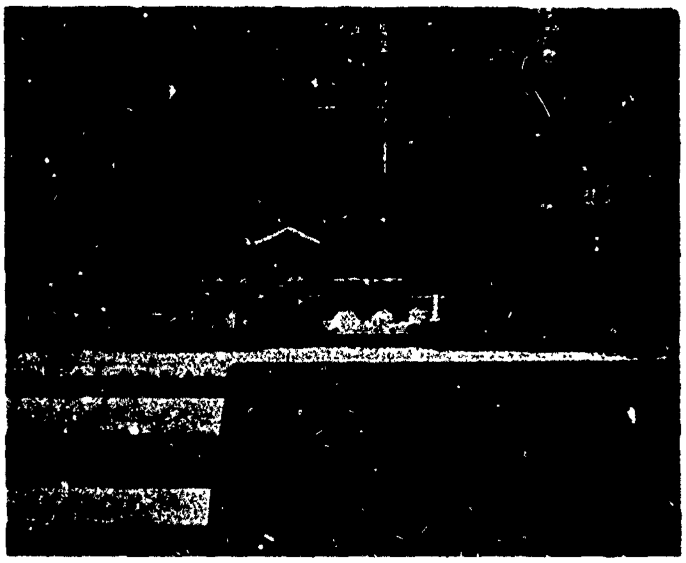

SGC/440

(b) Warp Approximately One-Half Complete

Figure 95. Warping Process

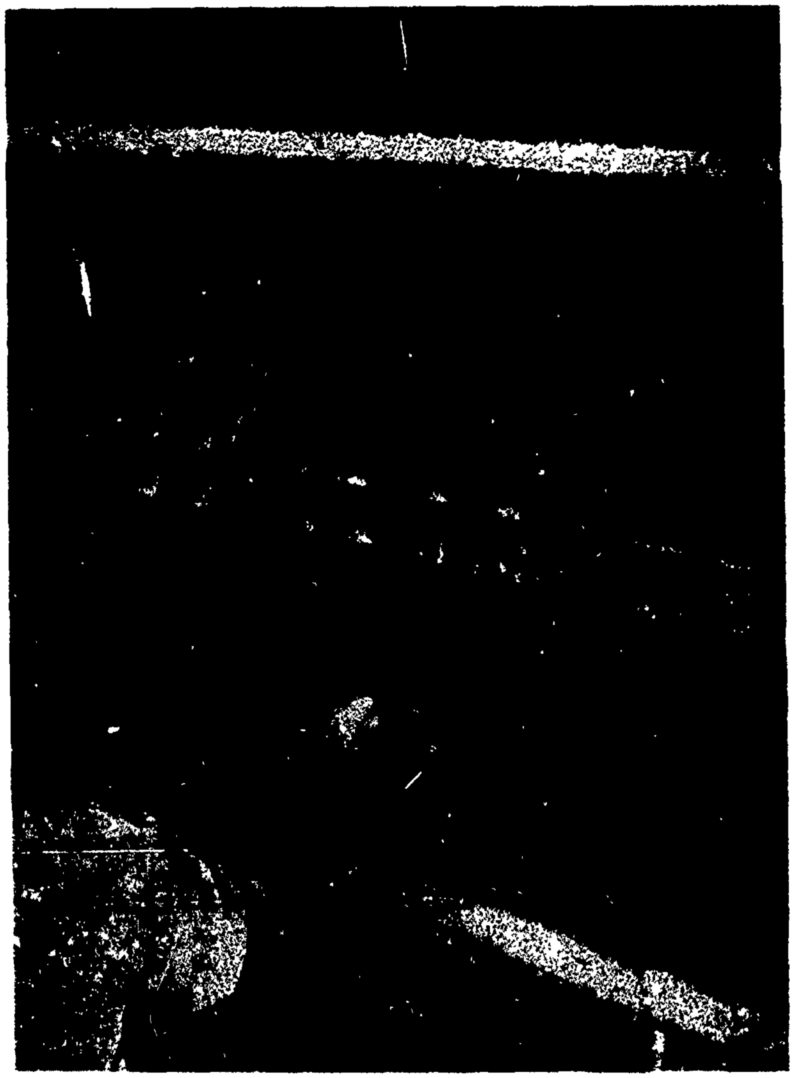

SGC/431

Figure 96. Drawing Yarn Ends Through the Heddle

yarn as it was pulled off the end of the quill in the shuttle during weaving. Figure 97(a) shows the filling winder with quills in the automatic supply hopper. The tension used in winding the filling averaged 600 grams. The yarn packages (bobbins) received from FRL were rolled off (de-reeled) directly to the quills. The quills were hand-fed to the winder to assure uniformity.

Filling for the tape loom was rolled directly from the yarn package onto special tape loom filling quills. The filling winder for tape is shown in Figure 97(b).

3.8.3.3.3 WEAVING OF WIDE FABRIC (BROAD GOODS)

The major problem encountered in weaving the wide fabric was obtaining balanced crimp in the warp and filling yarns. The crimp relationship is a function of relative yarn tensions, loom timing, and other factors while weaving. The discussion which follows will point out some of the special problems encountered in weaving metal fabric and modifications made to the equipment and process to obtain the best possible crimp balance and good fabric texture.

After drawing each individual end through a heddle and placing it in the proper reed dent, the complete warp, with harness assembly, was placed in the loom. The warp was then hand-tied to the canvas apron which had been inserted around the cloth take-up roll in the front of the loom, Figure 98(a). Care must be taken in tieing up any warp at the beginning to make sure the tensions are even across the width. Special precaution had to be taken with this particular warp because of the very high modulus of elasticity of the metal yarn.

Figure 98(b) shows the loom "head motion" which utilizes a harness chain having nylon rollers to control the raising and lowering of the harness. For the initial weaving setup, the harness was timed to cross (or close the "shed") 1-5/16-inch from front center. The whip roll was centered level with the eye of the heddles on crossing. The heddles were standard-eye, blue-diamond finish.

The loom used to weave the wide fabric was a Crompton Knowles Type W-3 broad goods loom with a friction band-type let-off for warp tensioning. Figure 99 shows the warp in the loom with heddle frames and warp beam in place. The weighted, band-type let-off mechanism may be seen at the end of the beam. Teflon lease rods were used for this weaving. This particular loom runs at 132 picks per minute.

Crow pickers with no temples were used to hold the fabric out at the full width. The timing on the crow picker is very important in that it must hold the pick until the shuttle is boxed and then release it. If this is not done properly, an excess amount of tension is placed upon the filling yarn and the crimp in the fabric is thrown out of balance. Placing the crow picker at several different locations with respect to the selvage was also tried.

SGC/442

(a) Filling Quills for Wide Fabric

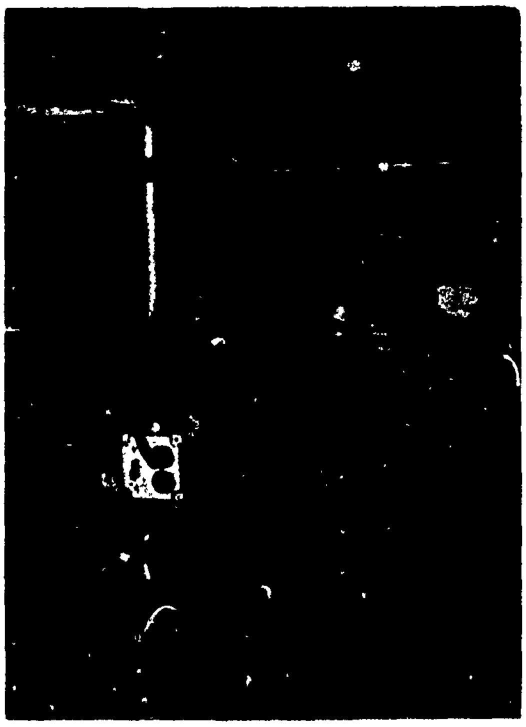

SGC/443

(b) Filling Tape Quills

Figure 97. Filling Winders

SGC/430

(a) Tying Warp to Apron

SGC/432

(b) "Head Motion" Showing Harness Chain

Figure 98. Loom Set-Up for Wide Fabric

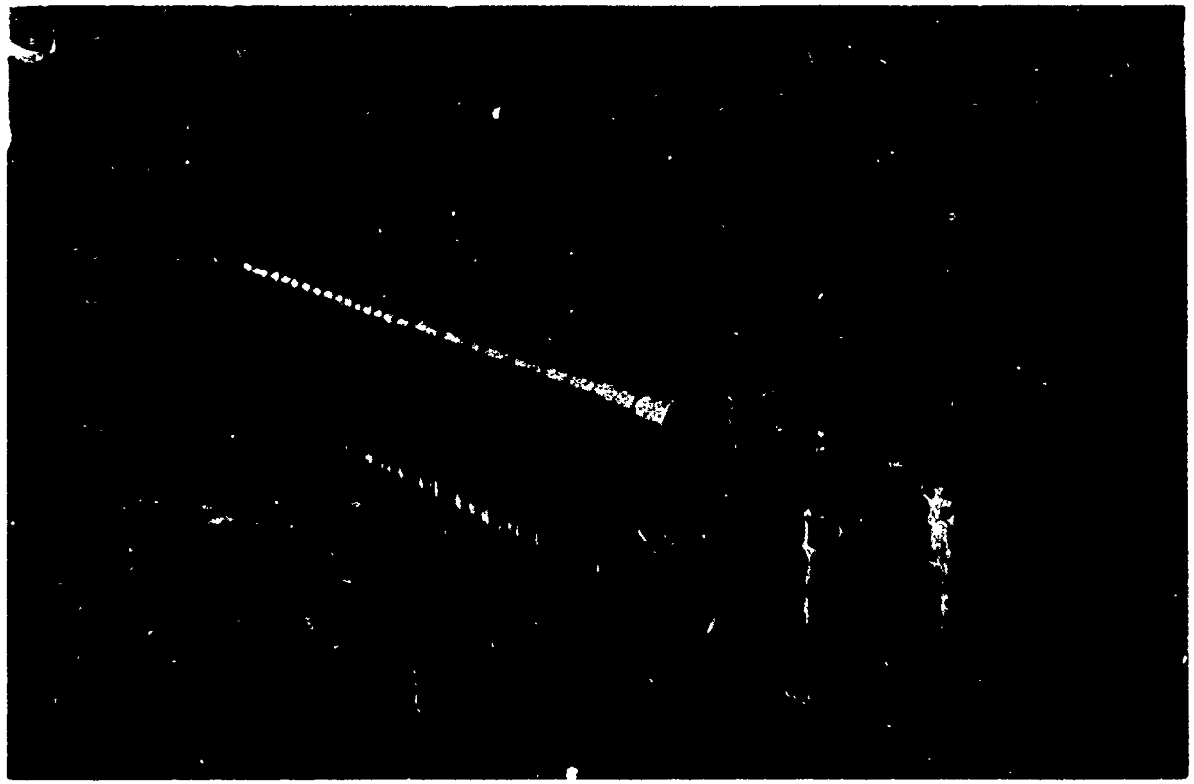
SGC/441

Figure 99. Warp in Place in Loom Showing Beam and Let-Off Mechanism

After an initial head end was woven and submitted for evaluation, it was necessary to make the following changes to achieve better crimp balance.

The harness timing was moved from 1-5/16-inch before front center to 2 inches before front center. The crow pickers were adjusted so that the pick would be held until the shuttle was approximately 2 inches into the box and then released. The harness pulldown springs usually placed on the bottom of the harness were removed and replaced by a positive pull-down mechanism. This was done to make a smaller shed in weaving.

The rolls were changed from whip rolls to drag rolls. One drag roll was covered with 40 durometer, 3/8-inch-thick neoprene in the hope that this would cause a more constant tension to be held on the warp throughout the shed cycle. The results were not sufficiently encouraging as indicated by the data for Sample D-1, Table XXVII. Because of the friction band-type let-off and the high modulus of the yarn, the warp tended to go slack when the shed closed. Since it was not advisable to slide the chromium-nickel alloy yarn over a carbon steel surface, the drag rolls were then chrome plated and the upper drag roll was locked and spring loaded as shown in Figure 100(a). The spring loading was intended to equalize difference in warp yarn tension between open and closed positions of the shed. In addition to the changes in the drag rolls, the harness timing was changed to 1/4-inch from front center along with a split cylinder. A split cylinder raises the harness at different times.

Selvage edge temples (pin-type) were added to aid in keeping the fabric at the proper width for weaving but this did not aid in improving filling crimp. The split cylinder was later abandoned in favor of a regular opening. A minimum shuttle tension of 25 grams was used.

The final loom set-up used chrome plated, locked drag rolls with one being spring loaded, harness timing of 1/4 inch from front center, and the minimum shuttle tension. This set-up, while not producing equal crimp in warp and fill, produced the most satisfactory results obtainable with this type of loom. See Sample F, Table XXVII.

The standard W-3 loom shuttle was modified using 40 pound monofilament whiskers pre-tensioned against the quill. The shuttle, with the nylon monofilament whiskers and oppossum fur liner, is shown in Figure 100(b). This shuttle was run at a minimum tension of 25 grams and quill changing, which is normally an automatic process, was done manually. The reason for changing quills manually was that the normal winding "bunch" could not be made on the quill due to reversing the direction of the winding spindle. Since this bunch of yarn triggers the automatic indexing of the W-3 loom, the quill feeding mechanism was inoperative.

A total of 161,000 picks were finally woven at the 61-3/4 inch width. This netted a total of 74 yards of wide fabric.

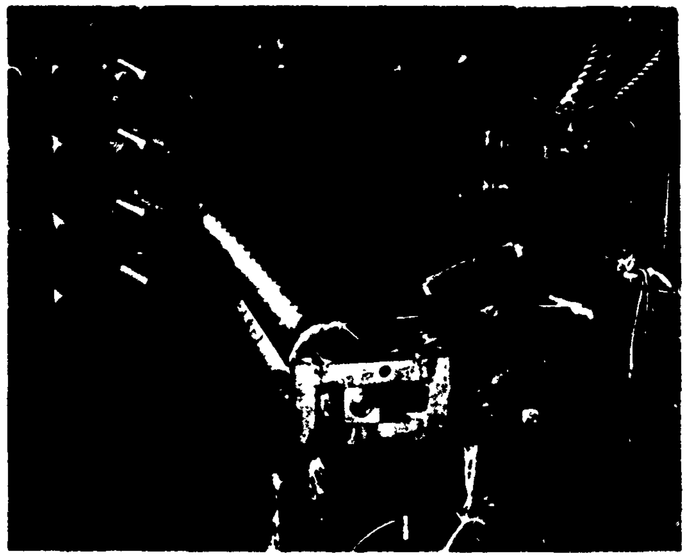

SGC/433

(a) Spring Loaded Upper Drag Roll

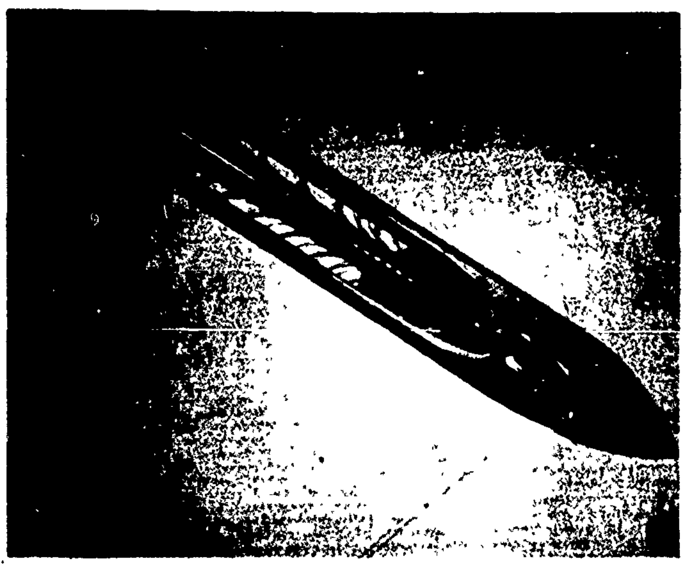

SGC/434

(b) Shuttle with Nylon Multifilament Whiskers

Figure 100. Equipment Modifications

One serious difficulty encountered in the weaving of this fabric was that areas of warp became very slack at several locations along the length of the warp. It was determined that this occurred in each area where paper had been inserted at about 25-yard intervals between the layers of yarn in the beaming operations. Figure 101 shows the effect of warp slackness as it is revealed in the fabric seen from the front of the loom. This unevenness in tension resulted in puckering of the fabric for approximately one-yard at each of three places.

3.8.3.3.4 WEAVING OF TAPE

The tape was to be woven at a width of 1.60, - .05, + 0 inches (approximately $1\frac{17''}{32} - 1\frac{19''}{32}$) and was woven concurrently in four spaces in the tape loom resulting in four separate lengths of tape. The warps were wrapped onto 3-inch wide Mossburg beams and drawn into the harness and the reed in the loom. This weaving set-up also utilized Teflon lease rods and standard blue-diamond finish heddles. Six ends were removed from each warp to obtain the proper width.

The tape loom utilizes a weight and rope device for warp tensioning. The tapes being woven are shown from the front of the loom in Figure 102(a). Unlike the W-3 loom which drives the shuttle across the fabric with a picker stick, the shuttles in the tape loom are gear driven and have positive motion from one side of the tape to the other. The shuttles are shown in Figure 102(b).

A piece of felt was added to the tensioning device of the tape loom shuttle to obtain more shuttle tension. The tensions used in the tape weaving were 20 grams shuttle tension, 400 grams warp tension and 200 grams filling winding tension.

Four tapes were woven, each approximately 100 yards long, for a total of 400 yards of tape fabric. There were 126 ends in each tape and the widths averaged 1-9/16 inches.

3.8.3.3.5 FINISHING

The finishing of the woven metal fabric, both broad goods and tapes, was done on scouring jigs. The tapes were scoured on the small jig in Prodesco's finishing laboratory, Figure 103(a). However, the 62-inch width made it necessary to fabricate a special jig, Figure 103(b), for scouring of the broad goods. The solution used for scouring the tapes and wide goods was a solution of 1 gram of Duponal-RA per liter of water. The average bath temperature for scouring the tapes and broad goods was approximately 205°F.

The number of tapes was kept at a maximum of two on the small jig during scouring. No unusual problems or difficulties arose in the scouring of the tapes.

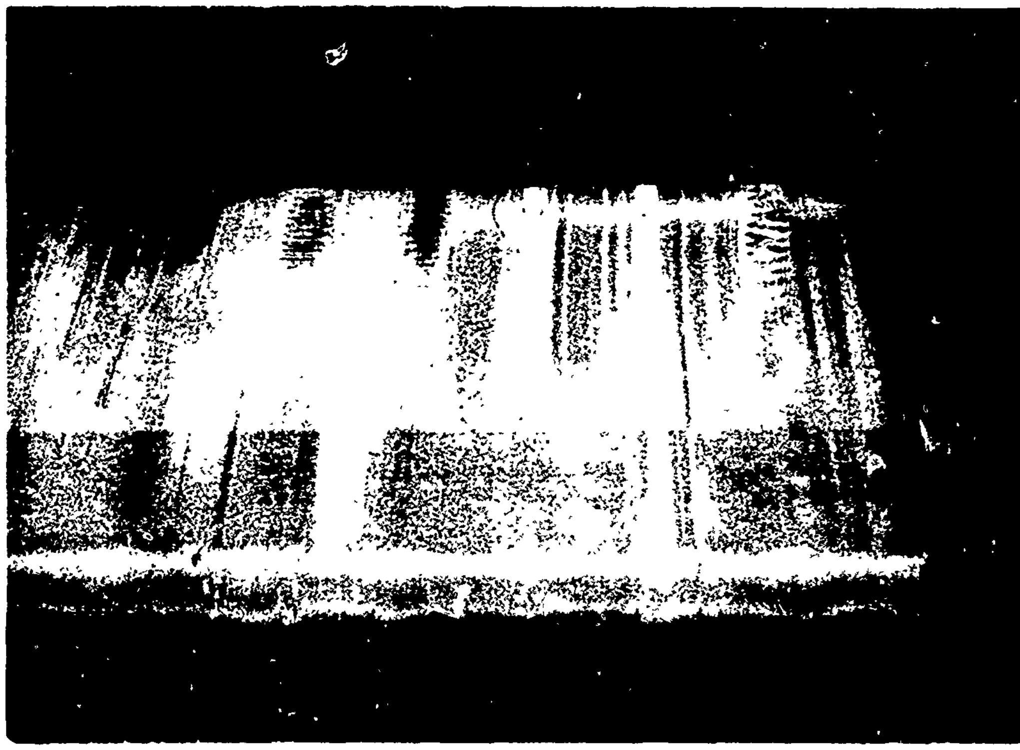

SGC/428

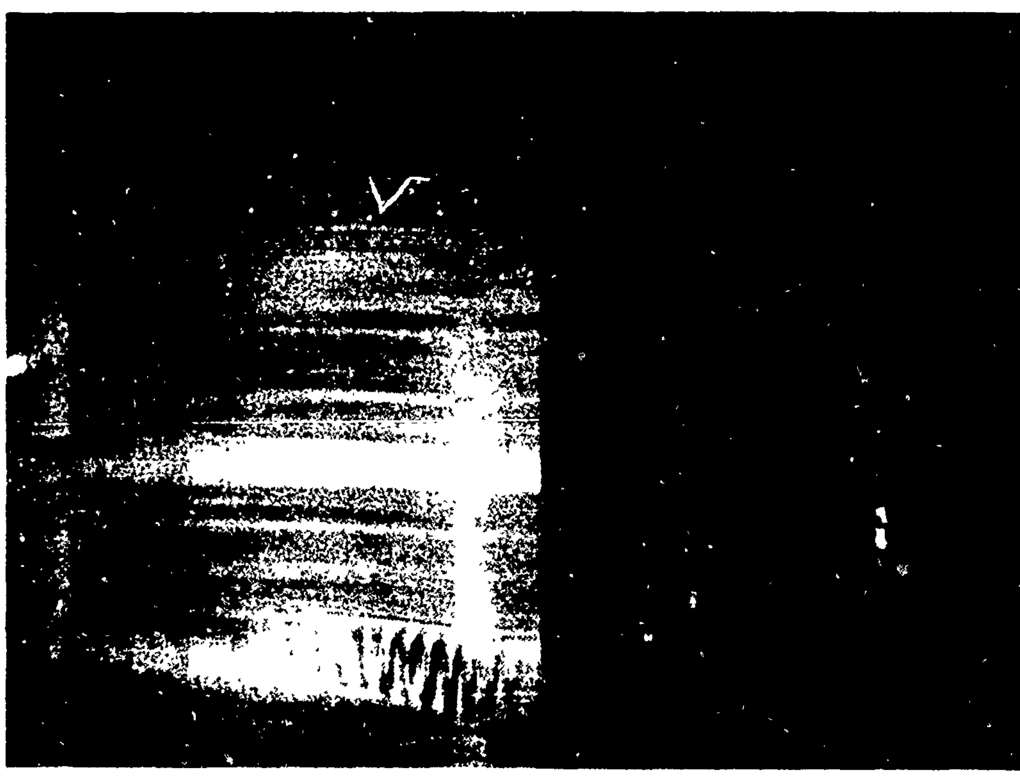

SGC/429

Figure 101. Fabric Defects Encountered During Weaving

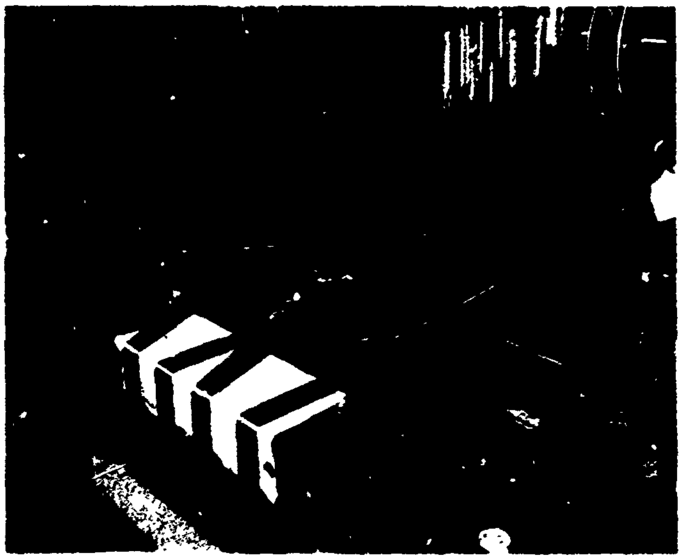

SGC/422

(a) Tape Weaving from Front of Loom

SGC/423

(b) Gear Driven Tape Shuttles

Figure 102. Weaving of Narrow Tapes

SGC/424

(a) Tape Scouring

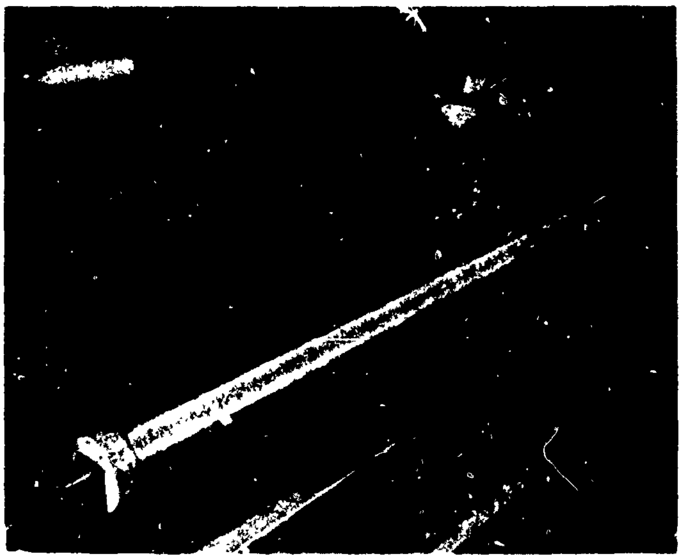

SGC/416

(b) Wide Goods Scouring

Figure 103. Scouring Jigs and Tanks

The broad goods scouring operation was preceded by transferring the fabric directly from the loom to the special jig, driving the fabric take-up roll with the motor on the jig. The fabric was then looped under a roller in the bottom of the tank and attached to the roll on the side of the jig. The scouring solution was added to the tank. Figure 103(b) shows the actual scouring of the wide fabric.

Tensioning and fabric control in the scouring operation was a major problem. Non-uniform tensions resulted from uneven contact between the straight roll in the bottom of the jig and the surface of the fabric. This created bows in the filling which were reduced somewhat by a subsequent beaming and re-beaming operation. After making two complete passes through the scouring solution, the bath was dropped and a cold water rinse was applied to the fabric. Inspection revealed that the wax was still not removed satisfactorily. It was also apparent that a different method of transporting the fabric would be necessary to minimize fabric deformation. The final arrangement was to run the fabric directly from one beam to the other on the jig while completely saturating it with hot scouring solution. This was accomplished by pumping the solution from the bottom of the tank through a hose which was passed manually back and forth across the fabric. The delivery roll was also tensioned by using pulleys and weights which assisted in straightening the pronounced filling bows which had occurred across the fabric.

Four complete passes while spraying with scouring solution, followed by two passes with hot clear water, resulted in a satisfactory scour.

Three additional passes back and forth from beam to beam were required to dry the fabric. Forced air was blown on the fabric during the first pass and the second and third passes were made using infrared lamps to evaporate the moisture from the fabric.

3.8.3.4 CONCLUSIONS AND RECOMMENDATIONS

The following conclusions are a result of the weaving and related fabrication studies conducted under this production phase, and are based on observations by Prodesco, Fabric Research Laboratories, and Space-General:

a. Yarns made from fine-diameter wire filaments can be handled on normal textile handling equipment provided the guide surfaces and tensions are carefully prepared and monitored.

b. Because of the high modulus of elasticity of the wire filaments, standard weaving techniques to achieve certain fabric characteristics with textiles did not have the same effect on wire yarns.

c. Jig scouring of wide metal fabrics requires more handling than a normal fabric, and more technology in both jig manufacture and scouring techniques.

d. The loom should have a small shed opening and positive let-off with maintenance of constant warp tension by hydraulic dash-pot or similar means. This may also help absorb beat-up shock and vibration.

e. The warp should be rolled on the beam with a continuous sheet of heavy paper or polyethylene sheet throughout.

3.9 SEMI-AUTOMATIC WELDER FOR METAL FABRIC

3.9.1 WELDER DESIGN AND CONSTRUCTION

The development work on the spot welding process described in Section 3.7.2 yielded the parameters necessary for design of a semi-automatic metal fabric welder. Some of the objectives undertaken in the design of the welder included application of "through" or "series welding" in which one electrode is on top of the seam and the other below; use of probe-type electrodes to minimize variation in electrode footprint area with number of layers of fabric; and use of a deep-throat welding frame to accommodate the long sections to be welded. The concept included provision for precise, incremental spacing of the welding spots by rubber-tired drive wheels over and under the fabric, and the production of two uniformly spaced rows of weld spots on one pass of the fabric through the machine.

The work with a hand-held welding gun, although ultimately unsuccessful, established much of the background and confidence level in the new concept. Some of the important design considerations for the new welder were as follows:

a. The secondary circuit inductance effect on the weld power available at the electrodes with a 7- to 9-foot throat was proven to be very small as a result of the testing. This proved the practicability of through welding, and the potential capability of welding through four or five layers of fabric. As previously discussed, this was not possible with both electrodes on the same side of the fabric.

b. After some analysis, it was decided that electrical solenoids operating a cam would be used to drive the electrode down to the fabric and provide the proper welding force. With this type of duty cycle, the solenoids would be energized for only a small portion of the cycle and the failure mode would be with the electrode in the raised position, thus avoiding possible damage to the fabric when it is advanced by the drive wheels. Although pneumatic electrode loading was considered, analysis indicated that the pneumatic response time was too limiting.

c. Re-evaluation of all welding test results indicated that there was no advantage to the use of the fabric drive wheels as the actual welding electrodes. The contact area of the wheel-type electrodes changes greatly with the change in the number of fabric layers. Based upon a 0.0035-inch per layer local compression due to electrode loading, the wheel contact area is increased by a factor of 2.2 when changing from two layers to five layers of fabric. This change in contact area results in variation of current density and work piece resistance.

The use of wheels as electrodes requires a sliding electrical contact for low-voltage, high-current weld pulse. This sliding contact is prone to electrical resistance variation and arc-pitting which could cause variation in delivered weld power.

The continuous rolling of the hard electrode wheels under welding loads presses the crimp out of the fabric, which causes it to elongate locally and pucker the material or dislocate the layers with respect to one another.

The heavily loaded wheels, rolling continuously, cause abrasion between filaments and yarns that may be degrading to the fabric as well as causing geometrical distortion. Calculations showed that the yield strength of the wires could be exceeded by the load needed to make the welding gun perform satisfactorily, and weakening due to notching probably occurred.

If the wheel rolled continuously, movement of the individual filaments and yarns would be occurring while the weld nugget was solidifying. This could cause cracks and other lack of homogeneity in the nugget. It would have been necessary to cause the wheel to pause momentarily after each weld pulse to avoid this. The use of vertically reciprocating electrodes permits proper sequential timing of the squeeze, preheat, weld pulse, and quenching time periods.

d. Use of vertically applied electrodes would permit variation of the electrode force without greatly changing the electrode contact area. This was not true of wheels.

e. By bringing the work piece to the welder, through development of a proper basting technique, the need for portability no longer existed and the problem of obtaining the proper electrode force was extremely simplified.

f. If the electrode force is removed from the fabric during the time the fabric is being advanced, a small fabric advancing force is required which can be provided by rubber-faced fabric drive wheels. These would not abrade the fabric and could advance it accurately because of minimum slip.

Figure 104 shows the welding heads temporarily assembled on the welder frame. Figure 105 shows separate parts of the welding heads prior to assembly.

The completely assembled welder with the bottom of the L-shaped arm in place is shown in Figure 106. This photo shows an inductance coil of copper tubing just behind the upper head. This coil was used to vary the secondary circuit inductance during further welding tests. Also shown adjacent to the welder arms are the insulated, flat copper conductors responsible for the low secondary circuit impedance. To the left rear of the photograph is the center welding arm. The small, portable, Duffers current analyzer is shown in the center of the picture (rear). This instrument indicates either peak or rms amperage in the secondary circuit for one pulse, or continuously, and also is capable of counting pulses. Mounted on the right rear of the machine is the General Electric size 3, square-pulse power supply. Above this is the Space-General-designed and constructed electromechanical sequence timer. A foot pedal is brought to the forward end of the machine so that the operator can control the speed of operation. The welder with the center arm in place is shown in Figure 107.

The lower and center support arms are interchangeable enabling the welder to accommodate all possible shapes of complex structures. The lower arm could be used for toroidal or cup-shaped objects; the horizontal arm would be used for structures generally of cylindrical or conical shape.

For making hoop seams or seams at orientations other than axial to the machine, the weld heads may be rotated in the horizontal plane to 24 different angular positions as determined by splined shafts and bushings incorporated in the support. The upper head is raised by use of the cam handle shown in Figures 106 and 107. The upper head is turned and lowered into the spline engagement position desired. The lower head angle is changed by loosening the lower nut so that the entire weld head can be raised clear of the splined parts and then turned and dropped into the desired position. It follows, of course, that both of the heads must be turned to the same angle so that the drive wheels are in the same plane when welding.

The sequencing timer control performs the functions of advancing the fabric, lowering one electrode, initiating a weld pulse, raising the electrode, lowering the second electrode, triggering another weld pulse, and concluding the cycle with raising of the second electrode. The overall welding speed is variable with the foot control from zero to approximately eight inches per minute. Each spot weld pulse must be of the same duration and, therefore, the weld pulse time period is controlled to a preset value by the

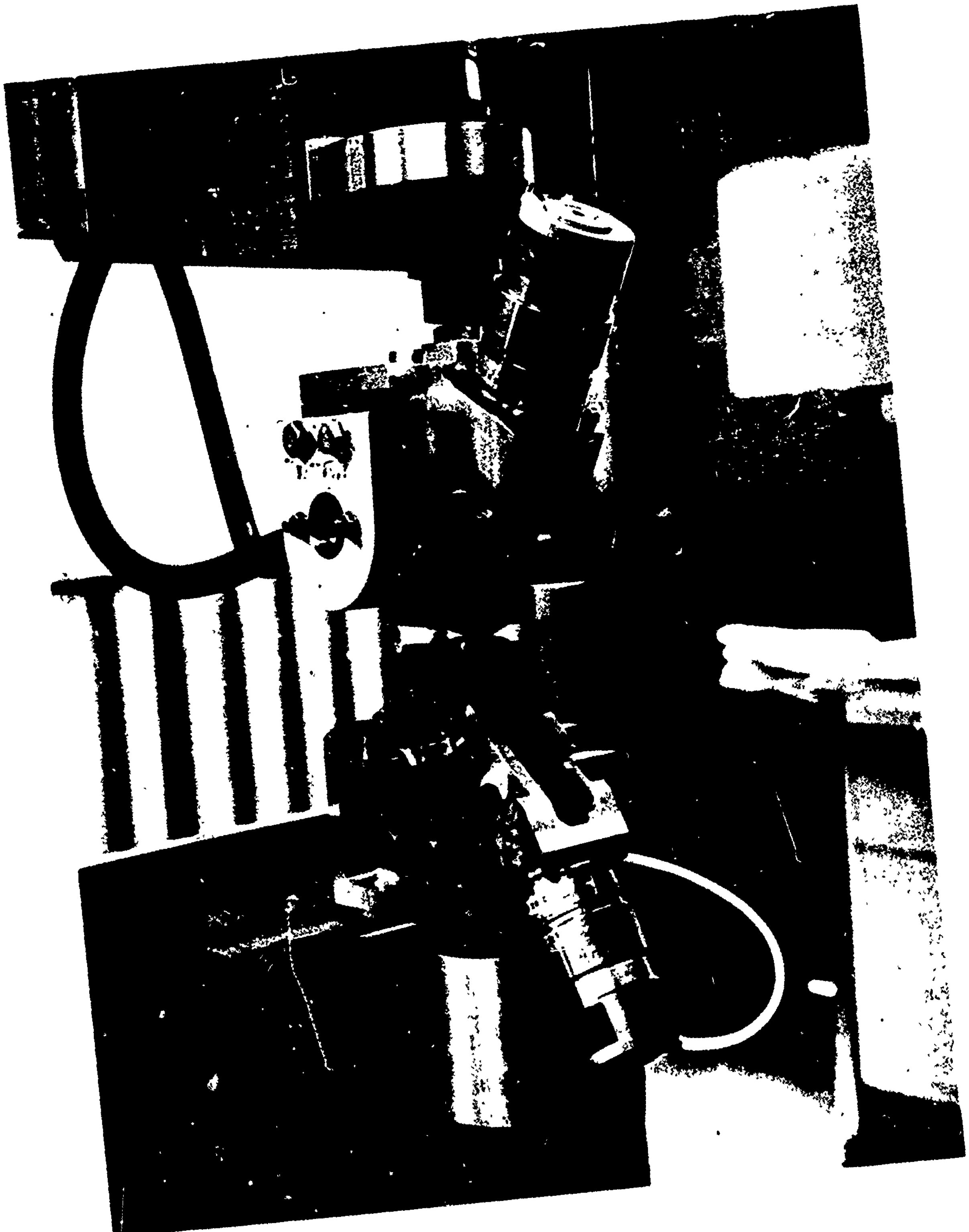

335/127

Figure 104. Welding Heads Temporarily Installed in Frame

333/280

Figure 105. Weld Head Parts

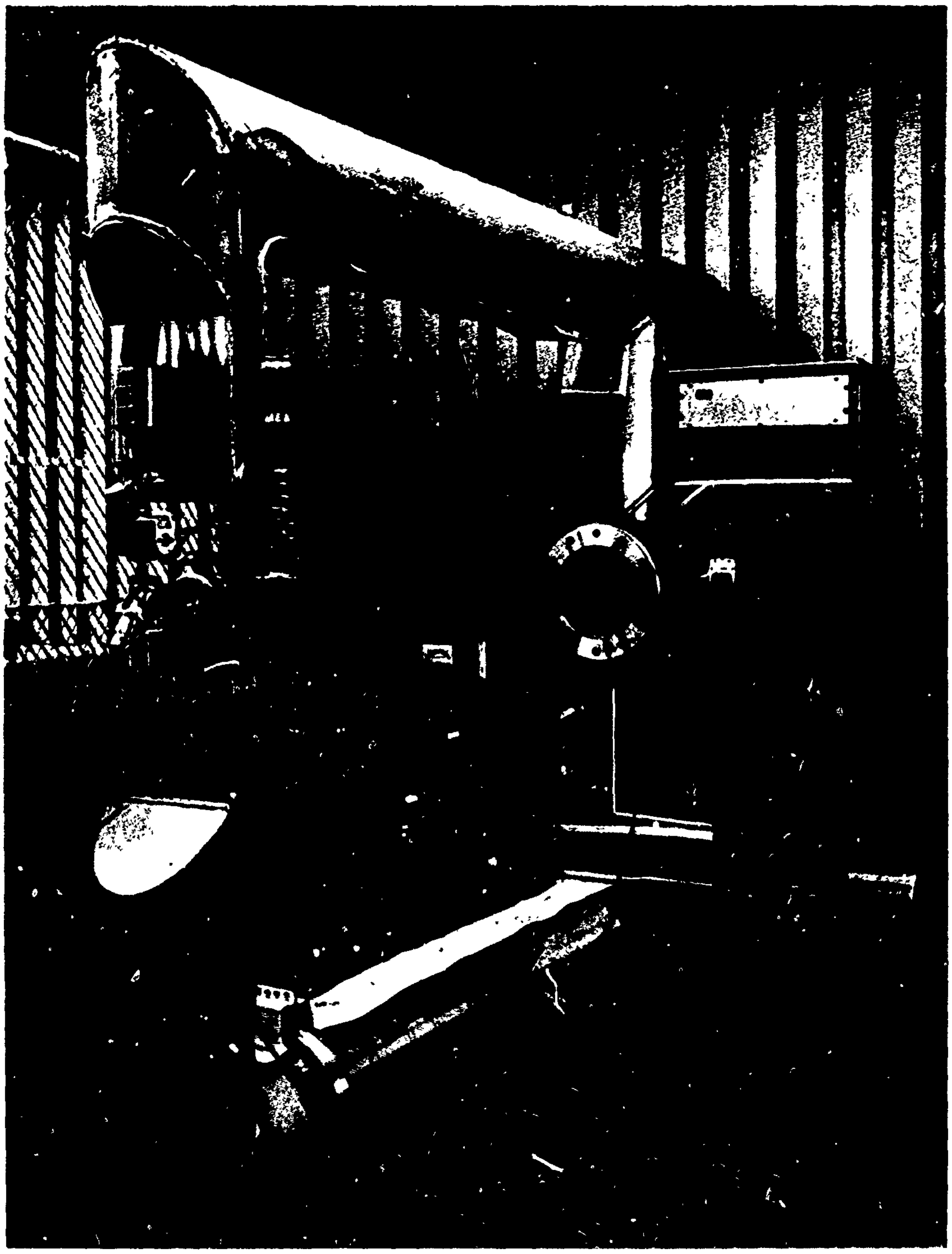

335/133

Figure 106. Completely Assembled Welder

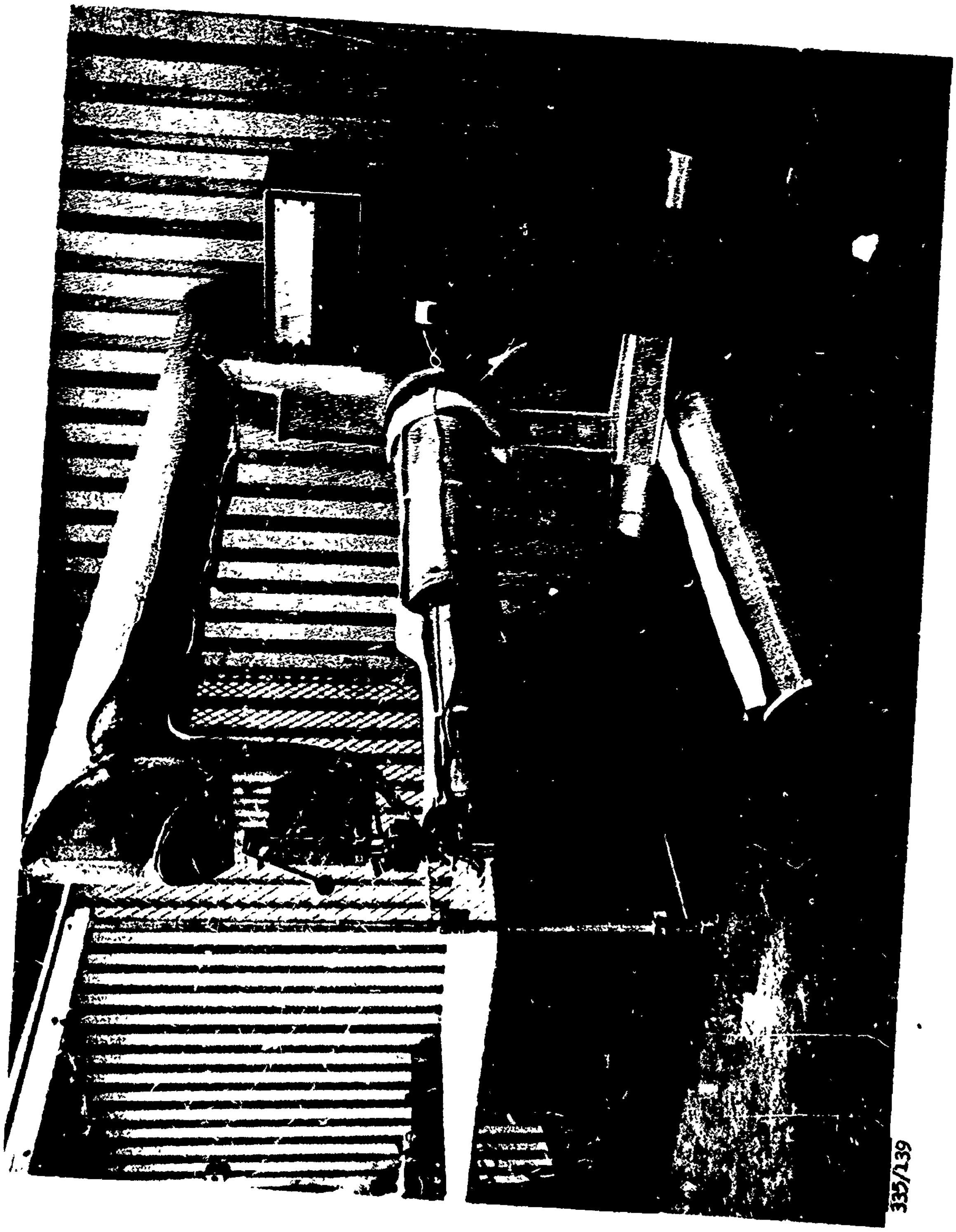

Figure 107. Welder with Horizontal Arm Installed

General Electric power supply itself. The remainder of the time cycle is regulated by the rotational speed of a wafer or commutator-type switch driven by a small motor. The speed is regulated by a second braking motor regulated by the foot control.

A transistor switching circuit is provided for each of the individual pulse signals required, i.e., fabric advance, electrode engagement, weld pulse, electrode disengagement, second electrode engagement, second weld pulse, and second electrode disengagement. The transistors are turned on by the rotating wafer switch and, in turn, transfer the power signals to the rotary solenoids (operating the electrodes), stepper motors (operating the fabric advancement wheels), and power supply.

A close-up view of the heads, with the horizontal arm, head raising and lowering handle, head mounting splines, and bushings in place, is shown in Figure 108. This photo, taken after the welder was in use for some time, shows the insulation of the conductor along the horizontal arm, insulation on the electrode shoes, and the use of separate flexible conductor wires to each movable shoe on the top head.

3.9.2 WELDER DEVELOPMENT

A number of significant technical problems had to be overcome before the welder was put into full operation. These problems are discussed below.

a. Electrode Life - The original electrode material used was too soft for acceptable life. This alloy (RWMA Class 3) had the characteristic of enlarging (mushrooming) rapidly at the electrode tips due to the combination of high temperature and impact loading. An improved sintered tungsten carbide alloy, Elkonite TC-10, manufactured by Mallory, was used and a significant increase in electrode life was achieved. The electrode life was initially increased from approximately 1 foot to 15 feet of welded seam using the lowest welding speed of 2 inches per minute.

   Later, the elimination of loose fit in the electrode shoes and splines (through hard chrome plating), and other improvements brought about the production of 184 feet of double seam on one set of electrodes during welding of the apex (at an average joint efficiency of 91.6 percent). This was at a speed of approximately 3.5 inches per minute.

b. Electrode Alignment - It proved difficult to align the welder electrodes after their installation because the electron supporting members were mounted with flat head counter-sunk screws so that no adjustment of the electrode tips in the horizontal plane was possible. This was overcome by changing the design to accommodate panhead screws.

335/152

Figure 108. Close-Up View of Welding Heads

Another type of electrode positioning problem was encountered in that the upper and center arms of the welder tended to vibrate so that proper electrode position could not be assured under dynamic conditions. This was corrected by adding approximately 50 pounds of sand to the tubular interior of both arms at the outer extremities. This decreased the natural frequency of the arms as well as the amplitude of vibration for a given amount of energy input.

c. Electrical Isolation of Welding Circuit - It was discovered that the metal fabric was grounding the welding circuit to the welder frame and to the metal parts of the welding heads. This was overcome by use of insulating tapes and plastic films on the small parts of the welder while a permanent insulation of the welder frame was obtained by applying Tygon insulating paint.

Another grounding effect was discovered, caused by metal adjusting shims inserted between the electrodes and their mountings. These shims would ground the welding circuit by connecting the electrode holder with the mounting member, an effect which occurred even though Mylar film was used to isolate the shims. Occasionally, a shim would contact the fabric driving wheel, creating a ground. These problems were overcome by using shims made of fibre glass epoxy laminate.

d. Cleaning - Most of the fabric used for the welder development was the fabric weavers experimental sample material. This material had not been subjected to the normal scouring process used by the weaver for the main bolts of fabric. Because of this, quantities of the soluble waxes used for yarn twisting and fabric weaving were left in the sample fabric and were not being completely removed by Space-General's solvent-acid cleaning process. A better process using Phos-It (a commercial metal cleaner) greatly increased the obtainable welding efficiency.

For small quantities of fabric or welding coupons, the fabric was stored in MEK to exclude oxygen and moisture after cleaning.

e. Welder Power Supply - The square pulse power supply on the welder was found to be pulsing erratically at fabric speeds higher than 3.75 inches per minute, although maximum design speed was substantially higher than this. It was found that inadequate power was available at higher speeds for firing the silicon-controlled rectifier which triggers the actual weld pulse discharge. This was corrected by adding a transistorized amplifier to the gating circuits for the SCR. After this modification, no pulses were missed at higher fabric speeds. A diagram of the welder function sequence timing is given in Figure 109. This figure shows the sequence, duration, and time relationship of the welder steps for the high- and low-speed phases, as regulated by the variable-speed, 48-contact rotary switch.

3.9.3 OPERATION OF WELDER

3.9.3.1 WELDER SET-UP AND MAINTENANCE

Alignment and maintenance of the electrodes is probably the most important consideration in the proper care of the welding machine.

Before installing or replacing electrodes, the relative position of the upper and lower heads and corresponding fabric drive wheels must be checked for proper adjustment. With the upper head in the lowered position, the rubber surface of the fabric drive wheels should barely touch. The upper head main deflection spring, shown immediately below the upper, white-colored housing in Figure 108, must be adjusted by use of the lock nuts located below the spring. With the rubber-tired drive wheels touching as described above, shim stock or feeler gages are placed between one of the electrode pairs so that electrical contact is made. A Chatillon, or equivalent compression spring gauge is placed slightly oblique from the vertical and pushed upward against the bottom of one of the rotary solenoid housings, shown as the white housings with curved lower surfaces on either side of the upper head in Figure 108. The compression gauge is pushed upward until electrical contact between upper and lower electrodes through the shim is broken, as indicated by an ohmmeter. The upper head compression spring is adjusted to give a spring force of 23-28 pounds on the Chatillon gauge at the point at which the ohmmeter circuit is interrupted. All power to the power supply and timer should be off for safety purposes during this check and adjustment.

The purpose of the upper spring is simply to load the drive wheels and allow the upper head to deflect upward when the wheels ride over a seam or other thicker section of a work piece. They do influence electrode force, however; hence, this adjustment must be performed carefully.

The lower electrodes may be adjusted up and down by use of the hexagonally-headed screws extending horizontally from either side of the lower head. The tip of the lower electrode is adjusted so that it is slightly below the horizontal plane tangent with the top of the lower drive wheel. An exact measurement cannot be made because the compression of the rubber coating on the drive wheel varies with the type and thickness of metal fabric being welded (the drape of the metal fabric also varies). The adjustment of these lower electrodes may be checked after all alignment is completed as

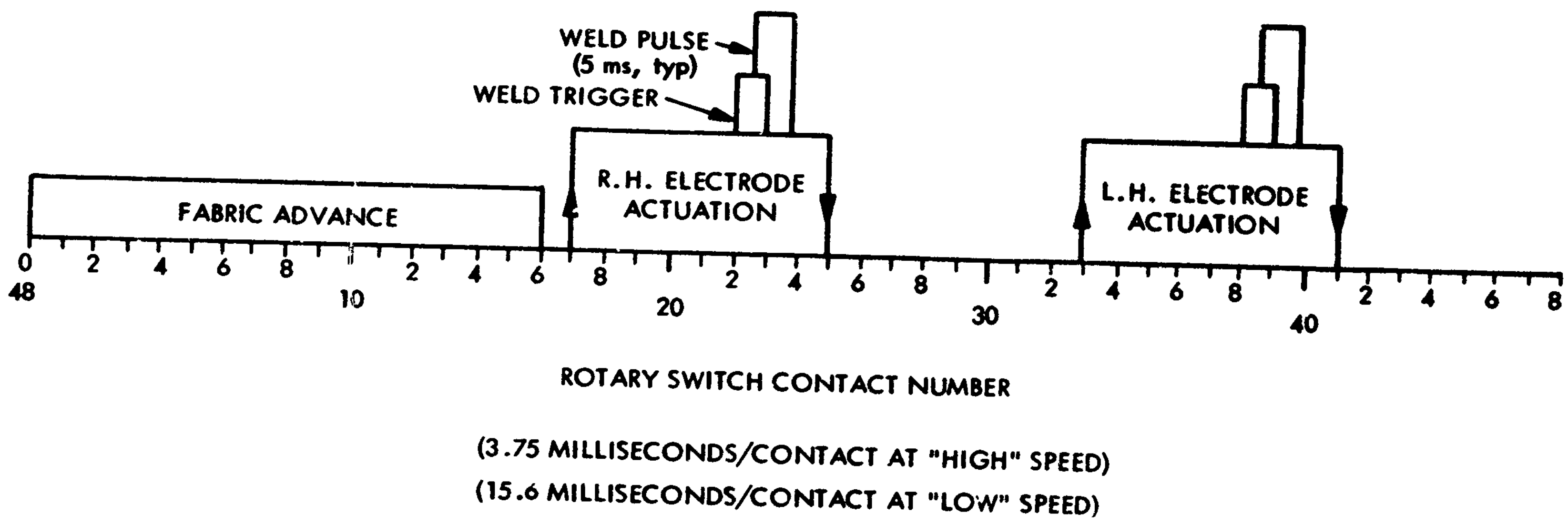

Figure 109. Welder Function Diagram, High-Speed Mode

described below. The tip of both lower electrodes should be at the same elevation, i.e., within $\pm$0.002 inches of the same horizontal plane. The plungers in the upper heads must be well lubricated with silicone grease and be free-operating. With the upper head raised, by use of the upper handle, the upper electrode plungers are adjusted for maximum travel by rotating the solenoid housings on either side of the head. This is accomplished through the mounting-screw hole clearance. The mounting screws are then tightened in the solenoid housing.

The upper head is then lowered, and alignment of the upper and the lower electrodes is made. The drive wheels must be rechecked to make certain they are touching, with negligible compression of the rubber tires. The gap between the upper and lower electrode is now adjusted to 0.023 inches $\pm$ 0.005 inches. This is done through modification of the stroke of the upper electrodes by loosening the screws in the upper solenoid housings and turning the housings very slightly. This can also be accomplished by changing the height of the lower electrodes but this should be done with care to retain the salient features of the lower electrode adjustment described above. When the electrodes are adjusted with the proper gap, the 110-volt power to the sequencing timer is turned on; however, the 220-Volt power to the main General Electric power supply should remain off. Using the single function "remote" switch position on the timer, an electrode can be made to descend and stay down with its solenoid being continuously energized by depressing the foot pedal (rather than allowing continuous operation through the entire cycle sequence). Causing one electrode to descend should cause the opposite pair of electrodes to separate 0.004 - 0.009 inches more than the original gap setting. In other words, a nominal 0.025-inch gap should increase to a nominal 0.031-inch gap. This gap can be easily checked with feeler gauges. This gap deflection should be checked on both sides by causing each of the opposing pair of electrodes to close.

The vertical alignment of the electrodes should now be rechecked assuring that the upper and lower electrodes are concentric within $\pm$0.005-inch by observing the closed electrodes with a lighted magnifier in two horizontal directions 90° apart. If the electrodes are not lined up, either upper or lower electrode holders must be loosened and moved accordingly.

The electrode head circuit should now be checked for shorts. The electrode is in contact with the electrode holder to which the flexible electrode conductors bring power from the main, large, flat copper conductors leading from the power supply. The electrode holder and electrodes, however, must be insulated from the stainless steel plungers. This should be checked with an ohmmeter. The panhead screws holding the electrode holders are screwed into nylon inserts in the stainless steel plungers. Occasionally these inserts break or become worn. If this happens they should be replaced. The proper height of the lower electrodes can be checked by running two or more layers of the fabric to be welded between the wheels and carefully observing the underside of the fabric. The lower electrode should not drag on the fabric. If the lower electrodes are too low, however, it will be impossible to obtain the proper forging pressure during welding as indicated by obtaining the proper deflection during the deflection tests described above. Final determination of proper adjustment, as well as proper power characteristics, must be made by welding tensile test coupons.

The above process is necessarily iterative in that one adjustment often affects another adjustment. With experience, however, the heads could be completely disassembled and reassembled with proper adjustment in 8-10 hours. Replacement and alignment of electrodes only should not require more than 1-2 hours. Electrodes may be dressed with a fine jewelers file and emery paper to give a square-ended, cylindrical shape after they have become mushroomed or chipped, but it has generally been found more expedient to replace the electrodes with new ones.

With the heads in good adjustment and sliding surfaces not too worn, as much as 180 feet of weld in two layers of metal fabric have been accomplished without replacing electrodes. Complete disassembly of the heads or replacement of the drive wheels rarely should be necessary. The rubber-tired surfaces on the drive wheels were replaced only once during approximately 2-1/2 years of welding on this program. Practically all of the welding in this program was done at a speed of approximately 3.5 inches per minute. Higher speeds cause shorter electrode life and make positioning or "steering" of the fabric difficult.

To maintain maximum welding speed, the rotary commutator switch, located in the timer control box, must be lubricated. Normally, the contact should be sprayed twice a day, during continuous operation, with "Spray-Clean" manufactured by GC Electronics, or equivalent. A one-half second spray per wafer has been found to be sufficient. Occasionally, perhaps once each week, the contacts should be wiped off with absorbent lint-free toweling or wipers.

3.9.3.2 WELDING OF METAL FABRIC

Most of the welding in this program has been done at a speed of 3.5 inches per minute although the welder is capable of operating to more than 8 inches per minute. Higher speeds shorten electrode life and make handling of metal fabric more difficult. The operator controls the speed so that he can direct the fabric, as in the use of a sewing machine, such that the weld seam proceeds down the exact center of the overlap in the fabric layers. Since an overlap of 0.75 inches was used in most of the components in this program, and the centerline of the electrodes is 0.3 inches apart, only about 0.2 inches clearance between electrode and edge of overlap remains on either side. The operator must never allow the welder to run off the edge of the fabric causing the electrodes to strike together when weld power is being supplied because this will seriously damage the electrodes. Also, care must be taken to trim all loose yarns or other metal filaments from the edges of the fabric so that these do not short out to the electrodes. It is customary to see a tiny spark each time a weld is made, but if electrodes are misaligned, chipped, or if superficial fuzz is encountered, serious arcing may occur.

If the welder is used on long seams, wherein the solenoid motors driving the wheels and energizing the electrodes are being used continuously, it is desirable to cool these motors with an electric blower or fan. If the machine is redesigned for high-production use, continuous operation, heavy-duty solenoid motors should be used.

After the operator is assured that the welder heads are in proper dimensional and force adjustment, he establishes the proper power characteristics by use of the adjustments on the front of the General Electric power supply and the automatic sequencing timer.

Primary circuit voltage is indicated on the voltmeter on the power supply and the adjacent tap switches determine the transformer taps which are being used. The upper lefthand selector has two tap steps and the righthand selector has four steps, giving a combination of eight transformer tap combinations. These tap switches not only affect the primary voltage but the "voltage adjust," rotary control on the power supply door is used to select the exact voltage desired. It has been found that this power supply should never be operated in excess of 185 primary Volts. The solid state circuitry is subject to damage at higher voltages.

Also on the door of the power supply are a main adjustment and vernier for selecting weld pulse time from 0.1 to 10.0 milliseconds.

With new fabrics and combinations of layers careful matrix optimization must be utilized to establish the proper combination of variables to give the best possible weld efficiency. Table XXVIII illustrates the optimized settings which have been determined for multiple layers of metal fabric tape and broad goods as used in this program. It will be noted that joint efficiencies range from 87 to 92 percent and two-through-five layers of metal fabric were welded.

The Duffers current analyzer has been found ideal for measuring the short duration pulses in the secondary welding circuit. The clamp of the analyzer is placed around the flexible conductors leading from the flat plate busses to the upper electrode holders. The instrument has usually been set to read the peak amperage continuously. The reading will be a general average of peak current flowing during all pulses. The instrument may also be set to read and retain the amperage on one weld pulse. The secondary circuit voltage is of the order of two-to-eight Volts so that there is little danger to the operator even though he is holding the metal fabric. Reasonable safety precautions should be taken, however, to assure that he is not grounded. It is also recommended that he wear protective eye glasses although there has never been any indication that particles are thrown out even when arcing happens to occur.

Table XXVIII

WELDER SCHEDULE FOR VARIOUS CONFIGURATIONS OF METAL FABRIC TAPE AND BROAD GOODS

Layers in Weld Joint		Welder Settings				
B. G.*	Tape**	Pulse (ms)	Taps	Primary (Volts)	Current (Amperes)	Joint Efficiency*** (%)
2	0	5	1-2	165	470-500	92
3	0	5	1-2	170	460-520	89
4	0	5	1-3	175	480-510	92
2	1	5	1-2	170	430-470	90
2	2	5	1-3	180	450-490	93
3	1	5	1-3	175	490-530	95
3	2	5	2-1	157	440-470	87
0	2	5	1-2	165	470-500	87

* Broad goods: 1/49/3Z-2Z, 58x58, parent strength cleaned fabric (warp) 316 lb/in.
** Tape: 1/49/3Z-2Z, 80x40, parent strength cleaned fabric (warp) 463 lb/in.
***Average of all weld check coupons tested during fabrication of apex.

3.9.3.3 WELDER CERTIFICATION

Soon after the welder was put into operation a qualification procedure was established. The plan given in Appendix IV was prepared to cover the range of thickness and layers of fabric and the welder speeds and configurations intended for making the paraglider test components in this program. It called for the welding and tensile testing of 154 Karma fabric coupons, with the tensile rupture values to be statistically analyzed to judge welder capability. At that time it was hoped to obtain assurance of 70 percent minimum welded joint efficiency at a confidence level of 90 percent. Actually, the results of the statistical analysis showed that there was more than a 99.95 percent confidence that the average joint efficiency exceeded 70 percent, and that the average joint efficiency exceeded 30 percent at the 90 percent level of confidence.

It was subsequent to the above qualification work that the welder heads were reworked, chromium plating the electrode plunger slots and reducing the play in the upper splines. Thus, much higher joint efficiencies were obtained. (See Table XXVIII.) To confirm the obviously improved performance an additional statistical analysis was made, as shown in Appendix V. This was done approximately nine months after the qualification testing presented in Appendix IV. The latter data shows that the statistical, two-layer weld efficiency had increased to 88.85 percent (of average parent fabric tensile strength) at the 90 percent confidence level. There was also 99.95 percent confidence that the weld efficiency exceeded 85 percent.

Coupons used in certification were cut at least 1-1/2 inches wide and approximately 3 inches long. They were then basted together with three basting spots using the hand-held welder and Unitek power supply. The double-row weld was then placed across the 3/4-inch overlap of the two coupons, straddling the three basting spots. The coupons were then raveled under a microscope, removing yarns from either side so that 58 yarns, corresponding to one-inch in width, were retained. Careful alignment of the two coupons during basting is necessary to assure uniform loading of the seam. Since most metal fabrics vary in strength between warp and fill directions, note must be made of the direction in which the coupon is being pulled so as to relate the weld strength to the proper parent fabric strength.

The coupon is inserted in tensile machine test jaws being careful that it is again accurately aligned in a vertical position. The tensile machine jaws should be lined with leather. Voltage, current, pulse time, head spring force, welding speed, and identification of the fabric should be recorded on the certification sheet, along with the time, date, and test results, including weld efficiency.

During actual qualification testing, all coupons were statistically analyzed and none discarded. No changes were made to the welder except for occasional redressing of electrodes or replacement of electrodes if required.